

**Use of satellite-based global Earth Observation  
products to support national mitigation  
strategies to reduce forest carbon emissions**

Joana Lisboa Brandão de Melo

Submitted in accordance with the requirements for the degree of

Doctor of Philosophy

The University of Leeds

School of Geography

December 2023



The candidate confirms that the work submitted is her own, except where work which has formed part of jointly-authored publications has been included. The contribution of the candidate and the other authors to this work has been explicitly indicated below. The candidate confirms that appropriate credit has been given within the thesis where reference has been made to the work of others.

**Chapter 2:** Melo, J., Baker, T., Nemitz, D., Quegan, S. & Ziv, G. (2023). Satellite-based global maps are rarely used in forest reference levels submitted to the UNFCCC, *Environmental Research Letters* 18(3): 03402. URL: <https://dx.doi.org/10.1088/1748-9326/acba31>

JM, TRB and GZ designed and conceived the study. JM and DN conceived the database for data collection. JM compiled and analysed the data. JM wrote the manuscript. All co-authors provided critical feedback to the text, figures and tables.

**Chapter 3:** Melo, J., Ziv, G., Baker, T., Carreiras, J., Pearson, T. & Vasconcelos, M. (2018) Striking divergences in earth observation products may limit their use for REDD+, *Environmental Research Letters* 13(10): 104020. URL: <https://dx.doi.org/10.1088/1748-9326/aae3f8>

JM, GZ and TRB designed and conceived the study. JM collected and analysed the data. JC, TP and MV supported the collection and analysis of Guinea-Bissau data, including the land cover maps and field data. JM wrote the manuscript with GZ and TB critical feedback. All co-authors reviewed the final text.

**Chapter 4:** Melo, J., Baker, T., Cassama, V., Chen S., Ziv, G., (in prep). Combining satellite-based global maps for improved estimates of deforestation in African savannas

JM, TRB and GZ designed and conceived the study. JM collected and analysed the data. VC supported the QAQC of the visual interpretation of the reference dataset. SC provided feedback on the sampling design and results to be undertaken as corrections. JM wrote the first draft manuscript.

**Introduction and Conclusions chapters:** during the years I was developing my PhD as a part-time student, I had many opportunities to collaborate with other academics or researchers and my work contributed to peer-reviewed articles or reports that fit within the wider context of the thesis. Some of my contributions to these publications (list below) are embedded in **Chapter 1: Introduction** and **Chapter 5: Thesis Conclusions**. When materials are used, they are explicitly mentioned in captions of Figures and Tables.

Bullock et al (2023) Estimating aboveground biomass density using hybrid statistical inference with GEDI lidar data and Paraguay's national forest inventory. Environ. Res. Lett. 18 085001 DOI [10.1088/1748-9326/acdf03](https://doi.org/10.1088/1748-9326/acdf03)

CEOS Earth Observation Handbook 2023 "Space data for the Global Stocktake". Available online at: <https://eohandbook.com/gst/> [contributions from Chapter 2, Figure 2.2, Table 2.1 and text]

Grassi et al (2022) Carbon fluxes from land 2000–2020: bringing clarity to countries' reporting, Earth Syst. Sci. Data, 14, 4643-4666, [10.5194/essd-14-4643-2022](https://doi.org/10.5194/essd-14-4643-2022)

Grassi et al (2023) Harmonising the land-use flux estimates of global models and national inventories for 2000–2020. Earth System Science Data, 15(3), 1093–1112. DOI [10.5194/essd-15-1093-2023](https://doi.org/10.5194/essd-15-1093-2023)

Heinrich et al (2023) Mind the gap: reconciling tropical forest carbon flux estimates from earth observation and national reporting requires transparency. Carbon Balance Manage 18, 22. DOI [10.1186/s13021-023-00240-2](https://doi.org/10.1186/s13021-023-00240-2)

Hunka et al (2023) On the NASA GEDI and ESA CCI biomass maps: aligning for uptake in the UNFCCC global stocktake. Environ. Res. Lett. 18 124042. DOI [10.1088/1748-9326/ad0b60](https://doi.org/10.1088/1748-9326/ad0b60)

Ochiai et al (2023) Towards a roadmap for space-based observations of the land sector for the UNFCCC global stocktake. iScience 26 106489. DOI [10.1016/j.isci.2023.106489](https://doi.org/10.1016/j.isci.2023.106489)

Poulter et al (2023) CEOS Roadmap for Space-Based Support of Agriculture, Forestry and Other Land Use (AFOLU) Emissions and Removals of Greenhouse Gases. Version 1.0 endorsed by the Principals at the 37<sup>th</sup> Committee on Earth Observation Satellites Plenary, Thailand November 2023. Available online at: [https://ceos.org/document\\_management/Meetings/Plenary/37/Supporting%20Documents/CEOS\\_AFOLU\\_roadmap\\_FINAL\\_V1.0.pdf](https://ceos.org/document_management/Meetings/Plenary/37/Supporting%20Documents/CEOS_AFOLU_roadmap_FINAL_V1.0.pdf) [contributed with Figure 2.2, Table 1.2, and text]

This copy has been supplied on the understanding that it is copyright material and that no quotation from the thesis may be published without proper acknowledgement.

*Assertion of moral rights:*

The right of Joana Lisboa Brandão de Melo to be identified as Author of this work has been asserted by her in accordance with the Copyright, Designs and Patents Act 1988.

© 2023 The University of Leeds and Joana Lisboa Brandão de Melo

# Acknowledgements



***“How vain it is to sit down to write when you have not stood up to live!”***

**Henry David Thoreau**

This thesis was easy to write because I lived it intensely. I lived it, even before starting it. I worked in many places, but it was my time in Guinea-Bissau that changed me from the forester-by-training into the forester-by-passion. I have a debt of gratitude to this beautiful country, its forests and its people and, therefore, first, I thank Guinea-Bissau for bringing passion into my work and into this thesis. From the very beginning to the very end.

I thank my supervisors, Timothy Baker and Guy Ziv, for bringing out the hidden scientist in me. For guiding me without breaking me. For teaching me how to write better and communicate science better. For trusting me.

To João, to Alice and to Gustavo (and to Radar, my dog), who cheered me and supported me unconditionally, for so many years. I would have quit a long time ago without your spirit and your love. I am very grateful for having done this with you by my side.

To my mum and to my dad, who behind the scenes, without me knowing, read my articles and shared them with family and friends, and are always so proud of me.



# Abstract

Forests are vitally important for the World to achieve carbon neutrality as called for in the Paris Agreement under the United Nations Framework Convention on Climate Change (UNFCCC). This thesis explores existing challenges in integrating global maps derived from satellite-based Earth observation to quantifying forest dynamics and fluxes (hereafter 'EO products') in national reporting to the UNFCCC. Focusing on developing tropical countries this thesis reveals a notable underutilization of EO products in national reporting (Chapter 2).

Chapters 3 and 4 delve into this low uptake, revealing striking divergences in deforestation maps, in its magnitude and spatial distribution (Chapter 3), and identify large omission and commission errors linked to shifting agriculture (Chapter 4). While combining maps can improve the accuracy of deforestation estimates, large errors remain. However, correcting the estimates with a reference sample renders relatively similar area estimates regardless of the map used to stratify the sample (Chapter 4). Using the maps for stratification is one of the practical demonstrations of how the EO products are ingested in national monitoring systems with such examples of uptake occurring mainly in the reporting of African States and Least Developed Countries (Chapter 2).

This thesis emphasizes the complexities of accurately mapping deforestation in tropical dry forests and concludes that EO products are not as widely employed nor as accurate as perceived within the EO community. The results from this thesis call for a stronger collaboration between national and global land monitoring experts to address the existing disconnect between the available EO products and the requirements of the IPCC Guidelines. By supporting the measurement reporting and verification capacity of Parties to the UNFCCC, the EO community fills an important information gap to both the national and global (Global Stocktake) understanding of land use carbon fluxes and trends.



# Table of Contents

Acknowledgements .....	iii
Abstract .....	v
Table of Contents .....	vii
List of Tables .....	xii
List of Figures .....	xiv
Abbreviations.....	xxi
1. Chapter 1: Introduction.....	1
1.1 The bigger picture and motivation for this thesis .....	1
1.2 Key definitions .....	7
1.3 Forests and land use under the UNFCCC and its Paris Agreement.....	7
1.3.1. So, what exactly is LULUCF?.....	9
1.3.2. REDD+ .....	10
1.3.3. The IPCC guidelines, methods and variables .....	11
1.3.4. Perspectives of tropical countries.....	13
1.4 Space agencies and the EO community in support of the UNFCCC.....	15
1.5. Literature review on EO stakeholders developing global to pantropical EO products for MRV .....	19
1.5.1. EO for monitoring forest land and changes in forest area.....	20
1.5.2. EO for biomass .....	26
1.5.3. Combining EO derived products to estimate land carbon fluxes.....	29
1.5.4. The uptake of EO products in national reporting.....	31
1.6 Thesis aims and objectives.....	33

1.7 Chapter outline .....	34
1.8 References .....	36
2. Chapter 2. Satellite-based global maps are rarely used in forest reference levels submitted to the UNFCCC .....	57
2.1 Contributions and Acknowledgements .....	58
2.2 Introduction.....	59
2.3 Methods.....	62
2.4 Results .....	64
2.5 Discussion .....	70
2.5.1. IPCC considerations for area representation: national definitions, spatial and temporal resolution, temporal coverage and consistency.....	70
2.5.2. Limited uptake of global biomass maps.....	72
2.5.3. Regional differences in the uptake of EO products .....	73
2.5.4. Transparency of reference level submissions and limitations of the analysis .....	73
2.6 Conclusions.....	74
2.7 References .....	75
3. Chapter 3. Striking divergences in Earth Observation products may limit their use for REDD+.....	85
3.1 Contributions and Acknowledgements .....	86
3.2 Introduction.....	87
3.3 Data.....	88
3.3.1. National deforestation and above-ground biomass data .....	88
3.3.2. Global forest cover data.....	89
3.3.3. AGB maps .....	89

3.4 Methods .....	90
3.4.1 Deforestation (Activity Data).....	90
3.4.2 Carbon assessment and emission factors .....	91
3.4.3 Estimating historic gross emissions from deforestation .....	91
3.4.4 Identifying spatial patterns of agreement .....	91
3.5 Results .....	92
3.5.1. Above-ground biomass and emission factors .....	92
3.5.2. Deforestation magnitude and spatial disagreement.....	93
3.5.3. Forest Reference Emission Level combinations .....	94
3.5.4. Relationship between spatial patterns.....	95
3.6 Discussion .....	96
3.6.1. Understanding spatial disagreements in deforestation (Activity Data).....	96
3.6.2. Opportunities and limitations for using available AGB datasets.....	98
3.6.3. Implications of observed differences in Forest Reference Emission Level estimates .....	99
3.7 Conclusions .....	100
3.8 References .....	100
4. Chapter 4. Combining satellite-based global maps for improved estimates of deforestation in African savannas .....	107
4.1 Contributions and Acknowledgements.....	108
4.2 Introduction .....	109
4.3 Materials and methods .....	110
4.3.1 Deforestation maps .....	110
4.3.2 Reference data.....	112

4.3.3	Map validation and bias correction of area estimates.....	115
4.3.4	Spatial distribution of the errors and causes of the classification errors.....	116
4.4	Results and discussion.....	117
4.4.1	Deforestation areas and classification errors of the maps.....	117
4.4.2	Sampling design as a source of bias.....	119
4.4.3	Causes of classification errors and drivers of deforestation.....	121
4.4.4	Trends in the 21 <sup>st</sup> century.....	124
4.5	Conclusions.....	125
4.6	References.....	126
5.	Thesis Conclusions.....	131
5.1	Cross chapter synthesis.....	131
5.1.1	Summary answers to the research questions raised in the previous chapters .....	132
5.2	Contributions to the overarching questions and future directions to science and policy.....	137
5.2.1	Provision of high quality EO data for maps and sampling approaches. ....	138
5.2.2	Improve mapping of shifting agriculture.....	139
5.2.3	Better alignment between EO products and IPCC categories.....	140
5.2.4	Link EO products to IPCC variables.....	142
5.2.5	Implement a collaborative interface between national and global land monitoring experts. ....	143
5.2.6	Reconcile the differences at national and global level.....	145
5.3	Closing Remarks.....	147
5.4	References.....	148
Appendix 1	.....	153

Appendix 2 ..... 167

Appendix 3 ..... 175

# List of Tables

**Table 1.1** IPCC categories for the land use, land use change and forestry (LULUCF) sector used in GHG inventories reported to the UNFCCC mapped to the variables used in the Global Carbon Budget (2023) and the Global Earth Observations flux model from Harris et al (2021) to identify which LULUCF categories are covered and where they are presented in the other two datasets..... 10

**Table 1.2** Variables used in the IPCC equations for estimating carbon stock changes in the AFOLU sector (Volume 4, Chapter 3, IPCC 2006). The first five variables correspond to the gain-loss method while the last two are used in the stock-difference method. [table also included in Poulter et al (2023) and in Supplementary information of Hunka et al (2023)]..... 13

**Table 2.1.** Examples of key uses and opportunities for Earth Observation products in the core elements of the Paris Agreement (UNFCCC, 2015)(corresponding article in brackets). Satellites can only measure the land surface, so only the above-ground biomass pool is considered here within emission and removal factors (EF/RF). .....60

**Table 2.2.** Examples of existing satellite-based global-scale maps (or Earth Observation products in the text) on land-cover, land-cover change, fire, and above-ground biomass (AGB) covering the tropics. Many of these products are identified as being key for the land sector by the research and systematic observation community (ESA, 2022). Because the focus of our study is on country uptake for domestic GHG inventories and on consistent global monitoring for the Global Stocktake, we have excluded datasets with spatial resolutions coarser than 1-km and with only regional to local coverage. Maps produced with Earth observations from airborne data are not included.....61

**Table 2.3.** All the global maps derived from satellite-data ('EO products') used by 26 out of the 56 countries that submitted a forest reference emission levels/forest reference levels (FREL/FRL) to the UNFCCC between 2014 and 2022 and ways in which these products were used: to directly derive Activity Data (AD; yellow box) and Emission Factors (EF; green box) or contributing indirectly to the FREL/FRL. Colours and symbols (yellow, green and • match the legend of **Figure 2-1** and **Figure 2-2**). Uses for AD are separated into deriving information on 'deforestation', on 'other REDD+ activities', as auxiliary data (e.g., as training data or to correct the maps), and to map fire occurrences. Uses for emission factors are separated into deriving information on 'deforestation' and 'other REDD+ activities'. Unlisted countries (from the 56 with submitted FREL/FRL) used no EO product in their FRLs, or if one was used, it is not clearly identified in the

submission and supporting documentation. Dash (-) denotes no use. \* Togo compared emission results with data from the Global Forest Watch relying on the Global Forest Change (Hansen et al., 2013) product. Totals are total number of countries. Note countries can appear repeated in the same column or row..... 68

**Table 2.4.** Examples of how this study classifies the different contributions from products derived from satellite data (EO products) found in forest reference emission level/forest reference level (FREL/FRL) submissions to the UNFCCC. The main classification of EO product uses is as i) a direct contribution to derive activity data (AD; highlighted in yellow), ii) a direct contribution to derive emission factors (EFs; in green; n.a. because no examples of uptake were found) and iii) indirect contributions related to either AD or EFs (in white). See more details at country level in **Table A.1.2** ..... 69

**Table 3.1.** The data sources used to derive deforestation estimates between 2007 and 2010. .... 89

**Table 3.2.** The above-ground biomass data sources used to derive emission factors. 90

**Table 3.3.** Forest Reference Emission Levels (in MtCO<sub>2</sub> yr<sup>-1</sup>) for the reference period 2007-2010 and country-wide spread given by the Coefficient of Variation (CV, %) for AD by fixing each AGB product, and for EF by fixing each deforestation product. The different FREL estimates are obtained as the product of Activity Data (AD, ha yr<sup>-1</sup>) derived from each dataset (National, GFC, GLCF, and JAXA) and Emission Factors (EF, tCO<sub>2</sub> ha<sup>-1</sup>) obtained by each dataset (National, SA11, BA12, CA12, BO18). .... 94

**Table 3.4.** Spearman’s rank correlation coefficient between per-pixel mean and coefficient of variation (CV, %) for AD and AGB. Correlation values above 0.3 are in boldface; p > 0.05 in round brackets. .... 95

**Table 4.1.** Aggregated deforestation between 2007 and 2010 obtained from the individual deforestation maps (National, GFC, and GLCF), the intersection of maps (National ∩ GFC; National ∩ GLCF; GFC ∩ GLCF; National ∩ GFC ∩ GLCF) and union of maps (National U GFC; National U GLCF; GFC U GLCF; National U GFC U GLCF) before and after correction of classification bias calculated as in Olofsson et al. 2014 ..... 118

**Table 5.1.** Preliminary reflections on the requirements in terms of spatial and temporal resolutions and temporal coverage for satellite-based products to estimate emissions and removals from the LULUCF, i.e., to the IPCC variable to report (IPCC, 2006). The options of products, uses and characteristics are not exhaustive and only builds on the

range of data and uses in Forest Reference Level submissions from the analysis in Chapter 2 ..... 143

## List of Figures

**Figure 1-1** Differences in the estimates of emissions from land use change between GCB2020 (left) (Friedlingstein et al., 2020) and the most recent GCB2023 (right) (Friedlingstein et al., 2023). Note the variability shown is not the uncertainty of the models but the variability from the estimates of the three bookkeeping models BLUE, H&N and OSCAR. ....2

**Figure 1-2** Estimates of global anthropogenic GHG emissions from different data sources for the period 1970–2019. Source: Figure 2.2b from the IPCC AR6. The estimates from the three bookkeeping models (BLUE, OSCAR and H&N) are those from the GCB2020 depicting on average an increasing trend of emissions from land use. Source of NGHGI is Grassi et al. (2021). ....3

**Figure 1-3** Global net CO<sub>2</sub> flux due to land use (LULUCF) calculated by different datasets, including the Global Earth Observation dataset from Harris et al. (2021) as the sum of the gross emissions and gross removals in non-intact forests. Source: Figure 1 from Heinrich et al. (2023a). ....4

**Figure 1-4** Comparison of emissions from deforestation from the last two decades (2000-2020) 1) in the tropics from the study of Feng et al. (2022) based on data from the Global Forest Change dataset (Hansen et al., 2013) and using a stratified random-sample approach (left figure), and 2) in non-Annex I Parties to the UNFCCC as the aggregation of emissions from deforestation from national GHG inventories. Sources: Figure 1 from Feng et al. (2022) and adapted Figure 2b from Grassi et al. (2022). ....4

**Figure 1-5** Information flows between key actors contributing to the elements of the Paris Agreement of the UNFCCC and placing this thesis in a wider scope of understanding the contributions from the satellite Earth Observation (EO) community to the UNFCCC and its Global Stocktake. The arrows show possible ways the satellite community can support the implementation of the Paris Agreement. The blue arrows/pathways show possible support through the provision of satellite data and derived EO products to national teams preparing their submissions – nationally determined contributions (NDCs), forest reference levels and REDD+ results under the REDD+ framework, GHG inventories in the biennial transparency reports under the enhanced transparency framework. These three sources of data are then ingested in the Global Stocktake for a collective view. In the blue pathway, to prepare their submissions, national teams follow the methodological

guidance developed by the IPCC Task Force on national GHG inventories. The EO community can also contribute to the science included in the IPCC assessment reports (ARs) (brown arrow/pathway), including the synthesis report and the independent reports from the three working groups (WGI - Physical Science Basis of Climate Change; WGII - Climate Change Impacts, Adaptation and Vulnerability; WGIII with Mitigation of Climate Change) who serve as input to the Global Stocktake (UNFCCC, 2019a). Finally, according to the same decision 19/CMA1 (UNFCCC, 2019a) the EO community can contribute directly to the Global Stocktake with independent estimates (black arrow/pathway). This thesis focuses on the ways EO products can be used according to the IPCC Guidelines to produce estimates of emissions from deforestation which are used in all country submissions (NDCs, REDD+ and NGHGI)..... 16

**Figure 1-6.** Link between the chapters and the research questions of the thesis to present the logical flow across the chapters..... 35

**Figure 2-1.** List of all data sources used in this study (accessed through the UNFCCC REDD+ Web platform, (UNFCCC, 2022a), and methodological steps in the analysis. For each of the 75 forest reference level (FRL) submissions, we checked if: i) satellite data (e.g., Landsat imagery) or ii) EO products (satellite-based global maps, see examples in **Table 2.2**) were used in their development; if so, for which element of the FRL (AD - activity data or EF - emission factors) and in which way (direct or indirect use). In addition, we identify iii) which method was used to derive AD. For clarity, the colour scheme and symbol • match the legend of the figures and tables in the results section. .... 64

**Figure 2-2.** Location of the 56 country Parties to the UNFCCC that submitted 75 forest reference emission levels / forest reference levels (FREL/FRL) to the UNFCCC from 2014 up to 2022. The colour scheme in the quadrant charts shows the use of satellite data (e.g., Landsat imagery) and derived products (i.e., satellite-based global maps in **Table 2.2** or ‘EO products’ in the text) to directly derive Activity Data (AD, left-hand quadrants in red and yellow respectively), and Emission Factors (EF, right-hand quadrants in teal and green respectively). Indirect uses of EO products are represented with a • mark in a quadrant (e.g., use for validation, to justify decisions, to adjust the FREL/FRL, or for comparison of reported estimates). See **Table 2.4** for more details on what is considered direct and indirect contributions and **Table A.1.2** for details on the specific ways country Parties use the data. Use of maps produced from airborne technology are not included. Panel a) shows the proportion of developing country Parties that have submitted at least one FREL/FRL (blue bars) and proportion within those that submitted at least one FREL/FRL using ‘EO products’ in their FREL/FRL (black bars; including direct and indirect use of EO products depicted in the widgets in yellow and

green and with a • mark). Country Parties are separated in panel a) by geopolitical regional groups recognized by the UN—Latin American and the Caribbean (LAC) States, African States, Asian States—and the negotiating Party group defined as Least Developed Countries (LDCs, marked with the & symbol). Note that the 56 countries with FREL/FRL submissions are part of one of the three regional groups while 20 of them are also designated by the UN as LDCs. See **Figure A.1.1** for more information on MRV capacity indicators separated by Party groupings. ....67

**Figure 2-3.** Number of forest reference emission levels / forest reference levels (FREL/FRL) submissions to the UNFCCC per year since 2014 and up to 2022 separated by technique employed to generate Activity Data (AD): pixel-counting, stratified area estimate, or sampling. Panel a) includes all the 75 submissions to date with a1) showing the trend of the annual proportion of submissions using each AD technique. The trend is statistically significant (at 95% CI) for 'pixel-counting' (p-value < 0.001) and 'sampling' approaches (p-value < 0.001) but not for 'stratified area estimate' (p-value = 0.374). Panel b) shows only those submissions using products derived from satellite data (n = 29; 29 submissions from 26 country-Parties with Madagascar, Nigeria and Zambia using Earth Observation products in their two submissions; see **Table 2.4**); and further separated into submissions using Earth Observation products b1) to directly derive AD for deforestation (n = 11 including all 9 countries in **Table 2.3**, with Madagascar and Nigeria using it in their two submissions) or b2) to directly derive any of the other REDD+ activities (n=6).....69

**Figure 3-1.** Map indicating the location of Guinea-Bissau in Western Africa showing terrestrial ecoregions (adapted from Olson et al., 2001) and precipitation gradient (mm yr<sup>-1</sup>, WorldClim) in the Guinea-Bissau subset. ....88

**Figure 3-2.** Distribution of above-ground biomass (AGB, t ha<sup>-1</sup>) estimates from SA11, BA12, CA12, and BO18, including minimum, first quartile, median, third quartile, maximum, and mean AGB. Estimates at the country level are highlighted in grey and the mean marked with the symbol ×. The remaining distributions describe data from SA11, BA12, CA12, and BO18 in areas mapped as deforested by each activity data product: GFC, GLCF, JAXA, and National (mean values marked with symbols △, □, ◇, \*, respectively). Right panel depicts National (N) mean AGB (t ha<sup>-1</sup>) and the error bars the 95% confidence interval (CI) obtained from data collected nationwide in 309 sampled field plots. The 95% CI is also depicted by a blue bar for comparison with the remaining country-wide estimates. **Table A.2.3** shows mean and standard deviation values for all distributions. The National mean AGB density for the entire country (62.8 t ha<sup>-1</sup>, **Table A.2.2**) is used directly as proxy of pre-deforestation carbon stock or EF. The IPCC default

AGB value for sub-tropical dry forests (130 t ha<sup>-1</sup>, Table 4.12, IPCC 2006) is also illustrated here with a dashed line. .... 92

**Figure 3-3.** Spatial patterns of above-ground biomass (AGB, t ha<sup>-1</sup>) in Guinea-Bissau at 10-km resolution, including: a) AGB distribution from different products (SA11, BA12, CA12 and BO18), and b) per-pixel statistics including average AGB of all products and measure of spread given by the coefficient of variation (CV, %) in each pixel. The National EF is not depicted as it is estimated as the area-weighted average AGB of all forest classes with the same value of 62.8 t ha<sup>-1</sup> used country-wide with no spatial variation. .... 93

**Figure 3-4.** Spatial patterns of deforestation in Guinea-Bissau between 2007 and 2010 derived from different products (GFC, GLCF, JAXA and National) at 10-km resolution: a) per-pixel deforestation values shown as the proportion (%) of deforestation by the land area of national territory (blue color denotes no change), and b) per-pixel statistics with average and measure of spread given by the coefficient of variation (CV, %). .... 94

**Figure 3-5.** Country-wide and regional spread analysis given by the Coefficient of Variation (CV, %) in Activity Data (AD) and Emission Factors (EF). Forest types or regions (F) were stratified based on mean annual precipitation. For Mangroves the BO18 dataset is excluded, as mangrove areas are masked in the original above-ground biomass map. .... 95

**Figure 3-6.** Example of deforestation in Mangrove through inspection of: a) very high spatial resolution imagery available in Google Earth (16 May 2004 and 23 January 2011) showing an area of mangrove in 2004 that in 2011 was a swamped rice field; and b) the Landsat archive with its higher temporal resolution (images ranging from May 2004 to April 2010 and displayed in RGB color composites: band 7, band 4, band 3) identifying 2007 as the conversion year. The high temporal resolution of Landsat images also highlight the different spectral signals of the cycle of rice production: from August to October rice is cultivated in swamped fields (green signal) while in November the field dries out and the rice is cropped. In this study, only AD-National and AD-GLCF identified this area as deforested between 2007 and 2010. .... 97

**Figure 3-7.** Example of bushfires in Guinea-Bissau. Figure shows a) high spatial resolution imagery from Google Earth identifying this area as forest in 2005 and remaining forest in 2012, regarding of the prevalence of fire as shown by the b) temporal analysis of Landsat imagery with annual evidence of active fires or fire scars (displayed in RGB color composites: band 7, band 4, band 3). The area marked (yellow square) was mapped as deforested only by the AD-National product which is based on Landsat

imagery from the dry season. Wildfires in African savannas typically occur in the beginning of the dry season (November-February) and their scars are very difficult to detect using remote sensing imagery from the late dry season (March-May) and growing season (June-October) .....97

**Figure 4-1.** Study area and data used in this study, including: a) the location of Guinea-Bissau in Western Africa showing terrestrial ecoregions (adapted from Olson et al 2001); b) Guinea-Bissau subset showing deforestation between 2007 and 2010 obtained as the sum of deforestation derived from three independent maps - a map produced in-house using Landsat imagery and used by Guinea-Bissau in its submissions to the UNFCCC, and deforestation derived from two global scale maps, the Global Forest Change (GFC, Hansen et al, 2013) and the Global Land Cover Facility (Sexton et al, 2013); c) Guinea-Bissau subset depicting the sample units following a stratified sampling approach and identifying the 899 sample units visually interpreted with Google Earth imagery and included in this study as reference dataset (in blue), and the remaining 341 sample units where Google Earth imagery was not available for the period 2007-2010 (in yellow). The example of a very high-resolution imagery from Google Earth corresponding to one 0.5 ha sample unit also depicts the 49-point grid used to determine the proportion of land use and tree cover in each sample unit. .... 111

**Figure 4-2.** Response design or decision tree for the classification of the sampling units using Google Earth imagery to determine the prevailing land use in the year 2007 and 2010 and eventual land use changes in the reference period. Sample unit classified as “temporarily unstocked” correspond to areas affected by fire, logging, or low intensity shifting agriculture where the percentage tree cover is not reduced more than 30% and is not below the threshold of the national definition of forest in 2010 (i.e., 10% in Guinea-Bissau). When the land use is not forest (NF), the interpreter takes note of prevailing land use and percentage tree cover before and after conversion. Imagery available between 2010 and 2022 was also assessed to support and increase trust in the decision. .... 115

**Figure 4-3.** Example of a time-series of google earth imagery between 2005 and 2019 used to classify one sampling unit and the use of the grid of 49 points used to determine land use and land use change between 2005 and 2010. For each sample unit, the proportion of a) tree cover and a) land use was assessed in at least two time points through visual interpretation of very high-resolution satellite images. In this example, mangrove is converted to swamp rice cultivation (deforestation) between 2005 and 2010 with a reduction of a) tree canopy cover from 71% (35/49 points) to 4% (4/49 points) and

a reduction of b) 88% (43/49 points) to 8% (4/49 points) of mangrove forest land use. An image from 2019 is also analysed to confirm the land use transition. .... 115

**Figure 4-4.** Omission and commission errors of the individual maps (National, GFC, and GLCF), intersection of maps (National  $\cap$  GFC; National  $\cap$  GLCF; GFC  $\cap$  GLCF; National  $\cap$  GFC  $\cap$  GLCF) and union of maps (National  $\cup$  GFC; National  $\cup$  GLCF; GFC  $\cup$  GLCF; National  $\cup$  GFC  $\cup$  GLCF) a) before and b) after correction of classification bias. The size of each circle is proportional to the area mapped as deforestation by each map (black circle), intersection of maps (red) or union of maps (blue), a) before, and b) after correction for classification bias..... 118

**Figure 4-5.** Number of the total 899 sampling units corresponding (correct, green) or not corresponding (wrong, red) to the classification of deforestation and stable forest or non-forest from the individual deforestation maps (National, GFC, and GLCF), the intersection of maps (National  $\cap$  GFC; National  $\cap$  GLCF; GFC  $\cap$  GLCF; National  $\cap$  GFC  $\cap$  GLCF) and union of maps (National  $\cup$  GFC; National  $\cup$  GLCF; GFC  $\cup$  GLCF; National  $\cup$  GFC  $\cup$  GLCF)..... 119

**Figure 4-6.** Percentage of classification errors of the satellite-based deforestation maps analysed by land use and land use conversion. Conversions from forest to other land uses (i.e., deforestation) is highlighted in red and errors in these classes are omission errors in the maps. Errors in the remaining classes with no red shading correspond to omission errors in the maps. In a) the individual maps (National, GFC, and GLCF) and b) the main errors of union and intersection of maps of the three maps. .... 121

**Figure 4-7.** Drivers of deforestation in Guinea-Bissau, estimated from the reference dataset comprising 899 sample units where Google Earth imagery was visually interpreted to assess the accuracy of existing deforestation maps. Forest land use is separated by classes: forest, degraded forest and mangrove. The proportion of these forest classes converted to other land use (crop/shifting agriculture, tree crops, swamp rice cultivation, urban, and other non forest land uses not clearly identified) between 2007 and 2010 is identified in the chart by the size of the channels. .... 123

**Figure 4-8.** Map of the study area (Guinea-Bissau) showing high concentrations or clusters of the 899 sample units wrongly (red) or correctly (green) classified in the maps as deforestation or stable land use. One figure of the study area for each of the 11 maps or combination of maps: individual deforestation maps - National, GFC, and GLCF; intersection of maps - National  $\cap$  GFC, National  $\cap$  GLCF, GFC  $\cap$  GLCF, National  $\cap$  GFC  $\cap$  GLCF; and union of maps - National  $\cup$  GFC, National  $\cup$  GLCF, GFC  $\cup$  GLCF, National  $\cup$  GFC  $\cup$  GLCF. .... 124

**Figure 5-1** Figure 7(d) from the Global Carbon Budget 2023 (Friedlingstein et al, 2023) overlaid with emissions from deforestation from the aggregated NGHGI in Figure 2(a) of Grassi et al (2022) (in black) and the global emissions from tree cover loss (Hansen et al., 2013) combined with the map of drivers from Curtis et al. (2018) to exclude emissions from shifting agriculture (in blue; from Global Forest Watch, GFW, 2023). The figure from Friedlingstein et al, (2023) shows the sub-components of “deforestation” and of “forest (re)growth” in the component of emissions from land use ( $E_{LUC}$ ): (i) deforestation in shifting cultivation cycles, (ii) permanent deforestation, (iii) forest (re)growth due to afforestation and/or reforestation, and (iv) forest regrowth in shifting cultivation cycles.  
..... 147

# Abbreviations

AD	Activity Data
AGB	Above-ground biomass
ALOS	Advanced Land Observing Satellite
BA12	Pantropical above-ground biomass map for African savannas published by (Baccini et al., 2012)
BAFTER	biomass stocks on land type i immediately after the conversion, t d.m. ha <sup>-1</sup>
BBEFORE	biomass stocks on land type i before the conversion, t d.m. ha <sup>-1</sup>
BLUE	Bookkeeping of Land Use Emissions
BO18	Above-ground biomass map for African savannas published by (Bouvet et al., 2018)
BTR	Biennial transparency report
BUR	Biennial Update Report
CA12	Above-ground biomass map for Guinea-Bissau published by (Carreiras et al., 2012)
CCI	ESA Climate Change Initiative
CE	Commission Error
CEOS	Committee on Earth Observation Satellites
CI	Confidence Interval
CMA	Conference of the Parties serving as the meeting of the Parties to the Paris Agreement
CO <sub>2</sub>	Carbon dioxide
CV	Coefficient of Variation
DEF	Deforestation
DEG	Forest Degradation
DETER	Real-Time System for Detection of Deforestation
DRC	Democratic Republic of the Congo
ECS	Enhancement of forest Carbon Stocks
EF	Emission Factor
E <sub>LUC</sub>	Emissions from land-use change in the Global Carbon Budget
EO	Earth observation
ESA	European Space Agency
F/NF	Forest/Non-Forest
FAO	Food and Agriculture Organization of the United Nations
FL	Forest Land
FRA	Forest Resource Assessment
FREL	Forest Reference Emission Level
FRL	Forest Reference Level
GCB	Global Carbon Budget
GEDI	Global Ecosystem Dynamics Investigation
GEO	Group on Earth Observations
GFC	Global Forest Change
GFOI	Global Forest Observations Initiative
GGGW	Global Greenhouse Gas Watch monitoring infrastructure
GHG	Greenhouse gases
GLAS	Geoscience Laser Altimeter System
GLCF	Global Land Cover Facility

HILDA	Historic Land Dynamics Assessment
HYDE	History database of the Global Environment
IBAP	Institute for Biodiversity and Protected Areas of Guinea-Bissau
ICESat	Ice, Cloud and land Elevation Satellite
IPCC	Intergovernmental Panel on Climate Change
JAXA	Japan Aerospace Exploration Agency
JICA	Japan International Cooperation Agency
JPL	NASA Jet Propulsion Laboratory
LAC	Latin America and the Caribbean (region)
LDC	Least Developed Countries
LIDAR	Light Detection and Ranging
LUH2	Land-Use Harmonization model
LULUCF	Land Use, Land-use Change and Forestry
MESA	Monitoring for Environment and Security in Africa
MGD	GFOI Methods and Guidance Document
MODIS	MODerate-resolution Imaging Spectroradiometer
MPGs	Modalities, procedures and guidelines for the transparency framework for action and support referred to in Article 13 of the Paris Agreement
MRV	Measurement, Reporting and Verification
MSS	Multispectral Scanner
NA	Not Available
NASA	National Aeronautics and Space Administration
NDC	Nationally Determined Contribution
NDVI	Normalized Difference Vegetation Index
NF	Non Forest
NFI	National Forest Inventory
NGHGi	National Greenhouse Gas inventories
NISAR	NASA-ISRO Synthetic Aperture Radar
NOAA	National Oceanic and Atmospheric Administration
OA	Overall Accuracy
OE	Omission Error
OSCAR	A compact Earth system model
PALSAR	Phased Array L-band Synthetic Aperture Radar
PRODES	Projeto de Monitoramento do Desmatamento na Amazônia Legal por Satélite
QuikSCAT	Quick Scatterometer
RADAMBRASIL	Projeto Radar da Amazônia
REDD+	Reducing emissions from deforestation and forest degradation in developing countries
RF	Removal Factor
RGB	Red, green and blue
SA11	Above-ground biomass map published by (Saatchi et al., 2011)
SAR	Synthetic Aperture Radar
SBSTA	Subsidiary Body for Scientific and Technological Advice
SEPAL	System for Earth Observation Data Access, Processing and Analysis for Land Monitoring
S <sub>LAND</sub>	The terrestrial CO <sub>2</sub> sink in the Global Carbon Budget
SMF	Sustainable Management of Forests
SPOT	Satellite Pour l'Observation de la Terre

TAR	Technical Assessment Report
TM	Thematic Mapper
TMF	Tropical Moist Forest cover change dataset
UN	United Nations
UNFCCC	United Nations Framework Convention on Climate Change
VCF	Vegetation Continuous Fields
VHR	Very-high resolution
WHRC	Woodwell Climate Research Center
WMO	World Meteorological Organization



# Chapter 1: Introduction

## 1.1 The bigger picture and motivation for this thesis

The climate crisis is the major challenge humanity is facing during this century (IPCC, 2023; UNEP, 2023). Under the United Nations Framework Convention on Climate Change (UNFCCC), all countries, developed and developing, large and small, are making policy decisions to address this challenge and strive for a universal shift towards a low carbon future. Forests are vitally important to support this transition to carbon neutrality as they are the only proven large-scale carbon removal technology that is available to compensate part of our fossil fuel emissions in the most immediate years of transition (Mo et al., 2023; Anderson et al., 2023). In the future, forests and land use will also continue to play an important role to compensate unavoidable emissions from the remaining sectors. But accurate and timely information on forest and land use GHG fluxes is required to plan mitigation actions and align ambition with reality (Korosuo et al., 2023).

Satellite Earth observations (EO) have great potential to support more accurate and complete estimates of land use GHG fluxes at national and global scales by providing information that is consistent over space and time and by covering all of the Earth's surface, including remote and inaccessible forests in the tropical biome (Defries et al., 2007; Achard and House, 2015; Romijn et al., 2018; Herold et al., 2019; GFOI, 2020). Accordingly, EO products are used in global estimates of carbon fluxes from land in satellite-based studies (Baccini et al., 2017; Harris et al., 2021; Chevallier, 2021; Feng et al., 2022), and in the three bookkeeping models H&N (Houghton and Nassikas, 2017), BLUE (Hansis et al., 2015) and OSCAR (Gasser et al., 2020) that contribute to the Global Stocktake through the IPCC assessment reports (AR; IPCC, 2022). Furthermore, large investments continue to be made by the international Space Agencies to support space-based observations of the land sector. Such data directly supports UNFCCC processes such as the reducing emissions from deforestation and forest degradation in tropical countries (REDD+) (e.g. Goetz et al., 2015) and the Global Stocktake (Ochiai et al., 2023; Poulter et al., 2023).

The first Global Stocktake ran during 2021-2023 and will now be repeated in 5-year cycles to assess the collective, continual progress in achieving the objectives of the Paris Agreement. This process uses information on GHG fluxes from the models in the IPCC ARs and also aggregated information from national GHG inventories (NGHGI) submitted by nations to the UNFCCC (UNFCCC, 2019a; Decision 19/CMA.1, para 37). However,

for the process to be effective in informing policy makers on the role of forests and land use in achieving carbon neutrality, the high levels of uncertainty (Friedlingstein et al, 2023) and large divergence of the GHG flux estimates from different sources, both in terms of its trends and magnitude, must be reduced or explained (Grassi et al 2023; Heinrich et al 2023a, Gidden et al 2023).

An example of this large divergence in magnitude and trends can ironically be found in the history of the Global Carbon Budget (GCB), a key “living document” for carbon-cycle researchers, that provides a historic record of changes in the state of carbon cycle science. Firstly, a reversal in the trend was observed between GCB2020 and the budgets of the subsequent years (**Figure 1-1**). Secondly, the annual CO<sub>2</sub> emissions trend from land use change (E<sub>LUC</sub> component) shows a large variability among the three bookkeeping models, with H&N showing a decreasing trend while BLUE and OSCAR show an increasing emissions from land-use change, or E<sub>LUC</sub> (from the latest IPCC assessment report, AR6, **Figure 1-2**). Comparing the estimates from the bookkeeping models used in the IPCC 6<sup>th</sup> Assessment Report and in the first Global Stocktake (GCB2020, IPCC AR6, **Figure 1-2**) with those from the global aggregation of NGHGs, highlights a large difference and an opposite sign between the estimates, with the NGHGs presenting the LULUCF sector as a small increasing carbon sink (negative sign) and the average of the bookkeeping models reporting this sector as an increasing large source (positive sign).

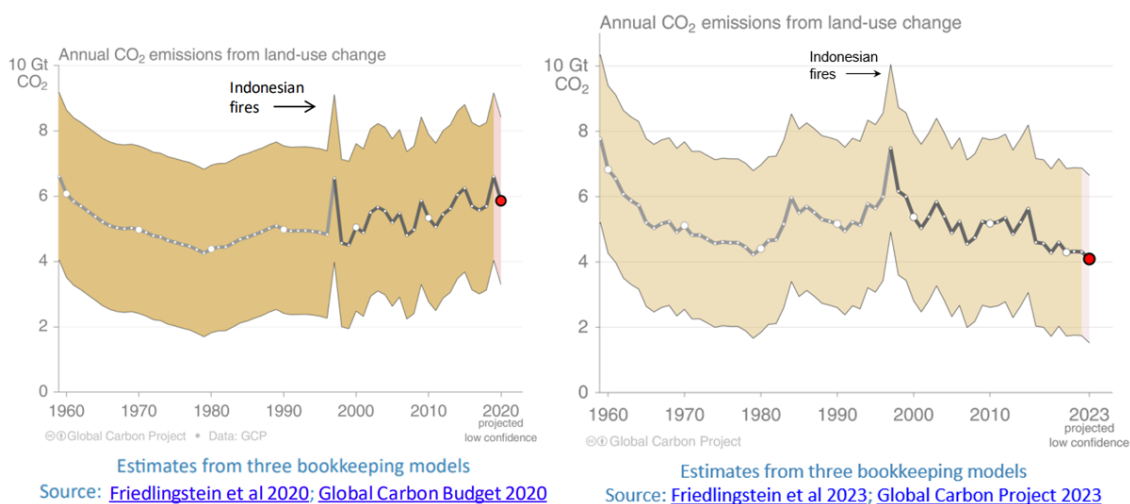


**Figure 1-1** Differences in the estimates of emissions from land use change between GCB2020 (left) (Friedlingstein et al., 2020) and the most recent GCB2023 (right) (Friedlingstein et al., 2023). Note the variability shown is not the uncertainty of the models but the variability from the estimates of the three bookkeeping models BLUE, H&N and OSCAR.

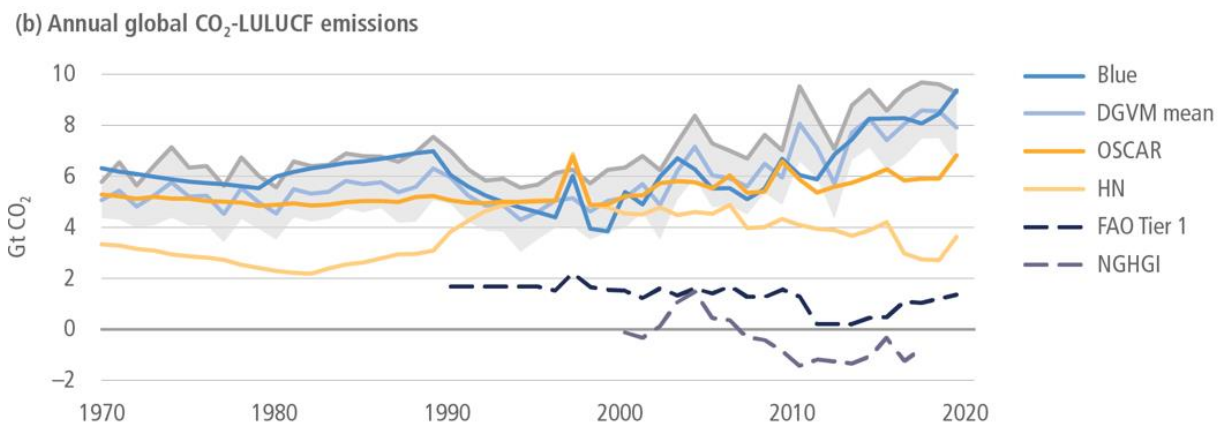


**Figure 1-2** Estimates of global anthropogenic GHG emissions from different data sources for the period 1970–2019. *Source:* Figure 2.2b from the IPCC AR6. The estimates from the three bookkeeping models (BLUE, OSCAR and H&N) are those from the GCB2020 depicting on average an increasing trend of emissions from land use. *Source of NGHGI is Grassi et al. (2021).*

The apparently contradictory estimates and large mismatch between the average of the bookkeeping models (version GCB2023) and the aggregation of NGHGI is quantified as a staggering  $6.7 \text{ GtCO}_2\text{yr}^{-1}$  (Grassi et al., 2023). This large gap, which is greater than the current fossil fuel emissions of the USA (Friedlingstein et al 2023), can be mainly explained by conceptual differences in how the two sources of information estimate the anthropogenic and natural land CO<sub>2</sub> fluxes. Grassi et al. (2023) reconcile this difference by adding part of the sinks estimated by DGVMs to the bookkeeping models so that the GCB and IPCC ARs are comparable to the aggregation of NGHGIs when assessing progress under the Global Stocktake of the Paris Agreement.

So far, the independent estimates of global GHG flux models based primarily on EO products to quantify forest dynamics and carbon fluxes (Harris et al., 2021; Feng et al., 2022), are not contributing to adding clarity to our understanding of land use CO<sub>2</sub> flux estimates and the mitigation role of forests (**Figure 1-3**). The 2001 to 2020 global average net emissions from forests and forest conversion (gross emissions plus gross removals; not including emissions and removals from other land use categories such as croplands and grasslands) from Harris et al. (2021) in Heinrich et al. (2023a) is estimated as a large net sink of  $-6.7 \text{ GtCO}_2\text{yr}^{-1}$ . It represents a difference of  $4.8 \text{ GtCO}_2\text{yr}^{-1}$  compared to the aggregated NGHGIs for LULUCF, or  $11.5 \text{ GtCO}_2\text{yr}^{-1}$  compared to the average of bookkeeping models for  $E_{\text{LUC}}$ , which is comparable to the fossil fuel emissions of China (Friedlingstein et al 2023).

Similar discrepancies emerge when focusing on the most fundamental issue of estimating emissions from deforestation in the tropics. Feng et al. (2022) used different high-resolution satellite datasets, including the Hansen et al. (2013) global forest change (GFC) dataset also used by Harris et al. (2012), to show a doubling of gross tropical forest carbon loss from  $0.97 \pm 0.16 \text{ PgC yr}^{-1}$  (or  $3.6 \pm 0.6 \text{ GtCO}_2\text{yr}^{-1}$ ) in 2001–2005 to

1.99 ± 0.13 PgC yr<sup>-1</sup> (or 7.3 ± 0.5 GtCO<sub>2</sub>yr<sup>-1</sup>) in 2015–2019. Although the magnitude of emissions from deforestation is of the same order of magnitude of the aggregated emissions from deforestation in Non-Annex I Parties to the UNFCCC (including all tropical countries from the study but also China, Mongolia, Southern Africa and Southern South America), the trend is opposite (**Figure 1-4**). The Feng et al. (2022) increasing trend in emissions from deforestation is consistent with Harris et al. (2012), and the IPCC AR6 (IPCC, 2022) (**Figure 1-2**) using data from the GCB2020 (Friedlingstein et al., 2020). However, it is contrasting to the slightly decreasing trend from the aggregation of NGHGI, from the average of bookkeeping models in the GCB2023 and other pan-tropical studies (e.g., Vancutsem et al., 2021).

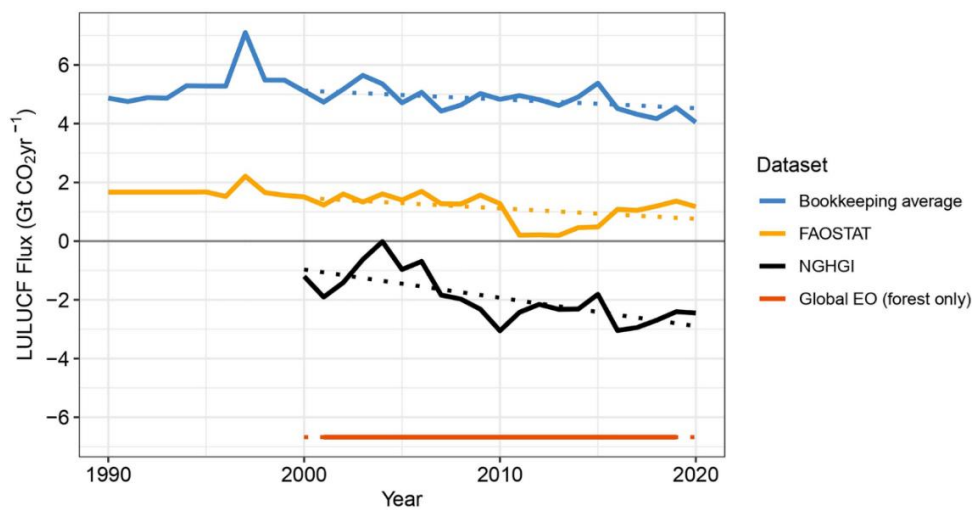


**Figure 1-3** Global net CO<sub>2</sub> flux due to land use (LULUCF) calculated by different datasets, including the Global Earth Observation dataset from Harris et al. (2021) as the sum of the gross emissions and gross removals in non-intact forests. *Source:* Figure 1 from Heinrich et al. (2023a).

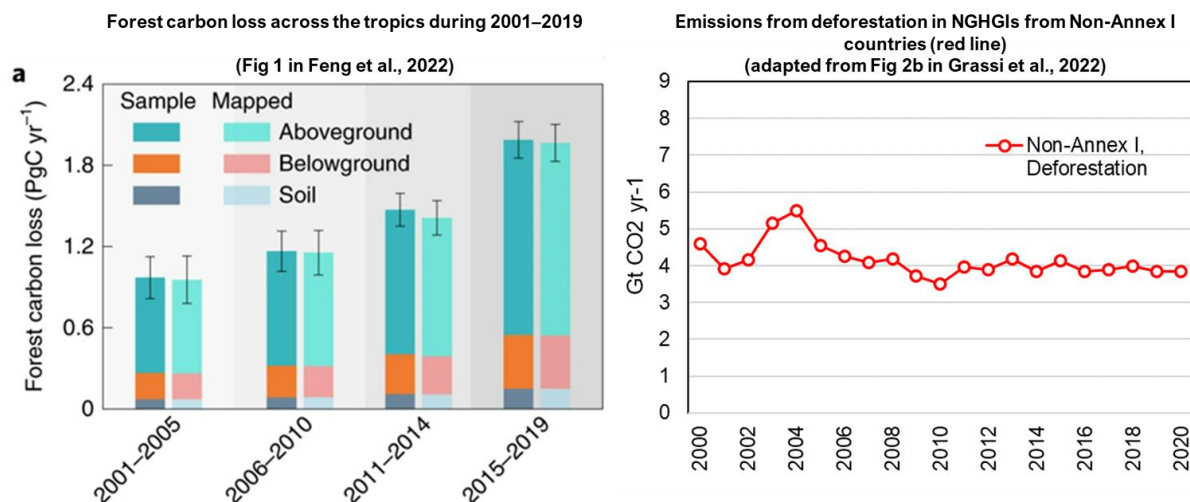


**Figure 1-4** Comparison of emissions from deforestation from the last two decades (2000-2020) 1) in the tropics from the study of Feng et al. (2022) based on data from the Global Forest Change dataset (Hansen et al., 2013) and using a stratified random-sample approach (left figure), and 2) in non-Annex I Parties to the UNFCCC as the aggregation of emissions from deforestation from national GHG inventories. *Sources:* Figure 1 from Feng et al. (2022) and adapted Figure 2b from Grassi et al. (2022).

Vancutsem et al (2021) do not document fluxes, but areas of deforestation, forest degradation and recovery of global tropical moist forests (TMF) over the past three decades (TMF dataset). The authors compare the TMF areas of deforestation with the GFC (Hansen et al., 2013) and note the TMF depicts 61.4% more deforested area than the GFC for the 2001-2010 decade but, for the 2010-2019 decade, the GFC maps as forest loss all the deforestation areas in TMF plus 5.7% of the areas mapped in TMF as forest degradation. This sharp increase in detected forest loss between the two decades by the GFC was highlighted in other studies as well (Galiatsatos et al., 2020; Palahi et al., 2021; Ceccherini et al., 2021). The different definitions and approaches used by these datasets must be considered when explaining the differences with NGHGI. The TMF (Vancutsem et al., 2021) shows a marked increase in forest degradation in recent years. The GFC (Hansen et al., 2013) does not map forest degradation, only tree cover loss, including harvest (Ceccherini et al., 2020). However, harvest is reported in NGHGI in the category forest land remaining forest land, and not in a forest conversion category, and therefore is not included in the class “deforestation” in Grassi et al. (2022) (**Figure 1-4**).

The writing of this thesis ends at the same time as the conclusion of the first Global Stocktake, a mechanism under the Paris Agreement to course correct and reflect urgency to address ambition and implementation gaps (UNFCCC, 2019a). According to the synthesis report prepared by the co-facilitators of the technical dialogues of the Global Stocktake, “*around half of net AFOLU emissions result from land-use change: predominantly CO<sub>2</sub> from deforestation*” and “*despite a decline in deforestation since 2000, the rate remains high, with 95 per cent of global deforestation occurring in the tropics but incentivized by consumers globally*” (UNFCCC, 2023a). This observation contrasts to that of many sources of information from the EO community, who seem to be unable to agree on the fundamental question “*has deforestation increased or decreased in the past 20 years?*”. The apparent disconnect between the EO community and the processes under the UNFCCC raises the overarching questions:

***Why do we get conflicting estimates from the aggregation of land carbon fluxes from GHG inventories submitted to the UNFCCC and independent global estimates from EO products?***

***How has the EO community contributed to the first Global Stocktake if their estimates of land carbon fluxes diverge from the conclusions from the Global Stocktake?***

These are the wider questions this thesis will address and contribute to. They are of particular relevance to tropical developing countries where EO products have for long been expected to substantially bolster the understanding, and reduce the uncertainty, of historical emissions from deforestation.

**Box 1.1.** *Additional motivation for this study*

For most of the time of my PhD studies I was funded by the Natural Environment Research Council (NERC, UK), through the Leeds–York NERC Doctoral Training Partnership. NERC encourages and invites researchers to apply for work placements during their doctoral training programs. In this context, in 2017, I was on placement at the UNFCCC secretariat in Bonn (Germany), in the transparency division, AFOLU unit. My responsibilities included compiling data from REDD+ reference levels, identifying main insights and trends in methods used by Parties in their submission, and supporting programme officers during the climate change conference (COP23). The insight I gained on UNFCCC processes was invaluable. Following my work placement, I was nominated to the Roster of UNFCCC experts by the national focal point of Guinea-Bissau with whom I had worked with for many years prior to my PhD and continued to work with throughout my PhD. My work placement and longstanding collaboration with Guinea-Bissau steered my research interests to contributing to the objectives of and processes under the UNFCCC, and to exploring the existing opportunities provided by the EO community to level out the playing field in forest monitoring and MRV by supporting developing countries who don't have accurate in-house data or forest monitoring capacity to comply with the requirements of the Paris Agreement and effectively plan mitigation actions in the forest and land use sector.

## 1.2 Key definitions

In the previous background section 1.1, which sets the motivation for this thesis, some terms were introduced, such as “EO data”, “EO products” and “EO community”. Because these are key terms used throughout this thesis, this section of the introduction defines them, or clarified their meaning. "Earth observations" (EO) is a commonly accepted term within the field of remote sensing for describing the use of satellite data to study the Earth. Satellites do not directly "observe" the surface of the Earth, they detect and measure electromagnetic radiation emitted or reflected by objects on the Earth's surface which are then processed to create images. Consequently, EO is considered by some scientists to be an inaccurate designation. Nevertheless, it is a simplification adopted in this thesis when referring to:

- “EO data” as satellite imagery, for example Landsat scenes or mosaics, or very-high resolution imagery available in Google Earth;
- “EO products” as analytical products derived from satellite data, such as land cover or tree cover maps, or biomass maps;
- “EO community” as the diverse group of stakeholders involved in the collection and analysis of EO data, and development of EO products, including Space Agencies, remote sensing scientists and researchers.

The overarching questions raised in section 1.1 above link these key terms on EO with the needs of governments and national technical teams of tropical countries, which are the main actors in this thesis. Some terms related to this group of actors, such as “deforestation”, “LULUCF”, “REDD+”, the “Global Stocktake”, are discussed in the following section 1.3. This is then followed by two sections (1.4 and 1.5) with a description of ongoing efforts and opportunities envisioned by the EO community to better support the UNFCCC processes, and a literature review on EO stakeholders developing global to pantropical EO products to include more detail on the existing maps. These last two sections introduce the other main group of actors in this thesis, the EO community wishing to assist UNFCCC processes.

## 1.3 Forests and land use under the UNFCCC and its Paris Agreement

The academic and scientific communities are generally somewhat disconnected from policy (Oliver and Cairney 2019, Findlater et al 2021). This section of the introduction will therefore briefly describe the policy background and the modalities and guidelines

countries use in preparing their NGHGI and in reporting to the UNFCCC. It builds on the reflections from the previous section related to the discrepancies in the data from different sources which, in theory, are measuring the same thing – land dynamics and GHG fluxes from the land sector – and with the same objective of informing the UNFCCC and its Global Stocktake.

In 2015 a near universal agreement was achieved under the UNFCCC. By signing the Paris Agreement, countries agreed to limit global warming to below 2.0°C or 1.5°C above pre-industrial levels and to reach GHG neutrality in the second half of the century (UNFCCC, 2015). These objectives are to be achieved through the implementation of national climate plans, or nationally determined contributions (NDCs). The Paris Agreement has an emphasis on transparency and includes a new set of rules for measurement, reporting and verification (MRV) applicable to all Parties (UNFCCC, 2019b). The enhanced transparency framework (Article 13 of the Paris Agreement; UNFCCC, 2015), which supersedes the previous MRV arrangements, establishes that each Party is to regularly provide a national inventory report of anthropogenic emissions by sources and removals by sinks of GHGs (NGHGI). Among other contributions, the NGHGIs submitted to the UNFCCC enable the availability of regular and up to date quantitative information on domestic GHG emissions and removals, and of the progress towards meeting domestic targets of the NDCs. In 5-year cycles, such information is also aggregated to provide a collective view through the Global Stocktake process (UNFCCC, 2019a).

Forests cover approximately 4 billion hectares, or one third of the Earth's land surface, with 45% located in the tropics (FAO, 2020). Net CO<sub>2</sub> emissions from land-use change (mainly deforestation) accounted for about 11% of anthropogenic CO<sub>2</sub> emissions in the last decade (IPCC, 2022). According to the IPCC AR6, after solar energy, reducing deforestation is the mitigation option with the largest potential contribution to net emission reduction by 2030 (IPCC, 2022). At the same time, forests can act as a powerful sink working as an efficient, safe, natural, long-lasting and cost-effective carbon capture and storage technology (Mo et al., 2023; Heinrich et al., 2023b; Cook-Patton et al., 2020). As of September 2022, 54% of the submitted NDCs mentioned the mitigation measures afforestation, reforestation and revegetation (UNFCCC, 2022). Other terrestrial systems in addition to forest land, such as croplands, grasslands, wetlands, trees outside forests such as tree crops and urban trees, are all part of land use, land use change and forestry (LULUCF) and can also play an important role in climate change mitigation (Skole et al., 2021; Hart et al., 2023). In some of these cases, most of the carbon stocks are found in the below-ground plant organic matter and soil.

Consequently, mitigation actions in the land use, land use change and forestry (LULUCF) sector are strategically important to achieve the long-term goal of the Paris Agreement (UNFCCC, 2015; Den Elzen et al., 2022; UNFCCC, 2023a; IPCC, 2023). It is therefore not surprising that the sector plays a key role in the pledges made by many countries towards meeting the Paris Agreement targets with 43% of Parties including related quantitative mitigation targets in their NDCs (UNFCCC, 2022; Grassi et al., 2017).

### 1.3.1. So, what exactly is LULUCF?

Land use, land use change and forestry (LULUCF) is one of the sectors in the national GHG inventory (NGHGi), it is the land component of AFOLU (Agriculture, forestry and other land use) and is reported in the NGHGi separately from agriculture. While the 2006 IPCC Guidelines refer to AFOLU as a single sector (IPCC, 2006), the rules for the transparency framework (MPGs) (UNFCCC, 2019b) refer to the agriculture sector and the LULUCF sector separately. For reporting to the UNFCCC, the MPGs take precedence. Agriculture in the NGHGi refers to GHG emissions mainly from livestock, fertilizers and burning of crop residues, while LULUCF covers all anthropogenic emissions and removals from lands in a land-based approach.

Understanding how reporting GHG fluxes from LULUCF works, how the sector is split in categories of land use and land use change (**Table 1.1**), helps understanding where possible divergences with independent estimates can occur (as mentioned in chapter 1.1). To handle and present the data in a way that makes sense to the users under the UNFCCC, the latest global carbon budget (GCB2023; Friedlingstein et al 2023) includes a section splitting the land use ( $E_{LUC}$ ) components to partially map the global models' fluxes to the categories in the NGHGi. Sources and sinks are presented aggregated into (i) gross sources from deforestation; (ii) afforestation, reforestation, and wood harvest; (iii) emissions from organic soils (peat drainage and peat fire); and (iv) sources and sinks related to other land-use transitions. In addition, in one of the appendices, the authors add part of the land sinks component ( $S_{LAND}$ ) in managed forest from the DGVM simulations to  $E_{LUC}$  estimates (following Grassi et al., 2021) to the bookkeeping  $E_{LUC}$  estimate.

Understanding these categories is important because they affect the comparability of the results with values calculated using different approaches. For example, it is not straightforward to link the maps and estimates of “forest net fluxes” and “gross emissions” and “gross removals” from the global EO flux model of Harris et al (2021) to the IPCC categories in the NGHGI. For example, the “net forest GHG fluxes” in the EO flux model corresponds in the NGHGI to GHG fluxes in the categories “Forest Land” but

also on the sub-categories “Forest Land converted to Cropland” (which is reported in the Cropland main category), “Forest Land converted to Grassland” (in the Grassland main category), “Forest Land converted to Wetlands” (in the Wetlands main category), “Forest Land converted to Settlement” (in the Settlement main category) and Forest Land converted to Other land” (in the Other Land main category), depending on the post-deforestation land use in the EO flux model for each Landsat pixel. Furthermore, the LULUCF net fluxes in the NGHGI may also include sinks from other land use categories and therefore it is not comparable with the net fluxes from the EO flux model – this is stated by the authors (Harris et al., 2021) but may be confusing to readers of these papers.

**Table 1.1** IPCC categories for the land use, land use change and forestry (LULUCF) sector used in GHG inventories reported to the UNFCCC mapped to the variables used in the Global Carbon Budget (2023) and the Global Earth Observations flux model from Harris et al (2021) to identify which LULUCF categories are covered and where they are presented in the other two datasets.

IPCC land-use categories and sub-categories	Global Carbon Budget (2023)	Global EO flux model (Harris et al)
forest land remaining forest land (4.A.1.)	SLAND (land sinks) ELUC (harvest, forest degradation, reforestation, fallow of shifting agriculture cycles)	Gross losses (harvest) Gross removals (forest land remaining forest land)
land converted to forest land (4.A.2.a-e)	ELUC (afforestation)	Gross removals (from forest gain)
cropland remaining cropland (4.B.1.)	ELUC (other transitions)	n.a.
land converted to cropland (4.B.2.)		
forest land converted to cropland (4.B.2.a)	ELUC (deforestation)	Gross losses (deforestation)
other land uses converted to cropland (4.B.2.b-e)	ELUC (other transitions)	n.a.
grassland remaining grassland (4.C.1.)	ELUC (other transitions)	n.a.
land converted to grassland (4.C.2.)		
forest land converted to grassland (4.C.2.a)	ELUC (deforestation)	Gross losses (deforestation)
other land uses converted to grassland (4.C.2.b-e)	ELUC (other transitions)	n.a.
wetlands remaining wetlands (4.D.1.)	ELUC (other transitions)	n.a.
land converted to wetlands (4.D.2.)		
forest land converted to wetlands (4.D.2.a)	ELUC (deforestation)	Gross losses (deforestation)
other land uses converted to wetlands (4.D.2.b-e)	ELUC (other transitions)	n.a.
settlements remaining settlements (4.E.1.)	ELUC (other transitions)	n.a.
land converted to settlements (4.E.2.)		
forest land converted to settlements (4.E.2.a)	ELUC (deforestation)	Gross losses (deforestation)
other land uses converted to settlements (4.E.2.b-e)	ELUC (other transitions)	n.a.
other land remaining other land (4.F.1.)	ELUC (other transitions)	n.a.
land converted to other land (4.F.2.)		
forest land converted to other land (4.F.2.a)	ELUC (deforestation)	Gross losses (deforestation)
other land uses converted to other land (4.F.2.b-e)	ELUC (other transitions)	n.a.

### 1.3.2. REDD+

Reducing emissions from deforestation and forest degradation in developing countries (REDD+) is a framework established under the UNFCCC for the implementation of activities to reduce GHG emissions from forests. These activities are to be implemented by national governments, at the national level, and in the context of results-based payments. Since the Warsaw Framework for REDD+ was agreed in COP 19, held in 2013 (UNFCCC, 2014), 60 developing countries have submitted at least one REDD+

Forest Reference Level / Forest Reference Emission Level (FRL/FREL) as benchmark for assessing performance in implementing REDD+ activities. To date, the submitted FRL/FRELS collectively cover a forest area of over 1.5 billion ha (over 1/3 of global forest area). The Paris Agreement reemphasizes in its Article 5 the importance of the existing efforts to mitigate climate change through land use activities, including those related to forests and REDD+. REDD+ is therefore a component of the Paris Agreement and REDD+ activities can be included in the NDCs. REDD+ results are submitted as an Annex to the biennial update report (BUR; 19 Parties have submitted REDD+ Annexes to the BUR so far). The BURs, which include the GHG inventory, are the main source of information to the collective view under the Global Stocktake.

Furthermore, REDD+ decisions establish that the data, methodologies and procedures used in FRL/FRELS should be consistent with corresponding anthropogenic forest related GHG emissions by sources and removals by sinks as contained in the national GHG inventory. Although methodologies are often not yet harmonized between REDD+ and GHGi, countries are working towards that objective. Accordingly, REDD+ activities (deforestation, forest degradation, sustainable management of forests and the conservation and enhancement of forest carbon stocks) can be mapped to the IPCC categories (see **Table A.1.1**) and many submissions already adopt a land based approach in their FRL/FRELS that allows an easy mapping between REDD+ FRL/FREL and their NGHGI. The REDD+ Framework, and the REDD+ Readiness investment from multilateral and bilateral arrangements triggered by it, has in fact substantially contributed to building national MRV capacity in developing countries and supporting them in the transition to the more stringent reporting requirements of the Paris Agreement (Federici et al., 2017; Grainger and Kim, 2020). For example, more than half of these countries submitted a FRL/FREL before their first NGHGI in the biennial update report (BUR; 53%) (UNFCCC, 2023b, 2023c). Going through the technical assessment process under the UNFCCC helps to build such MRV capacity and REDD+ submissions are typically more detailed, more complete and more transparent than national communications and even BURs (Grainger and Kim, 2020; Grassi et al., 2022). Accordingly, in their database of LULUCF CO<sub>2</sub> fluxes of countries submissions, Grassi et al. (2022), prioritise the most recent data source but also take into account the completeness of information and select REDD+ as data source in 22 countries because the data was more recent and complete.

### **1.3.3. The IPCC guidelines, methods and variables**

The IPCC provides internationally agreed methodologies for assessing and reporting on GHG emissions and removals. Under the enhanced transparency framework

arrangements, all countries "shall" use the 2006 IPCC Guidelines (IPCC, 2006), complemented by the 2019 refinement (IPCC, 2019), to prepare their NGHGI. This is different from the previous MRV arrangements where developing countries can still select any previous IPCC methodology. The simplest methodological approach to estimating emissions and removals is to combine information on the extent to which a human activity takes place (activity data or AD) with coefficients which quantify the emissions or removals per unit activity (emission/removal factors or EF/RF). For emissions from land use change this is given as:

$$Emissions (tCO_2e yr^{-1}) = AD (ha yr^{-1}) \times EF (tCO_2e ha^{-1})$$

Estimating changes in carbon pools and fluxes depends on national circumstances such as data and model availability, as well as resources and capacity to collect and analyse that information. According to IPCC guidance, moving to higher tiers improves the GHG inventory by reducing the uncertainty of the estimates (IPCC, 2019). Tier 1 methods are designed to be the simplest to use and default values are provided for estimating country-specific carbon stocks using globally available sources. Tier 2 can use the same methodological approach as Tier 1 but country- or regional-specific input data, such as emission factors that are more appropriate for the climatic regions and land-use systems in that country. Higher order methods are used in Tier 3 together with high-resolution data (spatial and temporal) disaggregated at sub-national level. Any model used in Tier 3 needs to be validated and thoroughly documented. These higher order methods provide estimates of greater certainty than lower tiers. However, the complexity of the infrastructure and resources required to conduct the inventories also increases with higher tiers. The 2019 IPCC refinement recognizes the role of remote sensing as a possible source of data in delivering GHG inventories for both the AD and EF components, and has a new section with guidance on the use of biomass density maps for national GHG inventories (IPCC, 2019; Herold et al., 2019).

Following IPCC guidance, two methods can be used to estimate the changes in carbon stock in forest lands remaining forest lands, and forest land conversion to and from other land use categories: *gain-loss* or *stock-difference*. The chosen method and some of the variables used in those methods (**Table 1.2**) determine the requirements in terms of characteristics of the data. The default *gain-loss* method estimates the net balance of additions to and removals from a carbon stock in all land-use categories. For example, changes in biomass carbon stocks on forest land *i* converted to cropland *j* are estimated by the difference between the biomass stocks of the forest type *i* before and immediately after the conversion ( $B_{AFTERi} - B_{BEFOREi}$ , t d.m.  $ha^{-1}yr^{-1}$ ) multiplied by the area change of forest type *i* to crop *j* ( $AD_{ij}$ ,  $ha yr^{-1}$ ; *i* and *j* are country specific strata). The initial change

in biomass stock is increased by the average annual biomass growth ( $\Delta C_G$ ) and decreased by the average annual biomass losses in crop  $j$  ( $\Delta C_L$ , t d.m.ha<sup>-1</sup>yr<sup>-1</sup>) on the land in the year of conversion (t d.m. ha<sup>-1</sup>yr<sup>-1</sup>). The alternative method is *stock-difference*, where carbon stocks are measured at two points in time to assess carbon stock changes (keeping the area of land in that category at times  $t_1$  and  $t_2$  identical). In this method, if using plot data (in t d.m. ha<sup>-1</sup>), the value is then multiplied by the total area within each stratum to obtain the total stock change estimate.

The decision on which approach to use is based on the availability of data, with most GHG inventories submitted to the UNFCCC using the default *gain-loss* approach. When national data is not available, Tier 1 methods are applied and default values are used. For forest land, for example, the IPCC Guidelines provided default values for estimating the variables for the *gain-loss* method using globally available sources, distinguishing climate domain, ecological zone, continent, forest age structure, and for plantation or natural forests. However, for key categories, or categories with significant influence on a country's total inventory of GHG in terms of absolute level, more advanced methods should be chosen (Tier 2, 3).

**Table 1.2** Variables used in the IPCC equations for estimating carbon stock changes in the AFOLU sector (Volume 4, Chapter 3, IPCC 2006). The first five variables correspond to the gain-loss method while the last two are used in the stock-difference method. [table also included in Poulter et al (2023) and in Supplementary information of Hunka et al (2023)]

Variable	Description	Equation from the IPCC 2006 Guidelines
$B_{AFTERi}$	biomass stocks on land type $i$ immediately after the conversion, t d.m. ha <sup>-1</sup>	Equation 2.16
$B_{BEFOREi}$	biomass stocks on land type $i$ before the conversion, t d.m. ha <sup>-1</sup>	Equation 2.16
$AD_{ij}$	area of land remaining in the same land-use category, or area of land use $i$ converted to land-use $j$ in a certain year, ha yr <sup>-1</sup>	Equation 2.9,
$\Delta C_G$	annual increase in carbon stocks in biomass due to growth on land converted to another land-use category or in land remaining in the same land-use category by vegetation type and climatic zone, in t C yr <sup>-1</sup>	Equation 2.7, 2.9
$\Delta C_L$	annual decrease in biomass carbon stocks due to losses from harvesting, fuel wood gathering and disturbances on land converted to other land-use category or in land remaining in the same land-use category, in t C yr <sup>-1</sup>	Equation 2.7, 2.11
$C_{t1}$	carbon stock in the pool at time $t_1$ , t C	Equation 2.5 and 2.8
$C_{t2}$	carbon stock in the pool at time $t_2$ , t C	Equation 2.5 and 2.8

### 1.3.4. Perspectives of tropical countries

When the UNFCCC entered into force in 1994, all the onus was put on developed countries to lead the way to stabilizing GHG concentrations "at a level that would prevent dangerous anthropogenic interference with the climate system". Industrialized countries were the source of most historical and current GHG emissions and, accordingly, were the ones expected to undertake most of the efforts to reduce their emissions to 1990 levels. Existing MRV arrangements under the UNFCCC are more stringent for developed countries, and with such stringency came also a legacy of developed capacity on repeated national forest inventory measurements (NFIs), forest monitoring and MRV

(Nesha et al., 2022). Developing countries were encouraged to start submitting biennial reports only in 2014, and with a lot of flexibility and consideration for their respective capabilities. To date (as of December 2023), from the 155 developing country-Parties to the UNFCCC, 111 (72%) have either never submitted a biennial update report with a GHG inventory to the UNFCCC (n=56 or 36% of total) or have submitted only one report (n=55, 35%) (UNFCCC, 2023b, 2023c). At the same time, developed countries have been following standardized requirements for reporting national inventories annually since 2003 and are in their 5<sup>th</sup> biennial report using the 2006 IPCC guidelines and detailed common reporting format tables.

While behind in MRV capacity, it is clear that a decade after the Warsaw Framework for REDD+ was adopted, and more than a decade of REDD+ momentum and REDD+ readiness investment played a crucial role in MRV and GHGi capacity in tropical countries (Federici et al., 2007; Nesha et al., 2021; FAO, 2022). REDD+ under the UNFCCC anticipated three phases (UNFCCC, 2011): Phase I, or readiness phase, including the development of national strategies or action plans and forest reference levels; Phase II consisting on the implementation of these plans which at this phase could be piloted at a subnational level; and phase III, where results-based actions are implemented and measured, reported and verified (UNFCCC, 2011; 2014). In parallel to, and in support of, the UN negotiations and decisions on REDD+, several multi- and bi-lateral initiatives started mobilizing resources focusing on “readiness activities” (e.g., the World Bank Forest Carbon Partnership Facility (FCPF), and the UN Collaborative Programme UN-REDD) which enhanced MRV capacity. The Green Climate Fund (GCF) launched a pilot programme for results-based payments in 2017, but its envelope was depleted in 2020 (FAO, 2022). The World Bank FCPF’s Carbon Fund and other private jurisdictional REDD+ accounting standards emerged, providing new opportunities for countries engaged in REDD+ activities and seeking results-based payments. Although these standards build on UNFCCC MRV requirements they go beyond the UNFCCC MRV requirements, for example by including additional verification and determining countries’ choices when constructing their reference levels.

With more than a decade of investment in REDD+ readiness and REDD+ MRV capacity, inequity persists. Firstly, countries from the African regional group and the group of least developed countries represent an almost negligible proportion of historical reported results and corresponding payments (FAO, 2022). This means the investment in REDD+ readiness was either lower in these UN groupings or less effective. Secondly, but linked with the lack of effectiveness factor, while financial assistance can help in enhancing capacity, adequate levels of monitoring capacity and data are not achieved immediately (Herold and Skutsch, 2011). It is therefore important to reflect on how the international

community and academia can assist countries that are currently being left behind in the transition to the more stringent reporting requirements of the Paris Agreement. One way of doing so, is by developing research to increase knowledge. National monitoring of land dynamic and associated carbon fluxes is essential to achieve result-based emissions-reduction (e.g., Gibbs et al., 2007; Joseph et al., 2013), as is understanding the drivers and causes of forest and biomass loss through space and time for the development of appropriate mitigation strategies. These complex but fundamental components can potentially benefit from existing capabilities of readily available EO data, methods and products.

## **1.4 Space agencies and the EO community in support of the UNFCCC**

Space agencies and the Earth Observation (EO) community play a crucial role in monitoring the Earth surface and in supporting the UNFCCC. The Paris Agreement, particularly in its Article 7 on adaptation and Article 8 on loss and damage, identifies the need to enhance and strengthen systematic observation, climate services and knowledge sharing and that systematic observation and early warning systems are areas of cooperation and facilitation to enhance understanding, action and support. Satellites collect data on the land surface systematically in space and time, and therefore are also considered fundamental to provide a global overview of land dynamics and associated carbon stocks and fluxes (Baccini et al., 2017; Harris et al., 2021; Chevallier, 2021; Feng et al., 2022). Accordingly, the international EO community monitoring the land surface stepped up in support of the UNFCCC (Hegglin et al., 2022; Byrne et al., 2023) targeting mitigation and the AFOLU sector (Poulter et al., 2023; Ochiai et al., 2023; Chevallier, 2021).

For the processes under the UNFCCC and specifically the operationalization of the Paris Agreement, the availability of land carbon fluxes obtained from satellite data presents opportunities for the enhancement of NDCs, for national reporting under the Enhanced Transparency Framework (ETF, Art 13), for REDD+ (Art 5), and for the Global Stocktake (Art 14) (see blue path in **Figure 1-5** and **Table 2.1** in Chapter 2 to avoid duplication here). By supporting the completeness and timeliness of domestic NGHGI the EO community would contribute to a stronger Global Stocktake, informing policy makers on the effective role of forests and the land use sector in achieving the carbon neutrality objectives of the Paris Agreement. **Figure 1-5** illustrates the wider scope of this thesis identifying the possible ways the EO community can contribute to processes under the UNFCCC, including the Global Stocktake. Because the Global Stocktake process is

Party-driven, it consists mostly of the analysis of the aggregation of country-Parties submissions (blue pathways) complemented with science from the IPCC assessment reports (ARs, brown pathway) and independent contributions (black pathway) (see UNFCCC 2019a, paragraph 37). The EO community can contribute through all these pathways. However, the focus of this thesis (yellow pathway) is on the specificities of the IPCC guidelines and UNFCCC modalities to ingest EO products in national reporting. Exploring if and how these products are ingested in national GHG inventory reporting can help answer the wider questions of this thesis i) why do we get conflicting estimates and ii) how has the EO community contributed to the Global Stocktake.

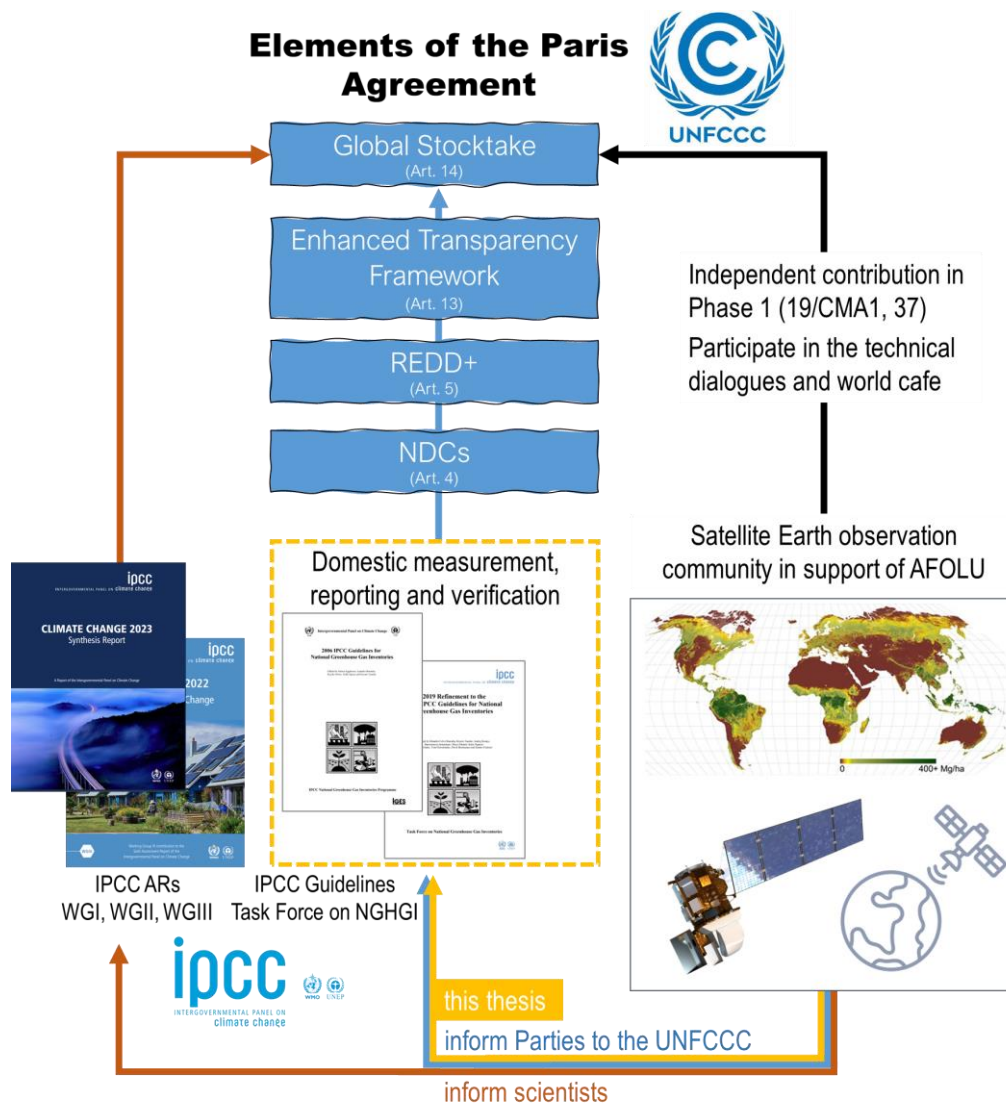


**Figure 1-5** Information flows between key actors contributing to the elements of the Paris Agreement of the UNFCCC and placing this thesis in a wider scope of understanding the contributions from the satellite Earth Observation (EO) community to the UNFCCC and its Global Stocktake. The arrows show possible ways the satellite community can support the implementation of the Paris Agreement. The blue arrows/pathways show possible support through the provision of satellite data and derived EO products to national teams preparing their submissions – nationally determined contributions (NDCs), forest reference levels and REDD+ results under the REDD+ framework, GHG inventories in the biennial transparency reports under the enhanced transparency framework. These three sources of data are then ingested in the Global Stocktake for a collective view. In the blue pathway, to prepare their submissions, national teams follow the methodological guidance developed by the IPCC Task Force on national GHG inventories. The EO community can also contribute to the science included in the IPCC assessment reports (ARs) (brown arrow/pathway), including the synthesis report and the independent reports from the three working groups [continues in next page...]

*(WGI - Physical Science Basis of Climate Change; WGII - Climate Change Impacts, Adaptation and Vulnerability; WGIII with Mitigation of Climate Change) who serve as input to the Global Stocktake (UNFCCC, 2019a). Finally, according to the same decision 19/CMA.1 (UNFCCC, 2019a) the EO community can contribute directly to the Global Stocktake with independent estimates (black arrow/pathway). This thesis focuses on the ways EO products can be used according to the IPCC Guidelines to produce estimates of emissions from deforestation which are used in all country submissions (NDCs, REDD+ and NGHGI).*

The EO community, including through the World Meteorological Organization (WMO), the Committee on Earth Observation Satellites (CEOS), and the Group on Earth Observations (GEO), has ongoing efforts and working groups to facilitate the coordination on data collection and research. For example, the WMO is taking the lead in coordinating an international effort to establish top-down GHG monitoring in support of the implementation of the Paris Agreement. The Global GHG Watch monitoring infrastructure (GGGW) (WMO, 2023) will rely on satellite and surface (airborne and in situ) atmospheric observations and include modelling and data assimilation capabilities in an integrated framework to provide estimates of total net GHG fluxes on a global scale but potentially useful at national scales. The ambition of the GGGW infrastructure includes the support to UNFCCC processes by delivering “actionable information that supports the Paris Agreement Global Stocktake and national government policy objectives” (WMO, 2023) **(Figure 1-5)** Given the complexities of the AFOLU sector, the existing prototypes (Chevallier, 2021; Deng et al., 2022; Byrne et al., 2023) indicate this is still very much an active research area. The estimates are given at a spatial scale that is too coarse, and any comparison attempt with NGHGI is only possible in very large, or aggregated, countries. The uncertainties are also very high. For example, Byrne et al (2023) overestimate CO<sub>2</sub> fluxes for the EU+UK by over a GtCO<sub>2</sub>, and in Chevallier et al (2021), the uncertainties in some countries are more than 4GtCO<sub>2</sub>, which is an order of magnitude close to the fossil fuel emissions of the USA. Because of the issues with the large uncertainty ranges, the conclusion from these studies is that there is no significant difference between NGHGI and inversions.

In parallel, CEOS has recently endorsed a roadmap to provide a framework for long-term (+15 years) coordination of space agencies observing programmes in support of the needs of society for AFOLU-related information, with a particular focus on the needs and ambition cycle of the Global Stocktake (Poulter et al., 2023). The AFOLU EO community does not use atmospheric measurements and inversions, but satellite-based measurements of the land surface and its structure. The large investments made by the space agencies to launch new missions dedicated to measuring land dynamics (e.g., with the continuation of programmes such as Landsat, Sentinel, MODIS), and forest structure and biomass (e.g., GEDI, BIOMASS, NISAR) (Quegan et al., 2019; Dubayah et al., 2020) have the potential to be used for land GHG emissions and removals and improve national measurement, reporting and verification capacity (Nesha et al., 2021).

Accordingly, a CEOS AFOLU roadmap was endorsed by the space agencies' Principals at the CEOS Plenary in November 2023. The roadmap includes a set of recommendations to the space agencies and the EO research community (see **Box 1.2**) and lists the current and planned satellite missions using a combination of sensor types (Ochiai et al., 2023). Among the recommendations, which will develop into specific activities, there is the aim of improving the use of EO data in UNFCCC reporting (recommendation 2). The definition of "data" in the recommendation encompasses datasets or what is defined here in this thesis as EO products. This aim is also emphasized in the CEOS EO handbook, mentioning that "the primary expected outcome of the CEOS AFOLU efforts is an enhanced uptake of EO satellite data sets in support of the Global Stocktake process on a global and country level" (CEOS, 2023).

**Box 1.2** Recommendations provided in the CEOS Roadmap for AFOLU (Poulter et al., 2023) to serve as a guide for active implementation by the CEOS agencies and partners.

Recommendation 0:	Ensure that every country that wishes to has the land satellite data required to report to UNFCCC under IPCC guidance.
Recommendation 1:	Ensure long-term continuity and backward compatibility for missions providing activity data and emission factors.
Recommendation 2:	Improve use of Earth observation data in UNFCCC reporting and IPCC Guidelines.
Recommendation 3:	Recognizing that different countries have various requirements to support their system for reporting, enable dialog between inventory practitioners and CEOS community.
Recommendation 4:	Support efforts to reconcile bottom-up, top-down, and inventory estimates of GHG emissions and removals.
Recommendation 5:	Integration of New Space and commercial partnerships in supporting national GHG inventories.
Recommendation 6:	Ensure consistency of CEOS AFOLU and GHG Roadmaps to support an integrated national GHG inventory system, GHG+.
Recommendation 7:	Development of actions to support the CEOS AFOLU recommendations.

The release of new state-of-the-art EO products at such rapid speed is promising and timely. However, the fact that the existing CO<sub>2</sub> flux estimates diverge in the magnitude (Heinrich et al., 2023a) and their trend (Feng et al., 2022) with the aggregation of NGHGI and the bookkeeping models (Grassi et al 2023), highlights the necessity for clearer definitions, and for map validation and correction. Large biases from map classification errors make the maps inaccurate (Stehman, 2013; McRoberts, 2011; Olofsson et al., 2014). These biases could come, for example, from the lack of backward compatibility which could prevent a consistent time-series. The risk of temporal inconsistencies exists in all EO products, even those from the long-running Landsat programme, because of

sensor degradation or sensor and technology changes between successive missions (Roy et al., 2016; Vogeler et al., 2018). Accordingly, this concern is reflected in the CEOS AFOLU roadmap (**Box 1.2, recommendation 1**), and Achard et al. (2002), Vancutsem et al. (2021), Feng et al. (2022) are a few examples of the use of deforestation maps as hotspots for stratification with the estimates being derived from the stratified sample. The same process for area correction (Olofsson et al., 2014) is recommended in the Global Forest Watch portal, where data from Hansen et al (2013) is available, due to changes in the GFC algorithm (Ceccherini et al., 2021; Palahi et al., 2021). Reflecting on the overarching questions raised in section 1.1, the suggested best practice of correcting the areas derived from maps highlights potential issues of accuracy of the maps or difficulty in the attribution of mapped categories to actual land use or land use changes according to national definitions. Low accuracy and attribution could explain the differences in the global estimates or hinder the uptake of these datasets in UNFCCC processes.

## **1.5. Literature review on EO stakeholders developing global to pantropical EO products for MRV**

The CEOS AFOLU roadmap (Poulter et al., 2023) mentioned in the previous section identifies several global products or maps derived from satellite-data that could potentially provide information compatible with the IPCC variables related to AD and EF/RF described above (section 1.2.3). **Table 2.2** (in Chapter 2 to avoid duplication) lists those products and expands on those identified in the roadmap to include datasets on land cover, fire and biomass with spatial resolutions finer than 1 km and with global to pantropical coverage.

Some of these global maps or products (**Table 2.2**) that provide information on land dynamics (Friedl et al., 2010; Sexton et al., 2013; Hansen et al., 2013; Shimada et al., 2014) biomass distribution (Saatchi et al., 2011; Baccini et al., 2012) and fire disturbances (e.g., MODIS active fire and burned area, (Giglio et al., 2016; Giglio et al., 2018)) have existed for more than 10 years. The research community has had plenty of opportunity to explore their application to estimate CO<sub>2</sub> fluxes from land from national (Tyukavina et al., 2013) to pantropical (Zarin et al., 2016; Achard et al., 2014) or global scales (Harris et al., 2012; Harris et al., 2021; Feng et al., 2022). The methods used to obtain CO<sub>2</sub> flux estimates in these studies are similar to the basic concept in the IPCC Guidelines of multiplying AD and EF/RF, or “stratify and multiply” to obtain more adequate AD and EF/RFs according to the chosen stratification and land definitions. In more recent years there has been an explosion in the number of maps being released, likely due to the greater availability of satellite data from different sensor types, for land

cover and land cover change (Zanaga et al., 2021; Karra et al., 2021; Arevalo et al., 2022) and biomass (Santoro et al., 2021; Baccini et al., 2021; Duncanson et al., 2022; Dubayah et al., 2022; Simard et al., 2019). However, the main questions raised in this thesis remain – in which way have these EO products, widely explored by the research community, contributed to inform the UNFCCC, including through country uptake? The following subsections reflect on how the scientific community has been contributing with EO products that could be used for activity data (AD; section 1.5.1), emission/removal factors (EF/RF, section 1.5.2) or the combination of both to derive carbon fluxes from land use (section 1.5.3).

### **1.5.1. EO for monitoring forest land and changes in forest area**

The use of satellite data and remote sensing for forest cover and forest/non-forest mapping is well advanced. Methodologies using multispectral Landsat Thematic Mapper (TM) data are considered core for this purpose due to the available time-series and long-term continuity of the programme (TM since 1984), its spatial resolution (30-m), and demonstrated applicability in tropical forest mapping contexts (e.g., reviewed in Gomez et al., 2016). The 10-m resolution Satellite Pour l'Observation de la Terre (SPOT) missions have also been orbiting the Earth for over 30 years providing optical data used in cartography, land classification and change detection (e.g., Kanellopoulos et al., 1992). The more recently launched Sentinel-2 providing free, full and open data access to high resolution optical imagery and continuity of SPOT and Landsat missions is equally promising (Drusch et al., 2012). Also sensitive to vegetation structure and applicable for stand-alone forest cover mapping are: the optical Moderate Resolution Imaging Spectroradiometer (MODIS) (e.g., Friedl et al., 2002, 2010) and the Advanced Very High Resolution Radiometer (AVHRR) (e.g., DeFries and Townshend, 1994; Gopal et al., 1999) at coarser resolution, and the very high resolution optical RapidEye, and microwave sensors such as ALOS PALSAR (Advanced Land Observing Satellite Phased Array type L-band Synthetic Aperture Radar) (Shimada et al., 2014; Shiraishi et al., 2014) and Sentinel-1 (Torres et al., 2012). Furthermore, methodologies incorporating different data sources (e.g., optical and microwave sensors) have increased potential (De Alban et al., 2018; Sirro et al., 2018) when the use of optical data alone is less suitable, e.g. due to permanent cloud cover (Rignot et al., 1997).

For forest cover mapping, several single date wall-to-wall land cover maps were produced based on different data sources and methods through national or international initiatives worldwide. Some of the global land cover maps composites are even available periodically, although they are usually too coarse and have low local accuracy to be useful for national land monitoring, reporting and planning (Alfieri et al., 2007; Herold et

al., 2008; Fritz et al., 2010). Some examples are the International Geosphere-Biosphere Programme DISCover (IGBP DISC), the University of Maryland (UMD) global land cover classification, MODIS land cover, and the Global Land Cover Map (GLC-2000), ranging from 300-m to 1-km spatial resolution. At finer resolution, although not available for tropical regions there is CORINE Land Cover 2000 (CLC) in Europe based on Landsat data. The Food and Agriculture Organization of the United Nations (FAO), which is the standard reference for global scale forest resource information usually based on national statistics and tabular data, developed a Global Forest Resources Assessment (FRA) Remote Sensing Survey (FAO & JRC, 2012; Keenan et al., 2015) in partnership with the European Commission Joint Research Centre (JRC) and using for the first time a systematic sample of Landsat satellite imagery and remote sensing techniques to calculate and report global forest land-use and change rates (deforestation and afforestation) for 1990, 2000, 2005, 2010, and 2015 (Keenan et al., 2015). This work was based in sampling methods and aggregated estimates without providing spatially explicit information. It can, therefore, be considered less practical for spatial planning of mitigation activities.

The monitoring of forest loss and disturbances, although with considerable uncertainty and varying estimates, is equally well documented, with several studies demonstrating a variety of robust methods using particularly optical data, but also Synthetic Aperture Radar (SAR) data to map clear cut and fire in tropical regions (e.g., van der Werf et al. (2010); Walker et al. (2010)). Fusing and integration of optical and radar data has also been considered a promising alternative (reviewed in Joshi et al., 2016). In more recent years, and to overcome the knowledge gap on global forest trends and particularly forest lost in the tropics, available global datasets of tree cover and tree cover loss (Hansen et al., 2013; Sexton et al., 2013; Vancutsem et al., 2021) and periodic forest and non-forest (F/NF) cover maps (Shimada et al., 2014) based on automated classification algorithms of Landsat and ALOS PALSAR imagery were developed and are now freely available covering all tropical nations. Furthermore, such automatic systems are continuously updated and made freely available in Google Earth Engine or other web-mapping tools such as the Global Forest Watch (GFW), or the JRC Tropical Moist Forest (TMF) Explorer.

Three of these initiatives - the Global Forest Change (GFC) dataset, the Global Land Cover Facility tree cover dataset (Sexton et al., 2013) and the Japan Aerospace Exploration Agency (JAXA) forest/non-forest maps (Shimada et al., 2014) - are worth discussing in more detail because they are more complete in the extent covered (compared to the TMF dataset covering only moist forests), they are of finer spatial resolution (in contrast to the previous generation of coarser resolution IGBP DISC,

MODIS land cover, and GLC-2000), and have shown some continuity in their updates. They are therefore hypothetically more useful for national forest monitoring systems and for MRV.

Worldwide coverage of Landsat sensor data was used by Hansen et al (2013) from the University of Maryland to develop a Global Forest Change (GFC) dataset mapping global forest cover extent and forest change between 2000 and 2012. This dataset is being updated in terms of algorithmic improvements and extending the time series – currently covering the period 2000-2023 available for download in the GFW platform. With a spatial resolution of 30-m this product is globally consistent and potentially locally and regionally relevant (McRoberts et al., 2016). The dataset includes a global tree cover extent map from 2000 and a map identifying the year when removal of all tree cover was observed (Hansen et al., 2013; 2014). The global dataset is divided into 10x10 degree tiles and users can easily download the tiles corresponding to their area of interest. An advantage of this EO product is that continuity of this appears to be secured, with constant updates made available in the GFW web platform. It has been widely used by researchers from many different fields and for a variety of applications through their integration with other datasets. For example, with forest types as in Johnson (2015); or protected areas as in Spracklen et al. (2015) and Lui and Coomes (2016); or to estimate carbon fluxes from forest dynamics in Harris et al. (2021). However, because it is described as a “forest change” dataset, misconceptions about some definitions and methods employed in the creation of the product may lead to its inappropriate use or interpretation (Tropek et al., 2014; Hansen et al., 2014). Namely, the specific definition of forests used, as all vegetation taller than 5-m in height (supplementary information in Hansen et al., 2013), renders some limitations such as failing in distinguishing between natural forests and plantations (Lui and Coomes, 2015; Zarin et al., 2016). Other misconceptions can apply in the use of the “loss” and “gain” datasets. The mapping process is entirely signal-driven and forest loss represents a complete removal of tree cover (~0% crown cover), which depending on the percentage cover threshold defined by the end user can determine an under estimation of converted areas. Also, although this dataset includes a map of forest gain in the period 2000-2012, the “gain” only includes densities of >50% tree cover of areas originally mapped as non-forest, and the year of that “gain” is not identified which may cause some confusion when analysing the dynamics of loss and gain in a same area and in estimating net emissions. Moreover, by using images from the growing season some confusion with herbaceous vegetation occurs, especially considering the optical data sensitivity to foliage cover (e.g., Lui and Coomes, 2015). Some consideration should also be given to the potential issues arising from the Landsat 7 slc off and consequent “banding effects”, which can cause artefacts

and consequently an incorrect interpretation of the product. And finally, more specifically for the dry forests and woodlands of Africa, it is considered particularly difficult to correctly extract tree cover percentages for low tree cover densities of 10-30% which can lead to its inaccuracy (Achard et al., 2014; Bastin et al., 2017).

Existing studies analysed the agreement among GFC and locally produced maps and estimates of forest loss (e.g., Lui and Coomes, 2015; Richards and VanWey, 2016; Sannier et al., 2016; Mermoz and Toan, 2016; Zarin et al., 2016; Bastin et al., 2017). For example, at a global level Bastin et al. (2017) indicate an underestimation of dry forests by the GFC when comparing GFC to their forest map based on a reference sample. Mermoz and Toan (2016) in their study over Vietnam, Cambodia and Lao (together covering a total area of approximately 750,000 km<sup>2</sup>) reported a consistent overestimation of forest loss from the GFC dataset in all three countries when compared to their map of forest loss derived from ALOS PALSAR data. Consistently, Zarin et al. (2016) in their pan-tropical study of GHG emissions from deforestation reported a significant reduction of the estimated forest loss in the Democratic Republic of Congo and Malaysia after plantations were excluded from the UMD GFC dataset (from 0.581 to 0.110 and 0.387 to 0.162 Mha yr<sup>-1</sup>, respectively). Two other studies had a focus in the forest-savanna transitions of West Africa. Lui and Coomes (2015) in a study over a region of Sierra Leone (West Africa) which included the Gola Rainforest National Park (covering an area of 710 km<sup>2</sup>) showed that three different EO products, i) one using a traditional pixel-based supervised land classification technique using Landsat imagery, ii) the forest cover and forest cover change maps obtained with the Carnegie Landsat Analysis System lite (CLASlite) software package, and iii) the UMD GFC dataset, all generated maps with high overall accuracy (using high-resolution imagery and photo interpretation to generate truth data). Of the three maps, the CLASlite was the more accurate and analytically capable of both mapping deforestation and distinguishing natural forests and plantation stands. However, the authors also report a significant underestimation of forest loss from both the CLASlite and the GFC maps when compared to the supervised classification, and showing deforestation rates close to zero. The underestimation of forest loss by this product was also documented in the studies of Tropek et al. (2014) at global level and Milodowski et al. (2017) in the Amazon. Sannier et al. (2016) in their study in Gabon (267,667 km<sup>2</sup>) also report comparable overall accuracies for all forest cover maps but highlight that overall accuracy can be misleading by itself, and that the GFC dataset should be calibrated at national and more local level if it is to offer an alternative to national wall-to-wall forest maps. The authors identify an overestimation of tree cover and consequently forest area, a tendency for overestimation of deforestation, and an underestimation of regeneration or “gain” with consequences for net change estimates

as the main limitations of the product. One should also note that in the case of Gabon, very few changes occurred during the period analysed by this study, with close to zero net changes. In conclusion, the findings from the existing studies using GFC at national levels are conflicting, i.e. the underestimation of forest loss in Lui and Coomes (2015), Tropek et al. (2014) and Milodowski et al. (2017) is contrasting to the overestimation of forest loss in the Mermoz & Toan (2016), Zarin et al (2016) and Sannier et al. (2016) studies. All studies highlight issues of accuracy, which underlines the need for further studies at national scales to increase confidence in the use of such product for reporting in the land use sector.

The Global Land Cover Facility (GLCF), also in the University of Maryland Department of Geographical Sciences, published on the same year another global dataset of tree cover at 30-m resolution described by Sexton et al. (2013). The final product is also a tree cover global map but, differently from GFC, this dataset uses the 250-m MODIS VCF rescaled to 30-m resolution using Landsat data. Additionally, contrarily to the GFC that used a single tree cover map for a reference year and through spectral metrics detected changes in the study interval based only on this reference map, this product includes a tree cover layer for 2000, 2005, 2010 and 2015. Landsat scenes acquisition dates varied greatly (between October 1999 and April 2002 for the 2000 product, between November 2005 and December 2006 for the 2005 product, and between October 2009 and November 2010 for the 2010 product) but largely correspond to the dry season in West Africa, making it hard to compare to GFC map based on imagery from the growing season in the region. Bastin et al. (2017) compared the area of forest obtained from Sexton et al (2013) and Hansen et al (2013) with their estimates from a reference data of 210,000 sample units and concluded both maps underestimated the area of dry forests, in particular Sexton et al. (2013). Seasonality of imagery acquisition date could be a possible explanation for underestimation in Sexton et al. (2013) compared to Hansen et al. (2013) although further studies comparing the two products are needed to derive a conclusion. Seasonality causing under- or over-estimation can also have an impact on the suitability of these products for national reporting following IPCC guidelines and the IPCC good practice of neither over- nor under-estimate emissions.

Global mosaics between 2007 and 2010 with a spatial resolution of 25-m from the Japan Aerospace Exploration Agency (JAXA) Advanced Land Observing Satellite (ALOS) Phased Array L-band Synthetic Aperture Radar (PALSAR) were used by Shimada et al. (2014) to produce annual Forest/Non-Forest maps. This mission collected two cloud-free global coverages per annum producing an archive that until then only existed for coarse-resolution sensors. Although the mission ended, ALOS-2 PALSAR-2 was launched in

2014 and is providing continuity to this product (Rosenqvist et al., 2014), with new annual composites for 2015-2022 being available. The Forest/Non-Forest product uses the lower levels of L-band backscatter as a threshold for mapping the transition of forest to non-forest, with forests being defined as areas of woody vegetation above 10% tree cover. While the University of Maryland products require a cloud screening and a stack of layers to create a per-pixel set of cloud-free observations, SAR penetrates through clouds (a unique ability when compared to optical and LiDAR data) and therefore does not require multiple acquisitions and repeat mapping. However, potential limitations of the product should be considered when interpreting results. According to the authors, forests and woodlands at the lower threshold might be missed in the classification due to the still too coarse resolution of PALSAR for such detailed mapping (Shimada et al., 2014). Studies evaluating the relationship between ALOS PALSAR L-Band Backscatter and AGB reported that the signal saturation is influenced by the sensitivity to surface moisture conditions (Lucas et al., 2010). Also, contrarily to Hansen et al. (2013) who used a single tree cover map for a reference year and through spectral metrics detected changes in the study interval based only on this reference map, the JAXA product includes independent F/NF annual maps that do not necessarily ensure consistency in the observed transitions, although they can be subsequently combined by the user to identify changes. More studies are needed at local scale to understand the accuracy of this product given the signal saturation and influence of surface moisture.

The use of global datasets such as these examples mentioned above opens a possibility for developing countries, in particular countries with low capacity and insufficient support (such as finance from REDD+ readiness), to quickly produce estimates of forest loss, and potentially use them for a critical analysis on the spatial patterns of deforestation and associated drivers. Additionally, the continuous global monitoring of land use processes is only expected to expand in the future, with initiatives such as the opening up of the Landsat archives to the public and the continuation of the programme, the start of the Sentinel family of missions from the European Space Agency (ESA) with an open data policy, and the availability of powerful cloud-based geospatial storage and processing platforms such as Google Earth Engine. However, the wider availability of data does not guarantee by itself a higher uptake by national teams in their reporting (Ochieng et al., 2016). Ochieng et al., (2016) identify a high acquisition of remote sensing data but low use in reporting to the UN-REDD programme from FAO, while Nesha et al. (2021) concluded that in more recent years, remote sensing and forest monitoring capacity of developing countries have increased significantly in reporting to the FAO FRA. However, there are no studies on the uptake of EO products derived from EO data by national teams in official reporting to the UNFCCC.

### 1.5.2. EO for biomass

As a global store of carbon, particularly in tropical forest ecosystems, above-ground biomass (AGB) has a stabilizing effect on the Earth's climate system (Pan et al., 2011; Friedlingstein et al., 2023). Therefore, understanding its dynamics and climatic feedbacks is essential. In the context of REDD+ and for reporting carbon fluxes from the land use sector, countries must quantify and map the carbon content, losses and gains in their forests, both for producing a benchmark and historical reference, and to quantify the impact of REDD+ interventions or NDCs. Essentially, the information on land dynamics discussed above (section 1.5.1.) needs to be combined with information on carbon stocks and biomass changes to quantify fluxes of carbon to and from the atmosphere. Methods to determine AGB include direct measurement through forest inventories and allometry (Tomppo et al., 2010), and estimation of AGB from EO instruments sensitive to AGB content (Houghton et al., 2001; McRoberts et al., 2010). However, although this is a controversial subject, many authors argue that mapping AGB over large areas without the support of EO data is insufficient (Goetz et al., 2009), and highlight the risk of assigning an average carbon stock to an entire area or even to forest strata that do not capture the large inter-variability in carbon content of the forest (e.g., Houghton et al., 2012).

Different methods have been explored to estimate AGB directly through a combination of EO data calibrated with field AGB measurements (e.g., Mitchard et al., 2011; Saatchi et al., 2011; Ryan et al., 2012; Baccini et al., 2012; Asner, 2009; Asner et al., 2014; Baccini et al., 2021; Duncanson et al., 2022; Dubayah et al., 2022; Simard et al., 2019), including approaches for biomass retrieval algorithms using optical, light detection and ranging (LiDAR) and/or Synthetic Aperture Radar (SAR) data either as primary inputs or as auxiliary datasets. Optical EO data are often used to investigate forest structure, cover, and processes through vegetation indices and spectral signatures (e.g., the spectral mixture analysis CLASlite method described in Asner et al., 2009), and have even been shown to have some capability to spatialize field measurements and produce estimates of biomass (Foody et al., 2003; Foody et al., 2001; Baccini et al., 2004; Avitabile et al., 2012). However, these data are spectrally more sensitive to leaves than wood and offer great limitations for direct biomass retrieval (e.g., saturation, limited transferability). They are therefore rarely used for this purpose unless complemented by additional data (e.g., Saatchi et al., 2011).

Active sensors such as LiDAR can penetrate the canopy of trees and measure the signal reflected either from the ground or top canopy, which is useful to have an estimate of canopy height, a biophysical indicator strongly linked to AGB (e.g., Lefsky et al., 1999).

LiDAR spaceborne systems such as the Geoscience Laser Altimeter System (GLAS) with 70-m footprints available throughout the globe have the potential to measure large areas if upscaled, but have limitations for biomass estimation as the instrument was design to measure ice-sheet and was not optimized for vegetation. Furthermore, it is more suitable for estimating height and not biomass directly; its measurements are sparse and require interpolation to obtain full coverage of a given area, with higher associated uncertainty, and are sensitive to topography. Airborne systems though have proven ability to more precisely estimate AGB (Zhao et al., 2009) but are very expensive to use in large areas (Mascaro et al., 2014). Nevertheless, such capabilities led to the planning and development of the Global Ecosystems Dynamics Investigation Lidar (GEDI) from the National Aeronautics and Space Administration (NASA) launched in 2018 to collect high-resolution observations of the vertical structure of tropical and temperate forests used to predict AGB at fine spatial resolution (Dubayah et al., 2020). Two products were released recently, one provided at 25-m footprint-level samples of waveform lidar over the globe up to  $\pm 51.6^\circ$  latitude and publicly available as Level 4A (L4A) product (Duncanson et al., 2022); and a gridded product at 1-km spatial resolution and publicly available as Level 4B (L4B) product (Dubayah et al., 2022; Healey et al., 2022). The application of these datasets leveraging millions of satellite observations over small areas is very promising to improve NFIs, but due to their very recent release few studies and no guidance with practical demonstration of their use is available for countries. Furthermore, the existing studies at national levels warn the users to the fact that L4A model-building data may not reflect local conditions if local data is not used to calibrate the model (e.g., Bullock et al., 2023).

SAR transmits a microwave signal and measures the reflected backscatter intensity which is related with AGB (e.g., Toan et al., 1992; Kasischke et al., 1997; Englhart et al., 2011; Sinha et al., 2015). Its capabilities in tropical regions (in cases of cloud cover and haze) and the different sensitivity to vegetation structure, including AGB, depending on the length of the transmitted wavelength (X, C, L and P bands) or operating mode (e.g., polarization, interferometry) is an advantage of these data. However, SAR also shows some disadvantages in terms of uncertainties in the estimates, particularly in moist tropical forests where the backscattered intensity is less sensitive to the high levels of AGB. Nevertheless, reported saturation levels vary considerably depending on the wavelength used (e.g. co- vs. cross-polarization), and vegetation type. For example, in dry tropical forests and savanna ecosystems, saturation (L-band HV backscatter) has been reported to occur at higher AGB values of around 150-200 t ha<sup>-1</sup> (Collins et al., 2009; Mitchard et al., 2009). Other related limitation is the sensitivity to vegetation water content and surface moisture conditions influencing the capacity to retrieve AGB (Lucas

et al., 2010; Carreiras et al., 2012). Finally, it is also worth noting that SAR requires an advanced degree of technical expertise for data processing, making it less attractive for developing countries when considering alternatives for the development and operationalization of their monitoring systems (Reiche et al., 2016). The European Space Agency (ESA) Climate Change Initiative (CCI) biomass map (Santoro et al., 2021) is an example of the use of satellite radar sensors, specifically SAR data from Sentinel-1 satellites and other international SAR missions such as the Japanese ALOS PALSAR, to generate a global, spatially explicit forest AGB dataset at a spatial resolution of 1-ha.

The capabilities offered by these different data sources and methods described above to derive AGB estimates have been explored at different scales. For example, maps using EO data have been developed at national level in tropical countries either using primarily optical data (e.g., Avitabile et al., 2012), LiDAR (Asner et al., 2014), or SAR (Carreiras et al., 2012; Avtar et al., 2013; Cartus et al., 2014; Mermoz et al., 2014). Part of these national studies (Avitabile et al., 2012; Carreiras et al., 2012; Mermoz et al., 2014) and other studies at sub-national levels (e.g., Mitchard et al., 2009; Ryan et al., 2012; Carreiras et al., 2013) had a particular focus on sub-Saharan Africa and its tropical dry forests. However, only a few large-scale maps of biomass have been published so far (e.g., Saatchi et al., 2011; Baccini et al., 2012; Santoro et al., 2021; Duncanson et al., 2022; Dubayah et al., 2022; see **Table 2.2** to avoid duplication here).

Two freely available pantropical maps at grid scales of 1 km (Saatchi et al., 2011) and 500 m (Baccini et al., 2012) have been available for over a decade. These two maps used similar GLAS LiDAR data sources but are based on different ground data for calibration and different MODIS layers and spatial modelling methodologies (Maxent and Random Forests, respectively) for upscaling. Their reference year is 2000 and 2007-2008 for Saatchi et al. (2011) and Baccini et al. (2012) respectively. Saatchi et al. (2011) also produced a map with a per pixel error estimate. This approach of combining remote sensing and field data was considered a milestone (Morton, 2016) and several subsequent studies explored their application for estimating carbon fluxes. For example, Langner et al. (2014) combined the two maps to produce AGB values per eco-zones as an alternative to IPCC Tier 1 values. Mitchard et al. (2013) compared the two already existing pantropical maps, founding overall agreement and lower uncertainties when data is aggregated at larger scales, but significant differences otherwise. Some other studies concluded the same at the regional and local scales, using independent data to further assess the precision of those maps (e.g., Hill et al., 2013; Mitchard et al., 2014), recommending better uncertainty assessments. Others proposed fusion and calibration methods to correct for spatial bias (Langner et al., 2015; Avitabile et al., 2016). However, more important than identifying agreement and disagreement, and harmonizing

methods, is understanding their cause and spatial pattern, and the accuracy (i.e. agreement with the truth) of those products rather than their precision (i.e. good agreement), to ultimately understand their usefulness for reporting and decision making at national to sub-national level (Araza et al., 2022). Furthermore, it is unclear how extensively these maps have in fact been used in national reporting in support of country MRV.

### **1.5.3. Combining EO derived products to estimate land carbon fluxes**

Ultimately, what we want in the context of the UNFCCC and in applying the IPCC guidance, is to derive estimates of carbon fluxes from land and land use changes. Following on the description of existing products and their capabilities for land use change assessments and AGB content, EO global datasets, and in particular readily available automatic products, are a potentially interesting alternative to derive these estimates of carbon fluxes at very low cost. This can be especially true given the frequently limited capacity of developing countries to timely produce their own complex datasets and maintain operational forest monitoring systems (Romijn et al., 2015; Goetz et al., 2015; Nisha et al., 2021).

There are examples of studies developing estimates of emissions from tropical deforestation using a combination of different EO data and several EO techniques (e.g., DeFries et al. (2002); Pan et al. (2011); Ryan et al. (2012); Baccini et al. (2012); Tyukavina et al. (2013); Harris et al. (2012); Achard et al. (2014); Tyukavina et al. (2015); Mermoz and Toan (2016); Zarin et al. (2016); McNicol et al., 2018). At the pan-tropical level (Pan et al., 2011; Baccini et al., 2012; Harris et al., 2012; Achard et al., 2014; Tyukavina et al., 2015; Zarin et al., 2016), the derived biomass loss estimates for the decade of 2000 vary considerably (0.81 to 2.9 Pg yr<sup>-1</sup>) and the reasons for the major differences between emissions reported in these studies range from the type of data used (EO data, forest inventory, or tabular reference data), the analytical approach (e.g., bookkeeping, sampling, wall to wall), and forest loss definition (net vs. gross emissions).

From the pan-tropical emission baseline studies, the most recent ones (Harris et al., 2012; Achard et al., 2014; Tyukavina et al., 2015; Zarin et al., 2016; Harris et al., 2021; Feng et al., 2022) all use at least one of the EO products described above either directly or with some form of modification. Focusing on REDD+ needs and requirements and highlighting the unreliability of FAO data and the many assumptions inherent to bookkeeping models, Harris et al (2012) match areas of forest loss (Hansen et al. 2010; AD) with pre-deforestation carbon stocks (Saatchi et al 2011; EF) to quantify gross carbon emissions from deforestation in tropical regions. Achard et al. (2014) used a

systematic sampling approach of Landsat-TM imagery to map forest area changes and estimate emissions between 1990 and 2010 with small statistical standard errors (due to large sample size). The author used average biomass density values from Saatchi et al (2011) and Baccini et al (2012) within the sampled units as sources of carbon data (EF). Gross emissions averaged by continent were obtained by combining the two factors. Tyukavina et al (2015) used a 'stratify and multiply' approach where GLAS footprints from Baccini et al. (2012) were used directly to derive a mean carbon density estimate for each pre-deforestation forest stratum (stratification was based on Landsat-derived structural characteristics). Using the GLAS footprints as EFs rather than relating forest loss to the coarser biomass map, which may include mixed pixels, was deemed by the authors as more appropriate, particularly when considering spatially heterogeneous regions. For AD, the authors use the GFC forest cover loss dataset (Hansen et al., 2013) following a probability sampling approach for classification error adjustment. Zarin et al. (2016) established a 2001–2013 benchmark for annual carbon emissions from gross tropical deforestation by also compiling and modifying or expanding on some of the datasets described in the previous sections. More specifically, the GFC dataset (Hansen et al., 2013) was modified to correct for some of the confusion between natural forests and plantations and used as AD, while the Baccini et al. (2012) methodology was expanded to include additional GLAS footprints and correlate those with additional RS and biophysical variables to map AGB density at 30-m, which was then used as the EFs. The baseline estimate of carbon emissions from the AGB pool for the reference period 2001-2013 was subsequently calculated through the combination of these two products. At a regional level, Mermoz and Toan (2016) developed an algorithm based on ALOS PALSAR data to map and quantify disturbances in Cambodia, Vietnam and Lao, and assessed the associated emissions aggregated by ecological zones by combining their map of change (AD) with the AGB values of Saatchi et al. (2011) and Baccini et al. (2012) at the pixel level (EF). Finally, at global level, Harris et al. (2021) used the GFC dataset of tree cover change, fires data from MODIS burned area product and information of the post deforestation land use from Curtis et al (2018), combined with geospatial data (e.g., removal factors for naturally regenerating forests from Cook-Patton et al 2020) and IPCC Tier 1 default values (IPCC 2019). The more recent study from Feng et al. (2022) also extensively used the GFC product and document a significant increase in carbon loss from forest conversion in the tropics during the early twenty-first century.

All these studies based on EO products at larger scales (global or pantropical) converge in their conclusion that there has been a significant increase in carbon emissions from deforestation in the tropics during the early twenty-first century. As discussed in section 1.1, this collective agreement from the EO community at large scale is contradictory to

the stable trend or slight decline in emissions from deforestation as reported in the GHG inventories of developing countries (Grassi et al., 2022; **Figure 1-6**), the Global Carbon Budget (Friedlingstein et al., 2023) and the synthesis reports used in the UNFCCC Global Stocktake (UNFCCC, 2019a). The conclusions are also more divergent at the local and national levels, as discussed in section 1.5.1.

#### **1.5.4. The uptake of EO products in national reporting**

The previous sections discussed the different studies using different approaches to develop baselines of carbon emissions and describing methodologies for matching carbon density to the area of deforestation. I showed that existing EO products to measure carbon fluxes from land at relatively high resolution are becoming widely popular. These research efforts from the EO community to produce data and explore their capabilities can therefore contribute to enhance forest monitoring capacity (Romijn et al., 2015; Nisha et al., 2021), promote consistency and transparency across regions and contribute to tracking global progress on reducing GHG emissions in a transparent way. However, there is i) a large variation between the estimates at pan tropical level both on biomass distribution (Hunka et al., 2023) and land cover mapping (Herold et al., 2008), ii) a divergent trend between EO global estimates and the Global Stocktake, and iii) many studies warn of the dangers of over- and underestimation when using EO products at national levels. Therefore, the operational usefulness or accuracy for application of EO products at national scales needs to be further explored if these EO products are to be considered in the context of supporting processes under the UNFCCC. Nisha et al (2021) and Romijn et al (2015) assessed the forest monitoring capacity using EO data for reporting to the FAO, not the UNFCCC, and Ochieng et al. (2016) assessed MRV capacity but using country reports to the UN-REDD+ programme from FAO, not the UNFCCC. Therefore, to my knowledge, at the time of developing the research in this thesis, there has been no systematic review of the uptake of EO products in national reporting to the UNFCCC nor an explanation of the technical factors hindering their uptake.

As discussed above, the UNFCCC REDD+ framework had an important role in developing the MRV capacity in developing countries (Federici et al., 2017; Nisha et al., 2021). We now count on more than 15 years of REDD+ readiness investments, namely investments in forest monitoring and MRV using satellite data and remote sensing techniques such as those discussed above (Gibbs et al., 2007, Gibbs and Herold, 2007; Goetz et al., 2015). Since the start of the negotiations on REDD+, the EO community has been arguing that methods and data are available for immediate use (Herold and Johns, 2007; Gibbs et al., 2007; Gibbs and Herold, 2007; Achard and House, 2015; Bucki

et al., 2012). If not at national levels, at least to be used in priority areas at subnational levels where measurements can be more rigorous and independently verified (Herold and Skutsch, 2011). The same discourse continues to date with the space agencies at the higher level expressing the readiness to contribute to UNFCCC processes (Ochiai et al., 2023; Poulter et al., 2023).

Some studies reflect on the lessons learned from the more than 15 years of investment in REDD+ readiness and highlight the challenges faced by developing countries in effectively implementing REDD+ (Joseph et al., 2013; Ochieng et al., 2016). For example, Ochieng et al. (2016) added an institutional dimension in the assessment of MRV capacity by analysing 'ownership of technical methods', 'administrative capacity' and 'good governance'. The findings underscore the importance of addressing governance issues, capacity building, and stakeholder engagement for a successful MRV. The authors argue that countries have high ownership of EO data and methods for reporting Activity Data (consistent with findings from Romijn et al., 2015 and Nesha et al., 2021) but do not have MRV systems in place due to low administrative and low levels of good governance. However, a question arises from the conclusion of this study regarding the link between data acquisition (the indicator used by the authors to score countries' technical ownership) and the use of EO data in reporting. The fact that countries acquired data due to REDD+ readiness support from international agencies but then did not use it in reporting may not necessarily be linked to administrative and good governance issues. As De Sy et al (2012) point out, it is not enough to assume that just because EO data is available, it is useful for developing countries. There are constraints in the operational usefulness of the data, for example those linked to lack of consistency or continuous coverage or the use of appropriate methodologies or classification protocols for data interpretation depending on the national circumstances (De Sy et al., 2012; DeFries et al., 2007). This thesis focuses on these technical capabilities or limitations of using readily available EO products because focusing on administrative and governance issues, although important, can hide or dismiss existing problems in the EO products. The contrasting trend of emissions from deforestation between global EO-based studies and aggregation of country reporting to the UNFCCC (e.g., Feng et al., 2022 vs. Grassi et al 2022; **Figure 1-4**; section 1.5.3), the difficulty in comparing different land cover maps, understanding their utility and the knowledge that they have limited ability to discriminate some classes (Herold et al., 2008; Bastin et al., 2017) further suggests that mapping land use and land use change following IPCC guidance with EO products is not trivial. Effective MRV needs institutional arrangements and ownership of data at the national level by sovereign governments (Ochieng et al, 2016; Ochieng et al, 2018). This is not something the EO community can directly interfere

with but rather support through the provision of essential data to inform policy decisions and strategies (Herold et al., 2019). The onus is on the EO community to exercise scientific humility and question the data that is being provided. Because there is a possibility that the EO community may not fully understand the requirements of national teams reporting to the UNFCCC and that the way EO products are handled and present can be improved to better fit the national and international requirements for MRV and support the transparency framework of the Paris Agreement.

## 1.6 Thesis aims and objectives

This section summarizes the research gaps identified in the literature review (**Box 1.3**) and provides a concise list of the research questions which the thesis will address. It is followed by section 1.7 showing the workflow and how the different chapters are addressing these research questions.

### **Box 1.3** Summary research gaps from the literature review

- Forests and land use (LULUCF) have an important role to play in climate change mitigation but the CO<sub>2</sub> fluxes from the sector are complex to measure and the contrasting trend from global EO carbon flux estimates creates confusion to policy makers, and can hinder action and uptake of EO products.
- EO products are assumed to be highly relevant for MRV under the UNFCCC and for the Global Stocktake but so far there has been no systematic review of the uptake of EO products in national reporting to the UNFCCC nor an explanation of the technical factors hindering or facilitating their uptake.
- There is a scarcity of studies solely combining EO products for both land dynamics and biomass.
- Studies analysing the agreement between EO products and *in situ* data at national scales emphasise issues of under- or over-estimation of the EO products.
- Existing EO products show large variation between the estimates at pan tropical level both on biomass distribution and land cover mapping but the causes of such disagreements are poorly studied.
- High ownership of EO data is not the same thing as using it in MRV. Focusing on lack of governance and capacity gaps can hide problems inherent to the way the EO products are being handled and presented to national teams.
- The accuracy of existing EO products at national scales and the causes of errors remains largely unknown.
- There are no examples on if and how the estimates can be improved with the combination of existing EO products.

The overarching aim of this thesis is to explore how the capabilities offered by the fast-growing availability of global maps and products derived from satellite data to measure land use, fire, and tree above-ground biomass (referred to as “EO products” throughout this thesis) are and could be harnessed by the developing world to quantify and report

land use dynamics and fluxes to the UNFCCC. By supporting the completeness and timeliness of domestic NGHGI the EO community would contribute to a stronger Global Stocktake, informing policy makers on the effective role of forests and the land use sector in achieving the carbon neutrality objectives of the Paris Agreement. The research questions raised in this thesis aim to inform two main actors: i) the national teams reporting to the UNFCCC and the policy makers using their GHG inventories to make decisions on land mitigation actions, and ii) the EO community eager to contribute to the UNFCCC Global Stocktake. The research questions emerging from the literature gaps and to be addressed in this thesis are very practical in focus. Focusing on available EO products to measure carbon fluxes from land, this thesis will answer the questions:

- How extensively are the wide range of EO products offered by the EO community being used in national reporting and are thus contributing to the Global Stocktake?
- Is the uncertainty in the EO-based carbon flux estimates mostly linked to land and land use change (Activity Data) or biomass (Emission/Removal factors)?
- What are the reasons for the main discrepancies and errors?
- How can the combination of maps improve the estimates?

Answering these research questions will contribute to the understanding of the overarching questions:

***Why do we get conflicting estimates from the aggregation of land carbon fluxes from GHG inventories submitted to the UNFCCC and independent global estimates from EO products?***

***How has the EO community contributed to the first Global Stocktake if their estimates of land carbon fluxes diverge from the conclusions from the Global Stocktake?***

## **1.7 Chapter outline**

To answer the overarching questions, three chapters were prepared. **Figure 1-6** presents the logical flow of the thesis by linking the chapters to the research questions.

Overarching questions:	<p><i>Why do we get conflicting estimates from the aggregation of land carbon fluxes from GHG inventories submitted to the UNFCCC and independent global estimates from EO products?</i></p> <p><i>How has the EO community contributed to the first Global Stocktake if their estimates of land carbon fluxes diverge from the conclusions from the Global Stocktake?</i></p>	
Research questions:	How extensively are the wide range of EO products offered by the EO community being used in national reporting and are thus contributing to the Global Stocktake?	<p><b>Chapter 2</b> <i>(pan-tropical study)</i></p>
	Is the uncertainty in the EO-based estimates mostly linked to land and land use change (Activity Data) or biomass (Emission/Removal factors)?	<p><b>Chapter 3</b> <i>(case study: Guinea-Bissau)</i></p>
	What are the reasons for the main discrepancies and map errors?	<p><b>Chapter 4</b></p>
	How can the combination of maps improve the estimates?	<p><i>(case study: Guinea-Bissau)</i></p>
<p><b>Chapter 5</b> <i>Thesis discussion and final conclusions</i></p>		

**Figure 1-6.** Link between the chapters and the research questions of the thesis to present the logical flow across the chapters.

Chapter 2 starts by evaluating if the global capabilities provided by existing EO products are being used in the national reporting obligations to the UNFCCC and provides the basis for identifying which products are effective in this sector, and why. It also highlights the challenges to wider use of existing and planned products. The data sources used in analysis of this chapter timely coincided with the end of the input phase for the first Global Stocktake and the results can therefore serve as a baseline to assess progress on uptake of EO products for the next cycles of the Global Stocktake. Furthermore, Chapter 2 helps identifying i) existing EO products, ii) which are considered more relevant by national teams, and iii) how national teams adapted them to fit with the national definitions and which methods were used to correct mapping errors. Such information is useful for the subsequent chapters.

Chapter 3 assesses the impact of using different combinations of EO products for producing estimates of historical carbon emissions from deforestation. Using Guinea-Bissau (a Least Developed Country in West Africa) as a case study, I compare historical gross emissions from deforestation obtained by combining several EO products (for AD and EF), including nationally produced ones. I investigate how well global EO products agree between them, and how they agree with in-situ data, and explore the causes of existing variations.

Chapter 4 uses the same EO products from Chapter 3 and assesses their accuracies. The chapter describes a sampling scheme and the collection of a reference dataset of very high-resolution data to quantify the errors of the AD maps used in Chapter 3 and

test if the errors are reduced with the combination of maps. Similar approaches and methods used by national teams identified in Chapter 2 were explored here, namely the sampling design and classification protocol.

Chapter 5 includes the thesis discussion and final conclusions, binding the work carried out across the chapters and linking the work to the overarching questions. It also concludes with some practical contributions from the results of this thesis and perspectives for future work.

## 1.8 References

Achard, F. and House, J. I.: Reporting carbon losses from tropical deforestation with Pan-tropical biomass maps, *Environmental Research Letters*, 10, 3, 10.1088/1748-9326/10/10/101002, 2015.

Achard, F., Eva, H. D., Stibig, H. J., Mayaux, P., Gallego, J., Richards, T., and Malingreau, J. P.: Determination of deforestation rates of the world's humid tropical forests, *Science*, 297, 999-1002, 10.1126/science.1070656, 2002.

Achard, F., Beuchle, R., Mayaux, P., Stibig, H.-J., Bodart, C., Brink, A., Carboni, S., Desclee, B., Donnay, F., Eva, H. D., Lupi, A., Rasi, R., Seliger, R., and Simonetti, D.: Determination of tropical deforestation rates and related carbon losses from 1990 to 2010, *Global Change Biology*, 20, 2540-2554, 10.1111/gcb.12605, 2014.

Alfieri, J. G., Niyogi, D., LeMone, M. A., Chen, F., and Fall, S.: A simple reclassification method for correcting uncertainty in land Use/Land cover data sets used with land surface models, *Pure and Applied Geophysics*, 164, 1789-1809, 10.1007/s00024-007-0241-4, 2007.

Anderson, K., Buck, H. J., Fuhr, L., Geden, O., Peters, G. P., and Tamme, E.: Controversies of carbon dioxide removal, *Nature Reviews Earth & Environment*, 4, 808-814, 10.1038/s43017-023-00493-y, 2023.

Araza, A., de Bruin, S., Herold, M., Quegan, S., Labriere, N., Rodriguez-Veiga, P., Avitabile, V., Santoro, M., Mitchard, E., Ryan, C., Phillips, O., Willcock, S., Verbeeck, H., Carreiras, J., Hein, L., Schelhaas, M., Pacheco-Pascagaza, A., Bispo, P., Laurin, G., Vieilledent, G., Slik, F., Wijaya, A., Lewis, S., Morel, A., Liang, J., Sukhdeo, H., Schepaschenko, D., Cavlovic, J., Gilani, H., and Lucas, R.: A comprehensive framework for assessing the accuracy and uncertainty of global above-ground biomass maps, *Remote Sensing of Environment*, 272, 10.1016/j.rse.2022.112917, 2022.

Arevalo, P., Stanimirova, R., Bullock, E., Zhang, Y., Tarrío, K., Turlej, K., Hu, K., McAvoy, K., Pasquarella, V., Woodcock, C., Olofsson, P., Zhu, Z., Gorelick, N., Loveland, T., Barber, C., and Friedl, M.: Global Land Cover Mapping and Estimation Yearly 30 m V001 [Data set]. NASA EOSDIS Land Processes DAAC. Available at

<https://doi.org/10.5067/MEaSURES/GLanCE/GLanCE30.001> (last accessed December 2022), 2022.

Asner, G. P.: Tropical forest carbon assessment: integrating satellite and airborne mapping approaches, *Environmental Research Letters*, 4, 11, 10.1088/1748-9326/4/3/034009, 2009.

Asner, G. P., Knapp, D. E., Balaji, A., and Paez-Acosta, G.: Automated mapping of tropical deforestation and forest degradation: CLASlite, *Journal of Applied Remote Sensing*, 3, 24, 10.1117/1.3223675, 2009.

Asner, G. P., Knapp, D. E., Martin, R. E., Tupayachi, R., Anderson, C. B., Mascaro, J., Sinca, F., Chadwick, K. D., Higgins, M., Farfan, W., Llactayo, W., and Silman, M. R.: Targeted carbon conservation at national scales with high-resolution monitoring, *Proceedings of the National Academy of Sciences of the United States of America*, 111, E5016-E5022, 10.1073/pnas.1419550111, 2014.

Avitabile, V., Baccini, A., Friedl, M. A., and Schullius, C.: Capabilities and limitations of Landsat and land cover data for aboveground woody biomass estimation of Uganda, *Remote Sensing of Environment*, 117, 366-380, 10.1016/j.rse.2011.10.012, 2012.

Avitabile, V., Herold, M., Heuvelink, G. B. M., Lewis, S. L., Phillips, O. L., Asner, G. P., Armston, J., Ashton, P. S., Banin, L., Bayol, N., Berry, N. J., Boeckx, P., de Jong, B. H. J., DeVries, B., Girardin, C. A. J., Kearsley, E., Lindsell, J. A., Lopez-Gonzalez, G., Lucas, R., Malhi, Y., Morel, A., Mitchard, E. T. A., Nagy, L., Qie, L., Quinones, M. J., Ryan, C. M., Ferry, S. J. W., Sunderland, T., Laurin, G. V., Gatti, R. C., Valentini, R., Verbeeck, H., Wijaya, A., and Willcock, S.: An integrated pan-tropical biomass map using multiple reference datasets, *Global Change Biology*, 22, 1406-1420, 10.1111/gcb.13139, 2016.

Avtar, R., Suzuki, R., Takeuchi, W., and Sawada, H.: PALSAR 50 m Mosaic Data Based National Level Biomass Estimation in Cambodia for Implementation of REDD plus Mechanism, *Plos One*, 8, 11, 10.1371/journal.pone.0074807, 2013.

Baccini, A., Friedl, M. A., Woodcock, C. E., and Warbington, R.: Forest biomass estimation over regional scales using multisource data, *Geophysical Research Letters*, 31, 4, 10.1029/2004gl019782, 2004.

Baccini, A., Walker, W., Carvalho, L., Farina, M., Sulla-Menashe, D., and Houghton, R.: Tropical forests are a net carbon source based on aboveground measurements of gain and loss, *Science*, 358, 230-233, 10.1126/science.aam5962, 2017.

Baccini, A., Walker, W., Carvalho, L. E., Farina, M. K., Solvik, K. K., and Sulla-Menashe, D.: Aboveground Biomass Change for Amazon Basin, Mexico, and Pantropical Belt, 2003-2016, 10.3334/ORNLDAAC/1824, 2021.

Baccini, A., Goetz, S. J., Walker, W. S., Laporte, N. T., Sun, M., Sulla-Menashe, D., Hackler, J., Beck, P. S. A., Dubayah, R., Friedl, M. A., Samanta, S., and Houghton, R. A.: Estimated carbon dioxide emissions from tropical deforestation improved by carbon-density maps, *Nature Climate Change*, 2, 182-185, 10.1038/nclimate1354, 2012.

Bastin, J., Berrahmouni, N., Grainger, A., Maniatis, D., Mollicone, D., Moore, R., Patriarca, C., Picard, N., Sparrow, B., Abraham, E., Aloui, K., Atesoglu, A., Attorre, F., Bassullu, C., Bey, A., Garzuglia, M., Garcia-Montero, L., Groot, N., Guerin, G., Laestadius, L., Lowe, A., Mamane, B., Marchi, G., Patterson, P., Rezende, M., Ricci, S., Salcedo, I., Diaz, A., Stolle, F., Surappaeva, V., and Castro, R.: The extent of forest in dryland biomes, *Science*, 356, 635-+, 10.1126/science.aam6527, 2017.

Bucki, M., Cuypers, D., Mayaux, P., Achard, F., Estreguil, C., and Grassi, G.: Assessing REDD plus performance of countries with low monitoring capacities: the matrix approach, *Environmental Research Letters*, 7, 10.1088/1748-9326/7/1/014031, 2012.

Bullock, E., Healey, S., Yang, Z., Acosta, R., Villalba, H., Insfran, K., Melo, J., Wilson, S., Duncanson, L., Naesset, E., Armston, J., Saarela, S., Stahl, G., Patterson, P., and Dubayah, R.: Estimating aboveground biomass density using hybrid statistical inference with GEDI lidar data and Paraguay's national forest inventory, *Environmental Research Letters*, 18, 10.1088/1748-9326/acdf03, 2023.

Byrne, B., Baker, D. F., Basu, S., Bertolacci, M., Bowman, K. W., Carroll, D., Chatterjee, A., Chevallier, F., Ciais, P., Cressie, N., Crisp, D., Crowell, S., Deng, F., Deng, Z., Deutscher, N. M., Dubey, M. K., Feng, S., García, O. E., Griffith, D. W. T., Herkommer, B., Hu, L., Jacobson, A. R., Janardan, R., Jeong, S., Johnson, M. S., Jones, D. B. A., Kivi, R., Liu, J., Liu, Z., Maksyutov, S., Miller, J. B., Miller, S. M., Morino, I., Notholt, J., Oda, T., O'Dell, C. W., Oh, Y. S., Ohyama, H., Patra, P. K., Peiro, H., Petri, C., Philip, S., Pollard, D. F., Poulter, B., Remaud, M., Schuh, A., Sha, M. K., Shiomi, K., Strong, K., Sweeney, C., Té, Y., Tian, H., Velazco, V. A., Vrekoussis, M., Warneke, T., Worden, J. R., Wunch, D., Yao, Y., Yun, J., Zammit-Mangion, A., and Zeng, N.: National CO<sub>2</sub> budgets (2015–2020) inferred from atmospheric CO<sub>2</sub> observations in support of the global stocktake, *Earth Syst. Sci. Data*, 15, 963-1004, 10.5194/essd-15-963-2023, 2023.

Carreiras, J. M. B., Vasconcelos, M. J., and Lucas, R. M.: Understanding the relationship between aboveground biomass and ALOS PALSAR data in the forests of Guinea-Bissau (West Africa), *Remote Sensing of Environment*, 121, 426-442, 10.1016/j.rse.2012.02.012, 2012.

Cartus, O., Kellndorfer, J., Walker, W., Franco, C., Bishop, J., Santos, L., and Fuentes, J. M. M.: A National, Detailed Map of Forest Aboveground Carbon Stocks in Mexico, *Remote Sensing*, 6, 5559-5588, 10.3390/rs6065559, 2014.

Ceccherini, G., Duveiller, G., Grassi, G., Lemoine, G., Avitabile, V., Pilli, R., and Cescatti, A.: Abrupt increase in harvested forest area over Europe after 2015, *Nature*, 583, 72-+, 10.1038/s41586-020-2438-y, 2020.

Ceccherini, G., Duveiller, G., Grassi, G., Lemoine, G., Avitabile, V., Pilli, R., and Cescatti, A.: Concerns about reported harvests in European forests Reply to Wernick, I. K. et al.; Palahi, M. et al., *Nature*, 592, E18-E23, 10.1038/s41586-021-03294-9, 2021.

CEOS Earth Observation Handbook 2023 "Space data for the Global Stocktake". Available online at: <https://eohandbook.com/gst/>

Chevallier, F.: Fluxes of Carbon Dioxide From Managed Ecosystems Estimated by National Inventories Compared to Atmospheric Inverse Modeling, *Geophysical Research Letters*, 48, 10.1029/2021GL093565, 2021.

Collins, J. N., Hutley, L. B., Williams, R. J., Boggs, G., Bell, D., and Bartolo, R.: Estimating landscape-scale vegetation carbon stocks using airborne multi-frequency polarimetric synthetic aperture radar (SAR) in the savannahs of north Australia, *International Journal of Remote Sensing*, 30, 1141-1159, 10.1080/01431160802448935, 2009.

Cook-Patton, S., Leavitt, S., Gibbs, D., Harris, N., Lister, K., Anderson-Teixeira, K., Briggs, R., Chazdon, R., Crowther, T., Ellis, P., Griscom, H., Herrmann, V., Holl, K., Houghton, R., Larrosa, C., Lomax, G., Lucas, R., Madsen, P., Malhi, Y., Paquette, A., Parker, J., Paul, K., Routh, D., Roxburgh, S., Saatchi, S., van den Hoogen, J., Walker, W., Wheeler, C., Wood, S., Xu, L., and Griscom, B.: Mapping carbon accumulation potential from global natural forest regrowth, *Nature*, 585, 545-+, 10.1038/s41586-020-2686-x, 2020.

Curtis, P., Slay, C., Harris, N., Tyukavina, A., and Hansen, M.: Classifying drivers of global forest loss, *Science*, 361, 1108-1111, 10.1126/science.aau3445, 2018.

De Alban, J., Connette, G., Oswald, P., and Webb, E.: Combined Landsat and L-Band SAR Data Improves Land Cover Classification and Change Detection in Dynamic Tropical Landscapes, *Remote Sensing*, 10, 10.3390/rs10020306, 2018.

De Sy, V., Herold, M., Achard, F., Asner, G. P., Held, A., Kellndorfer, J., and Verbesselt, J.: Synergies of multiple remote sensing data sources for REDD+ monitoring, *Current Opinion in Environmental Sustainability*, 4, 696-706, 10.1016/j.cosust.2012.09.013, 2012.

DeFries, R., Achard, F., Brown, S., Herold, M., Murdiyarso, D., Schlamadinger, B., and de Souza, C.: Earth observations for estimating greenhouse gas emissions from deforestation in developing countries, *Environmental Science & Policy*, 10, 385-394, 10.1016/j.envsci.2007.01.010, 2007.

DeFries, R. S. and Townshend, J. R. G.: NDVI-DERIVED LAND-COVER CLASSIFICATIONS AT A GLOBAL-SCALE, *International Journal of Remote Sensing*, 15, 3567-3586, 1994.

DeFries, R. S., Houghton, R. A., Hansen, M. C., Field, C. B., Skole, D., and Townshend, J.: Carbon emissions from tropical deforestation and regrowth based on satellite observations for the 1980s and 1990s, *Proceedings of the National Academy of Sciences of the United States of America*, 99, 14256-14261, 10.1073/pnas.182560099, 2002.

den Elzen, M., Dafnomilis, I., Forsell, N., Fragkos, P., Fragkiadakis, K., Höhne, N., Kuramochi, T., Nascimento, L., Roelfsema, M., van Soest, H., and Sperling, F.: Updated nationally determined contributions collectively raise ambition levels but need strengthening further to keep Paris goals within reach, *Mitigation and Adaptation Strategies For Global Change*, 27, 10.1007/s11027-022-10008-7, 2022.

Deng, Z., Ciais, P., Tzompa-Sosa, Z., Saunois, M., Qiu, C., Tan, C., Sun, T., Ke, P., Cui, Y., Tanaka, K., Lin, X., Thompson, R., Tian, H., Yao, Y., Huang, Y., Lauerwald, R., Jain,

A., Xu, X., Bastos, A., Sitch, S., Palmer, P., Lauvaux, T., d'Aspremont, A., Giron, C., Benoit, A., Poulter, B., Chang, J., Petrescu, A., Davis, S., Liu, Z., Grassi, G., Albergel, C., Tubiello, F., Perugini, L., Peters, W., and Chevallier, F.: Comparing national greenhouse gas budgets reported in UNFCCC inventories against atmospheric inversions, *Earth System Science Data*, 14, 1639-1675, 10.5194/essd-14-1639-2022, 2022.

Drusch, M., Del Bello, U., Carlier, S., Colin, O., Fernandez, V., Gascon, F., Hoersch, B., Isola, C., Laberinti, P., Martimort, P., Meygret, A., Spoto, F., Sy, O., Marchese, F., and Bargellini, P.: Sentinel-2: ESA's Optical High-Resolution Mission for GMES Operational Services, *Remote Sensing of Environment*, 120, 25-36, 10.1016/j.rse.2011.11.026, 2012.

Dubayah, R., Armston, J., Healey, S., Bruening, J., Patterson, P., Kellner, J., Duncanson, L., Saarela, S., Stahl, G., Yang, Z., Tang, H., Blair, J., Fatoyinbo, L., Goetz, S., Hancock, S., Hansen, M., Hofton, M., Hurtt, G., and Luthcke, S.: GEDI launches a new era of biomass inference from space, *Environmental Research Letters*, 17, 10.1088/1748-9326/ac8694, 2022.

Dubayah, R., Blair, J. B., Goetz, S., Fatoyinbo, L., Hansen, M., Healey, S., Hofton, M., Hurtt, G., Kellner, J., Luthcke, S., Armston, J., Tang, H., Duncanson, L., Hancock, S., Jantz, P., Marselis, S., Patterson, P. L., Qi, W., and Silva, C.: The Global Ecosystem Dynamics Investigation: High-resolution laser ranging of the Earth's forests and topography, *Science of Remote Sensing*, 1, 100002, <https://doi.org/10.1016/j.srs.2020.100002>, 2020.

Duncanson, L., Kellner, J., Armston, J., Dubayah, R., Minor, D., Hancock, S., Healey, S., Patterson, P., Saarela, S., Marselis, S., Silva, C., Bruening, J., Goetz, S., Tang, H., Hofton, M., Blair, B., Luthcke, S., Fatoyinbo, L., Abernethy, K., Alonso, A., Andersen, H., Aplin, P., Baker, T., Barbier, N., Bastin, J., Biber, P., Boeckx, P., Bogaert, J., Boschetti, L., Boucher, P., Boyd, D., Burslem, D., Calvo-Rodriguez, S., Chave, J., Chazdon, R., Clark, D., Clark, D., Cohen, W., Coomes, D., Corona, P., Cushman, K., Cutler, M., Dalling, J., Dalponte, M., Dash, J., de-Miguel, S., Deng, S., Ellis, P., Erasmus, B., Fekety, P., Fernandez-Landa, A., Ferraz, A., Fischer, R., Fisher, A., Garcia-Abril, A., Gobakken, T., Hacker, J., Heurich, M., Hill, R., Hopkinson, C., Huang, H., Hubbell, S., Hudak, A., Huth, A., Imbach, B., Jeffery, K., Katoh, M., Kearsley, E., Kenfack, D., Kljun, N., Knapp, N., Kral, K., Krucek, M., Labriere, N., Lewis, S., Longo, M., Lucas, R., Main, R., Manzanera, J., Martinez, R., Mathieu, R., Memiaghe, H., Meyer, V., Mendoza, A., Moneris, A., Montesano, P., Morsdorf, F., Naesset, E., Naidoo, L., Nilus, R., O'Brien, M., Orwig, D., Papathanassiou, K., Parker, G., Philipson, C., Phillips, O., Pisek, J., Poulsen, J., Pretzsch, H., Rudiger, C., Saatchi, S., Sanchez-Azofeifa, A., Sanchez-Lopez, N., Scholes, R., Silva, C., Simard, M., Skidmore, A., Sterenczak, K., Tanase, M., Torresan, C., Valbuena, R., Verbeeck, H., Vrska, T., Wessels, K., White, J., White, L., Zahabu, E., and Zraggen, C.: Aboveground biomass density models for NASA's Global Ecosystem Dynamics Investigation (GEDI) lidar mission, *Remote Sensing of Environment*, 270, 10.1016/j.rse.2021.112845, 2022.

Englhart, S., Keuck, V., and Siegert, F.: Aboveground biomass retrieval in tropical forests - The potential of combined X- and L-band SAR data use, *Remote Sensing of Environment*, 115, 1260-1271, 10.1016/j.rse.2011.01.008, 2011.

FAO: Global Forest Resources Assessment 2020: Main report. Rome. Available at: <https://doi.org/10.4060/ca9825en> (last accessed December 2022), 2020.

FAO & JRC: Global forest land-use change 1990–2005, by E.J. Lindquist, R. D'Annunzio, A. Gerrand, K. MacDicken, F. Achard, R. Beuchle, A. Brink, H.D. Eva, P. Mayaux, J. San-Miguel-Ayanz & H-J. Stibig. FAO Forestry Paper No. 169. Food and Agriculture Organization of the United Nations and European Commission Joint Research Centre. Rome, FAO, 2012

Federici, S., Grassi, G., Harris, N., Lee, D., Neeff, T., Penman, J., Sanz, M. J., and Wolosin, M.: GHG Fluxes from Forests: An assessment of national GHG estimates and independent research in the context of the Paris Agreement., Available at: <https://www.climateandlandusealliance.org/reports/ghg-fluxes-forests/> (last access October 2022), 2017.

Feng, Y., Zeng, Z., Searchinger, T., Ziegler, A., Wu, J., Wang, D., He, X., Elsen, P., Ciais, P., Xu, R., Guo, Z., Peng, L., Tao, Y., Spracklen, D., Holden, J., Liu, X., Zheng, Y., Xu, P., Chen, J., Jiang, X., Song, X., Lakshmi, V., Wood, E., and Zheng, C.: Doubling of annual forest carbon loss over the tropics during the early twenty-first century, *Nature Sustainability*, 5, 444-451, 10.1038/s41893-022-00854-3, 2022.

Findlater, K., Webber, S., Kandlikar, M., and Donner, S.: Climate services promise better decisions but mainly focus on better data, *Nature Climate Change*, 11, 731+, 10.1038/s41558-021-01125-3, 2021.

Foody, G. M., Boyd, D. S., and Cutler, M. E. J.: Predictive relations of tropical forest biomass from Landsat TM data and their transferability between regions, *Remote Sensing of Environment*, 85, 463-474, 10.1016/s0034-4257(03)00039-7, 2003.

Foody, G. M., Cutler, M. E., McMorrow, J., Pelz, D., Tangki, H., Boyd, D. S., and Douglas, I.: Mapping the biomass of Bornean tropical rain forest from remotely sensed data, *Global Ecology and Biogeography*, 10, 379-387, 10.1046/j.1466-822X.2001.00248.x, 2001.

Friedl, M. A., Sulla-Menashe, D., Tan, B., Schneider, A., Ramankutty, N., Sibley, A., and Huang, X. M.: MODIS Collection 5 global land cover: Algorithm refinements and characterization of new datasets, *Remote Sensing of Environment*, 114, 168-182, 10.1016/j.rse.2009.08.016, 2010.

Friedl, M. A., McIver, D. K., Hodges, J. C. F., Zhang, X. Y., Muchoney, D., Strahler, A. H., Woodcock, C. E., Gopal, S., Schneider, A., Cooper, A., Baccini, A., Gao, F., and Schaaf, C.: Global land cover mapping from MODIS: algorithms and early results, *Remote Sensing of Environment*, 83, 287-302, 10.1016/s0034-4257(02)00078-0, 2002.

Friedlingstein, P., O'Sullivan, M., Jones, M., Andrew, R., Hauck, J., Olsen, A., Peters, G., Peters, W., Pongratz, J., Sitch, S., Le Quere, C., Canadell, J., Ciais, P., Jackson, R., Alin, S., Aragao, L., Arneeth, A., Arora, V., Bates, N., Becker, M., Benoit-Cattin, A., Bittig, H., Bopp, L., Bultan, S., Chandra, N., Chevallier, F., Chini, L., Evans, W., Florentie, L., Forster, P., Gasser, T., Gehlen, M., Gilfillan, D., Gkritzalis, T., Gregor, L., Gruber, N., Harris, I., Hartung, K., Haverd, V., Houghton, R., Ilyina, T., Jain, A., Joetzjer, E., Kadono, K., Kato, E., Kitidis, V., Korsbakken, J., Landschutzer, P., Lefevre, N., Lenton, A., Lienert,

S., Liu, Z., Lombardozzi, D., Marland, G., Metzl, N., Munro, D., Nabel, J., Nakaoka, S., Niwa, Y., O'Brien, K., Ono, T., Palmer, P., Pierrot, D., Poulter, B., Resplandy, L., Robertson, E., Rodenbeck, C., Schwinger, J., Seferian, R., Skjelvan, I., Smith, A., Sutton, A., Tanhua, T., Tans, P., Tian, H., Tilbrook, B., Van der Werf, G., Vuichard, N., Walker, A., Wanninkhof, R., Watson, A., Willis, D., Wiltshire, A., Yuan, W., Yue, X., and Zaehle, S.: Global Carbon Budget 2020, *Earth System Science Data*, 12, 3269-3340, 10.5194/essd-12-3269-2020, 2020.

Friedlingstein, P., O'Sullivan, M., Jones, M. W., Andrew, R. M., Bakker, D. C. E., Hauck, J., Landschützer, P., Le Quéré, C., Lujikx, I. T., Peters, G. P., Peters, W., Pongratz, J., Schwingshackl, C., Sitch, S., Canadell, J. G., Ciais, P., Jackson, R. B., Alin, S. R., Anthoni, P., Barbero, L., Bates, N. R., Becker, M., Bellouin, N., Decharme, B., Bopp, L., Brasika, I. B. M., Cadule, P., Chamberlain, M. A., Chandra, N., Chau, T. T. T., Chevallier, F., Chini, L. P., Cronin, M., Dou, X., Enyo, K., Evans, W., Falk, S., Feely, R. A., Feng, L., Ford, D. J., Gasser, T., Ghattas, J., Gkritzalis, T., Grassi, G., Gregor, L., Gruber, N., Gürses, Ö., Harris, I., Hefner, M., Heinke, J., Houghton, R. A., Hurtt, G. C., Iida, Y., Ilyina, T., Jacobson, A. R., Jain, A., Jarníková, T., Jersild, A., Jiang, F., Jin, Z., Joos, F., Kato, E., Keeling, R. F., Kennedy, D., Klein Goldewijk, K., Knauer, J., Korsbakken, J. I., Körtzinger, A., Lan, X., Lefèvre, N., Li, H., Liu, J., Liu, Z., Ma, L., Marland, G., Mayot, N., McGuire, P. C., McKinley, G. A., Meyer, G., Morgan, E. J., Munro, D. R., Nakaoka, S. I., Niwa, Y., O'Brien, K. M., Olsen, A., Omar, A. M., Ono, T., Paulsen, M., Pierrot, D., Pockock, K., Poulter, B., Powis, C. M., Rehder, G., Resplandy, L., Robertson, E., Rodenbeck, C., Rosan, T. M., Schwinger, J., Séférian, R., Smallman, T. L., Smith, S. M., Sospedra-Alfonso, R., Sun, Q., Sutton, A. J., Sweeney, C., Takao, S., Tans, P. P., Tian, H., Tilbrook, B., Tsujino, H., Tubiello, F., van der Werf, G. R., van Ooijen, E., Wanninkhof, R., Watanabe, M., Wimart-Rousseau, C., Yang, D., Yang, X., Yuan, W., Yue, X., Zaehle, S., Zeng, J., and Zheng, B.: Global Carbon Budget 2023, 15, 5301-5369, 2023.

Fritz, S., See, L., and Rembold, F.: Comparison of global and regional land cover maps with statistical information for the agricultural domain in Africa, *International Journal of Remote Sensing*, 31, 2237-2256, 10.1080/01431160902946598, 2010.

Galiatsatos, N., Donoghue, D., Watt, P., Bholanath, P., Pickering, J., Hansen, M., and Mahmood, A.: An Assessment of Global Forest Change Datasets for National Forest Monitoring and Reporting, *Remote Sensing*, 12, 10.3390/rs12111790, 2020.

Gasser, T., Crepin, L., Quilcaille, Y., Houghton, R., Ciais, P., and Obersteiner, M.: Historical CO<sub>2</sub> emissions from land use and land cover change and their uncertainty, *Biogeosciences*, 17, 4075-4101, 10.5194/bg-17-4075-2020, 2020.

GFOI: Integration of remote-sensing and ground-based observations for estimation of emissions and removals of greenhouse gases in forests: Methods and Guidance from the Global Forest Observations Initiative, Edition 3.0., 2020.

Gibbs, H. and Herold, M.: Tropical deforestation and greenhouse gas emissions, *Environmental Research Letters*, 2, 10.1088/1748-9326/2/4/045021, 2007.

Gibbs, H. K., Brown, S., Niles, J. O., and Foley, J. A.: Monitoring and estimating tropical forest carbon stocks: making REDD a reality, *Environmental Research Letters*, 2, 10.1088/1748-9326/2/4/045023, 2007.

Gidden, M. J., Gasser, T., Grassi, G., Forsell, N., Janssens, I., Lamb, W. F., Minx, J., Nicholls, Z., Steinhauser, J., and Riahi, K.: Aligning climate scenarios to emissions inventories shifts global benchmarks, *Nature*, 10.1038/s41586-023-06724-y, 2023.

Giglio, L., Schroeder, W., and Justice, C.: The collection 6 MODIS active fire detection algorithm and fire products, *Remote Sensing of Environment*, 178, 31-41, 10.1016/j.rse.2016.02.054, 2016.

Giglio, L., Boschetti, L., Roy, D., Humber, M., and Justice, C.: The Collection 6 MODIS burned area mapping algorithm and product, *Remote Sensing of Environment*, 217, 72-85, 10.1016/j.rse.2018.08.005, 2018.

Goetz, S. J., Hansen, M., Houghton, R. A., Walker, W., Laporte, N., and Busch, J.: Measurement and monitoring needs, capabilities and potential for addressing reduced emissions from deforestation and forest degradation under REDD, *Environmental Research Letters*, 12, 10.1088/1748-9326/10/12/123001, 2015.

Goetz, S. J., Baccini, A., Laporte, N. T., Johns, T., Walker, W., Kellndorfer, J., Houghton, R. A., and Sun, M.: Mapping and monitoring carbon stocks with satellite observations: a comparison of methods, *Carbon balance and management*, 4, 2, 10.1186/1750-0680-4-2, 2009.

Gomez, C., White, J. C., and Wulder, M. A.: Optical remotely sensed time series data for land cover classification: A review, *Isprs Journal of Photogrammetry and Remote Sensing*, 116, 55-72, 10.1016/j.isprsjprs.2016.03.008, 2016.

Gopal, S., Woodcock, C. E., and Strahler, A. H.: Fuzzy neural network classification of global land cover from a 1 degrees AVHRR data set, *Remote Sensing of Environment*, 67, 230-243, 10.1016/s0034-4257(98)00088-1, 1999.

Grainger, A. and Kim, J.: Reducing Global Environmental Uncertainties in Reports of Tropical Forest Carbon Fluxes to REDD plus and the Paris Agreement Global Stocktake, *Remote Sensing*, 12, 10.3390/rs12152369, 2020.

Grassi, G., House, J., Dentener, F., Federici, S., den Elzen, M., and Penman, J.: The key role of forests in meeting climate targets requires science for credible mitigation, *Nature Climate Change*, 7, 220-+, 10.1038/NCLIMATE3227, 2017.

Grassi, G., Conchedda, G., Federici, S., Vinas, R., Korosuo, A., Melo, J., Rossi, S., Sandker, M., Somogyi, Z., Vizzarri, M., and Tubiello, F.: Carbon fluxes from land 2000-2020: bringing clarity to countries' reporting, *Earth System Science Data*, 14, 4643-4666, 10.5194/essd-14-4643-2022, 2022.

Grassi, G., Stehfest, E., Rogelj, J., van Vuuren, D., Cescatti, A., House, J., Nabuurs, G., Rossi, S., Alkama, R., Vinas, R., Calvin, K., Ceccherini, G., Federici, S., Fujimori, S., Gusti, M., Hasegawa, T., Havlik, P., Humpenoder, F., Korosuo, A., Perugini, L., Tubiello, F., and Popp, A.: Critical adjustment of land mitigation pathways for assessing countries' climate progress, *Nature Climate Change*, 11, 425-+, 10.1038/s41558-021-01033-6, 2021.

Grassi, G., Schwingshackl, C., Gasser, T., Houghton, R., Sitch, S., Canadell, J., Cescatti, A., Ciais, P., Federici, S., Friedlingstein, P., Kurz, W., Sanchez, M., Vinas, R., Alkama, R., Bultan, S., Ceccherini, G., Falk, S., Kato, E., Kennedy, D., Knauer, J., Korosuo, A., Melo, J., McGrath, M., Nabel, J., Poulter, B., Romanovskaya, A., Rossi, S., Tian, H., Walker, A., Yuan, W., Yue, X., and Pongratz, J.: Harmonising the land-use flux estimates of global models and national inventories for 2000-2020, *Earth System Science Data*, 15, 1093-1114, 10.5194/essd-15-1093-2023, 2023.

Hansen, M., Potapov, P., Margono, B., Stehman, S., Turubanova, S., and Tyukavina, A.: Response to Comment on "High-resolution global maps of 21st-century forest cover change", *Science*, 344, 1, 10.1126/science.1248817, 2014.

Hansen, M. C., Stehman, S. V., and Potapov, P. V.: Quantification of global gross forest cover loss, *Proceedings of the National Academy of Sciences of the United States of America*, 107, 8650-8655, 10.1073/pnas.0912668107, 2010.

Hansen, M. C., Potapov, P. V., Moore, R., Hancher, M., Turubanova, S. A., Tyukavina, A., Thau, D., Stehman, S. V., Goetz, S. J., Loveland, T. R., Kommareddy, A., Egorov, A., Chini, L., Justice, C. O., and Townshend, J. R. G.: High-Resolution Global Maps of 21st-Century Forest Cover Change, *Science*, 342, 850-853, 10.1126/science.1244693, 2013.

Hansis, E., Davis, S., and Pongratz, J.: Relevance of methodological choices for accounting of land use change carbon fluxes, *Global Biogeochemical Cycles*, 29, 1230-1246, 10.1002/2014GB004997, 2015.

Harris, N., Gibbs, D., Baccini, A., Birdsey, R., de Bruin, S., Farina, M., Fatoyinbo, L., Hansen, M., Herold, M., Houghton, R., Potapov, P., Suarez, D., Roman-Cuesta, R., Saatchi, S., Slay, C., Turubanova, S., and Tyukavina, A.: Global maps of twenty-first century forest carbon fluxes, *Nature Climate Change*, 11, 10.1038/s41558-020-00976-6, 2021.

Harris, N. L., Brown, S., Hagen, S. C., Saatchi, S. S., Petrova, S., Salas, W., Hansen, M. C., Potapov, P. V., and Lotsch, A.: Baseline Map of Carbon Emissions from Deforestation in Tropical Regions, *Science*, 336, 1573-1576, 10.1126/science.1217962, 2012.

Hart, D., Yeo, S., Almaraz, M., Beillouin, D., Cardinael, R., Garcia, E., Kay, S., Lovell, S., Rosenstock, T., Sprenkle-Hyppolite, S., Stolle, F., Suber, M., Thapa, B., Wood, S., and Cook-Patton, S.: Priority science can accelerate agroforestry as a natural climate solution, *Nature Climate Change*, 10.1038/s41558-023-01810-5, 2023.

Healey, S. P., Patterson, P. L. & Armston, J.: Algorithm theoretical basis document (atbd) for GEDI level-4b (l4b) gridded aboveground biomass density. version 1.0, ORNL Distributed Active Archive Center, 2022

Hegglin, M. I., Bastos, A., Bovensmann, H., Buchwitz, M., Fawcett, D., Ghent, D., Kulk, G., Sathyendranath, S., Shepherd, T. G., Quegan, S., Röthlisberger, R., Briggs, S., Buontempo, C., Cazenave, A., Chuvieco, E., Ciais, P., Crisp, D., Engelen, R., Fadnavis, S., Herold, M., Horwath, M., Jonsson, O., Kpaka, G., Merchant, C. J., Mielke, C., Nagler, T., Paul, F., Popp, T., Quaife, T., Rayner, N. A., Robert, C., Schröder, M., Sitch, S., Venturini, S., van der Schalie, R., van der Vliet, M., Wigneron, J.-P., and Woolway, R. I.:

Space-based Earth observation in support of the UNFCCC Paris Agreement, *Frontiers in Environmental Science*, 10, 10.3389/fenvs.2022.941490, 2022.

Heinrich, V., House, J., Gibbs, D. A., Harris, N., Herold, M., Grassi, G., Cantinho, R., Rosan, T. M., Zimbres, B., Shimbo, J. Z., Melo, J., Hales, T., Sitch, S., and Aragão, L. E. O. C.: Mind the gap: reconciling tropical forest carbon flux estimates from earth observation and national reporting requires transparency, *Carbon Balance and Management*, 18, 22, 10.1186/s13021-023-00240-2, 2023a.

Heinrich, V., Vancutsem, C., Dalagnol, R., Rosan, T., Fawcett, D., Silva, C., Cassol, H., Achard, F., Jucker, T., Silva, C., House, J., Sitch, S., Hales, T., and Aragao, L.: The carbon sink of secondary and degraded humid tropical forests, *Nature*, 615, 436+, 10.1038/s41586-022-05679-w, 2023b.

Herold, M. and Johns, T.: Linking requirements with capabilities for deforestation monitoring in the context of the UNFCCC-REDD process, *Environmental Research Letters*, 2, 10.1088/1748-9326/2/4/045025, 2007.

Herold, M. and Skutsch, M.: Monitoring, reporting and verification for national REDD plus programmes: two proposals, *Environmental Research Letters*, 6, 10.1088/1748-9326/6/1/014002, 2011.

Herold, M., Mayaux, P., Woodcock, C. E., Baccini, A., and Schullius, C.: Some challenges in global land cover mapping: An assessment of agreement and accuracy in existing 1 km datasets, *Remote Sensing of Environment*, 112, 2538-2556, 10.1016/j.rse.2007.11.013, 2008.

Herold, M., Carter, S., Avitabile, V., Espejo, A., Jonckheere, I., Lucas, R., McRoberts, R., Naesset, E., Nightingale, J., Petersen, R., Reiche, J., Romijn, E., Rosenqvist, A., Rozendaal, D., Seifert, F., Sanz, M., and De Sy, V.: The Role and Need for Space-Based Forest Biomass-Related Measurements in Environmental Management and Policy, *Surveys in Geophysics*, 40, 757-778, 10.1007/s10712-019-09510-6, 2019.

Hill, T. C., Williams, M., Bloom, A. A., Mitchard, E. T. A., and Ryan, C. M.: Are Inventory Based and Remotely Sensed Above-Ground Biomass Estimates Consistent?, *Plos One*, 8, 8, 10.1371/journal.pone.0074170, 2013.

Houghton, R. and Nassikas, A.: Global and regional fluxes of carbon from land use and land cover change 1850-2015, *Global Biogeochemical Cycles*, 31, 456-472, 10.1002/2016GB005546, 2017.

Houghton, R. A., Lawrence, K. T., Hackler, J. L., and Brown, S.: The spatial distribution of forest biomass in the Brazilian Amazon: a comparison of estimates, *Global Change Biology*, 7, 731-746, 10.1046/j.1365-2486.2001.00426.x, 2001.

Houghton, R. A., House, J. I., Pongratz, J., van der Werf, G. R., DeFries, R. S., Hansen, M. C., Le Quere, C., and Ramankutty, N.: Carbon emissions from land use and land-cover change, *Biogeosciences*, 9, 5125-5142, 10.5194/bg-9-5125-2012, 2012.

Hunka et al, N.: On the NASA GEDI and ESA CCI biomass maps: aligning for uptake in the UNFCCC global stocktake, *Environ. Res. Lett.* 18 124042 DOI 10.1088/1748-9326/ad0b60, 2023.

IPCC: *Climate Change 2022: Mitigation of Climate Change. Contribution of Working Group III to the Sixth Assessment Report of the Intergovernmental Panel on Climate Change*, 2022.

IPCC: Summary for Policymakers. In: *Climate Change 2023: Synthesis Report. Contribution of Working Groups I, II and III to the Sixth Assessment Report of the Intergovernmental Panel on Climate Change*, IPCC, Geneva, Switzerland, pp. 1-34, 2023.

Johnson, B. A.: Combining national forest type maps with annual global tree cover maps to better understand forest change over time: Case study for Thailand, *Applied Geography*, 62, 294-300, 10.1016/j.apgeog.2015.05.011, 2015.

Joseph, S., Herold, M., Sunderlin, W. D., and Verchot, L. V.: REDD plus readiness: early insights on monitoring, reporting and verification systems of project developers, *Environmental Research Letters*, 8, 10.1088/1748-9326/8/3/034038, 2013.

Joshi, N., Baumann, M., Ehammer, A., Fensholt, R., Grogan, K., Hostert, P., Jepsen, M. R., Kuemmerle, T., Meyfroidt, P., Mitchard, E. T. A., Reiche, J., Ryan, C. M., and Waske, B.: A Review of the Application of Optical and Radar Remote Sensing Data Fusion to Land Use Mapping and Monitoring, *Remote Sensing*, 8, 23, 10.3390/rs8010070, 2016.

Kanellopoulos, I., Varfis, A., Wilkinson, G. G., and Megier, J.: LAND-COVER DISCRIMINATION IN SPOT HRV IMAGERY USING AN ARTIFICIAL NEURAL NETWORK - A 20-CLASS EXPERIMENT, *International Journal of Remote Sensing*, 13, 917-924, 1992.

Karra, K., Kontgis, C., Statman-Weil, Z., Mazzariello, J., Mathis, M., and Brumby, S.: *Global land use/land cover with Sentinel-2 and deep learning*, 2021.

Kasischke, E. S., Melack, J. M., and Dobson, M. C.: The use of imaging radars for ecological applications - A review, *Remote Sensing of Environment*, 59, 141-156, 10.1016/s0034-4257(96)00148-4, 1997.

Keenan, R., Reams, G., Achard, F., de Freitas, J., Grainger, A., and Lindquist, E.: Dynamics of global forest area: Results from the FAO Global Forest Resources Assessment 2015, *Forest Ecology and Management*, 352, 9-20, 10.1016/j.foreco.2015.06.014, 2015.

Korosuo, A., Pilli, R., Viñas, R., Blujdea, V., Colditz, R., Fiorese, G., Rossi, S., Vizzarri, M., and Grassi, G.: The role of forests in the EU climate policy: are we on the right track?, *Carbon Balance and Management*, 18, 10.1186/s13021-023-00234-0, 2023.

Langner, A., Achard, F., and Grassi, G.: Can recent pan-tropical biomass maps be used to derive alternative Tier 1 values for reporting REDD plus activities under UNFCCC?, *Environmental Research Letters*, 9, 12, 10.1088/1748-9326/9/12/124008, 2014.

- Langner, A., Achard, F., Vancutsem, C., Pekel, J. F., Simonetti, D., Grassi, G., Kitayama, K., and Nakayama, M.: Assessment of Above-Ground Biomass of Borneo Forests through a New Data-Fusion Approach Combining Two Pan-Tropical Biomass Maps, *Land*, 4, 656-669, 10.3390/land4030656, 2015.
- Lefsky, M. A., Harding, D., Cohen, W. B., Parker, G., and Shugart, H. H.: Surface lidar remote sensing of basal area and biomass in deciduous forests of eastern Maryland, USA, *Remote Sensing of Environment*, 67, 83-98, 10.1016/s0034-4257(98)00071-6, 1999.
- Lucas, R., Armston, J., Fairfax, R., Fensham, R., Accad, A., Carreiras, J., Kelley, J., Bunting, P., Clewley, D., Bray, S., Metcalfe, D., Dwyer, J., Bowen, M., Eyre, T., Laidlaw, M., and Shimada, M.: An Evaluation of the ALOS PALSAR L-Band Backscatter-Above Ground Biomass Relationship Queensland, Australia: Impacts of Surface Moisture Condition and Vegetation Structure, *IEEE Journal of Selected Topics in Applied Earth Observations and Remote Sensing*, 3, 576-593, 10.1109/jstars.2010.2086436, 2010.
- Lui, G. V. and Coomes, D. A.: A Comparison of Novel Optical Remote Sensing-Based Technologies for Forest-Cover/Change Monitoring, *Remote Sensing*, 7, 2781-2807, 10.3390/rs70302781, 2015.
- Lui, G. V. and Coomes, D. A.: Tropical nature reserves are losing their buffer zones, but leakage is not to blame, *Environmental Research*, 147, 580-589, 10.1016/j.envres.2015.11.008, 2016.
- Mascaro, J., Asner, G. P., Davies, S., Dehgan, A., and Saatchi, S.: These are the days of lasers in the jungle, *Carbon balance and management*, 9, 7, 10.1186/s13021-014-0007-0, 2014.
- McNicol, I., Ryan, C., and Mitchard, E.: Carbon losses from deforestation and widespread degradation offset by extensive growth in African woodlands, *Nature Communications*, 9, 10.1038/s41467-018-05386-z, 2018.
- McRoberts, R.: Satellite image-based maps: Scientific inference or pretty pictures?, *Remote Sensing of Environment*, 115, 715-724, 10.1016/j.rse.2010.10.013, 2011.
- McRoberts, R., Tomppo, E., and Næsset, E.: Advances and emerging issues in national forest inventories, *Scandinavian Journal of Forest Research*, 25, 368-381, 10.1080/02827581.2010.496739, 2010.
- McRoberts, R. E., Vibrans, A. C., Sannier, C., Naesset, E., Hansen, M. C., Walters, B. F., and Lingner, D. V.: Methods for evaluating the utilities of local and global maps for increasing the precision of estimates of subtropical forest area, *Canadian Journal of Forest Research*, 46, 924-932, 10.1139/cjfr-2016-0064, 2016.
- Mermoz, S. and Toan, T. L.: Forest Disturbances and Regrowth Assessment Using ALOS PALSAR Data from 2007 to 2010 in Vietnam, Cambodia and Lao PDR, *Remote Sensing*, 8, 22, 10.3390/rs8030217, 2016.

Mermoz, S., Toan, T. L., Villard, L., Rejou-Mechain, M., and Seifert-Granzin, J.: Biomass assessment in the Cameroon savanna using ALOS PALSAR data, *Remote Sensing of Environment*, 155, 109-119, 10.1016/j.rse.2014.01.029, 2014.

Milodowski, D., Mitchard, E., and Williams, M.: Forest loss maps from regional satellite monitoring systematically underestimate deforestation in two rapidly changing parts of the Amazon, *Environmental Research Letters*, 12, 10.1088/1748-9326/aa7e1e, 2017.

Mitchard, E. T., Saatchi, S. S., Baccini, A., Asner, G. P., Goetz, S. J., Harris, N. L., and Brown, S.: Uncertainty in the spatial distribution of tropical forest biomass: a comparison of pan-tropical maps, *Carbon balance and management*, 8, 10, 10.1186/1750-0680-8-10, 2013.

Mitchard, E. T. A., Saatchi, S. S., Lewis, S. L., Feldpausch, T. R., Woodhouse, I. H., Sonke, B., Rowland, C., and Meir, P.: Measuring biomass changes due to woody encroachment and deforestation/degradation in a forest-savanna boundary region of central Africa using multi-temporal L-band radar backscatter, *Remote Sensing of Environment*, 115, 2861-2873, 10.1016/j.rse.2010.02.022, 2011.

Mitchard, E. T. A., Saatchi, S. S., Woodhouse, I. H., Nangendo, G., Ribeiro, N. S., Williams, M., Ryan, C. M., Lewis, S. L., Feldpausch, T. R., and Meir, P.: Using satellite radar backscatter to predict above-ground woody biomass: A consistent relationship across four different African landscapes, *Geophysical Research Letters*, 36, 6, 10.1029/2009gl040692, 2009.

Mitchard, E. T. A., Feldpausch, T. R., Brienen, R. J. W., Lopez-Gonzalez, G., Monteagudo, A., Baker, T. R., Lewis, S. L., Lloyd, J., Quesada, C. A., Gloor, M., ter Steege, H., Meir, P., Alvarez, E., Araujo-Murakami, A., Aragao, L., Arroyo, L., Aymard, G., Banki, O., Bonal, D., Brown, S., Brown, F. I., Ceron, C. E., Moscoso, V. C., Chave, J., Comiskey, J. A., Cornejo, F., Medina, M. C., Da Costa, L., Costa, F. R. C., Di Fiore, A., Domingues, T. F., Erwin, T. L., Frederickson, T., Higuchi, N., Coronado, E. N. H., Killeen, T. J., Laurance, W. F., Levis, C., Magnusson, W. E., Marimon, B. S., Marimon, B. H., Polo, I. M., Mishra, P., Nascimento, M. T., Neill, D., Vargas, M. P. N., Palacios, W. A., Parada, A., Molina, G. P., Pena-Claros, M., Pitman, N., Peres, C. A., Poorter, L., Prieto, A., Ramirez-Angulo, H., Correa, Z. R., Roopsind, A., Roucoux, K. H., Rudas, A., Salomao, R. P., Schiatti, J., Silveira, M., de Souza, P. F., Steininger, M. K., Stropp, J., Terborgh, J., Thomas, R., Toledo, M., Torres-Lezama, A., van Andel, T. R., van der Heijden, G. M. F., Vieira, I. C. G., Vieira, S., Vilanova-Torre, E., Vos, V. A., Wang, O., Zartman, C. E., Malhi, Y., and Phillips, O. L.: Markedly divergent estimates of Amazon forest carbon density from ground plots and satellites, *Global Ecology and Biogeography*, 23, 935-946, 10.1111/geb.12168, 2014.

Mo, L., Zohner, C. M., Reich, P. B., Liang, J., de Miguel, S., Nabuurs, G.-J., Renner, S. S., van den Hoogen, J., Araza, A., Herold, M., Mirzagholi, L., Ma, H., Averill, C., Phillips, O. L., Gamarra, J. G. P., Hordijk, I., Routh, D., Abegg, M., Adou Yao, Y. C., Alberti, G., Almeyda Zambrano, A. M., Alvarado, B. V., Alvarez-Dávila, E., Alvarez-Loayza, P., Alves, L. F., Amaral, I., Ammer, C., Antón-Fernández, C., Araujo-Murakami, A., Arroyo, L., Avitabile, V., Aymard, G. A., Baker, T. R., Bałazy, R., Banki, O., Barroso, J. G., Bastian, M. L., Bastin, J.-F., Birigazzi, L., Birnbaum, P., Bitariho, R., Boeckx, P., Bongers,

F., Bouriaud, O., Brancalion, P. H. S., Brandl, S., Brearley, F. Q., Brienen, R., Broadbent, E. N., Bruelheide, H., Bussotti, F., Cazzolla Gatti, R., César, R. G., Cesljar, G., Chazdon, R. L., Chen, H. Y. H., Chisholm, C., Cho, H., Cienciala, E., Clark, C., Clark, D., Colletta, G. D., Coomes, D. A., Cornejo Valverde, F., Corral-Rivas, J. J., Crim, P. M., Cumming, J. R., Dayanandan, S., de Gasper, A. L., Decuyper, M., Derroire, G., DeVries, B., Djordjevic, I., Dolezal, J., Dourdain, A., Engone Obiang, N. L., Enquist, B. J., Eyre, T. J., Fandohan, A. B., Fayle, T. M., Feldpausch, T. R., Ferreira, L. V., Finér, L., Fischer, M., Fletcher, C., Frizzera, L., Gianelle, D., Glick, H. B., Harris, D. J., Hector, A., Hemp, A., Hengeveld, G., Hérault, B., Herbohn, J. L., Hillers, A., Honorio Coronado, E. N., Hui, C., Ibanez, T., Imai, N., Jagodziński, A. M., Jaroszewicz, B., Johannsen, V. K., Joly, C. A., Jucker, T., Jung, I., Karminov, V., Kartawinata, K., Kearsley, E., Kenfack, D., Kennard, D. K., Kepfer-Rojas, S., Keppel, G., Khan, M. L., Killeen, T. J., Kim, H. S., Kitayama, K., Köhl, M., Korjus, H., Kraxner, F., Kucher, D., Laarmann, D., Lang, M., Lu, H., Lukina, N. V., Maitner, B. S., Malhi, Y., Marcon, E., Marimon, B. S., Marimon-Junior, B. H., Marshall, A. R., Martin, E. H., Meave, J. A., Melo-Cruz, O., Mendoza, C., Mendoza-Polo, I., Miscicki, S., Merow, C., Monteagudo Mendoza, A., Moreno, V. S., Mukul, S. A., Mundhenk, P., Nava-Miranda, M. G., Neill, D., Neldner, V. J., Nevenic, R. V., Ngugi, M. R., Niklaus, P. A., Oleksyn, J., Ontikov, P., Ortiz-Malavasi, E., Pan, Y., Paquette, A., Parada-Gutierrez, A., Parfenova, E. I., Park, M., Parren, M., Parthasarathy, N., Peri, P. L., Pfautsch, S., Picard, N., Piedade, M. T. F., Piotta, D., Pitman, N. C. A., Poulsen, A. D., Poulsen, J. R., Pretzsch, H., Ramirez Arevalo, F., Restrepo-Correa, Z., Rodeghiero, M., Rolim, S. G., Roopsind, A., Rovero, F., Rutishauser, E., Saikia, P., Salas-Eljatib, C., Saner, P., Schall, P., Schelhaas, M.-J., Schepaschenko, D., Scherer-Lorenzen, M., Schmid, B., Schöngart, J., Searle, E. B., Seben, V., Serra-Diaz, J. M., Sheil, D., Shvidenko, A. Z., Silva-Espejo, J. E., Silveira, M., Singh, J., Sist, P., Slik, F., Sonké, B., Souza, A. F., Stereńczak, K. J., Svenning, J.-C., Svoboda, M., Swanepoel, B., Targhetta, N., Tchebakova, N., ter Steege, H., Thomas, R., Tikhonova, E., Umunay, P. M., Usoltsev, V. A., Valencia, R., Valladares, F., van der Plas, F., Van Do, T., van Nuland, M. E., Vasquez, R. M., Verbeeck, H., Viana, H., Vibrans, A. C., Vieira, S., von Gadow, K., Wang, H.-F., Watson, J. V., Werner, G. D. A., Wisser, S. K., Wittmann, F., Woell, H., Wortel, V., Zagt, R., Zawila-Niedzwiecki, T., Zhang, C., Zhao, X., Zhou, M., Zhu, Z.-X., Zo-Bi, I. C., Gann, G. D., and Crowther, T. W.: Integrated global assessment of the natural forest carbon potential, *Nature*, 10.1038/s41586-023-06723-z, 2023.

Morton, D. C.: FOREST CARBON FLUXES A satellite perspective, *Nature Climate Change*, 6, 346-348, 2016.

Nesha, K., Herold, M., De Sy, V., Duchelle, A., Martius, C., Branthomme, A., Garzuglia, M., Jonsson, O., and Pekkarinen, A.: An assessment of data sources, data quality and changes in national forest monitoring capacities in the Global Forest Resources Assessment 2005-2020, *Environmental Research Letters*, 16, 10.1088/1748-9326/abd81b, 2021.

Nesha, K., Herold, M., De Sy, V., de Bruin, S., Araza, A., Málaga, N., Gamarra, J., Hergoualc'h, K., Pekkarinen, A., Ramirez, C., Morales-Hidalgo, D., and Tavani, R.: Exploring characteristics of national forest inventories for integration with global space-based forest biomass data, *Science of the Total Environment*, 850, 10.1016/j.scitotenv.2022.157788, 2022.

Ochiai, O., Poulter, B., Seifert, F. M., Ward, S., Jarvis, I., Whitcraft, A., Sahajpal, R., Gilliams, S., Herold, M., Carter, S., Duncanson, L. I., Kay, H., Lucas, R., Wilson, S. N., Melo, J., Post, J., Briggs, S., Quegan, S., Dowell, M., Cescatti, A., Crisp, D., Saatchi, S., Tadono, T., Steventon, M., and Rosenqvist, A.: Towards a roadmap for space-based observations of the land sector for the UNFCCC global stocktake, *iScience*, 106489, <https://doi.org/10.1016/j.isci.2023.106489>, 2023.

Ochieng, R., Arts, B., Brockhaus, M., and Visseren-Hamakers, I.: Institutionalization of REDD plus MRV in Indonesia, Peru, and Tanzania: progress and implications, *Ecology and Society*, 23, 10.5751/ES-09967-230208, 2018.

Ochieng, R., Visseren-Hamakers, I., Arts, B., Brockhaus, M., and Herold, M.: Institutional effectiveness of REDD plus MRV: Countries progress in implementing technical guidelines and good governance requirements, *Environmental Science & Policy*, 61, 42-52, 10.1016/j.envsci.2016.03.018, 2016.

Oliver, K. and Cairney, P.: The dos and don'ts of influencing policy: a systematic review of advice to academics, *Palgrave Communications*, 5, 10.1057/s41599-019-0232-y, 2019.

Olofsson, P., Foody, G., Herold, M., Stehman, S., Woodcock, C., and Wulder, M.: Good practices for estimating area and assessing accuracy of land change, *Remote Sensing of Environment*, 148, 42-57, 10.1016/j.rse.2014.02.015, 2014.

Palahi, M., Valbuena, R., Senf, C., Acil, N., Pugh, T., Sadler, J., Seidl, R., Potapov, P., Gardiner, B., Hetemaki, L., Chirici, G., Francini, S., Hlásny, T., Lerink, B., Olsson, H., Olabarria, J., Ascoli, D., Asikainen, A., Bauhus, J., Berndes, G., Donis, J., Fridman, J., Hanewinkel, M., Jactel, H., Lindner, M., Marchetti, M., Marusak, R., Sheil, D., Tome, M., Trasobares, A., Verkerk, P., Korhonen, M., and Nabuurs, G.: Concerns about reported harvests in European forests, *Nature*, 592, E15-E17, 10.1038/s41586-021-03292-x, 2021.

Pan, Y., Birdsey, R. A., Fang, J., Houghton, R., Kauppi, P. E., Kurz, W. A., Phillips, O. L., Shvidenko, A., Lewis, S. L., Canadell, J. G., Ciais, P., Jackson, R. B., Pacala, S. W., McGuire, A. D., Piao, S., Rautiainen, A., Sitch, S., and Hayes, D.: A Large and Persistent Carbon Sink in the World's Forests, *Science*, 333, 988-993, 10.1126/science.1201609, 2011.

Poulter, B., Ochiai, O., Siefert, F.-M., Albergel, C., Dowell, M., Duncanson, L., Gilliams, S., Harris, N., Herold, M., Hunka, N., Friendship-Kay, H., Jarvis, I., Lucas, R., Meijer, Y., Melo, J., Quegan, S., Rosenqvist, A., Sloat, L., Sohl, T., Requena Suarez, D., Viciano, L., Ward, S., Whitcraft, A., and Wilson, S.: CEOS Roadmap for Space-Based Support of Agriculture, Forestry and Other Land Use (AFOLU) Emissions and Removals of Greenhouse Gases. Version 1.0 endorsed by the Principals at the 37th Committee on Earth Observation Satellites Plenary, Thailand November 2023. Last accessed online at: [https://ceos.org/document\\_management/Meetings/Plenary/37/Supporting%20Documents/CEOS\\_AFOLU\\_roadmap\\_FINAL\\_V1.0.pdf](https://ceos.org/document_management/Meetings/Plenary/37/Supporting%20Documents/CEOS_AFOLU_roadmap_FINAL_V1.0.pdf), 2023.

Quegan, S., Toan, L., Chave, J., Dall, J., Exbrayat, J., Minh, D., Lomas, M., D'Alessandro, M., Paillou, P., Papathanassiou, K., Rocca, F., Saatchi, S., Scipal, K.,

Shugart, H., Smallman, T., Soja, M., Tebaldini, S., Ulander, L., Villard, L., and Williams, M.: The European Space Agency BIOMASS mission: Measuring forest above-ground biomass from space, *Remote Sensing of Environment*, 227, 44-60, 10.1016/j.rse.2019.03.032, 2019.

Reiche, J., Lucas, R., Mitchell, A. L., Verbesselt, J., Hoekman, D. H., Haarpaintner, J., Kellndorfer, J. M., Rosenqvist, A., Lehmann, E. A., Woodcock, C. E., Seifert, F. M., and Herold, M.: Combining satellite data for better tropical forest monitoring, *Nature Climate Change*, 6, 120-122, 2016.

Richards, P. D. and VanWey, L.: Farm-scale distribution of deforestation and remaining forest cover in Mato Grosso, *Nature Climate Change*, 6, 418-+, 10.1038/nclimate2854, 2016.

Rignot, E., Salas, W. A., and Skole, D. L.: Mapping deforestation and secondary growth in Rondonia, Brazil, using imaging radar and thematic mapper data, *Remote Sensing of Environment*, 59, 167-179, 10.1016/s0034-4257(96)00150-2, 1997.

Romijn, E., Lantican, C. B., Herold, M., Lindquist, E., Ochieng, R., Wijaya, A., Murdiyarso, D., and Verchot, L.: Assessing change in national forest monitoring capacities of 99 tropical countries, *Forest Ecology and Management*, 352, 109-123, 10.1016/j.foreco.2015.06.003, 2015.

Romijn, E., De Sy, V., Herold, M., Bottcher, H., Roman-Cuesta, R., Fritz, S., Schepaschenko, D., Avitabile, V., Gaveau, D., Verchot, L., and Martius, C.: Independent data for transparent monitoring of greenhouse gas emissions from the land use sector - What do stakeholders think and need?, *Environmental Science & Policy*, 85, 101-112, 10.1016/j.envsci.2018.03.016, 2018.

Rosenqvist, A., Shimada, M., Suzuki, S., Ohgushi, F., Tadono, T., Watanabe, M., Tsuzuku, K., Watanabe, T., Kamijo, S., and Aoki, E.: Operational performance of the ALOS global systematic acquisition strategy and observation plans for ALOS-2 PALSAR-2, *Remote Sensing of Environment*, 155, 3-12, 10.1016/j.rse.2014.04.011, 2014.

Roy, D., Kovalsky, V., Zhang, H., Vermote, E., Yan, L., Kumar, S., and Egorov, A.: Characterization of Landsat-7 to Landsat-8 reflective wavelength and normalized difference vegetation index continuity, *Remote Sensing of Environment*, 185, 57-70, 10.1016/j.rse.2015.12.024, 2016.

Ryan, C. M., Hill, T., Woollen, E., Ghee, C., Mitchard, E., Cassells, G., Grace, J., Woodhouse, I. H., and Williams, M.: Quantifying small-scale deforestation and forest degradation in African woodlands using radar imagery, *Global Change Biology*, 18, 243-257, 10.1111/j.1365-2486.2011.02551.x, 2012.

Saatchi, S. S., Harris, N. L., Brown, S., Lefsky, M., Mitchard, E. T. A., Salas, W., Zutta, B. R., Buermann, W., Lewis, S. L., Hagen, S., Petrova, S., White, L., Silman, M., and Morel, A.: Benchmark map of forest carbon stocks in tropical regions across three continents, *Proceedings of the National Academy of Sciences of the United States of America*, 108, 9899-9904, 10.1073/pnas.1019576108, 2011.

Sannier, C., McRoberts, R. E., and Fichet, L. V.: Suitability of Global Forest Change data to report forest cover estimates at national level in Gabon, *Remote Sensing of Environment*, 173, 326-338, 10.1016/j.rse.2015.10.032, 2016.

Santoro, M., Cartus, O., Carvalhais, N., Rozendaal, D., Avitabile, V., Araza, A., de Bruin, S., Herold, M., Quegan, S., Rodriguez-Veiga, P., Balzter, H., Carreiras, J., Schepaschenko, D., Korets, M., Shimada, M., Itoh, T., Martinez, A., Cavlovic, J., Gatti, R., Bispo, P., Dewnath, N., Labriere, N., Liang, J., Lindsell, J., Mitchard, E., Morel, A., Pascagaza, A., Ryan, C., Slik, F., Laurin, G., Verbeeck, H., Wijaya, A., and Willcock, S.: The global forest above-ground biomass pool for 2010 estimated from high-resolution satellite observations, *Earth System Science Data*, 13, 3927-3950, 10.5194/essd-13-3927-2021, 2021.

Sexton, J. O., Song, X. P., Feng, M., Noojipady, P., Anand, A., Huang, C. Q., Kim, D. H., Collins, K. M., Channan, S., DiMiceli, C., and Townshend, J. R.: Global, 30-m resolution continuous fields of tree cover: Landsat-based rescaling of MODIS vegetation continuous fields with lidar-based estimates of error, *International Journal of Digital Earth*, 6, 427-448, 10.1080/17538947.2013.786146, 2013.

Shimada, M., Itoh, T., Motooka, T., Watanabe, M., Shiraishi, T., Thapa, R., and Lucas, R.: New global forest/non-forest maps from ALOS PALSAR data (2007–2010), *Remote Sensing of Environment*, 155, 13-31, <http://dx.doi.org/10.1016/j.rse.2014.04.014>, 2014.

Shiraishi, T., Motohka, T., Thapa, R. B., Watanabe, M., and Shimada, M.: Comparative Assessment of Supervised Classifiers for Land Use-Land Cover Classification in a Tropical Region Using Time-Series PALSAR Mosaic Data, *Ieee Journal of Selected Topics in Applied Earth Observations and Remote Sensing*, 7, 1186-1199, 10.1109/jstars.2014.2313572, 2014.

Simard, M., Fatoyinbo, T., Smetanka, C., Rivera-monroy, V. H., Castaneda, E., Thomas, N., and Van der stocken, T.: Global Mangrove Distribution, Aboveground Biomass, and Canopy Height [dataset], 2019.

Sinha, S., Jeganathan, C., Sharma, L. K., and Nathawat, M. S.: A review of radar remote sensing for biomass estimation, *International Journal of Environmental Science and Technology*, 12, 1779-1792, 10.1007/s13762-015-0750-0, 2015.

Sirro, L., Häme, T., Rauste, Y., Kilpi, J., Hämäläinen, J., Gunia, K., de Jong, B., and Pellat, F.: Potential of Different Optical and SAR Data in Forest and Land Cover Classification to Support REDD plus MRV, *Remote Sensing*, 10, 10.3390/rs10060942, 2018.

Skole, D., Mbow, C., Mugabowindekwe, M., Brandt, M., and Samek, J.: Trees outside of forests as natural climate solutions, *Nature Climate Change*, 11, 1013-1016, 10.1038/s41558-021-01230-3, 2021.

Spracklen, B. D., Kalamandeen, M., Galbraith, D., Gloor, E., and Spracklen, D. V.: A Global Analysis of Deforestation in Moist Tropical Forest Protected Areas, *Plos One*, 10, 10.1371/journal.pone.0143886, 2015.

- Stehman, S.: Estimating area from an accuracy assessment error matrix, *Remote Sensing of Environment*, 132, 202-211, 10.1016/j.rse.2013.01.016, 2013.
- Toan, T.L., Beaudoin, A., Riom, J. and Guyon, D.: Relating forest biomass to SAR data. *IEEE Transactions on Geoscience and Remote Sensing*. 30(2), pp.403-411, 1992.
- Tomppo, E., Gschwantner, T., Lawrence, M., McRoberts R.E.: *National Forest Inventories: Pathways for Common Reporting*, Springer, Netherlands, 10.1007/978-90-481-3233-1, 2010
- Torres, R., Snoeij, P., Geudtner, D., Bibby, D., Davidson, M., Attema, E., Potin, P., Rommen, B., Floury, N., Brown, M., Traver, I., Deghaye, P., Duesmann, B., Rosich, B., Miranda, N., Bruno, C., L'Abbate, M., Croci, R., Pietropaolo, A., Huchler, M., and Rostan, F.: GMES Sentinel-1 mission, *Remote Sensing of Environment*, 120, 9-24, 10.1016/j.rse.2011.05.028, 2012.
- Tropek, R., Sedlacek, O., Beck, J., Keil, P., Musilova, Z., Simova, I., and Storch, D.: Comment on "High-resolution global maps of 21st-century forest cover change", *Science*, 344, 3, 10.1126/science.1248753, 2014.
- Tyukavina, A., Baccini, A., Hansen, M. C., Potapov, P. V., Stehman, S. V., Houghton, R. A., Krylov, A. M., Turubanova, S., and Goetz, S. J.: Aboveground carbon loss in natural and managed tropical forests from 2000 to 2012, *Environmental Research Letters*, 10, 14, 10.1088/1748-9326/10/7/074002, 2015.
- Tyukavina, A., Stehman, S. V., Potapov, P. V., Turubanova, S. A., Baccini, A., Goetz, S. J., Laporte, N. T., Houghton, R. A., and Hansen, M. C.: National-scale estimation of gross forest aboveground carbon loss: a case study of the Democratic Republic of the Congo, *Environmental Research Letters*, 8, 10.1088/1748-9326/8/4/044039, 2013.
- UNEP: *Emissions Gap Report 2023: Broken Record – Temperatures hit new highs, yet world fails to cut emissions (again)*, Nairobi, 2023.
- UNFCCC: 'Report of the Conference of the Parties on its sixteenth session, held in Cancun from 29 November to 10 December 2010'. Addendum (FCCC/CP/2010/7/Add.1), 2011.
- UNFCCC: *The Warsaw Framework for REDD-plus*, 2014.
- UNFCCC: 'Decision 19/CMA.1: Adoption of the Paris Agreement', 2015.
- UNFCCC: 'Decision 19/CMA.1: Matters relating to article 14 of the Paris Agreement and paragraphs 99–101 of decision 1/CP.21', 2019a.
- UNFCCC: 'Annex to decision 18/CMA.1: Modalities, procedures and guidelines for the transparency framework for action and support referred to in Article 13 of the Paris Agreement'. 2019b.
- UNFCCC: *Nationally determined contributions under the Paris Agreement. Synthesis report by the secretariat*, 2022.

UNFCCC: Technical dialogue of the first global stocktake. Synthesis report by the co-facilitators on the technical dialogue, 2023a.

UNFCCC: REDD+ web platform. Technical assessment process of forest reference level/forest reference emission level (FREL/FRL) submissions (available at: <https://redd.unfccc.int/fact-sheets/forest-reference-emission-levels.html>) (Accessed December 2023b)

UNFCCC: BUR portal. Biennial Update Report submissions by Non-Annex I Parties (available at: <https://unfccc.int/BURs>) (Accessed December 2023c)

van der Werf, G. R., Randerson, J. T., Giglio, L., Collatz, G. J., Mu, M., Kasibhatla, P. S., Morton, D. C., DeFries, R. S., Jin, Y., and van Leeuwen, T. T.: Global fire emissions and the contribution of deforestation, savanna, forest, agricultural, and peat fires (1997-2009), *Atmospheric Chemistry and Physics*, 10, 11707-11735, 10.5194/acp-10-11707-2010, 2010.

Vancutsem, C., Achard, F., Pekel, J., Vieilledent, G., Carboni, S., Simonetti, D., Gallego, J., Aragao, L., and Nasi, R.: Long-term (1990-2019) monitoring of forest cover changes in the humid tropics, *Science Advances*, 7, 10.1126/sciadv.abe1603, 2021.

Vogeler, J., Braaten, J., Slesak, R., and Falkowski, M.: Extracting the full value of the Landsat archive: Inter-sensor harmonization for the mapping of Minnesota forest canopy cover (1973-2015), *Remote Sensing of Environment*, 209, 363-374, 10.1016/j.rse.2018.02.046, 2018.

Walker, W. S., Stickler, C. M., Kellndorfer, J. M., Kirsch, K. M., and Nepstad, D. C.: Large-Area Classification and Mapping of Forest and Land Cover in the Brazilian Amazon: A Comparative Analysis of ALOS/PALSAR and Landsat Data Sources, *IEEE Journal of Selected Topics in Applied Earth Observations and Remote Sensing*, 3, 594-604, 10.1109/jstars.2010.2076398, 2010.

WMO: World Meteorological Congress approves Global Greenhouse Gas Watch. Press Release Number: 24052023, 24 May 2023. Last access online at: <https://public-old.wmo.int/en/media/press-release/world-meteorological-congress-approves-global-greenhouse-gas-watch>, 2023.

Zanaga, D., Van De Kerchove, R., De, Keersmaecker, W., Souverijns, N., Brockmann, C., Quast, R., Wevers, J., Grosu, A., Paccini, A., Vergnaud, S., Cartus, O., Santoro, M., Fritz, S., Georgieva, I., Lesiv, M., Carter, S., Herold, M., Li, L., Tsendbazar, N. E., Ramoino, F., and Arino, O.: ESA WorldCover 10 m 2020 v100 (Version v100) [Data set], 2021.

Zarin, D. J., Harris, N. L., Baccini, A., Aksenov, D., Hansen, M. C., Azevedo-Ramos, C., Azevedo, T., Margono, B. A., Alencar, A. C., Gabris, C. S., Allegretti, A., Potapov, P., Farina, M., Walker, W. S., Shevade, V. S., Loboda, T. V., Turubanova, S., and Tyukavina, A.: Can carbon emissions from tropical deforestation drop by 50% in 5 years?, *Global Change Biology*, 22, 1336-1347, 10.1111/gcb.13153, 2016.

Zhao, K. G., Popescu, S., and Nelson, R.: Lidar remote sensing of forest biomass: A scale-invariant estimation approach using airborne lasers, *Remote Sensing of Environment*, 113, 182-196, 10.1016/j.rse.2008.09.009, 2009.



## **Chapter 2. Satellite-based global maps are rarely used in forest reference levels submitted to the UNFCCC**

### **Abstract**

The Earth Observation (EO) community is coordinating a range of activities in support of the Global Stocktake. One objective is to enhance the uptake of satellite-based global-scale maps (hereafter ‘EO products’) in national GHG inventories submitted to the UNFCCC. To measure progress towards this objective, we compile information on the use of EO products on land cover, fire, and above-ground biomass to derive carbon flux estimates in forest reference levels from 56 tropical countries submitted to the UNFCCC between 2014-2022. The Global Forest Change (GFC) was the only EO product used to measure land extent and change, and was used by almost half the countries. Only two countries used existing EO products for fire mapping. Four countries used biomass maps, although only indirectly, such as for comparing with biomass estimates from field plot measurements or with IPCC defaults. The uptake is limited but improved the MRV capacity of 22 countries. The relatively high uptake of the GFC demonstrates the importance of meeting essential conditions in the IPCC guidance when developing EO products, including conditions on spatial and temporal resolution, temporal coverage and consistency, and the flexibility to adapt to biophysical thresholds in national definitions. The limited use of other global land EO products underlines the need for developers of EO products to interact with groups responsible for GHG inventories and experts familiar with IPCC guidance so that their products are suitable for national reporting, and thus contribute to more complete aggregated estimates in the Global Stocktake.

**Keywords:** tropical forests, REDD+, LULUCF, GHG inventory, global stocktake, research & systematic observation, Earth observation

## 2.1 Contributions and Acknowledgements

The following research chapter was published in Environmental Research Letters on 21 February 2023. Its full content is presented here as it appears in its published form having only been re-formatted and Tables and Figures renumbered for a uniform layout through the thesis. Supplementary information for this chapter is available in Appendix 1 of this thesis. The citation of the published paper is:

Melo J, Baker T, Nemitz D, Quegan S and Ziv G 2023 Satellite-based global maps are rarely used in forest reference levels submitted to the UNFCCC. Environ. Res. Lett. 18 034021. <https://doi.org/10.1088/1748-9326/acba31>

**Authors:** Joana Melo<sup>1</sup>, Timothy Baker<sup>1</sup>, Dirk Nemitz<sup>2</sup>, Shaun Quegan<sup>3</sup> and Guy Ziv<sup>1</sup>

### Affiliations and addresses

<sup>1</sup>School of Geography, University of Leeds, Woodhouse Lane, Leeds LS2 9JT, United Kingdom

<sup>2</sup>Basque Centre For Climate Change (BC3), Edificio Sede, Campus EHU, Leioa, Spain

<sup>3</sup>School of Mathematics and Statistics, University of Sheffield, Sheffield S3 7RH, United Kingdom

**Author contributions:** JM, TRB and GZ designed and conceived the study. JM and DN conceived the database for data collection. JM compiled and analysed the data. JM wrote the manuscript. All co-authors provided critical feedback to the text, figures and tables.

**Acknowledgements:** JM was funded by the Natural Environment Research Council (NERC), UK, through the Leeds–York NERC Doctoral Training Partnership (grant number NE/L002574/1). JM acknowledges the Committee on Earth Observation Satellites (CEOS) task teams working on contributions from the AFOLU sector to the Global Stocktake and the Biomass Harmonization sub-group for the exchange of views and feedback provided. The authors thank Marieke Sandker for her contribution to the quality control of the attribution of AD method used in the submissions flagged as low confidence in our study. The authors acknowledge the constructive comments from two anonymous reviewers.

## 2.2 Introduction

Forests play a key role in the pledges made by countries towards meeting Paris Agreement (UNFCCC, 2015) targets, mostly through reducing carbon emissions from deforestation or enhancement of carbon removals from large afforestation programmes (Grassi et al., 2017). However, measuring and tracking these contributions from the land use, land use change and forestry (LULUCF) sector is complex, and the corresponding estimates of greenhouse gas (GHG) fluxes have high uncertainties (Friedlingstein et al., 2022). The Global Stocktake, running in 2021-2023 and to be repeated in 5-year cycles, will use aggregated information from national submissions to the United Nations Framework Convention on Climate Change (UNFCCC), complemented by independent inputs (e.g., IPCC assessment reports), to assess the collective progress in achieving the objectives of the Paris Agreement. For the process to be effective in informing policy makers on the role of forests and land use in achieving carbon neutrality, the high levels of uncertainty in the estimates of GHG fluxes from land must be reduced.

Global maps derived from satellite-based Earth observation (hereafter 'EO products') are considered fundamental in addressing this problem, as a practical means to consistently monitor large-scale and remote land areas at high spatial and temporal resolutions (Defries et al., 2007; Achard and House, 2015; Romijn et al., 2018; Herold et al., 2019). Such global capabilities can support country Parties to the UNFCCC in measuring fluxes from LULUCF and in fulfilling their reporting obligations, namely the national GHG inventories that form an integral part of the Global Stocktake (**Table 2.1**). This is particularly relevant for tropical countries, where domestic GHG inventories are neither frequent nor complete (Grassi et al., 2022; Federici et al., 2017).

The international EO community monitoring the land surface has responded spectacularly to the needs of the Global Stocktake (CEOS, 2021; ESA, 2022; Hegglin et al., 2022). Firstly, space agencies are making large investments to launch new missions (e.g. Landsat 8, GEDI, BIOMASS, NISAR) dedicated to measuring land dynamics, forest structure and biomass using a combination of sensor types (Quegan et al., 2019; Dubayah et al., 2020). Secondly, there is an unprecedented degree of collaboration between international groups on harmonizing methods and improving the accuracy and policy-relevance of EO products (Araza et al., 2022; Tsendbazar et al., 2021; Szantoi et al., 2020; Labriere et al., 2022). Finally, partnerships with technology platforms allow free and easy dissemination and processing of EO products (Gorelick et al., 2017) which should facilitate their uptake in reports to the UNFCCC and support the operationalization of the Paris Agreement (**Table 2.1**). Nonetheless, it is unclear how extensively the wide

range of EO products offered by the EO community (**Table 2.2**) are being used in national reporting and thus is contributing to the Global Stocktake.

**Table 2.1.** Examples of key uses and opportunities for Earth Observation products in the core elements of the Paris Agreement (UNFCCC, 2015)(corresponding article in brackets). Satellites can only measure the land surface, so only the above-ground biomass pool is considered here within emission and removal factors (EF/RF).

Element of the Paris Agreement	Opportunities for satellite data and derived products ('EO products')
updating nationally determined contributions (NDCs)  (Art. 4)	<ul style="list-style-type: none"> <li>- quantitative metrics to derive quantitative targets and to obtain GHG targets from non-GHG targets.</li> </ul>
reducing emissions from deforestation and forest degradation in developing countries (REDD+)  (Art. 5)	<ul style="list-style-type: none"> <li>- estimation of activity data (land area change, AD) and emission/removal factors (biomass change, EF/RF) for establishing forest reference levels (FRLs) and report REDD+ results in a technical annex to the Biennial Transparency Report (BTR) in the context of accessing results-based payments,</li> <li>- assessment of drivers of forest changes and corresponding carbon fluxes for REDD+ strategies,</li> <li>- independent data sources for comparison by the assessment teams / UNFCCC LULUCF experts or to constraint the estimates by the Party (verification).</li> </ul>
national reporting under the enhanced transparency framework  (Art. 13)	<ul style="list-style-type: none"> <li>- estimation of carbon emissions and removals from forests, and non-forest areas with significant woody biomass (i.e., cropland/ grassland) in the GHG inventory (GHGi) and biennial transparency reports (BTRs; including AD and EF/RFs for all categories), and to track progress of the quantitative indicators of the NDCs,</li> <li>- supporting tools for Parties with lower Measurement, Reporting and Verification (MRV) capacity who will need to adapt to the more stringent reporting rules (previous non-Annex I Parties),</li> <li>- Independent data sources for verification and to support assessment teams in the technical expert review of BTRs.</li> </ul>
global stocktake  (Art. 14)	<ul style="list-style-type: none"> <li>- contribution to inputs (first phase) to each cycle of the Global Stocktake (taking place every five years), and its collective view on progress to achieve the objectives of the Paris Agreement, through country-Party submissions (NDCs, REDD+, GHGi/BTR, see above) and independent estimates by non-Party stakeholders.</li> </ul>

**Table 2.2.** Examples of existing satellite-based global-scale maps (or Earth Observation products in the text) on land-cover, land-cover change, fire, and above-ground biomass (AGB) covering the tropics. Many of these products are identified as being key for the land sector by the research and systematic observation community (ESA, 2022). Because the focus of our study is on country uptake for domestic GHG inventories and on consistent global monitoring for the Global Stocktake, we have excluded datasets with spatial resolutions coarser than 1-km and with only regional to local coverage. Maps produced with Earth observations from airborne data are not included.

Earth Observation products (global/pantropical scope)		spatial resolution	temporal coverage	theme/units
<b>land cover and land cover change</b>				
NASA MODIS Land Cover MCD12Q1	(Friedl et al., 2010)	500-m	2001-present (yearly)	class (in 6 different legends)
Global Land Cover Facility Tree-canopy	(Sexton et al., 2013)	30-m	2000, 2005, 2010, 2015	percent tree-cover
Global Forest Change	(Hansen et al., 2013)	30-m	2000 2000-present (yearly)	percent tree-cover class loss
JAXA Forest Non-Forest maps	(Shimada et al., 2014)	25-m	2000-present 2007-2010 (yearly), 2015-2021 (yearly)	class year of gain class (Forest, Non-Forest)
CCI Land cover maps	(ESA, 2017)	300-m	1992-present (yearly)	class (hierarchical)
Global Mangrove Watch	(Bunting et al., 2018)	25-m	1996, 2007-2010 (yearly), 2015-2020 (yearly)	class
Copernicus Land Cover	(Buchhorn et al., 2020)	100-m	2015-2019 (yearly)	class (hierarchical) + cover fraction
Global Mangrove Loss drivers	(Goldberg et al., 2020)	30-m	2000-2005; 2005-2010; 2010-2015	Class
HILDA+ Global Land-Use Change reconstruction	(Winkler et al., 2021)	1-km	1960-2019 (yearly)	class (6 + change)
WorldCover	(Zanaga et al., 2021)	10-m	2020; 2021 (planned)	Class
Sentinel-2 Land-Use/Land-Cover	(Karra et al., 2021)	10-m	2017-2021 (yearly)	class (10, including "trees")
Global Land Cover Mapping and Estimation (GLanCE)	(Arevalo et al., 2022)	30-m	2001-2019 (yearly)	class (7, including 'tree-cover')
<b>fire</b>				
Copernicus Burned Area	(Tansey et al., 2008)	300-m	2014-present	class
MODIS Active Fire MOD14A1	(Giglio et al., 2016)	1-km	2000-present (monthly)	class
MODIS Burned Area MCD64A1	(Giglio et al., 2018)	500-m	2001-present (daily)	class
VIIRS S-NPP NOAA-20 hotspots	(Schroeder and Giglio, 2018)	375-m	2012-present	class
CCI-Fire Burned Area	(Lizundia-Loiola et al., 2020)	250-m	2001-present	class
<b>above-ground biomass</b>				
NASA JPL	(Saatchi et al., 2011)	1-km	2003-2004	Mg/ha
WHRC Pantropical AGB map	(Baccini et al., 2012)	500-m	2007-2008	MgC/ha
GEOCARBON (map fusion)	(Avitabile et al., 2016)	1-km	2003-2008	Mg/ha
GlobBiomass growing stock and AGB	(Santoro et al., 2018; Santoro et al., 2021)	100-m	2010	m <sup>3</sup> /ha; Mg/ha
Global Mangrove AGB	(Simard et al., 2019)	30-m	2000	Mg/ha
CCI Biomass	(Santoro et al., 2021)	100-m	2010, 2017, 2018	Mg/ha
AGB Change, Pantropical Belt	(Baccini et al., 2021)	500-m	2003-2016	Mg C/ha/yr
NASA GEDI footprint product	(Duncanson et al., 2022)	25-m	2019-2021	Mg/ha
NASA GEDI gridded product	(Dubayah et al., 2022)	1-km	2019-2021	Mg/ha

We therefore present a compilation of information on the use of satellite data, specifically global EO products developed from satellite data, for estimating carbon fluxes from the LULUCF sector in the reporting from country Parties to the UNFCCC. The overall objective is to evaluate if the global capabilities provided by these new opportunities are being exploited in the national reporting obligations to the UNFCCC, and thus to assess the extent to which the decade-long investment in developing EO products is effective in supporting national aspects of international climate policy (Oliver and Cairney, 2019; Findlater et al., 2021). While other studies aggregate data from reports to the UNFCCC to explain the large differences in carbon flux estimates from different sources (Deng et al., 2022; Grassi et al., 2022), here we focus on the satellite-based data and methods that are used to ingest EO products. We also focus on tropical developing countries, where remote sensing contributions to forest monitoring are larger (Nesha et al., 2021), GHG inventories are scarcer and less complete, and Measurement, Reporting and Verification (MRV) capacity has improved through REDD+ (Federici et al., 2017). We include data from 56 countries with 75 submissions to the UNFCCC under the MRV for REDD+ Framework (UNFCCC, 2014) from 2014 and up to 2022. We seek to understand: i) if satellite data, and specifically the numerous products offered by the EO community, are being used; ii) which ones are used; and iii) how they contribute to quantifying the domestic carbon fluxes from the LULUCF sector. This provides a basis for identifying which products are effective in this sector, and why. It also highlights the challenges to wider use of existing and planned products.

## **2.3 Methods**

We compile data from all the forest reference emission levels/forest reference levels (FREL/FRLs) to date submitted voluntarily to the UNFCCC over the almost 10 years of the REDD+ framework (UNFCCC, 2014). We use the term FRL regardless of whether removals are included (typically FRL) or only emissions are reported (typically FREL). Our analysis covers 56 countries and 75 FRLs submitted since 2014. Combined, these submissions cover a forest area of over 1.5 billion ha, which is over 1/3 of global forest area and more than 80% of the forest land in the tropical domain (Fao, 2020b). We group the submissions by geopolitical regional groups recognized by the UN and the group of Least Developed Countries (LDCs) which overlap with the regional groups. Of the 75 FRLs included in our analysis, six are still undergoing technical assessment (cut-off date December 2022). For the 69 that have completed the assessment we also extracted information from the technical reports prepared by the LULUCF expert reviewers. Annexes to the 75 FRLs or other auxiliary information, if made available by the Party, were also reviewed. All the information used is accessible in the REDD+ portal

(UNFCCC, 2022a) and through web links within each submission. The overview database prepared by the UNFCCC secretariat (UNFCCC, 2022b) was used for quality control and as an alert for new submissions or for submissions completing the technical assessment process and with technical assessment reports available for inspection (**Figure 2-1**).

In each submission we identify the use of satellite data (e.g., Landsat imagery) and EO products (or satellite-based global maps as in **Table 2.2**) for land cover and land cover change, fire and above-ground biomass to estimate the IPCC variables related to activity data (area and area change, AD), and emission or removal factors (biomass and biomass change, EF/RF). We separate the different ways in which EO products can contribute to estimating AD from i) 'deforestation', and ii) 'other REDD+ activities' (all classes can be mapped to the IPCC categories used in GHG inventories, see Appendix 1; **Table A.1.1**), and also whether they were used iii) as auxiliary data, or iv) to map fire occurrences associated with either deforestation or forest degradation. These are 'direct' contributions to deriving AD. The use of EO products for EFs is only disaggregated into uses to directly estimate carbon fluxes from i) 'deforestation' and ii) 'other REDD+ activities'. We further identify 'indirect contributions' of EO products if they are not used directly to estimate one of the variables (AD or EF) but are used, for example, to support decisions and compare/constrain national estimates (verification).

Finally, to understand if other methodological choices determine the use or preference for certain satellite data sources, including EO products, we identify which of three methods was selected by the country to derive AD: i) 'pixel-counting', where areas of change are obtained by comparing two (or more) wall-to-wall maps or direct change detection wall-to-wall maps are produced; ii) 'stratified area estimation' (Olofsson et al., 2014), where the classification bias of the areas from the wall-to-wall map is corrected using a reference dataset (i.e., better quality data, such as photo-interpretation from higher resolution imagery or use of field data); and iii) 'sampling', when AD estimates are derived from a reference dataset and calculated directly from sample proportions without using areas from a map.

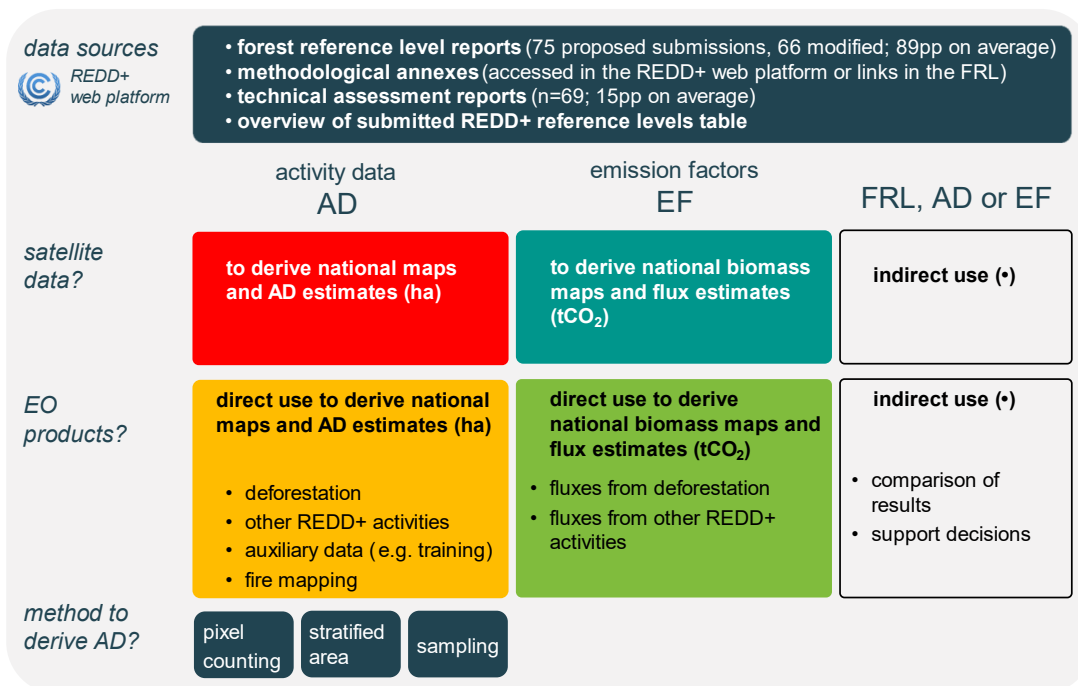


**Figure 2-1.** List of all data sources used in this study (accessed through the UNFCCC REDD+ Web platform, (UNFCCC, 2022a), and methodological steps in the analysis. For each of the 75 forest reference level (FRL) submissions, we checked if: i) satellite data (e.g., Landsat imagery) or ii) EO products (satellite-based global maps, see examples in **Table 2.2**) were used in their development; if so, for which element of the FRL (AD - activity data or EF - emission factors) and in which way (direct or indirect use). In addition, we identify iii) which method was used to derive AD. For clarity, the colour scheme and symbol • match the legend of the figures and tables in the results section.

## 2.4 Results

Satellite data, mostly Landsat imagery or imagery accessed through the Collect Earth platform (combining a time series of Google Earth, Bing Maps, Landsat, Sentinel, SPOT and RapidEye images), were used by all countries to produce their own maps or estimates for the FRL, in particular as a data source for forest change data (AD; red quadrants, **Figure 2-2**). EO products were used by 46% of the countries (n=26; lower quadrants **Figure 2-2**), but this proportion varied with geopolitical/negotiating groupings: 70% of LDCs (noting the overlap with regional groups), 65% of African States, 50% of Asian States, but only 25% of Latin American and the Caribbean (LAC) States used EO products. Hence, the regional group with highest proportion of countries submitting FRLs (more than 60% of LAC countries submitted at least one FRL) is also the group relying less on EO products to derive their FRLs (**Figure 2-2a**; **Figure A.1.1**).

All countries using EO products to derive AD (n=24 or 43% of the total countries with FRL submissions; yellow quadrants, **Figure 2-2**) relied on a single product—the Global Forest Change (GFC) product (Hansen et al., 2013). Submitted FRLs show that national technical teams found ingenious ways to adapt and integrate the GFC product into their monitoring systems, even to directly estimate deforestation and other forest dynamics

and land-use transitions ('other REDD+ activities') (n=16; **Table 2.3, Table 2.4, Table A.1.2**). For example, tree cover or tree cover loss or gain data were resampled to pixel blocks matching the minimum mapping unit of the national definition and combined with domestic maps or a reference dataset for the correct attribution of land uses in cases of tree crops, shifting agriculture, harvest and oil palm plantations (e.g., Bhutan, Equatorial Guinea, Madagascar, Sri Lanka). The GFC product was also used in combination with other data, including very high resolution imagery, to train a map classifier (e.g., Ethiopia, Zambia, Tanzania) or to correct mapped areas (e.g., Honduras). Furthermore, 14 countries used it indirectly, e.g., for quality control or verification by comparing the estimates produced with national data with the deforestation magnitude and trends of the GFC product (n=9).

Technical teams found creative ways of using the GFC product regardless of the technique employed to derive AD (**Figure 2-3, Table 2.4**), although more than half of the available examples are from FRLs using a 'stratified area estimate' approach. There is a trend for countries to move away from purely pixel-counting techniques using wall-to-wall mapping ( $p < 0.001$ , 95%CI) to a combination of wall-to-wall maps with a reference dataset to correct the bias of the map-based estimates (as recommended by Olofsson et al (2014b) and GFOI (2020);  $p > 0.1$ , 95%CI) or to probabilistic sampling methods using either a stratified or systematic approach ( $p < 0.001$ , 95%CI). This trend is closely linked to a change in preferred data sources, since the latter two methods rely heavily on very high resolution imagery. It is noteworthy that in the past two years there are no examples of use of EO products to directly estimate AD.

The use of satellite data to derive information on biomass and biomass change (EF/RF) is much less common. Just three countries used satellite imagery to produce their own biomass maps, from ALOS (Zambia 2017) or Landsat (Honduras for forest degradation and Togo, 2020) and no country used available global biomass maps (**Table 2.3, Table 2.4**). National Forest Inventory (NFI) plot measurements are the main source of biomass data (61%), sometimes complemented with IPCC defaults and additional field data (23%). If an NFI was not available, countries used a combination of other sources such as harmonized plot data, literature, and IPCC defaults (38%), or even biomass data from neighbouring countries (n=2) (**Table A.1.2**). Two biomass maps (Saatchi et al., 2011; Baccini et al., 2012) were explored in four (5%) submissions (from Congo, Equatorial Guinea, Guyana, and Mozambique; **Table 2.3, Table A.1.2**). However, they were only used indirectly, for example to compare estimates with the reported values in the FRL (verification). The use of EO products is also negligible for fire mapping (**Table 2.3**). Of the 16 countries including emissions from forest fires or non-CO<sub>2</sub> emissions from

biomass burning from deforestation, only two used EO products to estimate AD for burnt areas (Ghana and Indonesia), and another (Equatorial Guinea) used them simply to justify omitting these fluxes.

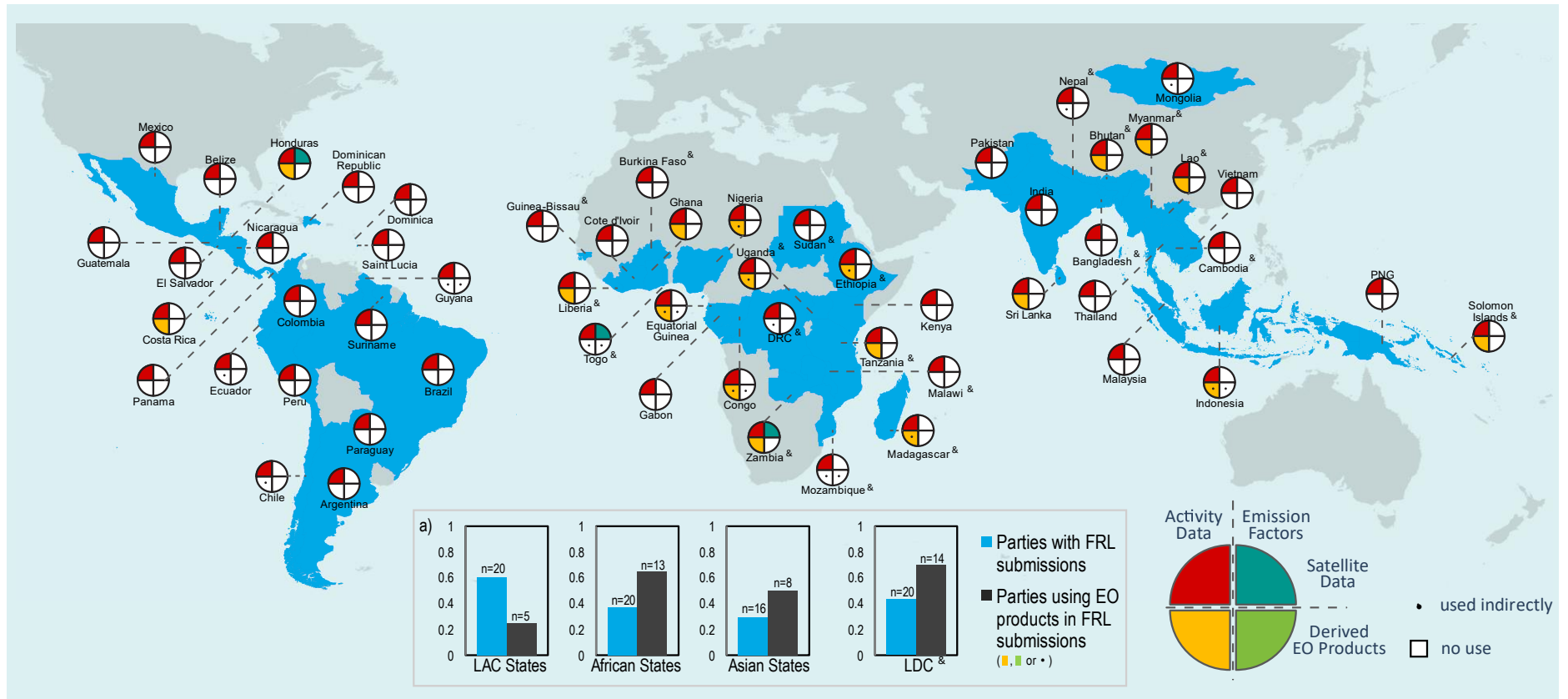


**Figure 2-2.** Location of the 56 country Parties to the UNFCCC that submitted 75 forest reference emission levels / forest reference levels (FREL/FRL) to the UNFCCC from 2014 up to 2022. The colour scheme in the quadrant charts shows the use of satellite data (e.g., Landsat imagery) and derived products (i.e., satellite-based global maps in **Table 2.2** or ‘EO products’ in the text) to directly derive Activity Data (AD, left-hand quadrants in red and yellow respectively), and Emission Factors (EF, right-hand quadrants in teal and green respectively). Indirect uses of EO products are represented with a • mark in a quadrant (e.g., use for validation, to justify decisions, to adjust the FREL/FRL, or for comparison of reported estimates). See **Table 2.4** for more details on what is considered direct and indirect contributions and **Table A.1.2** for details on the specific ways country Parties use the data. Use of maps produced from airborne technology are not included. Panel a) shows the proportion of developing country Parties that have submitted at least one FREL/FRL (blue bars) and proportion within those that submitted at least one FREL/FRL using ‘EO products’ in their FREL/FRL (black bars; including direct and indirect use of EO products depicted in the widgets in yellow and green and with a • mark). Country Parties are separated in panel a) by geopolitical regional groups recognized by the UN—Latin American and the Caribbean (LAC) States, African States, Asian States—and the negotiating Party group defined as Least Developed Countries (LDCs, marked with the & symbol). Note that the 56 countries with FREL/FRL submissions are part of one of the three regional groups while 20 of them are also designated by the UN as LDCs. See **Figure A.1.1** for more information on MRV capacity indicators separated by Party groupings.

**Table 2.3.** All the global maps derived from satellite-data ('EO products') used by 26 out of the 56 countries that submitted a forest reference emission levels/forest reference levels (FREL/FRL) to the UNFCCC between 2014 and 2022 and ways in which these products were used: to directly derive Activity Data (AD; yellow box) and Emission Factors (EF; green box) or contributing indirectly to the FREL/FRL. Colours and symbols (yellow, green and • match the legend of **Figure 2-1** and **Figure 2-2**). Uses for AD are separated into deriving information on 'deforestation', on 'other REDD+ activities', as auxiliary data (e.g., as training data or to correct the maps), and to map fire occurrences. Uses for emission factors are separated into deriving information on 'deforestation' and 'other REDD+ activities'. Unlisted countries (from the 56 with submitted FREL/FRL) used no EO product in their FRLs, or if one was used, it is not clearly identified in the submission and supporting documentation. Dash (-) denotes no use. \* Togo compared emission results with data from the Global Forest Watch relying on the Global Forest Change (Hansen et al., 2013) product. Totals are total number of countries. Note countries can appear repeated in the same column or row.

EO products used	activity data				emission factors		indirect contribution (*)		total countries
	deforestation	other REDD+ activities	auxiliary data	fire mapping	deforest.	other REDD+ activities	support decisions assumptions adjustments	comparison of results	
<b>land cover and land cover change</b>									
Global Forest Change (GFC)	(10) Bhutan Congo Costa Rica Equat.Guinea Liberia Madagascar Myanmar Nigeria Solom.Islands Sri Lanka	(6) Bhutan Costa Rica Equat.Guinea Liberia Solom.Islands Sri Lanka	(6) Ethiopia Honduras Lao Tanzania Uganda Zambia	-	-	-	(6) Congo DRC Indonesia Madagascar Nigeria	(9) Chile Ecuador Ethiopia Indonesia Mongolia Mozambique Nepal Togo* Uganda Zambia	<b>24</b>
<b>fire</b>									
MODIS Burned Area	-	-	-	(1) Ghana	-	-	(1) Equatorial Guinea	-	<b>2</b>
MODIS Active Fire	-	-	-	(1) Indonesia	-	-	-	-	<b>1</b>
NOAA fire hotspots	-	-	-	(1) Indonesia	-	-	-	-	<b>1</b>
<b>above-ground biomass</b>									
Saatchi et al. (2011)	-	-	-	-	-	-	-	(3) Congo Equat.Guinea Mozambique	<b>3</b>
Baccini et al., (2012)	-	-	-	-	-	-	(1) Guyana	(1) Congo	<b>2</b>
<b>total countries</b>		<b>18</b>			<b>0</b>		<b>16</b>		<b>26</b>

**Table 2.4.** Examples of how this study classifies the different contributions from products derived from satellite data (EO products) found in forest reference emission level/forest reference level (FREL/FRL) submissions to the UNFCCC. The main classification of EO product uses is as i) a direct contribution to derive activity data (AD; highlighted in yellow), ii) a direct contribution to derive emission factors (EFs; in green; n.a. because no examples of uptake were found) and iii) indirect contributions related to either AD or EFs (in white). See more details at country level in **Table A.1.2**

classes of EO product uses	examples of uses found in reference level submissions (Party, year of submission)	
activity data (AD)	direct use for 'deforestation'	- filling cloud gaps (Costa Rica 2016); - produce wall-to-wall forest non-forest maps by adjusting or tree-cover and tree-cover change to national definitions or combining it with national layers (Bhutan 2020, Congo 2016, Costa Rica 2016, Liberia 2020, Madagascar 2017 and 2018, Nigeria 2018 and 2019, Sri Lanka 2017); - support the classification of sample units (Solomon Islands 2019) or segments (Equatorial Guinea 2020);
	direct use for 'other REDD+ activities'	- 'pixel-counting' approach (Costa Rica 2016, Madagascar 2017); - stratification in a 'stratified area estimation' approach (Bhutan 2020, Congo 2016, Equatorial Guinea 2020, Liberia 2020, Madagascar 2018, Myanmar 2018, Nigeria 2018 and 2019, Sri Lanka 2017); - 'sampling' approach (Solomon Islands 2019).
	auxiliary data	- training data (Ethiopia 2016, Tanzania 2017, Uganda 2017, Zambia 2016); - map correction (Honduras 2017, Lao 2018, Zambia 2021).
	fire mapping	- burned areas mapping (Ghana 2017); - supporting the mapping (Indonesia 2022); - validating burned areas (Indonesia 2022).
emission factors (EF)	direct use for 'deforestation'	n.a.
	direct use for 'other REDD+ activities'	n.a.
indirect contribution (*)	- map validation (Madagascar 2017); - justification of omission of activities and gases (Equatorial Guinea 2020, Nigeria 2019); - supporting the choice of tree canopy threshold to define forest land (DRC 2018, Equatorial Guinea 2020); - adjusting the FRL (Guyana 2015; Congo 2016); - comparing estimates by the Party (Congo 2016, Equatorial Guinea 2020, Ethiopia 2016, Mozambique 2018, Nepal 2017, Togo 2020, Uganda 2017) or the assessment team (Chile 2016, Congo 2016, Ecuador 2015, Zambia 2016); - support decisions on the intensification of the sampling grid (Mongolia 2018); - stratification to support the spatial distribution of field plots for biomass measurements (Indonesia 2022).	

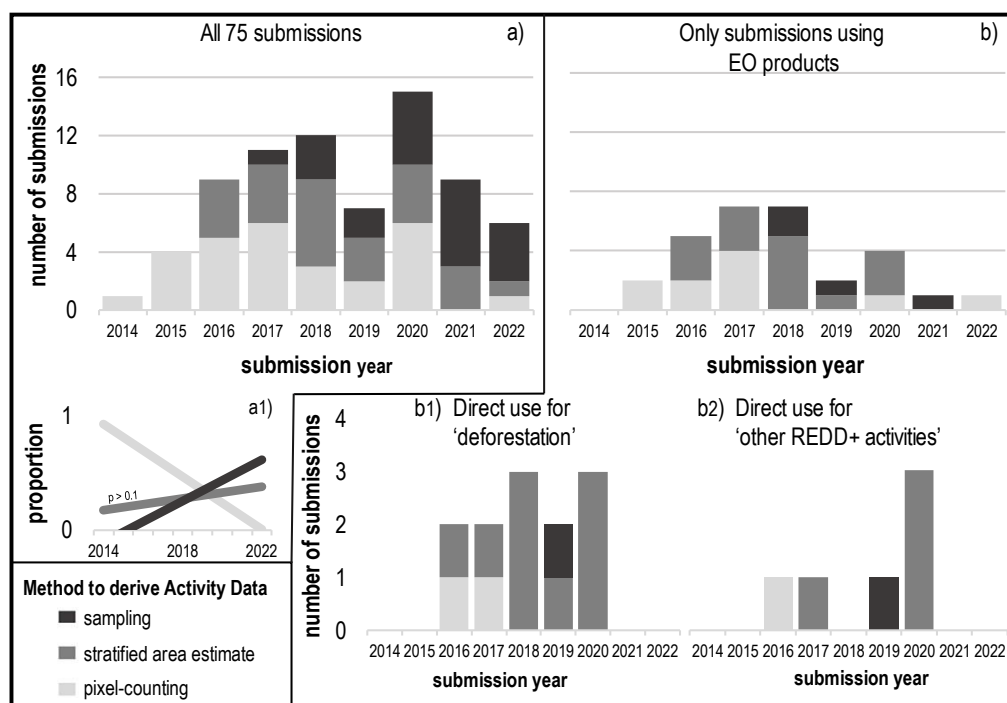


**Figure 2-3.** Number of forest reference emission levels / forest reference levels (FREL/FRL) submissions to the UNFCCC per year since 2014 and up to 2022 separated by technique employed to generate Activity Data (AD): pixel-counting, stratified area estimate, or sampling. [continues in next page.....]

Panel a) includes all the 75 submissions to date with a1) showing the trend of the annual proportion of submissions using each AD technique. The trend is statistically significant (at 95% CI) for 'pixel-counting' ( $p$ -value < 0.001) and 'sampling' approaches ( $p$ -value < 0.001) but not for 'stratified area estimate' ( $p$ -value = 0.374). Panel b) shows only those submissions using products derived from satellite data ( $n = 29$ ; 29 submissions from 26 country-Parties with Madagascar, Nigeria and Zambia using Earth Observation products in their two submissions; see **Table 2.4**); and further separated into submissions using Earth Observation products b1) to directly derive AD for deforestation ( $n = 11$  including all 9 countries in **Table 2.3**, with Madagascar and Nigeria using it in their two submissions) or b2) to directly derive any of the other REDD+ activities ( $n=6$ ).

## 2.5 Discussion

Given the wealth of products offered by the EO community (**Table 2.2** shows just the most prominent examples and some of their characteristics), the most striking finding from this study is the lack of diversity in those used for AD and their very limited use to map fire and support estimates of EFs. Below we explore some of the issues surrounding this observation.

### 2.5.1. IPCC considerations for area representation: national definitions, spatial and temporal resolution, temporal coverage and consistency

The GFC (Hansen et al., 2013) is the only EO product used to estimate AD, consistent with studies highlighting its suitability to produce estimates of forest area at both global (Harris et al., 2021) and national scales if local maps are not available (McRoberts et al., 2016). Reasons for its use in almost half the FRLs, and preference to other global land EO products, include its flexibility, which allows it to be adapted to different national definitions of forest land. The GFC includes a layer of percentage tree cover per Landsat pixel for the year 2000 and annual loss layers corresponding to the removal of all tree cover in a Landsat pixel. As a result, countries using the GFC selected the percentage tree cover matching the biophysical thresholds in their national definition of forest land (which always includes canopy cover thresholds, and varies between 10 and 60% among countries studied here, **Table A.1.2**) and integrated it with national data to produce AD. We found examples in 10 submissions (see **Table 2.4** and **Table A.1.2**). Alternative global maps with more rigid thematic classes (e.g., MODIS land cover, JAXA F/NF, CCI land cover; **Table 2.2**) are not broadly applicable and equally accurate at national level (Li et al., 2016; Tsendbazar et al., 2015; Tsendbazar et al., 2017) given the wide variation of canopy cover thresholds used to define forest, i.e., they cannot simultaneously match the forest definitions of all countries.

Land cover maps with a spatial resolution coarser than the minimum area that defines forest at national level were never used in FRL submissions. Most countries select either 0.5-ha or 1-ha as the minimum area of land in their national definitions (51% and 39% of submissions, respectively; **Table A.1.2**). EO products with spatial resolutions coarser or

finer than the corresponding 70-m and 100-m do not accurately depict forest and forest change extent. For example, coarser pixels may include mixed classes from the national definitions and miss small-scale dynamics (Milodowski et al., 2017a; Kalamandeen et al., 2018; Ganzenmuller et al., 2022). For finer resolutions, FRLs using the GFC (30-m pixels, or approximately 0.09-ha) resampled the data to the minimum mapping unit matching the national definition of forest so as not to overestimate the area of forest and deforestation. For example, Zambia in 2016 used the GFC aggregated into 5x5 pixel blocks to create an initial training dataset for stable forest, non-forest and deforestation (**Table A.1.2**; see also Bhutan, Congo).

Temporal resolution, coverage and consistency are also important considerations (IPCC, 2019; GFOI, 2020; Herold et al., 2019). FRLs estimate yearly fluxes and most have reference periods of 10 to 15 years. EO products need to be available and comparable over time, as well as consistently applied to the entire time series. Starting in the year 2000, with annual estimates of total tree cover loss, and described as globally consistent, the GFC product is the only example from **Table 2.2** meeting those requirements. Products that are not annual (i.e., coarser temporal resolutions) may miss land dynamics such as harvest and conversions to tree crops (Woodcock et al., 2020; Pengra et al., 2020). Discontinuation (e.g., GLCF; (Sexton et al., 2013)) or unexpected interruptions (JAXA Forest / Non-Forest; (Shimada et al., 2014)) of EO products at equivalent spatial resolutions could have prevented their use. Note that recent studies highlight a temporal inconsistency also in the GFC product attributed to changes in the algorithm (Ceccherini et al., 2021; Palahi et al., 2021). Temporal inconsistencies in fact exist in all EO products, even those from the long-running Landsat programme, because of sensor degradation or sensor and technology changes between successive missions (Roy et al., 2016; Vogeler et al., 2018).

Temporal inconsistencies and the biases they introduce may help explain why countries are relying more on reference data, most commonly a sample dataset of visually-interpreted imagery with high spatial resolution available through the Collect Earth platform (**Table A.1.2**; **Figure 2-3**). In the last three years 70% of the submissions used a reference dataset to estimate AD. While 40% stratified the sample with a map (including the GFC product), as recommended to reduce omission errors (Olofsson et al., 2020), 30% relied only on the samples. This trend towards reduced dependency on wall-to-wall maps to derive AD can partially explain the limited uptake of EO products. The need for compliance with IPCC good practice and reporting of uncertainty may also help explain this trend. Pixel-counting methods introduce bias in the estimate from map classification errors, and the map accuracies derived from error matrices do not quantify that bias, as required by the IPCC guidelines (McRoberts, 2011; Olofsson et al., 2013).

Another reason for the transition in methods to derive AD is related to attribution: while land cover can be obtained from EO, and is typically used as a proxy for land-use, the two are not the same. We find countries are using sampling methods and visual interpretation of very high resolution imagery to identify complex land dynamics, and to distinguish plantations, tree crops, shifting agriculture and trees outside forest, in order to attribute these areas to the correct class according to the national land classification. Such attribution is not possible with EO products alone (Tropek et al., 2014; Curtis et al., 2018; GFOI, 2020). For example, the Bangladesh FRL identifies that more than 50% of mapped tree canopy cover is from trees outside forest (Potapov et al., 2017). Solomon Islands used Collect Earth to correct cases of harvest and replanting of oil palm (cropland) identified in the GFC as forest loss. Similarly, Guinea-Bissau manually corrected the land cover maps and noted in its FRL that 74% of the corrected pixels corresponded to cashew trees (a tree crop) being mapped as forest (Melo et al., 2018). Ghana changed its AD approach from pixel-counting (in the 2017 submission) to systematic sampling (in the 2021 submission), resulting in a change in the deforestation (AD) estimate from around 312,000 to around 18,000 ha per year in the same reference period (i.e., deforestation estimate with the systematic sampling approach rendered a deforestation estimate which is only 6% of that obtained with pixel-counting). Ghana noted in its FRL that using very high resolution imagery as source of AD allowed the proper disaggregation of tree crops from forest which had led to the overestimation of the AD in the 2017 submission.

However, we note that in this transition towards sampling-based methods for deriving AD (including 'stratified area estimate' and 'sampling' in this study) the bias of the reference data is never quantified in the FRLs. Such bias can be substantial due to interpretation errors and to the temporal inconsistencies of the available imagery, given that the tropics do not have good coverage by very high resolution imagery, especially for a reference period of 10-15 years (McRoberts et al., 2018; Schepaschenko et al., 2019; Lesiv et al., 2018; Pengra et al., 2020).

### **2.5.2. Limited uptake of global biomass maps**

None of the available above-ground biomass EO products were used to estimate EFs. The only ways they were used, and only in the submissions of four countries, was as independent estimates to compare and enhance the confidence in the national above-ground biomass values used to derive EFs, or, in Guyana, to adjust the national historical emission trend with a global emission level to predict future emissions more accurately. Using EO products for verification (i.e., comparing with national estimates) was the only example of implementation of the 2019 Refinement to the 2006 IPCC Guidelines, now including a section on the use of above-ground biomass EO products. Similarly to AD,

when reporting the uncertainty of EFs, national teams need to document the precision of the estimates through confidence intervals. However, none of the biomass EO products from **Table 2.2**, except the most recent ones using GEDI data (Dubayah et al., 2022; Duncanson et al., 2022), provide the required variances and covariances (McRoberts et al., 2022; GFOI, 2020). There are examples on how to improve the precision of NFI plot-based estimates with global EO products of above-ground biomass (Naesset et al., 2016; Naesset et al., 2020; Malaga et al., 2022), but there has been no implementation of these methods in FRLs.

### **2.5.3. Regional differences in the uptake of EO products**

Our study reveals a higher uptake of EO products by countries from Party groupings with lower forest monitoring capacity (African States and LDCs; **Figure 2-2, Figure A.1.1**) and highlights the important role of EO products in enhancing these countries' MRV capacity. This finding is consistent with a recent study from Nisha et al (2021) on forest monitoring capacity in reporting to the FAO, where the authors conclude that despite remaining lower than in other regional groups, the remote sensing capacity of African States has increased significantly between 2015 and 2020. It also confirms that developing countries' capacity to report GHG fluxes from LULUCF to the UNFCCC has been increasing with REDD+ investments (Federici et al., 2017) (**Figure A.1.1**). For 80% (n=45) of the developing countries implementing REDD+ activities, submission of the FRL was their first experience of reporting GHG fluxes from LULUCF and going through a technical review under the UNFCCC (**Table A.1.3**). Half of those countries (n=22) did so while using EO products in their FRL. Furthermore, as of December 2022, there were 13 countries submitting a FRL with the support of EO products that have not yet submitted any biennial update report. The contribution of EO products can, therefore, be more prominent if the capacity built for FRLs leverages the development of GHG inventories. This is an important conclusion because strategically selecting collaborations with national teams with lower MRV capacity, who rely more on the EO products offered, will support their transition to the more stringent reporting requirements of the Paris Agreement. At the same time, it contributes to a more complete global time-series of carbon fluxes obtained from the aggregation of national GHG inventories in the Global Stocktake.

### **2.5.4. Transparency of reference level submissions and limitations of the analysis**

Of the 75 submissions included in our analysis, 69 have completed technical assessment. Of those, 75% (n=52) are described by the expert reviewers in the technical assessment report as being 'transparent and in overall accordance with the guidance'.

However, the remaining submissions ranged from ‘mostly transparent’ to ‘not sufficiently transparent’, with the experts flagging the need for including more detail on the data sources and methods. The limitations of this study due to lack of transparency in at least 25% of the submissions are twofold:

- Possible underestimation of the use of EO products due to our inability to find all data sources used. For example, maps were used for stratification but were not adequately documented in the FRL submission and accompanying methodological annexes. To minimize this source of bias we assumed that the technical assessment report had priority over the FRL, given that experts have access to more information that is not publicly shared. For example, Equatorial Guinea does not clearly describe how the GFC layers “were superimposed over the maps to help to classify AD” but because it is in the technical assessment report, we attributed a direct contribution of GFC in deriving AD.
- Possible underestimation of the direct use of EO products to derive AD due to poor descriptions of the methods. For example, any incorrect definitions of the AD method as ‘sampling’ instead of ‘stratified area estimate’ will lead to an incorrect classification of the use of the EO product as indirect instead of direct (e.g., Myanmar, Mongolia). In our analysis, eight submissions (10%) were flagged with low confidence in the attribution of the method used to derive AD because the FRL submission was not clear or our classification disagreed with FAO analysis on REDD+ FRL (FAO, 2020a). Of these eight submissions, three (4%) used the GFC product. To address this uncertainty, for these submissions, we relied on personal communications with the national technical teams to attribute the method used (e.g., Nigeria, see **Table A.1.2**).

## 2.6 Conclusions

Analysis of the use of satellite data and derived EO products by 56 developing country Parties to the UNFCCC in 75 REDD+ forest reference levels indicates that the only land EO product used was the GFC; this was used by 43% (n=24) of the countries, with 29% (n=16) using it directly to estimate AD. The number of countries using EO products to map burnt areas (n=2) and to estimate emission factors (n=0) is negligible. However, the GFC and pantropical biomass maps were used for verification (n=9 and n=3, respectively) by countries and expert reviewers. There is a trend towards using probabilistic sampling methods that do not rely on wall-to-wall mapping to quantify land dynamics ( $p < 0.001$ , 95%CI), which can partially explain a limited uptake of land maps. Nevertheless, overall, the availability of EO products enhances MRV capacity: 70% of LDCs and 65% of African States with FRL submissions relied on EO products, and for

22 of the countries using EO products in their submission, this was their first reviewing process under the UNFCCC. This analysis may help the EO community by clarifying the properties EO land products must have for their effective take-up by countries in their reporting for the land use sector. Fostering collaboration with experts familiar with IPCC guidance can help in the design of EO products and facilitate their integration into national reporting, and hence enable more complete GHG inventories and increase confidence in the data used by the Global Stocktake process.

## 2.7 References

Achard, F. & House, J. I. (2015) Reporting carbon losses from tropical deforestation with Pantropical biomass maps. *Environmental Research Letters*, 10(10), 3.

Araza, A., de Bruin, S., Herold, M., Quegan, S., Labriere, N., Rodriguez-Veiga, P., Avitabile, V., Santoro, M., Mitchard, E., Ryan, C., Phillips, O., Willcock, S., Verbeeck, H., Carreiras, J., Hein, L., Schelhaas, M., Pacheco-Pascagaza, A., Bispo, P., Laurin, G., Vieilledent, G., Slik, F., Wijaya, A., Lewis, S., Morel, A., Liang, J., Sukhdeo, H., Schepaschenko, D., Cavlovic, J., Gilani, H. & Lucas, R. (2022) A comprehensive framework for assessing the accuracy and uncertainty of global above-ground biomass maps. *Remote Sensing of Environment*, 272.

Arevalo, P., Stanimirova, R., Bullock, E., Zhang, Y., Tarrío, K., Turlej, K., Hu, K., McAvoy, K., Pasquarella, V., Woodcock, C., Olofsson, P., Zhu, Z., Gorelick, N., Loveland, T., Barber, C. & Friedl, M. (2022) Global Land Cover Mapping and Estimation Yearly 30 m V001 [Data set]. NASA EOSDIS Land Processes DAAC. Available at <https://doi.org/10.5067/MEaSURES/GLanCE/GLanCE30.001> (last accessed December 2022).

Avitabile, V., Herold, M., Heuvelink, G. B. M., Lewis, S. L., Phillips, O. L., Asner, G. P., Armston, J., Ashton, P. S., Banin, L., Bayol, N., Berry, N. J., Boeckx, P., de Jong, B. H. J., DeVries, B., Girardin, C. A. J., Kearsley, E., Lindsell, J. A., Lopez-Gonzalez, G., Lucas, R., Malhi, Y., Morel, A., Mitchard, E. T. A., Nagy, L., Qie, L., Quinones, M. J., Ryan, C. M., Ferry, S. J. W., Sunderland, T., Laurin, G. V., Gatti, R. C., Valentini, R., Verbeeck, H., Wijaya, A. & Willcock, S. (2016) An integrated pan-tropical biomass map using multiple reference datasets. *Global Change Biology*, 22(4), 1406-1420.

Baccini, A., Goetz, S. J., Walker, W. S., Laporte, N. T., Sun, M., Sulla-Menashe, D., Hackler, J., Beck, P. S. A., Dubayah, R., Friedl, M. A., Samanta, S. & Houghton, R. A. (2012) Estimated carbon dioxide emissions from tropical deforestation improved by carbon-density maps. *Nature Climate Change*, 2(3), 182-185.

Baccini, A., Walker, W., Carvalho, L. E., Farina, M. K., Solvik, K. K. & Sulla-Menashe, D. (2021) Aboveground Biomass Change for Amazon Basin, Mexico, and Pantropical Belt, 2003-2016. ORNL Distributed Active Archive Center.

Buchhorn, M., Lesiv, M., Tsendbazar, N., Herold, M., Bertels, L. & Smets, B. (2020) Copernicus Global Land Cover Layers-Collection 2. *Remote Sensing*, 12(6).

Bunting, P., Rosenqvist, A., Lucas, R. M., Rebelo, L.-M., Hilarides, L., Thomas, N., Hardy, A., Itoh, T., Shimada, M. & Finlayson, C. M. (2018) The Global Mangrove Watch—A New 2010 Global Baseline of Mangrove Extent. *Remote Sensing*, 10(10), 1669.

Ceccherini, G., Duveiller, G., Grassi, G., Lemoine, G., Avitabile, V., Pilli, R. & Cescatti, A. (2021) Concerns about reported harvests in European forests Reply to Wernick, I. K. et al.; Palahi, M. et al. *Nature*, 592(7856), E18-E23.

CEOS (2021) A Committee on Earth Observation Satellites Strategy to Support the Global Stocktake of the UNFCCC Paris Agreement, version 3.1. Available at: [https://ceos.org/observations/documents/GST\\_Strategy\\_Paper\\_V3.1.pdf](https://ceos.org/observations/documents/GST_Strategy_Paper_V3.1.pdf) (last accessed: October 2022).

Curtis, P., Slay, C., Harris, N., Tyukavina, A. & Hansen, M. (2018) Classifying drivers of global forest loss. *Science*, 361(6407), 1108-1111.

DeFries, R., Achard, F., Brown, S., Herold, M., Murdiyarso, D., Schlamadinger, B. & de Souza, C. (2007) Earth observations for estimating greenhouse gas emissions from deforestation in developing countries. *Environmental Science & Policy*, 10(4), 385-394.

Deng, Z., Ciais, P., Tzompa-Sosa, Z., Saunois, M., Qiu, C., Tan, C., Sun, T., Ke, P., Cui, Y., Tanaka, K., Lin, X., Thompson, R., Tian, H., Yao, Y., Huang, Y., Lauerwald, R., Jain, A., Xu, X., Bastos, A., Sitch, S., Palmer, P., Lauvaux, T., d'Aspremont, A., Giron, C., Benoit, A., Poulter, B., Chang, J., Petrescu, A., Davis, S., Liu, Z., Grassi, G., Albergel, C., Tubiello, F., Perugini, L., Peters, W. & Chevallier, F. (2022) Comparing national greenhouse gas budgets reported in UNFCCC inventories against atmospheric inversions. *Earth System Science Data*, 14(4), 1639-1675.

Dubayah, R., Armston, J., Healey, S., Bruening, J., Patterson, P., Kellner, J., Duncanson, L., Saarela, S., Stahl, G., Yang, Z., Tang, H., Blair, J., Fatoyinbo, L., Goetz, S., Hancock, S., Hansen, M., Hofton, M., Hurr, G. & Luthcke, S. (2022) GEDI launches a new era of biomass inference from space. *Environmental Research Letters*, 17(9).

Dubayah, R., Blair, J. B., Goetz, S., Fatoyinbo, L., Hansen, M., Healey, S., Hofton, M., Hurr, G., Kellner, J., Luthcke, S., Armston, J., Tang, H., Duncanson, L., Hancock, S., Jantz, P., Marselis, S., Patterson, P. L., Qi, W. & Silva, C. (2020) The Global Ecosystem Dynamics Investigation: High-resolution laser ranging of the Earth's forests and topography. *Science of Remote Sensing*, 1, 100002.

Duncanson, L., Kellner, J., Armston, J., Dubayah, R., Minor, D., Hancock, S., Healey, S., Patterson, P., Saarela, S., Marselis, S., Silva, C., Bruening, J., Goetz, S., Tang, H., Hofton, M., Blair, B., Luthcke, S., Fatoyinbo, L., Abernethy, K., Alonso, A., Andersen, H., Aplin, P., Baker, T., Barbier, N., Bastin, J., Biber, P., Boeckx, P., Bogaert, J., Boschetti, L., Boucher, P., Boyd, D., Burslem, D., Calvo-Rodriguez, S., Chave, J., Chazdon, R., Clark, D., Clark, D., Cohen, W., Coomes, D., Corona, P., Cushman, K., Cutler, M., Dalling, J., Dalponte, M., Dash, J., de-Miguel, S., Deng, S., Ellis, P., Erasmus, B., Fekety, P., Fernandez-Landa, A., Ferraz, A., Fischer, R., Fisher, A., Garcia-Abril, A., Gobakken, T., Hacker, J., Heurich, M., Hill, R., Hopkinson, C., Huang, H., Hubbell, S., Hudak, A., Huth, A., Imbach, B., Jeffery, K., Katoh, M., Kearsley, E., Kenfack, D., Kljun, N., Knapp, N., Kral, K., Krucek, M., Labriere, N., Lewis, S., Longo, M., Lucas, R., Main, R., Manzanera, J., Martinez, R., Mathieu, R., Memiaghe, H., Meyer, V., Mendoza, A., Moneris, A., Montesano, P., Morsdorf, F., Naesset, E., Naidoo, L., Nilus, R., O'Brien,

M., Orwig, D., Papathanassiou, K., Parker, G., Philipson, C., Phillips, O., Pisek, J., Poulsen, J., Pretzsch, H., Rudiger, C., et al (2022) Aboveground biomass density models for NASA's Global Ecosystem Dynamics Investigation (GEDI) lidar mission. *Remote Sensing of Environment*, 270.

ESA (2017) Land Cover CCI Product User Guide Version 2. Available at: [maps.elie.ucl.ac.be/CCI/viewer/download/ESACCI-LC-Ph2-PUGv2\\_2.0.pdf](https://maps.elie.ucl.ac.be/CCI/viewer/download/ESACCI-LC-Ph2-PUGv2_2.0.pdf) (last accessed: October 2022).

ESA (2022) The Role of Systematic Earth Observations in the Global Stocktake. Version 28 February. Available at: <https://unfccc.int/documents/462475> (last accessed: October 2022).

FAO (2020a) From reference levels to results reporting: REDD+ under the United Nations Framework Convention on Climate Change. 2020 update. Rome. FAO. Available at <https://doi.org/10.4060/cb1635en>.

FAO (2020b) Global Forest Resources Assessment 2020: Main report. Rome. Available at: <https://doi.org/10.4060/ca9825en> (last accessed December 2022).

Federici, S., Grassi, G., Harris, N., Lee, D., Neeff, T., Penman, J., Sanz, M. J. & Wolosin, M. (2017) GHG Fluxes from Forests: An assessment of national GHG estimates and independent research in the context of the Paris Agreement. Available at: <https://www.climateandlandusealliance.org/reports/ghg-fluxes-forests/> (last accessed October 2022).

Findlater, K., Webber, S., Kandlikar, M. & Donner, S. (2021) Climate services promise better decisions but mainly focus on better data. *Nature Climate Change*, 11(9), 731-+.

Friedl, M. A., Sulla-Menashe, D., Tan, B., Schneider, A., Ramankutty, N., Sibley, A. & Huang, X. M. (2010) MODIS Collection 5 global land cover: Algorithm refinements and characterization of new datasets. *Remote Sensing of Environment*, 114(1), 168-182.

Friedlingstein, P., Jones, M., O'Sullivan, M., Andrew, R., Bakker, D., Hauck, J., Le Quere, C., Peters, G., Peters, W., Pongratz, J., Sitch, S., Canadell, J., Ciais, P., Jackson, R., Alin, S., Anthoni, P., Bates, N., Becker, M., Bellouin, N., Bopp, L., Chau, T., Chevallier, F., Chini, L., Cronin, M., Currie, K., Decharme, B., Djeutchouang, L., Dou, X., Evans, W., Feely, R., Feng, L., Gasser, T., Gilfillan, D., Gkritzalis, T., Grassi, G., Gregor, L., Gruber, N., Gurses, O., Harris, I., Houghton, R., Hurtt, G., Iida, Y., Ilyina, T., Lujckx, I., Jain, A., Jones, S., Kato, E., Kennedy, D., Goldewijk, K., Knauer, J., Korsbakken, J., Kortzinger, A., Landschutzer, P., Lauvset, S., Lefevre, N., Lienert, S., Liu, J., Marland, G., McGuire, P., Melton, J., Munro, D., Nabel, J., Nakaoka, S., Niwa, Y., Ono, T., Pierrot, D., Poulter, B., Rehder, G., Resplandy, L., Robertson, E., Rodenbeck, C., Rosan, T., Schwinger, J., Schwingshackl, C., Seferian, R., Sutton, A., Sweeney, C., Tanhua, T., Tans, P., Tian, H., Tilbrook, B., Tubiello, F., van der Werf, G., Vuichard, N., Wada, C., Wanninkhof, R., Watson, A., Willis, D., Wiltshire, A., Yuan, W., Yue, C., Yue, X., Zaehle, S. & Zeng, J. (2022) Global Carbon Budget 2021. *Earth System Science Data*, 14(4), 1917-2005.

Ganzenmuller, R., Bultan, S., Winkler, K., Fuchs, R., Zabel, F. & Pongratz, J. (2022) Land-use change emissions based on high-resolution activity data substantially lower than previously estimated. *Environmental Research Letters*, 17(6).

GFOI (2020) Integration of remote-sensing and ground-based observations for estimation of emissions and removals of greenhouse gases in forests: Methods and Guidance from the Global Forest Observations Initiative, Edition 3.0.: Available at: <https://www.reddcompass.org/mgd/resources/GFOI-MGD-3.1-en.pdf> (last access October 2022).

Giglio, L., Boschetti, L., Roy, D., Humber, M. & Justice, C. (2018) The Collection 6 MODIS burned area mapping algorithm and product. *Remote Sensing of Environment*, 217, 72-85.

Giglio, L., Schroeder, W. & Justice, C. (2016) The collection 6 MODIS active fire detection algorithm and fire products. *Remote Sensing of Environment*, 178, 31-41.

Goldberg, L., Lagomasino, D., Thomas, N. & Fatoyinbo, T. (2020) Global declines in human-driven mangrove loss. *Global Change Biology*, 26(10), 5844-5855.

Gorelick, N., Hancher, M., Dixon, M., Ilyushchenko, S., Thau, D. & Moore, R. (2017) Google Earth Engine: Planetary-scale geospatial analysis for everyone. *Remote Sensing of Environment*, 202, 18-27.

Grassi, G., Conchedda, G., Federici, S., Abad Viñas, R., Korosuo, A., Melo, J., Rossi, S., Sandker, M., Somogyi, Z., Vizzarri, M. & Tubiello, F. N. (2022) Carbon fluxes from land 2000–2020: bringing clarity to countries' reporting. *Earth Syst. Sci. Data*, 14(10), 4643-4666.

Grassi, G., House, J., Dentener, F., Federici, S., den Elzen, M. & Penman, J. (2017) The key role of forests in meeting climate targets requires science for credible mitigation. *Nature Climate Change*, 7(3), 220-+.

Hansen, M. C., Potapov, P. V., Moore, R., Hancher, M., Turubanova, S. A., Tyukavina, A., Thau, D., Stehman, S. V., Goetz, S. J., Loveland, T. R., Kommareddy, A., Egorov, A., Chini, L., Justice, C. O. & Townshend, J. R. G. (2013) High-Resolution Global Maps of 21st-Century Forest Cover Change. *Science*, 342(6160), 850-853.

Harris, N., Gibbs, D., Baccini, A., Birdsey, R., de Bruin, S., Farina, M., Fatoyinbo, L., Hansen, M., Herold, M., Houghton, R., Potapov, P., Suarez, D., Roman-Cuesta, R., Saatchi, S., Slay, C., Turubanova, S. & Tyukavina, A. (2021) Global maps of twenty-first century forest carbon fluxes. *Nature Climate Change*, 11(3).

Hegglin, M. I., Bastos, A., Bovensmann, H., Buchwitz, M., Fawcett, D., Ghent, D., Kulk, G., Sathyendranath, S., Shepherd, T. G., Quegan, S., Röthlisberger, R., Briggs, S., Buontempo, C., Cazenave, A., Chuvieco, E., Ciais, P., Crisp, D., Engelen, R., Fadnavis, S., Herold, M., Horwath, M., Jonsson, O., Kpaka, G., Merchant, C. J., Mielke, C., Nagler, T., Paul, F., Popp, T., Quaife, T., Rayner, N. A., Robert, C., Schröder, M., Sitch, S., Venturini, S., van der Schalie, R., van der Vliet, M., Wigneron, J.-P. & Woolway, R. I. (2022) Space-based Earth observation in support of the UNFCCC Paris Agreement. *Frontiers in Environmental Science*, 10.

Herold, M., Carter, S., Avitabile, V., Espejo, A., Jonckheere, I., Lucas, R., McRoberts, R., Naesset, E., Nightingale, J., Petersen, R., Reiche, J., Romijn, E., Rosenqvist, A., Rozendaal, D., Seifert, F., Sanz, M. & De Sy, V. (2019) The Role and Need for Space-Based Forest Biomass-Related Measurements in Environmental Management and Policy. *Surveys in Geophysics*, 40(4), 757-778.

IPCC (2019) 2019 Refinement to the 2006 IPCC Guidelines for National Greenhouse Gas Inventories. Prepared by the IPCC Task Force on National Greenhouse Gas Inventories. Institute for Global Environmental Strategies (IGES). ISBN 978-4-88788-232-4.

Kalamandeen, M., Gloor, E., Mitchard, E., Quincey, D., Ziv, G., Spracklen, D., Spracklen, B., Adami, M., Aragao, L. & Galbraith, D. (2018) Pervasive Rise of Small-scale Deforestation in Amazonia. *Scientific Reports*, 8.

Karra, K., Kontgis, C., Statman-Weil, Z., Mazzariello, J., Mathis, M. & Brumby, S. (2021) Global land use/land cover with Sentinel-2 and deep learning. *IEEE International Geoscience and Remote Sensing Symposium IGARSS*, 2021, pp. 4704-4707, doi: 10.1109/IGARSS47720.2021.9553499.

Labriere, N., Davies, S., Disney, M., Duncanson, L., Herold, M., Lewis, S., Phillips, O., Quegan, S., Saatchi, S., Schepaschenko, D., Scipal, K., Sist, P. & Chave, J. (2022) Toward a forest biomass reference measurement system for remote sensing applications. *Global Change Biology*.

Lesiv, M., See, L., Bayas, J., Sturn, T., Schepaschenko, D., Karner, M., Moorthy, I., McCallum, I. & Fritz, S. (2018) Characterizing the Spatial and Temporal Availability of Very High Resolution Satellite Imagery in Google Earth and Microsoft Bing Maps as a Source of Reference Data. *Land*, 7(4).

Li, W., Ciais, P., MacBean, N., Peng, S. S., Defourny, P. & Bontemps, S. (2016) Major forest changes and land cover transitions based on plant functional types derived from the ESA CCI Land Cover product. *International Journal of Applied Earth Observation and Geoinformation*, 47, 30-39.

Lizundia-Loiola, J., Oton, G., Ramo, R. & Chuvieco, E. (2020) A spatio-temporal active-fire clustering approach for global burned area mapping at 250 m from MODIS data. *Remote Sensing of Environment*, 236.

Malaga, N., de Bruin, S., McRoberts, R., Olivos, A., Paiva, R., Montesinos, P., Suarez, D. & Herold, M. (2022) Precision of subnational forest AGB estimates within the Peruvian Amazonia using a global biomass map. *International Journal of Applied Earth Observation and Geoinformation*, 115.

McRoberts, R. (2011) Satellite image-based maps: Scientific inference or pretty pictures? *Remote Sensing of Environment*, 115(2), 715-724.

McRoberts, R., Naesset, E., Saatchi, S. & Quegan, S. (2022) Statistically rigorous, model-based inferences from maps. *Remote Sensing of Environment*, 279.

McRoberts, R., Stehman, S., Liknes, G., Naesset, E., Sannier, C. & Walters, B. (2018) The effects of imperfect reference data on remote sensing-assisted estimators of land cover class proportions. *Isprs Journal of Photogrammetry and Remote Sensing*, 142, 292-300.

McRoberts, R. E., Vibrans, A. C., Sannier, C., Naesset, E., Hansen, M. C., Walters, B. F. & Lingner, D. V. (2016) Methods for evaluating the utilities of local and global maps for increasing the precision of estimates of subtropical forest area. *Canadian Journal of Forest Research*, 46(7), 924-932.

Melo, J., Ziv, G., Baker, T., Carreiras, J., Pearson, T. & Vasconcelos, M. (2018) Striking divergences in Earth Observation products may limit their use for REDD. *Environmental Research Letters*, 13(10).

Milodowski, D., Mitchard, E. & Williams, M. (2017) Forest loss maps from regional satellite monitoring systematically underestimate deforestation in two rapidly changing parts of the Amazon. *Environmental Research Letters*, 12(9).

Naasset, E., McRoberts, R., Pekkarinen, A., Saatchi, S., Santoro, M., Trier, O., Zahabu, E. & Gobakken, T. (2020) Use of local and global maps of forest canopy height and aboveground biomass to enhance local estimates of biomass in miombo woodlands in Tanzania. *International Journal of Applied Earth Observation and Geoinformation*, 93.

Naasset, E., Orka, H. O., Solberg, S., Bollandasas, O. M., Hansen, E. H., Mauya, E., Zahabu, E., Malimbwi, R., Chamuya, N., Olsson, H. & Gobakken, T. (2016) Mapping and estimating forest area and aboveground biomass in miombo woodlands in Tanzania using data from airborne laser scanning, TanDEM-X, RapidEye, and global forest maps: A comparison of estimated precision. *Remote Sensing of Environment*, 175, 282-300.

Nesha, K., Herold, M., De Sy, V., Duchelle, A., Martius, C., Branthomme, A., Garzuglia, M., Jonsson, O. & Pekkarinen, A. (2021) An assessment of data sources, data quality and changes in national forest monitoring capacities in the Global Forest Resources Assessment 2005-2020. *Environmental Research Letters*, 16(5).

Oliver, K. & Cairney, P. (2019) *The dos and don'ts of influencing policy: a systematic review of advice to academics*. Palgrave Communications, 5.

Olofsson, P., Arevalo, P., Espejo, A., Green, C., Lindquist, E., McRoberts, R. & Sanz, M. (2020) Mitigating the effects of omission errors on area and area change estimates. *Remote Sensing of Environment*, 236.

Olofsson, P., Foody, G. M., Herold, M., Stehman, S. V., Woodcock, C. E. & Wulder, M. A. (2014) Good practices for estimating area and assessing accuracy of land change. *Remote Sensing of Environment*, 148, 42-57.

Olofsson, P., Foody, G. M., Stehman, S. V. & Woodcock, C. E. (2013) Making better use of accuracy data in land change studies: Estimating accuracy and area and quantifying uncertainty using stratified estimation. *Remote Sensing of Environment*, 129, 122-131.

Palahi, M., Valbuena, R., Senf, C., Acil, N., Pugh, T., Sadler, J., Seidl, R., Potapov, P., Gardiner, B., Hetemaki, L., Chirici, G., Francini, S., Hlásny, T., Lerink, B., Olsson, H., Olabarria, J., Ascoli, D., Asikainen, A., Bauhus, J., Berndes, G., Donis, J., Fridman, J., Hanewinkel, M., Jactel, H., Lindner, M., Marchetti, M., Marusak, R., Sheil, D., Tome, M., Trasobares, A., Verkerk, P., Korhonen, M. & Nabuurs, G. (2021) Concerns about reported harvests in European forests. *Nature*, 592(7856), E15-E17.

Pengra, B. W., Stehman, S. V., Horton, J. A., Dockter, D. J., Schroeder, T. A., Yang, Z. Q., Cohen, W. B., Healey, S. P. & Loveland, T. R. (2020) Quality control and assessment of interpreter consistency of annual land cover reference data in an operational national monitoring program. *Remote Sensing of Environment*, 238.

Potapov, P., Siddiqui, B. N., Iqbal, Z., Aziz, T., Zzaman, B., Islam, A., Pickens, A., Talero, Y., Tyukavina, A., Turubanova, S. & Hansen, M. C. (2017) Comprehensive monitoring

of Bangladesh tree cover inside and outside of forests, 2000-2014. *Environmental Research Letters*, 12(10).

Quegan, S., Toan, L., Chave, J., Dall, J., Exbrayat, J., Minh, D., Lomas, M., D'Alessandro, M., Paillou, P., Papathanassiou, K., Rocca, F., Saatchi, S., Scipal, K., Shugart, H., Smallman, T., Soja, M., Tebaldini, S., Ulander, L., Villard, L. & Williams, M. (2019) The European Space Agency BIOMASS mission: Measuring forest above-ground biomass from space. *Remote Sensing of Environment*, 227, 44-60.

Romijn, E., De Sy, V., Herold, M., Bottcher, H., Roman-Cuesta, R., Fritz, S., Schepaschenko, D., Avitabile, V., Gaveau, D., Verchot, L. & Martius, C. (2018) Independent data for transparent monitoring of greenhouse gas emissions from the land use sector - What do stakeholders think and need? *Environmental Science & Policy*, 85, 101-112.

Roy, D., Kovalskyy, V., Zhang, H., Vermote, E., Yan, L., Kumar, S. & Egorov, A. (2016) Characterization of Landsat-7 to Landsat-8 reflective wavelength and normalized difference vegetation index continuity. *Remote Sensing of Environment*, 185, 57-70.

Saatchi, S. S., Harris, N. L., Brown, S., Lefsky, M., Mitchard, E. T. A., Salas, W., Zutta, B. R., Buermann, W., Lewis, S. L., Hagen, S., Petrova, S., White, L., Silman, M. & Morel, A. (2011) Benchmark map of forest carbon stocks in tropical regions across three continents. *Proceedings of the National Academy of Sciences of the United States of America*, 108(24), 9899-9904.

Santoro, M., Cartus, O., Carvalhais, N., Rozendaal, D., Avitabile, V., Araza, A., de Bruin, S., Herold, M., Quegan, S., Rodriguez-Veiga, P., Balzter, H., Carreiras, J., Schepaschenko, D., Korets, M., Shimada, M., Itoh, T., Martinez, A., Cavlovic, J., Gatti, R., Bispo, P., Dewnath, N., Labriere, N., Liang, J., Lindsell, J., Mitchard, E., Morel, A., Pascagaza, A., Ryan, C., Slik, F., Laurin, G., Verbeeck, H., Wijaya, A. & Willcock, S. (2021) The global forest above-ground biomass pool for 2010 estimated from high-resolution satellite observations. *Earth System Science Data*, 13(8), 3927-3950.

Santoro, M., Cartus, O., Mermoz, S., Bouvet, A., Le Toan, T., Carvalhais, N., Rozendaal, D., Herold, M., Avitabile, V., Quegan, S., Carreiras, J., Rauste, Y., Balzter, H., Schmullius, C. & Seifert, F. M. (2018) GlobBiomass global above-ground biomass and growing stock volume datasets. Available at: <http://globbiomass.org/products/global-mapping> (last accessed October 2022)

Schepaschenko, D., See, L., Lesiv, M., Bastin, J., Mollicone, D., Tsendbazar, N., Bastin, L., McCallum, I., Bayas, J., Baklanov, A., Perger, C., Durauer, M. & Fritz, S. (2019) Recent Advances in Forest Observation with Visual Interpretation of Very High-Resolution Imagery. *Surveys in Geophysics*, 40(4), 839-862.

Schroeder, W. & Giglio, L. (2018) NASA VIIRS Land Science Investigator Processing System (SIPS) Visible Infrared Imaging Radiometer Suite (VIIRS) 375 m & 750 m Active Fire Products. In *Product User's Guide Version 1.4*: NASA. Available at: [https://viirsland.gsfc.nasa.gov/PDF/VIIRS\\_activefire\\_User\\_Guide.pdf](https://viirsland.gsfc.nasa.gov/PDF/VIIRS_activefire_User_Guide.pdf) (last accessed October 2022).

Sexton, J. O., Song, X. P., Feng, M., Noojipady, P., Anand, A., Huang, C. Q., Kim, D. H., Collins, K. M., Channan, S., DiMiceli, C. & Townshend, J. R. (2013) Global, 30-m resolution continuous fields of tree cover: Landsat-based rescaling of MODIS vegetation

continuous fields with lidar-based estimates of error. *International Journal of Digital Earth*, 6(5), 427-448.

Shimada, M., Itoh, T., Motooka, T., Watanabe, M., Shiraishi, T., Thapa, R. & Lucas, R. (2014) New global forest/non-forest maps from ALOS PALSAR data (2007–2010). *Remote Sensing of Environment*, 155, 13-31.

Simard, M., Fatoyinbo, T., Smetanka, C., Rivera-monroy, V. H., Castaneda, E., Thomas, N. & Van der stocken, T. (2019) *Global Mangrove Distribution, Aboveground Biomass, and Canopy Height*. ORNL DAAC, Oak Ridge, Tennessee, USA. DOI: 10.3334/ORNLDAAC/1665

Szantoi, Z., Geller, G., Tsendbazar, N., See, L., Griffiths, P., Fritz, S., Gong, P., Herold, M., Mora, B. & Obregon, A. (2020) Addressing the need for improved land cover map products for policy support. *Environmental Science & Policy*, 112, 28-35.

Tansey, K., Gregoire, J., Defourny, P., Leigh, R., Pekel, J., van Bogaert, E. & Bartholome, E. (2008) A new, global, multi-annual (2000-2007) burnt area product at 1 km resolution. *Geophysical Research Letters*, 35(1).

Tropek, R., Sedlacek, O., Beck, J., Keil, P., Musilova, Z., Simova, I. & Storch, D. (2014) Comment on "High-resolution global maps of 21st-century forest cover change". *Science*, 344(6187), 3.

Tsendbazar, N., Herold, M., Li, L., Tarko, A., de Bruin, S., Masiliunas, D., Lesiv, M., Fritz, S., Buchhorn, M., Smets, B., Van de Kerchove, R. & Duerauer, M. (2021) Towards operational validation of annual global land cover maps. *Remote Sensing of Environment*, 266.

Tsendbazar, N. E., de Bruin, S., Fritz, S. & Herold, M. (2015) Spatial Accuracy Assessment and Integration of Global Land Cover Datasets. *Remote Sensing*, 7(12), 15804-15821.

Tsendbazar, N. E., de Bruin, S. & Herold, M. (2017) Integrating global land cover datasets for deriving user-specific maps. *International Journal of Digital Earth*, 10(3), 219-237.

UNFCCC (2014) The Warsaw Framework for REDD-plus. In decisions 9-12/CP.19. Report No. FCCC/CP/2013/10/Add.1.

UNFCCC (2015) 'Decision 19/CMA.1: Adoption of the Paris Agreement'. Report No. FCCC/CP/2015/L.9/Rev.1. Paris, France.

UNFCCC (2021) 'SBSTA 52–55 agenda sub-item 14(a) Common reporting tables for the electronic reporting of the information in the national inventory reports of anthropogenic emissions by sources and removals by sinks of greenhouse gases.'. Available at: <https://unfccc.int/documents/308920> (last access: October 2022).

UNFCCC (2022a) REDD+ Web Platform, Database 'Overview of submitted REDD+ reference levels'. Available at: <https://redd.unfccc.int/> (last access: October 2022); UNFCCC Secretariat.

UNFCCC (2022b) REDD+ Web Platform. Technical Assessment process of Forest Reference Level/Forest Reference Emission Level (FREL/FRL) submissions. Available at: <https://redd.unfccc.int/fact-sheets/forest-reference-emission-levels.html> (last access: October 2022).

Vogeler, J., Braaten, J., Slesak, R. & Falkowski, M. (2018) Extracting the full value of the Landsat archive: Inter-sensor harmonization for the mapping of Minnesota forest canopy cover (1973-2015). *Remote Sensing of Environment*, 209, 363-374.

Winkler, K., Fuchs, R., Rounsevell, M. & Herold, M. (2021) Global land use changes are four times greater than previously estimated. *Nature Communications*, 12(1).

Woodcock, C. E., Loveland, T. R., Herold, M. & Bauer, M. E. (2020) Transitioning from change detection to monitoring with remote sensing: A paradigm shift. *Remote Sensing of Environment*, 238.

Zanaga, D., Van De Kerchove, R., De, Keersmaecker, W., Souverijns, N., Brockmann, C., Quast, R., Wevers, J., Grosu, A., Paccini, A., Vergnaud, S., Cartus, O., Santoro, M., Fritz, S., Georgieva, I., Lesiv, M., Carter, S., Herold, M., Li, L., Tsendbazar, N. E., Ramoino, F. & Arino, O. (2021) ESA WorldCover 10 m 2020 v100 (Version v100) [Data set]. Zenodo. Available at: <https://doi.org/10.5281/zenodo.5571936> (last access: October 2022).



# Chapter 3. Striking divergences in Earth Observation products may limit their use for REDD+

## Abstract

Countries are required to generate baselines of carbon emissions, or Forest Reference Emission Levels, for implementing REDD+ under the UNFCCC and to access results-based payments. Developing these baselines requires accurate maps of carbon stocks and historical deforestation. Global remote sensing products provide low-cost solutions for this information, but there has been little validation of these products at national scales. This study compares the ability of currently available products obtained from remote sensing data to deliver estimates of deforestation and associated carbon emissions in Guinea-Bissau, a West African country encompassing the climate and vegetation gradients that are typical of sub-Saharan Africa. We show that disagreements in estimates of deforestation are striking, and this variation leads to high uncertainty in derived emissions. For Guinea-Bissau, we suggest that higher temporal resolution of remote sensing products is required to reduce this uncertainty by overcoming current limitations in differentiating deforestation from seasonality. In contrast, existing datasets of carbon stocks show better agreement, and contribute much less to the variation in estimated emissions. We conclude that using global datasets based on Earth Observation data is a cost-effective solution to make REDD+ operational, but deforestation maps in particular should be derived carefully and their uncertainty assessed.

**Keywords:** REDD+; Forest Reference Emission Level; Measurement, Reporting and Verification; Deforestation; Carbon Emissions; Remote Sensing; Sub-Saharan Africa; Guinea-Bissau

### 3.1 Contributions and Acknowledgements

The following research chapter was published in Environmental Research Letters on 18 October 2018. Its full content is presented here as it appears in its published form having only been re-formatted and Tables and Figures renumbered for a uniform layout through the thesis. Supplementary information for this chapter is available in Appendix 2 of this thesis. The citation of the published paper is:

Melo J, Ziv G, Baker T, Carreiras J, Pearson T and Vasconcelos M 2018 Striking divergences in earth observation products may limit their use for REDD. Environ. Res. Lett. 13 104020. <https://doi.org/10.1088/1748-9326/aae3f8>

**Authors:** Joana Melo<sup>1</sup>, Guy Ziv<sup>1</sup>, Timothy R. Baker<sup>1</sup>, Joao M B Carreiras<sup>2</sup>, Timothy R H Pearson<sup>3</sup>, and Maria J Vasconcelos<sup>4</sup>

#### **Affiliations and addresses**

<sup>1</sup> School of Geography, University of Leeds, Woodhouse Lane, Leeds LS2 9JT, United Kingdom

<sup>2</sup> National Centre for Earth Observation, University of Sheffield, Sheffield, S3 7RH, UK

<sup>3</sup> Winrock International, 2121 Crystal Drive #500, Arlington, VA, 22180, USA

<sup>4</sup> Forest Research Center, School of Agriculture, University of Lisbon, Tapada da Ajuda 1349-017 Lisboa, Portugal

**Author contributions:** JM, GZ and TRB designed and conceived the study. JM collected and analysed the data. JMBC, TRHP and MJV supported the collection and analysis of Guinea-Bissau data, including the land cover maps and field data. JM wrote the manuscript with GZ and TB critical feedback. All co-authors reviewed the final text.

**Acknowledgements:** JM was funded by the Natural Environment Research Council (NERC), UK, through the Leeds–York NERC Doctoral Training Partnership. GZ acknowledges the support from the European Union’s Horizon 2020 Research and Innovation Programme under Grant Agreement No 641762 (Project: ‘ECOPOTENTIAL: Improving Future Ecosystem Benefits through Earth Observations’). J.M.B.C. was funded as part of NERC’s support of the National Centre for Earth Observation.

## 3.2 Introduction

Land-use change accounts for 12% of global carbon emissions (Le Quéré et al., 2018), and mitigation actions in this sector are strategically important under the United Nations Framework Convention on Climate Change (UNFCCC) and its Paris Agreement (UNFCCC, 2016; Grassi et al., 2017). Accordingly, efforts to reduce emissions from deforestation and forest degradation in tropical developing countries (REDD+) have also been high on the agenda. However, to be eligible to receive results-based payments for REDD+ efforts, countries need to fulfil certain technical requirements (Goetz et al., 2015) that include establishing baselines of historical greenhouse gas emissions, or Forest Reference Emissions Levels (FREL). FREL in UNFCCC terminology is given by the product of ‘activity data’ (AD) and ‘emission factors’ (EF), or area change and changes in carbon stock per unit of area. Existing global Earth Observation datasets for land-use change assessments (e.g., Hansen et al., 2013; Sexton et al., 2013; Shimada et al., 2014) and of above-ground biomass density (e.g., Saatchi et al., 2011; Baccini et al., 2012) may be useful in the context of REDD+ to establish emission baselines (Harris et al., 2012; Achard et al., 2014; Achard and House, 2015; Goetz et al., 2015; Tyukavina et al., 2015; Zarin et al., 2016). However, although Earth Observation capabilities to generate regional to global products can contribute to promote consistency and transparency across regions by tracking global progress on reducing emissions (Achard and House, 2015), the suitability of these products have rarely been tested for producing baselines at national scales.

Using existing Earth Observation (EO) products is less costly than developing and maintaining operational forest monitoring systems, including the high costs of sampling, and therefore is particularly attractive to some countries with less capacity and without substantial REDD+ readiness funding (Norman, 2015; Herold and Skutsch, 2011). However, limitations exist for their wider adoption at national and sub-national levels. Such limitations include the scarcity of studies analyzing the agreement between such products and *in-situ* data at national and subnational scales or the differences that may be found among the available studies. For example, studies have shown that although having high overall accuracies, some products still underestimate deforestation due to confusion between forests and plantations (Lui and Coomes, 2015; Tropek et al., 2014) or by failing to detect small-scale disturbances (Milodowski et al., 2017b). These products can also overestimate tree-cover and deforestation due to discrepancies in tree-cover thresholds (Mermoz and Toan, 2016; Sannier et al., 2016). As for biomass, studies comparing existing pantropical maps (Mitchard et al., 2013; Hill et al., 2013; Mitchard et al., 2014) found overall agreement and lower uncertainty when data is aggregated at larger scales, but significant differences otherwise, and thus recommended better uncertainty assessments of these pan-tropical products. Overall,

these studies compared different EO products for deriving either activity data (AD) or emission factors (EF). However, the combined analysis of these two components, which is a prerequisite for developing national REDD+ baselines, has rarely been performed.

This study therefore assesses the impact of using different available datasets obtained with state-of-the-art automated methods based on EO data for producing a national baseline of historical carbon emissions, using Guinea-Bissau (West Africa) as a case study. With an area of ~ 36,000 km<sup>2</sup>, this least-developed country is mostly covered with woodlands and mangroves (Vittek et al., 2014) and encompasses the climate and vegetation gradients that are typical of many areas of sub-Saharan Africa (**Figure 3-1**). We compare historical gross emissions from deforestation obtained by combining several products (for AD and EF), including nationally produced ones, and investigate a) if consistent FRELS are derived when using different EO products; b) if the variance is mostly due to the AD or EF component; and c) the reasons for observed discrepancies. Overall, we wish to explore whether the concern surrounding the use of global EO products at national scales to develop REDD+ baselines is warranted.

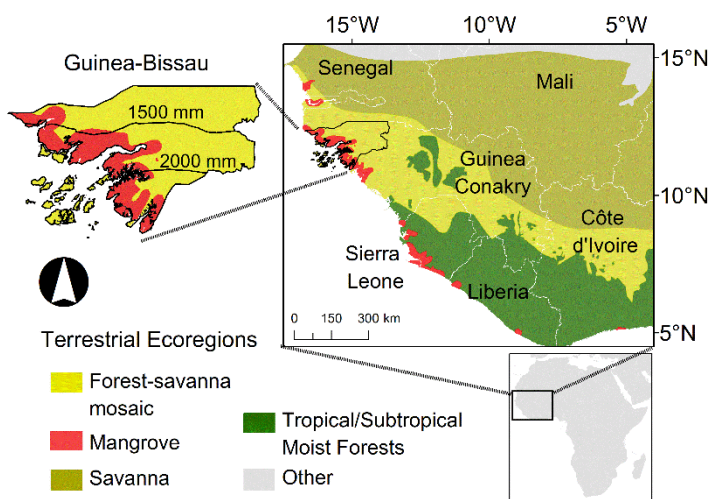


**Figure 3-1.** Map indicating the location of Guinea-Bissau in Western Africa showing terrestrial ecoregions (adapted from Olson et al., 2001) and precipitation gradient (mm yr<sup>-1</sup>, WorldClim) in the Guinea-Bissau subset.

### 3.3 Data

#### 3.3.1. National deforestation and above-ground biomass data

To comply with UNFCCC reporting requirements Guinea-Bissau compiled existing information on anthropogenic emissions by sources and removal by sinks in their national communications (Guinea-Bissau, 2011, 2018). The main source of data for the land-use sector, including information on deforestation and forest AGB, was the CARBOVEG-GB nation-wide project which ended in 2010. This project was latter extended by the Institute for Biodiversity and Protected Areas (IBAP) with the objective

of producing a baseline of emissions for the protected areas (Vasconcelos et al., 2015; IBAP, 2015). Information from these projects includes Landsat-based land-cover maps for 2007 and 2010 that stratify forests into four classes (**Table 3.1**), and *in-situ* AGB data collected nationwide in 309 plots (**Table 3.2**). These data are referred to hereafter as the *National* data (see Vasconcelos et al., 2015 and the Appendix 2 for detailed methods).

### 3.3.2. Global forest cover data

Available global datasets of tree-cover and tree-cover loss (Hansen et al., 2013; Sexton et al., 2013) and annual forest and non-forest cover maps (Shimada et al., 2014) based on automated classification algorithms of Landsat, the Vegetation Continuous Fields (VCF) derived from MODerate-resolution Imaging Spectroradiometer (MODIS), and Advanced Land Observing Satellite (ALOS) Phased Array L-band Synthetic Aperture Radar (PALSAR) imagery were used (**Table 3.1**, and Appendix 2). To estimate forest loss from 2007 to 2010, we firstly used the Global Forest Change (GFC; (Hansen et al., 2013)) 30-m resolution dataset based on a time-series of Landsat images from the growing season. Secondly, we used the global dataset of tree-cover made freely available by the Global Land Cover Facility (GLCF; (Sexton et al., 2013)). Although the final product is also a tree-cover global map, this dataset uses the 250-m MODIS VCF rescaled to 30-m resolution using Landsat data. Thirdly, we used the 25-m Forest/Non-Forest (F/NF) global mosaics for 2007 and 2010 from (Shimada et al., 2014) based on the Japan Aerospace Exploration Agency (JAXA) ALOS PALSAR. This product uses the lower levels of the L-band backscatter as a threshold for mapping the transition from forest to non-forest.

**Table 3.1.** *The data sources used to derive deforestation estimates between 2007 and 2010.*

Product	Reference	Scale	Remote sensing data sources	Spatial resolution	Imagery acquisition dates	Description of data used to derive deforestation
<i>GFC</i>	Hansen et al. (2012)	Global	Landsat	30-m	growing season	Tree-cover 2000 annual tree-cover loss 2000-2010
<i>GLCF</i>	Sexton et al. (2013)	Global	MODIS VCF rescaled with Landsat	30-m	all year	Tree-cover 2005, 2010
<i>JAXA</i>	Shimada et al. (2014)	Global	ALOS PALSAR	25-m	growing season	Forest/non-forest 2007, 2010
<i>National</i>	Guinea-Bissau (2012, 2018) Vasconcelos et al. (2015)	National	Landsat	25-m	dry season	Land-cover 2007, 2010

### 3.3.3. AGB maps

To assess pre-deforestation carbon stocks, we used four available maps of AGB (Table 3.2, and Appendix 2). Two were developed at a pantropical scale (Saatchi et al., 2011; Baccini et al., 2012) based on transects derived from the Lidar dataset obtained by the Geoscience Laser Altimeter System (GLAS) onboard the Ice, Cloud and land Elevation

Satellite (ICESat). Two additional AGB maps, based on Synthetic Aperture Radar (SAR) from ALOS PALSAR and developed for Africa savannas and dry forests (Bouvet et al., 2018) and at a national scale (Carreiras et al., 2012) with 25-m and 50-m spatial resolution, were also used. All products used field data for calibration and have reference years ranging from 2000 to 2010 (**Table 3.2**). Saatchi et al. (2011), Baccini et al. (2012), Carreiras et al. (2012), and Bouvet et al. (2018) products are referred to hereafter as *SA11*, *BA12*, *CA12*, and *BO18* respectively.

**Table 3.2.** The above-ground biomass data sources used to derive emission factors.

Product	Reference	Scale	Remote Sensing data sources	Spatial resolution	Reference year
<i>SA11</i>	Saatchi et al. (2011)	Pantropical	GLAS + MODIS + QuikSCAT	1-km	2000
<i>BA12</i>	Baccini et al. (2012)	Pantropical	GLAS + MODIS	500-m	2007-2008
<i>CA12</i>	Carreiras et al. (2012)	Guinea-Bissau	ALOS PALSAR	50-m	2008
<i>BO18</i>	Bouvet et al. (2018)	African savannas	ALOS PALSAR mosaic	25-m	2010
<i>National</i>	Guinea-Bissau (2012, 2018), Vasconcelos et al. (2015)	309 plots measured nationwide between 2007 and 2012			

## 3.4 Methods

### 3.4.1 Deforestation (Activity Data)

A spatial tracking approach was used to estimate gross deforestation over the 2007-2010 period. Firstly, F/NF layers were derived from all products. This included using a similar minimum mapping unit of 0.5-ha and tree-cover threshold of 10% to be consistent with the national forest definition (see Appendix 2 for details). The two *National* land-cover maps (2007, 2010) were reclassified into F/NF. For *GFC*, F/NF maps were generated for the years 2007 and 2010 using the 2000 tree-cover and annual loss maps; the 2000 tree-cover map was reclassified to F/NF with forest being defined as areas with tree-cover above 10%; loss in the period 2001-2007 was used to update the 2000 F/NF map and generate a 2007 F/NF map; the same approach was followed to obtain the 2010 F/NF map. For *GLCF*, F/NF maps were generated for the years 2005 and 2010 by reclassifying areas with tree-cover above 10% as forests in the tree-cover maps for the corresponding years. For *JAXA*, F/NF maps were already available for 2007 and 2010. For both *National* and *JAXA* the threshold for forest is 10% tree-cover, which is consistent with the national forest definition (FAO, 2015). Finally, deforestation maps were generated by reclassifying each of the combined maps from *forest* and *non-forest* to *deforestation* and *no-change*. A common projection, extent and water mask was applied as detailed in the Appendix 2.

### 3.4.2 Carbon assessment and emission factors

Due to lack of accurate information on the fate of post-deforestation land-uses and corresponding carbon stocks, and to ensure the integrity of their FRELs, most countries (all FREL submissions except five up to December 2017) and other pantropical studies (e.g., Harris et al., 2012; Achard et al., 2014; Tyukavina et al., 2015) chose to report gross instead of net emissions. This option is consistent with the stepwise approach for the development of REDD+ FRELs, which envisions the incorporation of better data and improved methodologies over time. In this study, we followed the same approach and estimated gross emissions, which means post-deforestation carbon stocks are assumed to be zero and any post-deforestation carbon sequestration is not accounted for. Additionally, tree AGB is the only carbon pool included. Field sampling methods were already described elsewhere (see Appendix 2). To estimate plot-level AGB from *National* field data, three different equations were selected: for forest trees (Chave et al., 2014), mangroves (best predictive model for mangroves from (Chave et al., 2005)) and palm trees (IPCC, 2003) (Table A1). AGB obtained at plot level was extrapolated to the area of 1-ha using a dimensional scaling factor (see Appendix 2). The *National* EF is the weighted average of the AGB density from all forest classes. For EFs derived from *SA11*, *BA12*, *CA12* and *BO18*, instead of country averages, the pre-deforestation AGB was used by extracting the values from pixels identified as deforested by each deforestation product. AGB was converted to  $\text{tCO}_2 \text{ ha}^{-1}$  by using the standard carbon factor of 0.47 (IPCC, 2006) and the 44/12 molecular weight ratio of carbon to carbon dioxide.

### 3.4.3 Estimating historic gross emissions from deforestation

For each combination of datasets, the product of deforested area ( $\text{AD}$ ,  $\text{ha yr}^{-1}$ ) and the associated AGB (EF,  $\text{tCO}_2 \text{ ha}^{-1}$ ) was summed to render total annual emissions (FREL,  $\text{tCO}_2 \text{ yr}^{-1}$ ). Four AD (*National*, *GFC*, *GLCF*, and *JAXA*) and five EF (*National*, *SA11*, *BA12*, *CA12*, and *BO18*) products were used in this analysis rendering 20 FREL combinations. The spread between emissions obtained by these products was estimated using the coefficient of variation (CV, %) computed as the ratio of the standard deviation to the mean of all products. To assess the source of variation in derived FRELs, the CV was calculated across deforestation products whilst fixing each AGB product, and vice-versa, fixing each deforestation product and calculating the CV across the AGB products.

### 3.4.4 Identifying spatial patterns of agreement

Datasets were overlaid and combined to identify agreement between both deforestation and AGB products. To facilitate the visual interpretation of different spatial patterns, datasets were aggregated to a 10-km spatial resolution with each pixel representing the

proportion of deforestation by area of national land (%) for AD and the mean AGB ( $t\ ha^{-1}$ ). Per-pixel statistics were computed including mean of all products, standard deviation and variation as a proportion of the mean given by the CV (%). The correlation between these statistical variables was assessed using the Spearman's rank correlation coefficient.

To understand the patterns of agreement between datasets we stratified the land area into four regions based on the *National* land-cover map (depicting Mangroves and Terrestrial Forests) stratified by climatic data (mean annual precipitation for the years 1970-2000 below or above 1500 and 2000  $mm\ yr^{-1}$ ) from WorldClim (Fick and Hijmans, 2017) version 2. The 20 FREL combinations and their CV (%) were calculated per region.

### 3.5 Results

#### 3.5.1. Above-ground biomass and emission factors

The aggregated AGB mean for the entire country varies little between products (**Figure 3-2**). All AGB estimates range between 54 and 65  $t\ ha^{-1}$  (SA11 and BA12 respectively), and are similar to estimates derived from *in-situ* data (National, 62.8  $t\ ha^{-1}$ ). They are also substantially lower than the IPCC default for sub-tropical dry forests (130  $t\ ha^{-1}$ , (IPCC, 2006)). Mean AGB densities from deforested areas tend to be lower than the aggregated national average indicating that deforestation occurs in areas of lower AGB (this is particularly evident for AD-*National* and true for all deforestation products except GFC in three of four AGB datasets). All AGB products show higher values in the south of Guinea-Bissau (**Figure 3-3**) where patches of sub-humid forest are documented (Malaisse, 1996). Some differences are observed elsewhere such as the lower densities in the North of the country in SA11, but overall variation in the AGB spatial distribution is low nationwide with 95% of 10-km pixels having a CV below 30% (**Figure 3-3**).

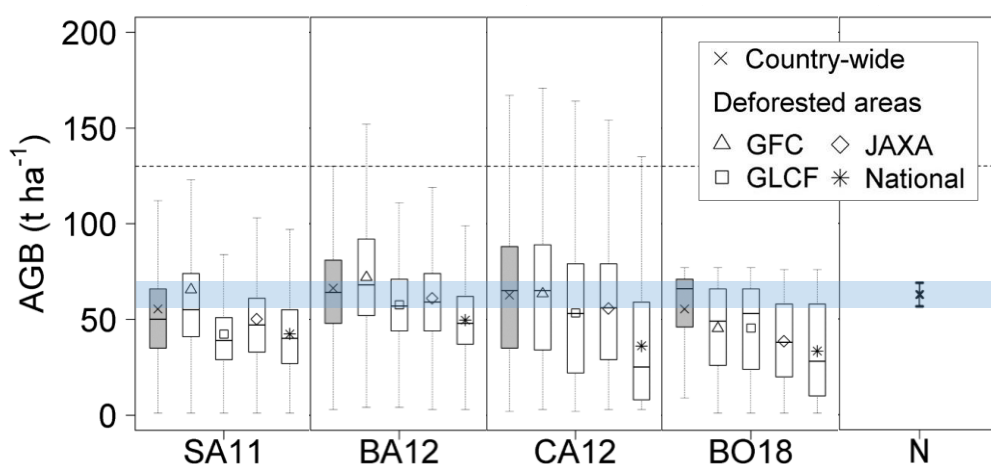


**Figure 3-2.** Distribution of above-ground biomass (AGB,  $t\ ha^{-1}$ ) estimates from SA11, BA12, CA12, and BO18, including minimum, first quartile, median, third quartile, maximum, [continues in next page.....]

and mean AGB. Estimates at the country level are highlighted in grey and the mean marked with the symbol  $\times$ . The remaining distributions describe data from SA11, BA12, CA12, and BO18 in areas mapped as deforested by each activity data product: GFC, GLCF, JAXA, and National (mean values marked with symbols  $\Delta$ ,  $\square$ ,  $\diamond$ ,  $*$ , respectively). Right panel depicts National (N) mean AGB ( $t\ ha^{-1}$ ) and the error bars the 95% confidence interval (CI) obtained from data collected nationwide in 309 sampled field plots. The 95% CI is also depicted by a blue bar for comparison with the remaining country-wide estimates. **Table A.2.3** shows mean and standard deviation values for all distributions. The National mean AGB density for the entire country ( $62.8\ t\ ha^{-1}$ , **Table A.2.2**) is used directly as proxy of pre-deforestation carbon stock or EF. The IPCC default AGB value for sub-tropical dry forests ( $130\ t\ ha^{-1}$ , Table 4.12, IPCC 2006) is also illustrated here with a dashed line.

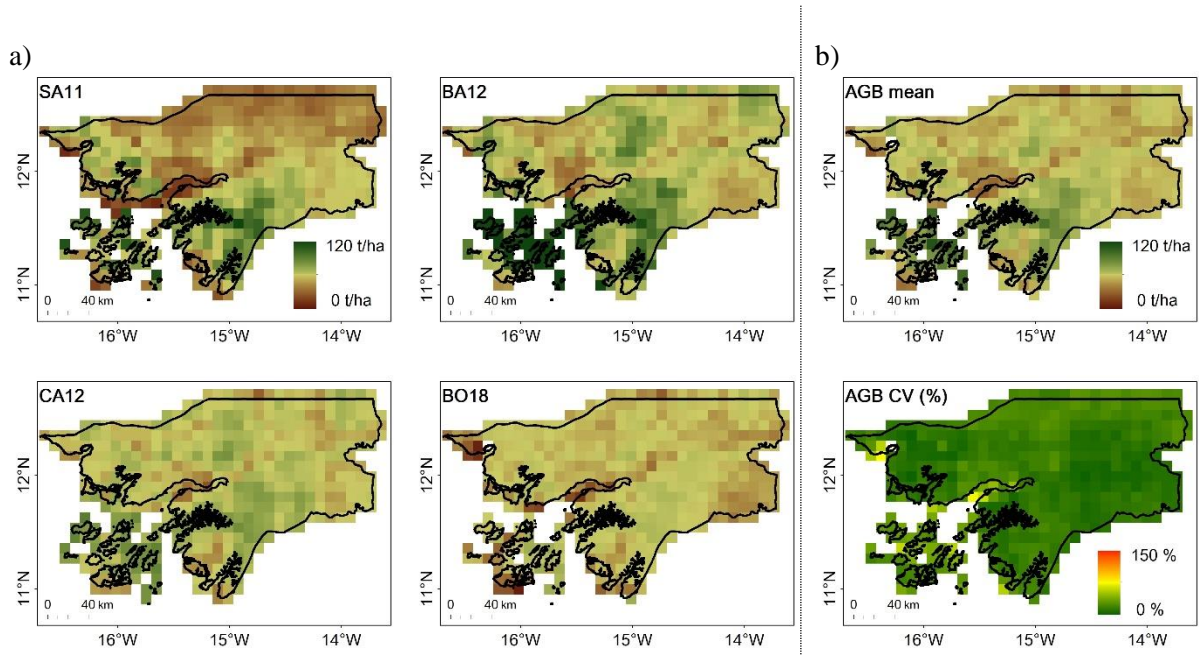


**Figure 3-3.** Spatial patterns of above-ground biomass (AGB,  $t\ ha^{-1}$ ) in Guinea-Bissau at 10-km resolution, including: a) AGB distribution from different products (SA11, BA12, CA12 and BO18), and b) per-pixel statistics including average AGB of all products and measure of spread given by the coefficient of variation (CV, %) in each pixel. The National EF is not depicted as it is estimated as the area-weighted average AGB of all forest classes with the same value of  $62.8\ t\ ha^{-1}$  used country-wide with no spatial variation.

### 3.5.2. Deforestation magnitude and spatial disagreement

In contrast to the AGB datasets, deforestation varies greatly among products with rates ranging between 0.3 and 1.8 %  $yr^{-1}$  for GFC and National maps respectively (**Table A.2.4**). Even more striking are the different spatial patterns of deforestation: the different products show almost complete disagreement (**Figure 3-4**). For instance, GFC identifies deforestation in the south of the country where the densest forests exist, while GLCF shows deforestation to the north in the border with Senegal and the Casamance region. Both National and JAXA highlight deforestation to the east of the country, in areas dominated by savannas, but these do not overlap. Variation as proportion of the mean (CV, %) is high to very high: over 90% of pixels have a CV above 50%.

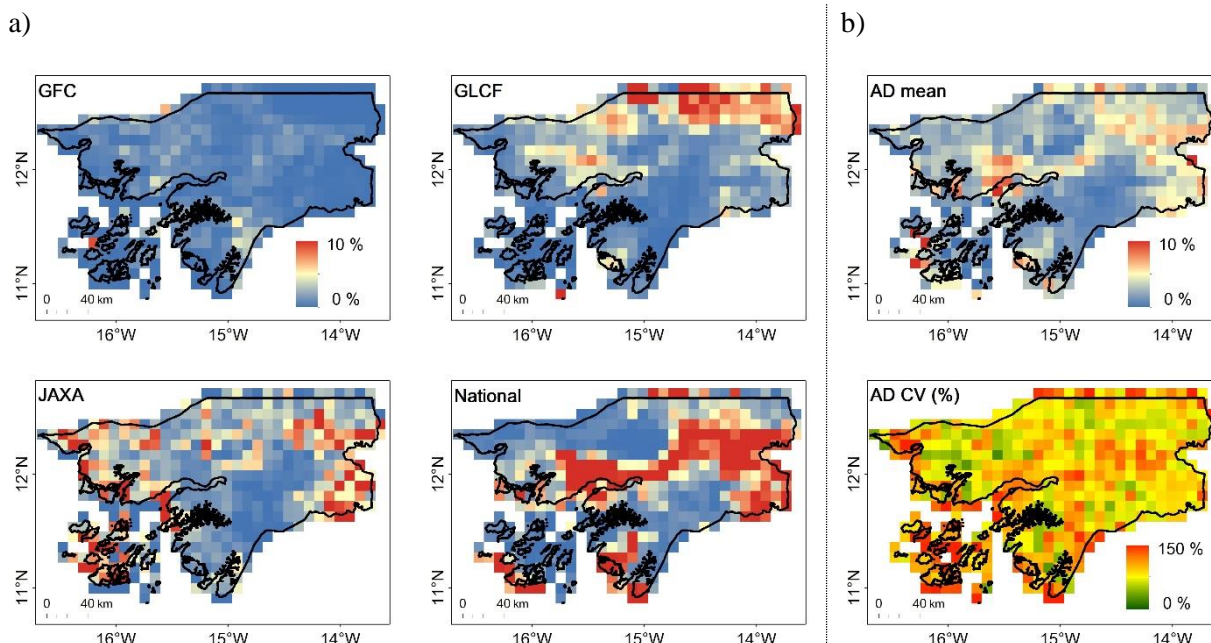


**Figure 3-4.** Spatial patterns of deforestation in Guinea-Bissau between 2007 and 2010 derived from different products (GFC, GLCF, JAXA and National) at 10-km resolution: a) per-pixel deforestation values shown as the proportion (%) of deforestation by the land area of national territory (blue color denotes no change), and b) per-pixel statistics with average and measure of spread given by the coefficient of variation (CV, %).

### 3.5.3. Forest Reference Emission Level combinations

Results for the 20 combinations of EO products show that AD and EF derived from different datasets render very different FRELs, or annual emissions ( $\text{MtCO}_2 \text{ yr}^{-1}$ ; **Table 3.3**). Using *National* data produced an estimate of  $5.71 \text{ MtCO}_2 \text{ yr}^{-1}$ , a value which is more than 10-times higher than the  $0.48 \text{ MtCO}_2 \text{ yr}^{-1}$  obtained when combining *GFC* (AD) and *BO18* (EF). While the spread of all FRELs is high (overall CV of 64%), the results highlight that the magnitude of variation is dominated by differences in the deforestation dataset (AD), with CV ranging between 58 and 71% when compared to the 20-32% variation in EFs. In both AD and EF higher spread is linked to *National* data, while the lowest spread in AD is obtained for the two EF products derived from L-band backscatter (*CA12* and *BO18*, 58% CV).

**Table 3.3.** Forest Reference Emission Levels (in  $\text{MtCO}_2 \text{ yr}^{-1}$ ) for the reference period 2007-2010 and country-wide spread given by the Coefficient of Variation (CV, %) for AD by fixing each AGB product, and for EF by fixing each deforestation product. The different FREL estimates are obtained as the product of Activity Data (AD,  $\text{ha yr}^{-1}$ ) derived from each dataset (National, GFC, GLCF, and JAXA) and Emission Factors (EF,  $\text{tCO}_2 \text{ ha}^{-1}$ ) obtained by each dataset (National, SA11, BA12, CA12, BO18).

	AD-GFC	AD-GLCF	AD-JAXA	AD-National	AD CV
EF-National	0.82	1.83	4.06	5.71	71 %
EF-SA11	0.79	1.17	2.97	3.60	64 %
EF-BA12	0.87	1.58	3.54	4.19	62 %
EF-CA12	0.79	1.49	3.46	3.15	58 %
EF-BO18	0.48	1.14	1.73	2.45	58 %
EF CV	21 %	20 %	28 %	32 %	64 %

### 3.5.4. Relationship between spatial patterns

As suggested by the analysis of AGB densities (**Figure 3-2**), there is a strong and significant relationship between higher deforestation estimates and lower AGB (**Table 3.4**, Spearman's correlation 0.641;  $p < 0.001$ ). There is no observed correlation between the variability of estimates of deforestation and mean AGB.

**Table 3.4.** Spearman's rank correlation coefficient between per-pixel mean and coefficient of variation (CV, %) for AD and AGB. Correlation values above 0.3 are in boldface;  $p > 0.05$  in round brackets.

	AD mean	AD CV	AGB mean
AD CV	0.112		
AGB mean	<b>-0.641</b>	(0.004)	
AGB CV	(0.047)	0.216	(-0.037)

No clear relationship between different emission estimates and regions defined based on vegetation and precipitation gradient is observed either (**Figure 3-5**), which was also suggested by the lack of spatial pattern in per-pixel spread (**Figure 3-4b**). Spread in AGB is always low with slightly higher values (30-47% CV) in forests with mean annual precipitation above 2000 mm. The spread in deforestation is always higher than that of AGB in all regions, and is particularly high in mangroves. However, mangroves are the least deforested biome and account for less than 3% of total deforestation in all datasets except JAXA, where it corresponds to 17% of total deforestation. Apart from mangrove areas, the disagreements in deforestation are not linked to specific vegetation types.

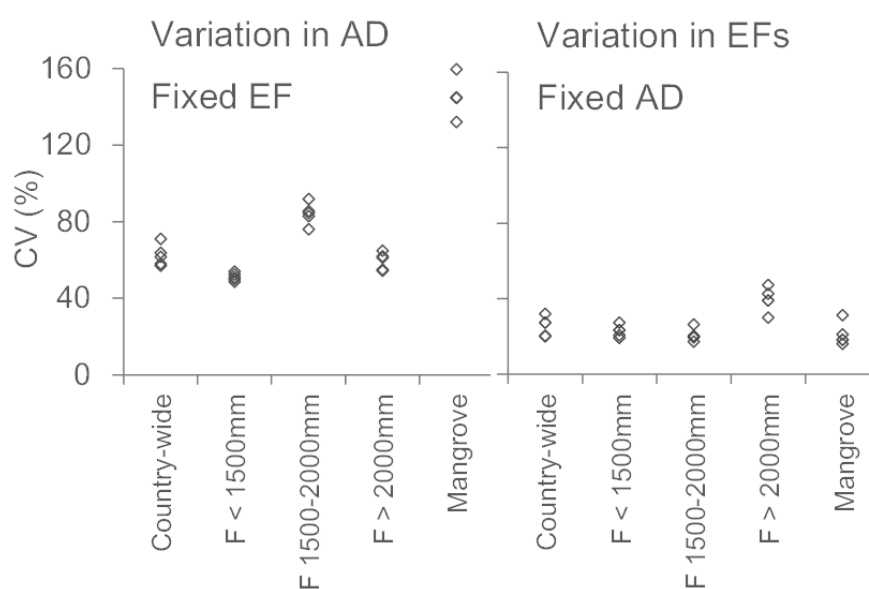


**Figure 3-5.** Country-wide and regional spread analysis given by the Coefficient of Variation (CV, %) in Activity Data (AD) and Emission Factors (EF). Forest types or regions (F) were stratified based on mean annual precipitation. For Mangroves the BO18 dataset is excluded, as mangrove areas are masked in the original above-ground biomass map.

## 3.6 Discussion

We produced different estimates of historical emissions from deforestation by combining pairs of deforestation and associated carbon stocks derived from different products. We show that there is a high variation in estimated emissions and that this is almost entirely due to variation in estimates of annual deforestation.

### 3.6.1. Understanding spatial disagreements in deforestation (Activity Data)

The observed differences in the patterns and magnitude of deforestation may be linked to different imagery acquisition dates coupled with difficulties in distinguishing seasonality from deforestation. For example, the seasonality of certain crops can have a spectral signal that is difficult to separate from deforestation events without imagery from the dry season. For example, in some cases of rice plantations that have been established in previously forested mangrove areas (**Figure 3-6**), images from the growing season depict a signal from swamped rice which is nearly identical to that of mangrove forest (they are “green” from August to October). As a result, the conversion from mangrove to another land-use may be missed. However, if images are acquired in the dry season when fields are drier and the rice has been cropped (between November and July) the spectral signal will be that of bare land (“red”). In this case, deforestation events are likely to be detected. The challenge of separating the temporal spectral signal of rice production from that of conversion of mangrove forest to rice fields may have contributed to the observed higher spread in emissions in this biome (**Figure 3-5**).

The occurrence of fire in dry biomes is another example of how seasonality may affect estimates of deforestation. African savanna fires are of low intensity and high frequency (Bowman and Murphy, 2010) and in the northern hemisphere burn extensively in the early dry season (Cahoon et al., 1992; Roberts et al., 2009). However, typically these wildfires burn primarily grass and tree litter (Van Wilgen and Scholes, 1997) and are not necessarily linked to conversion from forests to other land-uses. Consequently, the *National* deforestation product, relying on imagery from the dry season, may have incorrectly mapped bushfires in savannas as deforestation (**Figure 3-7**).

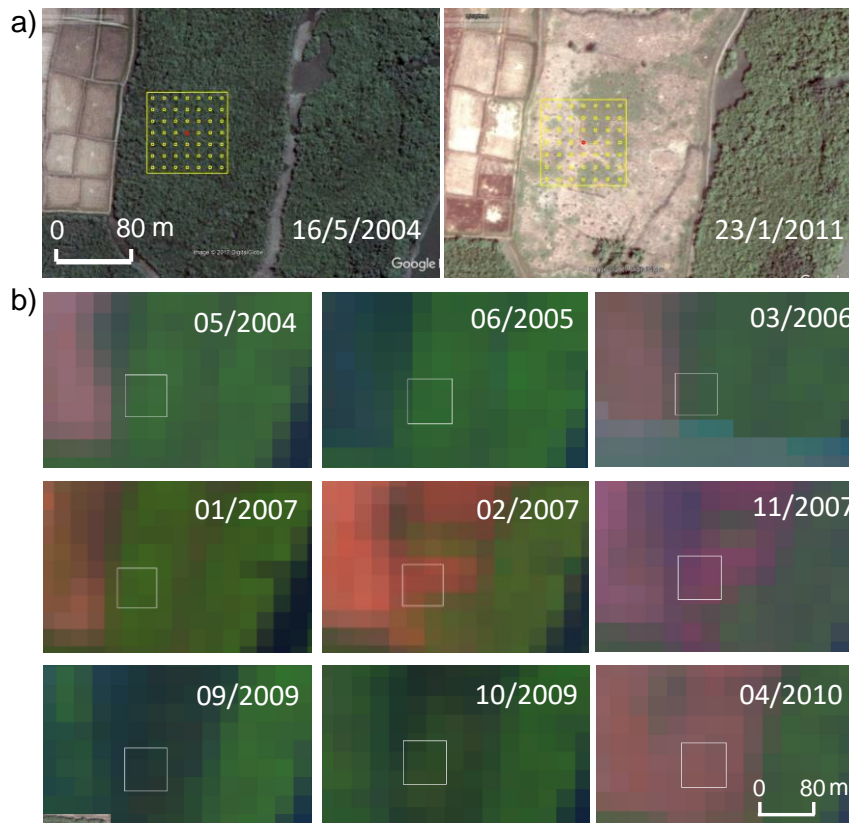


**Figure 3-6.** Example of deforestation in Mangrove through inspection of: a) very high spatial resolution imagery available in Google Earth (16 May 2004 and 23 January 2011) showing an area of mangrove in 2004 that in 2011 was a swamped rice field; and b) the Landsat archive with its higher temporal resolution (images ranging from May 2004 to April 2010 and displayed in RGB color composites: band 7, band 4, band 3) identifying 2007 as the conversion year. The high temporal resolution of Landsat images also highlight the different spectral signals of the cycle of rice production: from August to October rice is cultivated in swamped fields (green signal) while in November the field dries out and the rice is cropped. In this study, only AD-National and AD-GLCF identified this area as deforested between 2007 and 2010.

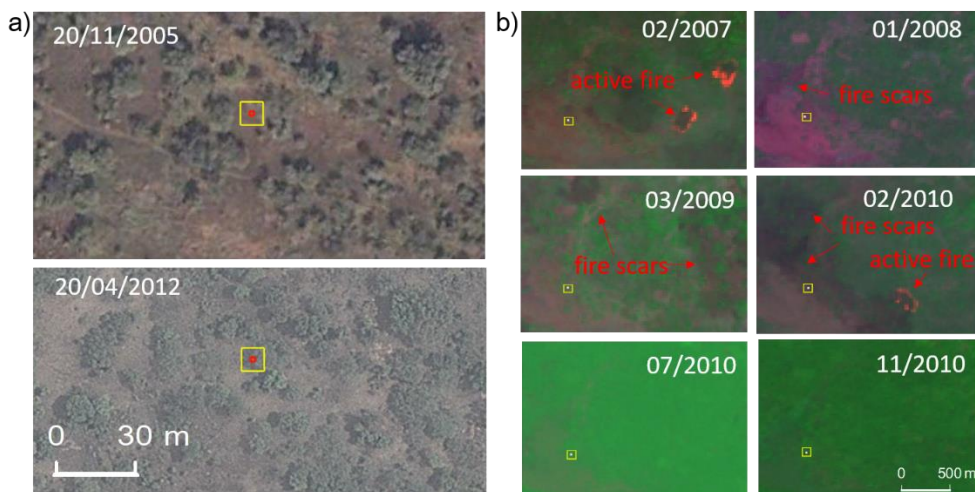


**Figure 3-7.** Example of bushfires in Guinea-Bissau. Figure shows a) high spatial resolution imagery from Google Earth identifying this area as forest in 2005 and remaining forest in 2012, regarding of the prevalence of fire as shown by the b) temporal analysis of Landsat imagery with annual evidence of active fires or fire scars (displayed in RGB color composites: band 7, band 4, band 3). The area marked (yellow square) was mapped as deforested only by the AD-National product which is based on Landsat imagery from the dry season. Wildfires in African savannas typically occur in the beginning of the dry season (November-February) and their scars are very difficult to detect using remote sensing imagery from the late dry season (March-May) and growing season (June-October)

Different acquisition dates and seasonality can therefore partially explain the lower estimates of deforestation rates in GFC and higher estimates of deforestation in *National*, and why, in this study, these products are associated with the lowest and highest

emission estimates respectively. Importantly, there is no single acquisition date that would resolve both problems: while relying on dry season imagery is helpful for the example of mangrove conversion, this season is not suitable for detecting deforestation in fire prone areas.

While seasonality appears to be the main issue, other possibilities for the differences in estimates of deforestation can be highlighted. One is linked to the different method that was used to quantify forest loss. The *GFC* is the only product that detects changes by directly comparing multi-temporal images. For the remaining products, detection of deforestation was made by comparing results from independent F/NF maps, which is considered to be less accurate and may lead to an overestimation of deforestation rates (GFOI, 2016). Another possible explanation for the disagreements in AD include the use of different data layers by these products. The L-band SAR backscatter has been reported to be very similar amongst mangroves, forests and plantations (Lucas et al., 2014) which could explain the higher estimates of deforestation in mangroves using the *JAXA* product. However, the same mapping limitation is known to exist with optical data (e.g., Lui and Coomes, 2015). Finally, it is also worth noting issues related with forest definitions and the complexities of using land-cover change and tree-cover change as proxy for land-use change. Although a tree-cover threshold consistent with that of national forest definition was used while processing all products, some limitations can still arise. It is considered particularly difficult to extract areas with low tree-cover densities using optical data (Achard et al., 2014; Hojas-Gascon, 2015). As a result, the use of 10% tree cover as a cut-off likely contributes to increased mapping errors and uncertainty in AD estimates. Additionally, defining forests using tree-cover thresholds fails to distinguish natural forests and plantations (Tropek et al., 2014; Lui and Coomes, 2015; Zarin et al., 2016).

Overall, to overcome all the identified issues and map deforestation more accurately, countries would need to use very high spectral resolution imagery or increased intra-annual temporal resolution when producing their maps and estimates.

### **3.6.2. Opportunities and limitations for using available AGB datasets**

While the development of emission factors is considered a major monitoring capacity gap for national GHG reporting (Romijn et al., 2015), our results show that for tree-AGB, using *in-situ* data from national inventories or available datasets, even when produced at a pantropical level, render relatively similar results. Our results also highlight that the magnitude of these estimates is in all cases lower than the IPCC Tier 1 default value, with the latter leading to estimates at least 2-times higher than with other EF alternatives (**Table A.2.5**). Moreover, it is expected that summing AGB values over larger areas

renders similar mean and total values (Mitchard et al., 2013), but in our study the spatial pattern of available datasets does not differ much either. The higher spread in EFs given by the CV in forests with mean annual precipitation above 2000 mm (30-47%) is likely not so much due to divergences in AGB products but more to limitations of data, such as the signal saturation of L-band SAR at higher levels of AGB. Nevertheless, a limitation for the use of AGB maps in baseline studies, and a possible explanation for some lower values observed in some products, is the reference year of these products. Using per-pixel AGB values as proxy for pre-deforested stock is only possible if the reference year of the AGB map precedes that of the start of the deforestation period. Finally, this study focuses only on tree-AGB, which is but one component of terrestrial carbon stocks influencing the global carbon cycle. Remote sensing products can only estimate the carbon content of other pools as a function of AGB (e.g. inclusion of below-ground biomass in Saatchi et al. 2011), which is a limitation of these products for countries wanting to include emissions from other pools in their FRELs over time (i.e. in a stepwise approach). However, including other pools here as a proportion of AGB would not alter the main findings of this study.

### **3.6.3. Implications of observed differences in Forest Reference Emission Level estimates**

This study finds that the variance in FRELs derived from different EO products is mostly due to the AD component. Although disagreement between products is not indicative of the accuracy of each product, it undoubtedly sheds suspicion over all products, confuses the user, and suggests producers are being overly confident in their products. While these AD products can be calibrated with reference data when developing a FREL (Olofsson et al., 2014b; Hojas-Gascon, 2015), there are consequences for the use of this information in the design of appropriate policy options and REDD+ strategies. Such strategies greatly rely on understanding where deforestation is occurring and the processes that are driving land-use change. Therefore, the risk of developing the FREL independently, and possibly favouring a product with higher historical deforestation in the hope of maximizing income from REDD+ results, may be counter-productive for the success of REDD+ implementation. The two REDD+ building blocks (the FREL and REDD+ strategy) should be developed in parallel, which requires accurate spatially explicit FRELs to guide the planning of interventions. Ultimately, and considering that the availability of products for continuous global monitoring of land-use processes is only expected to expand in the future (Wulder and Coops, 2014), it is important that products are carefully validated by their producers and users to quantify their uncertainty for national and subnational analysis.

### 3.7 Conclusions

Our study shows major differences are obtained in estimated emissions (FRELs) using different EO products and that those differences are mostly due to variation in estimates of deforestation. Although there are many calls for improving the accuracy of AGB maps, here we found that *in-situ* AGB data and AGB maps relying on more sophisticated remote sensing approaches have sufficient precision for national reporting, especially when compared to the deforestation component. Divergences in the latter are striking, with almost total spatial disagreement between datasets. This finding calls for better incorporation and reporting of accuracy in land-cover (and land-cover change) EO products. In the meantime, we suggest that users focus their efforts in assessing the adequacy and quality of deforestation maps for their national circumstances by relying on reference data with higher spatial and temporal resolution to validate and calibrate existing products. Furthermore, it is also important to understand the accuracy (i.e. agreement with the truth) of those products and the causes of disagreement. This is an essential step if countries wish to use any of these products for both their FRELs and within their national REDD+ strategies to identify the drivers of change and plan activities to reduce rates of deforestation.

### 3.8 References

- Achard, F. and House, J. I.: Reporting carbon losses from tropical deforestation with Pantropical biomass maps, *Environ Res Lett*, 10, 3, 10.1088/1748-9326/10/10/101002, 2015.
- Achard, F., Beuchle, R., Mayaux, P., Stibig, H.-J., Bodart, C., Brink, A., Carboni, S., Desclee, B., Donnay, F., Eva, H. D., Lupi, A., Rasi, R., Seliger, R., and Simonetti, D.: Determination of tropical deforestation rates and related carbon losses from 1990 to 2010, *Global Change Biology*, 20, 2540-2554, 10.1111/gcb.12605, 2014.
- Baccini, A., Goetz, S. J., Walker, W. S., Laporte, N. T., Sun, M., Sulla-Menashe, D., Hackler, J., Beck, P. S. A., Dubayah, R., Friedl, M. A., Samanta, S., and Houghton, R. A.: Estimated carbon dioxide emissions from tropical deforestation improved by carbon-density maps, *Nature Climate Change*, 2, 182-185, 10.1038/nclimate1354, 2012.
- Bouvet, A., Mermoz, S., Toan, T. L., Villard, L., Mathieu, R., Naidoo, L., and Asner, G. P.: An above-ground biomass map of African savannahs and woodlands at 25 m resolution derived from ALOS PALSAR, *Remote Sensing of Environment*, 206, 156-173, 10.1016/j.rse.2017.12.030, 2018.
- Bowman, D. M. J. S. and Murphy, B. P.: Fire and biodiversity, in: *Conservation Biology for All*, edited by: Sodhi, N. S., and Ehrlich, P. R., Oxford University Press, England, 163-181, 2010.

Cahoon, D. R., Stocks, B. J., Levine, J. S., Cofer, W. R., and Oneill, K. P.: Seasonal Distribution of African Savanna Fires, *Nature*, 359, 812-815, DOI 10.1038/359812a0, 1992.

Carreiras, J. M. B., Vasconcelos, M. J., and Lucas, R. M.: Understanding the relationship between aboveground biomass and ALOS PALSAR data in the forests of Guinea-Bissau (West Africa), *Remote Sensing of Environment*, 121, 426-442, 10.1016/j.rse.2012.02.012, 2012.

Chave, J., Andalo, C., Brown, S., Cairns, M. A., Chambers, J. Q., Eamus, D., Folster, H., Fromard, F., Higuchi, N., Kira, T., Lescure, J. P., Nelson, B. W., Ogawa, H., Puig, H., Riera, B., and Yamakura, T.: Tree allometry and improved estimation of carbon stocks and balance in tropical forests, *Oecologia*, 145, 87-99, 10.1007/s00442-005-0100-x, 2005.

Chave, J., Rejou-Mechain, M., Burquez, A., Chidumayo, E., Colgan, M. S., Delitti, W. B., Duque, A., Eid, T., Fearnside, P. M., Goodman, R. C., Henry, M., Martinez-Yrizar, A., Mugasha, W. A., Muller-Landau, H. C., Mencuccini, M., Nelson, B. W., Ngomanda, A., Nogueira, E. M., Ortiz-Malavassi, E., Pelissier, R., Ploton, P., Ryan, C. M., Saldarriaga, J. G., and Vieilledent, G.: Improved allometric models to estimate the aboveground biomass of tropical trees, *Global Change Biology*, 20, 3177-3190, 10.1111/gcb.12629, 2014.

Collins, J. N., Hutley, L. B., Williams, R. J., Boggs, G., Bell, D., and Bartolo, R.: Estimating landscape-scale vegetation carbon stocks using airborne multi-frequency polarimetric synthetic aperture radar (SAR) in the savannahs of north Australia, *International Journal of Remote Sensing*, 30, 1141-1159, 10.1080/01431160802448935, 2009.

FAO: Forest Resources Assessment 2015 Terms and Definitions, Food and Agriculture Organization of the United Nations, Rome, 2015.

Fick, S. E. and Hijmans, R. J.: WorldClim 2: new 1-km spatial resolution climate surfaces for global land areas, *International Journal of Climatology*, 37, 4302-4315, 10.1002/joc.5086, 2017.

GFOI: Integration of remote-sensing and ground-based observations for estimation of emissions and removals of greenhouse gases in forests: Methods and Guidance from the Global Forest Observations Initiative, Food and Agriculture Organization, Rome, 2016.

Goetz, S. J., Hansen, M., Houghton, R. A., Walker, W., Laporte, N., and Busch, J.: Measurement and monitoring needs, capabilities and potential for addressing reduced emissions from deforestation and forest degradation under REDD, *Environ Res Lett*, 12, 10.1088/1748-9326/10/12/123001, 2015.

Grassi, G., House, J., Dentener, F., Federici, S., den Elzen, M., and Penman, J.: The key role of forests in meeting climate targets requires science for credible mitigation, *Nature Climate Change*, 7, 220-+, 10.1038/Nclimate3227, 2017.

Guinea-Bissau, R. o.: Second National Communication of Guinea-Bissau to the UNFCCC, SEAT, Bissau, 2011.

Guinea-Bissau, R. o.: Third National Communication: Report to the United Nations Framework Convention on Climate Change, Bissau, 2018.

Hansen, M., Potapov, P., Margono, B., Stehman, S., Turubanova, S., and Tyukavina, A.: Response to Comment on "High-resolution global maps of 21st-century forest cover change", *Science*, 344, 1, 10.1126/science.1248817, 2014.

Hansen, M. C., Potapov, P. V., Moore, R., Hancher, M., Turubanova, S. A., Tyukavina, A., Thau, D., Stehman, S. V., Goetz, S. J., Loveland, T. R., Kommareddy, A., Egorov, A., Chini, L., Justice, C. O., and Townshend, J. R. G.: High-Resolution Global Maps of 21st-Century Forest Cover Change, *Science*, 342, 850-853, 10.1126/science.1244693, 2013.

Harris, N. L., Brown, S., Hagen, S. C., Saatchi, S. S., Petrova, S., Salas, W., Hansen, M. C., Potapov, P. V., and Lotsch, A.: Baseline Map of Carbon Emissions from Deforestation in Tropical Regions, *Science*, 336, 1573-1576, 10.1126/science.1217962, 2012.

Herold, M. and Skutsch, M.: Monitoring, reporting and verification for national REDD plus programmes: two proposals, *Environ Res Lett*, 6, 10.1088/1748-9326/6/1/014002, 2011.

Hill, T. C., Williams, M., Bloom, A. A., Mitchard, E. T. A., and Ryan, C. M.: Are Inventory Based and Remotely Sensed Above-Ground Biomass Estimates Consistent?, *Plos One*, 8, 8, 10.1371/journal.pone.0074170, 2013.

Hojas-Gascon, P. O. C., Hugh Eva, Robert Nasi and Christopher Martius: Monitoring deforestation and forest degradation in the context of REDD +: Lessons from Tanzania, Infobrief 124, Bogor, Indonesia, Center for International Forestry Research (CIFOR), 2015.

IBAP: Community Based Avoided Deforestation Project iin Guinea-Bissau; VCS Project Description, Instituto da Biodiversidade e das Áreas Protegidas (IBAP), 2015.

IPCC: IPCC Good Practice Guidance on Land Use, Land-Use Change and Forestry., Intergovernmental Panel on Climate Change, 2003.

IPCC: IPCC Guidelines for National Greenhouse Gas Inventories, IGES, Japan: National Greenhouse Gas Inventories Programme, 2006.

Le Quéré, C., Andrew, R. M., Friedlingstein, P., Sitch, S., Pongratz, J., Manning, A. C., Korsbakken, J. I., Peters, G. P., Canadell, J. G., Jackson, R. B., Boden, T. A., Tans, P. P., Andrews, O. D., Arora, V. K., Bakker, D. C. E., Barbero, L., Becker, M., Betts, R. A., Bopp, L., Chevallier, F., Chini, L. P., Ciais, P., Cosca, C. E., Cross, J., Currie, K., Gasser, T., Harris, I., Hauck, J., Haverd, V., Houghton, R. A., Hunt, C. W., Hurtt, G., Ilyina, T., Jain, A. K., Kato, E., Kautz, M., Keeling, R. F., Goldewijk, K. K., Kortzinger, A., Landschutzer, P., Lefevre, N., Lenton, A., Lienert, S., Lima, I., Lombardozzi, D., Metzl, N., Millero, F., Monteiro, P. M. S., Munro, D. R., Nabel, J. E. M. S., Nakaoka, S., Nojiri, Y., Padin, X. A., Peregón, A., Pfeil, B., Pierrot, D., Poulter, B., Rehder, G., Reimer, J., Rodenbeck, C., Schwinger, J., Seferian, R., Skjelvan, I., Stocker, B. D., Tian, H. Q., Tilbrook, B., Tubiello, F. N., van der Laan-Luijckx, I. T., van der Werf, G. R., van Heuven, S., Viovy, N., Vuichard, N., Walker, A. P., Watson, A. J., Wiltshire, A. J., Zaehle, S., and Zhu, D.: Global Carbon Budget 2017, *Earth Syst Sci Data*, 10, 405-448, 10.5194/essd-10-405-2018, 2018.

Lucas, R., Rebelo, L. M., Fatoyinbo, L., Rosenqvist, A., Itoh, T., Shimada, M., Simard, M., Souza, P. W., Thomas, N., Trettin, C., Accad, A., Carreiras, J., and Hilarides, L.: Contribution of L-band SAR to systematic global mangrove monitoring, *Marine and Freshwater Research*, 65, 589-603, 10.1071/mf13177, 2014.

Lucas, R., Armston, J., Fairfax, R., Fensham, R., Accad, A., Carreiras, J., Kelley, J., Bunting, P., Clewley, D., Bray, S., Metcalfe, D., Dwyer, J., Bowen, M., Eyre, T., Laidlaw, M., and Shimada, M.: An Evaluation of the ALOS PALSAR L-Band Backscatter-Above Ground Biomass Relationship Queensland, Australia: Impacts of Surface Moisture Condition and Vegetation Structure, *IEEE Journal of Selected Topics in Applied Earth Observations and Remote Sensing*, 3, 576-593, 10.1109/jstars.2010.2086436, 2010.

Lui, G. V. and Coomes, D. A.: A Comparison of Novel Optical Remote Sensing-Based Technologies for Forest-Cover/Change Monitoring, *Remote Sensing*, 7, 2781-2807, 10.3390/rs70302781, 2015.

Malaisse, F.: *Caractérisations Phytogéographique et Écologique des Forêts de Cantanhez (Région de Tombali, Guinée-Bissau), Acção para o Desenvolvimento, Bissau/Iemberem*, 95 p., 1996.

Mermoz, S. and Toan, T. L.: Forest Disturbances and Regrowth Assessment Using ALOS PALSAR Data from 2007 to 2010 in Vietnam, Cambodia and Lao PDR, *Remote Sensing*, 8, 22, 10.3390/rs8030217, 2016.

Milodowski, D. T., Mitchard, E. T. A., and Williams, M.: Forest loss maps from regional satellite monitoring systematically underestimate deforestation in two rapidly changing parts of the Amazon, *Environ Res Lett*, 12, ARTN 094003

10.1088/1748-9326/aa7e1e, 2017.

Mitchard, E. T., Saatchi, S. S., Baccini, A., Asner, G. P., Goetz, S. J., Harris, N. L., and Brown, S.: Uncertainty in the spatial distribution of tropical forest biomass: a comparison of pan-tropical maps, *Carbon balance and management*, 8, 10, 10.1186/1750-0680-8-10, 2013.

Mitchard, E. T. A., Saatchi, S. S., Woodhouse, I. H., Nangendo, G., Ribeiro, N. S., Williams, M., Ryan, C. M., Lewis, S. L., Feldpausch, T. R., and Meir, P.: Using satellite radar backscatter to predict above-ground woody biomass: A consistent relationship across four different African landscapes, *Geophysical Research Letters*, 36, 6, 10.1029/2009gl040692, 2009.

Mitchard, E. T. A., Feldpausch, T. R., Brienen, R. J. W., Lopez-Gonzalez, G., Monteagudo, A., Baker, T. R., Lewis, S. L., Lloyd, J., Quesada, C. A., Gloor, M., ter Steege, H., Meir, P., Alvarez, E., Araujo-Murakami, A., Aragao, L., Arroyo, L., Aymard, G., Banki, O., Bonal, D., Brown, S., Brown, F. I., Ceron, C. E., Moscoso, V. C., Chave, J., Comiskey, J. A., Cornejo, F., Medina, M. C., Da Costa, L., Costa, F. R. C., Di Fiore, A., Domingues, T. F., Erwin, T. L., Frederickson, T., Higuchi, N., Coronado, E. N. H., Killeen, T. J., Laurance, W. F., Levis, C., Magnusson, W. E., Marimon, B. S., Marimon, B. H., Polo, I. M., Mishra, P., Nascimento, M. T., Neill, D., Vargas, M. P. N., Palacios, W. A., Parada, A., Molina, G. P., Pena-Claros, M., Pitman, N., Peres, C. A., Poorter, L., Prieto, A., Ramirez-Angulo, H., Correa, Z. R., Roopsind, A., Roucoux, K. H., Rudas, A., Salomao, R. P., Schiatti, J., Silveira, M., de Souza, P. F., Steininger, M. K., Stropp, J., Terborgh, J., Thomas, R., Toledo, M., Torres-Lezama, A., van Andel, T. R., van der

Heijden, G. M. F., Vieira, I. C. G., Vieira, S., Vilanova-Torre, E., Vos, V. A., Wang, O., Zartman, C. E., Malhi, Y., and Phillips, O. L.: Markedly divergent estimates of Amazon forest carbon density from ground plots and satellites, *Global Ecology and Biogeography*, 23, 935-946, 10.1111/geb.12168, 2014.

Norman, M., Nakhouda, S.: *The State of REDD+ Finance*, 2015.

Olofsson, P., Foody, G. M., Herold, M., Stehman, S. V., Woodcock, C. E., and Wulder, M. A.: Good practices for estimating area and assessing accuracy of land change, *Remote Sensing of Environment*, 148, 42-57, 10.1016/j.rse.2014.02.015, 2014.

Olson, D. M., Dinerstein, E., Wikramanayake, E. D., Burgess, N. D., Powell, G. V. N., Underwood, E. C., D'Amico, J. A., Itoua, I., Strand, H. E., Morrison, J. C., Loucks, C. J., Allnutt, T. F., Ricketts, T. H., Kura, Y., Lamoreux, J. F., Wettengel, W. W., Hedao, P., and Kassem, K. R.: Terrestrial ecoregions of the worlds: A new map of life on Earth, *Bioscience*, 51, 933-938, Doi 10.1641/0006-3568(2001)051[0933:Teotwa]2.0.Co;2, 2001.

Pearson, T., Walker, S., and Brown, S.: *Sourcebook for land use, land-use change and forestry projects*, Winrock International, Little Rock, AK, 64 p., 2005.

Roberts, G., Wooster, M. J., and Lagoudakis, E.: Annual and diurnal african biomass burning temporal dynamics, *Biogeosciences*, 6, 849-866, DOI 10.5194/bg-6-849-2009, 2009.

Romijn, E., Lantican, C. B., Herold, M., Lindquist, E., Ochieng, R., Wijaya, A., Murdiyarto, D., and Verchot, L.: Assessing change in national forest monitoring capacities of 99 tropical countries, *Forest Ecology and Management*, 352, 109-123, 10.1016/j.foreco.2015.06.003, 2015.

Saatchi, S. S., Harris, N. L., Brown, S., Lefsky, M., Mitchard, E. T. A., Salas, W., Zutta, B. R., Buermann, W., Lewis, S. L., Hagen, S., Petrova, S., White, L., Silman, M., and Morel, A.: Benchmark map of forest carbon stocks in tropical regions across three continents, *Proceedings of the National Academy of Sciences of the United States of America*, 108, 9899-9904, 10.1073/pnas.1019576108, 2011.

Sannier, C., McRoberts, R. E., and Fichet, L. V.: Suitability of Global Forest Change data to report forest cover estimates at national level in Gabon, *Remote Sensing of Environment*, 173, 326-338, 10.1016/j.rse.2015.10.032, 2016.

Sexton, J. O., Song, X. P., Feng, M., Noojipady, P., Anand, A., Huang, C. Q., Kim, D. H., Collins, K. M., Channan, S., DiMiceli, C., and Townshend, J. R.: Global, 30-m resolution continuous fields of tree cover: Landsat-based rescaling of MODIS vegetation continuous fields with lidar-based estimates of error, *International Journal of Digital Earth*, 6, 427-448, 10.1080/17538947.2013.786146, 2013.

Shimada, M., Itoh, T., Motooka, T., Watanabe, M., Shiraishi, T., Thapa, R., and Lucas, R.: New global forest/non-forest maps from ALOS PALSAR data (2007–2010), *Remote Sensing of Environment*, 155, 13-31, <http://dx.doi.org/10.1016/j.rse.2014.04.014>, 2014.

Tropek, R., Sedlacek, O., Beck, J., Keil, P., Musilova, Z., Simova, I., and Storch, D.: Comment on "High-resolution global maps of 21st-century forest cover change", *Science*, 344, 3, 10.1126/science.1248753, 2014.

Tyukavina, A., Baccini, A., Hansen, M. C., Potapov, P. V., Stehman, S. V., Houghton, R. A., Krylov, A. M., Turubanova, S., and Goetz, S. J.: Aboveground carbon loss in natural and managed tropical forests from 2000 to 2012, *Environ Res Lett*, 10, 14, 10.1088/1748-9326/10/7/074002, 2015.

UNFCCC: Decision 1/CP.21, Adoption of the Paris Agreement, FCCC/CP/2015/10/Add.1, 2016.

van Wilgen, B. W. and Scholes, R. J.: The vegetation and fire regimes of southern-hemisphere Africa., in: *Fire in southern African savannas: ecological and atmospheric perspectives*, edited by: van Wilgen, B. W., Andreae, M. O., Goldammer, J. G., and Lindesay, J. A., Witwatersrand University Press, Johannesburg, 27-46, 1997.

Vasconcelos, M. J., Cabral, A. I. R., Melo, J. B., Pearson, T. R. H., Pereira, H. D., Cassama, V., and Yudelman, T.: Can blue carbon contribute to clean development in West-Africa? The case of Guinea-Bissau, *Mitigation and Adaptation Strategies for Global Change*, 20, 1361-1383, 10.1007/s11027-014-9551-x, 2015.

Vitteck, M., Brink, A., Donnay, F., Simonetti, D., and Desclee, B.: Land Cover Change Monitoring Using Landsat MSS/TM Satellite Image Data over West Africa between 1975 and 1990, *Remote Sensing*, 6, 658-676, 10.3390/rs6010658, 2014.

Wulder, M. A. and Coops, N. C.: Make Earth observations open access, *Nature*, 513, 30-31, DOI 10.1038/513030a, 2014.

Zarin, D. J., Harris, N. L., Baccini, A., Aksenov, D., Hansen, M. C., Azevedo-Ramos, C., Azevedo, T., Margono, B. A., Alencar, A. C., Gabris, C. S., Allegretti, A., Potapov, P., Farina, M., Walker, W. S., Shevade, V. S., Loboda, T. V., Turubanova, S., and Tyukavina, A.: Can carbon emissions from tropical deforestation drop by 50% in 5years?, *Global Change Biology*, 22, 1336-1347, 10.1111/gcb.13153, 2016.



# Chapter 4. Combining satellite-based global maps for improved estimates of deforestation in African savannas

## Abstract

Deforestation maps derived from satellite Earth Observations are attractive tools to developing countries monitoring their forests and plan actions to protect them. However, the accuracy of these maps is often unknown. We compared a national-scale deforestation map produced by Guinea-Bissau (West Africa) for the period 2007-2010 and used by the Government in national reporting to the UNFCCC, with deforestation maps derived from two global datasets. With a reference sample of 899 units, we validated and corrected the classification errors of the maps, both individually and when used in combination. We find that the errors associated with mapping deforestation are very high in all maps, but they are reduced when the maps are used together by combining them or intersecting them. Commission error varies from 29% to 60%, with the lowest commission error (CE = 29%) obtained by the intersection of all three deforestation maps. Omission error can reach as high as 99.9% with the lowest omission error (OE = 43%) obtained by the union of the three deforestation maps. The sources of errors are similar in all maps with most of the classification errors being linked to shifting agriculture (5-36%), swamped rice cultivation in mangrove areas (0-16%), or tree crops (3-11%). Most commission errors are in clusters around urban areas, where vegetation is expected to be more degraded, while most omission errors are in the western region dominated by dry forests. The practice of using wall-to-wall maps as stratified estimators and combining them with a reference sample to derive more accurate area estimates provides a better alternative for reporting areas than pixel-counting – the areas corrected for classification bias are relatively similar (CV=0.43 compared to CV=1.00 before correction) regardless of the deforestation map used as the basis for the stratification. Because the variation is still large, combining maps could be a good alternative to mitigate the effects of exacerbated omission areas corrections. To increase accuracy and confidence in the estimates, national definitions must clearly attribute shifting agriculture and trees outside forest to a land category (e.g., forest, cropland) used in the GHG inventory. Defining clear protocols for interpretation of sample units to be used either for map classification or for its validation and correction is also critical to harness the opportunities provided by satellite-based global maps to quantify deforestation and support the most vulnerable countries to protect their forests.

**Keywords:** drivers of deforestation, Earth observation, shifting agriculture, measurement reporting and verification, Guinea-Bissau

## 4.1 Contributions and Acknowledgements

The following research chapter is currently in preparation for submission to a scientific journal to be decided with co-authors. It is presented here as an initial draft to be distributed to co-authors for their comments. Supplementary information for this chapter is available in Appendix 3 of this thesis.

**Authors:** Joana Melo<sup>1</sup>, Timothy Baker<sup>1</sup>, Viriato Cassama<sup>2</sup>, Shijuan Chen<sup>3</sup>, Guy Ziv<sup>1</sup>

### **Affiliations and addresses**

<sup>1</sup> School of Geography, University of Leeds, Woodhouse Lane, Leeds LS2 9JT, United Kingdom

<sup>2</sup> Office of the President of the Republic of Guinea-Bissau, Bissau, Guiné-Bissau

<sup>3</sup> Yale School of the Environment, Yale University, New Haven, CT 06511, USA

**Author contributions:** JM, TRB and GZ designed and conceived the study. JM collected and analysed the data. VC supported the QAQC of the visual interpretation of the reference dataset. SC provided feedback on the sampling design and results to be undertaken as corrections. JM wrote the first draft manuscript.

## 4.2 Introduction

Tropical dry forests occupy a vast extent of land and support the livelihood of many people across the world (Mcnicol et al., 2018; Miles et al., 2006; Bastin et al., 2017). Although sub-Saharan Africa experienced the lowest rate of biomass loss in the tropics during the 2000s, the proportion of biomass loss in dry forests was comparable to that of humid tropical forests, contrasting with other regions of the world (Tyukavina et al., 2015). Highly dynamic and difficult to measure (Mcnicol et al., 2018), tropical dry forests remain under-studied and updated information on deforestation and forest degradation in these ecosystems remains a research priority (Sunderland et al., 2015; Tyukavina et al., 2015). In addition, given the increased urgency in acquiring near real-time information on forest dynamics and associated carbon fluxes to boost action towards climate change mitigation strategies (UNFCCC, 2015), such research is highly policy-relevant. This research is particularly important for East and West African countries dominated by savannas, where the land use sector is the larger contributor to domestic GHG emissions (Valentini et al., 2014).

Wall-to-wall deforestation maps provide information on the location and extent of deforestation events continuously in space and time (Hansen et al., 2013; Vancutsem et al., 2021). They are therefore widely used to spatially monitor forests and land dynamics and to report estimates of land change and associated GHG fluxes to the UNFCCC (Melo et al., 2023). However, large biases from map classification errors make the maps inaccurate (Stehman, 2013; McRoberts, 2011; Olofsson et al., 2014a). Therefore, to report a consistent and accurate time-series of deforestation, the good practice for area estimation using sample observations to correct the bias of the map introduced by classification errors (Olofsson et al., 2014a) must be employed. In this case, deforestation maps are used as hotspots for stratification and the estimates are derived from the stratified sample (Achard et al., 2002; Vancutsem et al., 2021; Feng et al., 2022). In addition to producing time-series estimates, wall-to-wall maps are very useful to prioritize and implement mitigation actions, to measure progress of those actions, or as alert systems for law enforcement (Reiche et al., 2021; Diniz et al., 2015; Doblus et al., 2022; Finer et al., 2018).

Guinea-Bissau is a least-developed country in West Africa. It is mostly covered by dry forests and mangroves (Vittekk et al., 2014) and encompasses the climate and vegetation gradients of many areas of sub-Saharan Africa (**Figure 4-1a**). Satellite-based global maps of deforestation are particularly interesting to explore in this context, given these UNFCCC Party groupings (i.e., the group of least developed countries and the geopolitical African group) with lower MRV capacity are also those who most benefit from the use of satellite-based global maps (Melo et al., 2023), and given the inherent

challenges of accurately measuring the highly dynamic dry forests. Previous studies highlighted striking differences in the mapped area of deforestation by different global maps (Hansen et al., 2013; Sexton et al., 2013; Shimada et al., 2014), both in terms of spatial distribution and its magnitude (Melo et al., 2018). Bastin et al. (2017) compared the areas of forest in the drylands as mapped by Hansen et al. (2013) and Sexton et al. (2013) using Landsat with a map based on VHR data and noted a large underestimation of dry forests in Africa by the two global products, in particular Sexton et al. However, the accuracy of the individual maps to quantify deforestation remains unknown.

Here, we therefore designed a sampling scheme to collect reference observations and quantify the errors of the deforestation maps and magnitude of those errors. We aim to understand i) which of the available deforestation maps is the most accurate ii) if combining deforestation maps reduces the classification errors of the estimates and iii) what are the main causes of classification errors in African mangroves and savanna ecosystems. Overall, we wish to understand the potential of global satellite-based maps to support developing countries dominated by dry forest ecosystems and with no domestic monitoring systems to respond to the urgent demands of the UNFCCC to achieve the objectives of its Paris Agreement.

## 4.3 Materials and methods

### 4.3.1 Deforestation maps

To estimate forest loss from 2007 to 2010 for Guinea-Bissau, three deforestation maps were generated (**Figure 4-1b**). The first deforestation map was produced using official national Landsat-based land-cover maps for 2007 and 2010 used in reporting to the UNFCCC (Guinea-Bissau, 2019, 2020). The land cover maps discriminating terrestrial forests and mangroves and non-forest were based on Landsat TM and ETM+ images collected during the late dry season in 2007 and 2010 and used supervised classification algorithms. Two available global datasets were also used for this study. The Global Forest Change (GFC; Hansen et al. (2013)) is a widely used 30-m resolution dataset based on automated classification algorithms of a time-series of Landsat images from the growing season. Specifically, here we used its tree cover map for 2000 and the annual tree-cover loss between 2000 and 2010. We also used the global dataset of tree-cover from the Global Land Cover Facility (GLCF; Sexton et al. (2013)). Although also a tree-cover global map, this dataset uses the 250-m MODerate-resolution Imaging Spectroradiometer (MODIS) Vegetation Continuous Fields (VCF) rescaled to 30-m resolution using Landsat data. Furthermore, imagery acquisition dates are not restricted to the wet season as in the GFC.

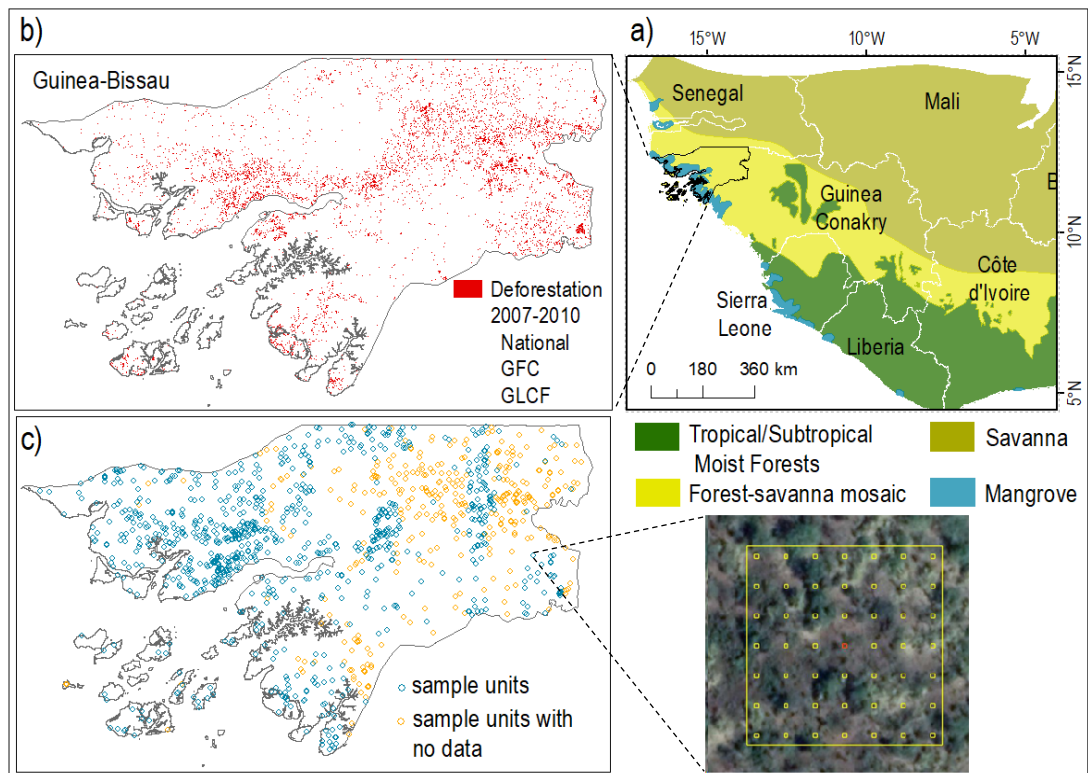


**Figure 4-1.** Study area and data used in this study, including: a) the location of Guinea-Bissau in Western Africa showing terrestrial ecoregions (adapted from Olson et al 2001); b) Guinea-Bissau subset showing deforestation between 2007 and 2010 obtained as the sum of deforestation derived from three independent maps - a map produced in-house using Landsat imagery and used by Guinea-Bissau in its submissions to the UNFCCC, and deforestation derived from two global scale maps, the Global Forest Change (GFC, Hansen et al, 2013) and the Global Land Cover Facility (Sexton et al, 2013); c) Guinea-Bissau subset depicting the sample units following a stratified sampling approach and identifying the 899 sample units visually interpreted with Google Earth imagery and included in this study as reference dataset (in blue), and the remaining 341 sample units where Google Earth imagery was not available for the period 2007-2010 (in yellow). The example of a very high-resolution imagery from Google Earth corresponding to one 0.5 ha sample unit also depicts the 49-point grid used to determine the proportion of land use and tree cover in each sample unit.

We spatially tracked and estimated gross deforestation from these three datasets over the 2007-2010 period. The reference period chosen for the analysis was determined by the availability of the national maps. The procedure to reclassify the data to *deforestation* and *no-change* was described in detail by Melo et al. (2018). In summary: the two National land-cover maps (2007, 2010) were reclassified into *forest* and *non-forest* (F/NF). For GFC, F/NF maps were generated for the years 2007 and 2010 using the 2000 tree-cover and annual loss maps; the 2000 tree-cover map was reclassified to F/NF with forest being defined as areas with tree-cover above 10%; loss in the period 2001-2007 was used to update the 2000 F/NF map and generate a 2007 F/NF map; the same approach was followed to obtain the 2010 F/NF map. For GLCF, F/NF maps were generated for the years 2005 and 2010 by reclassifying areas with tree-cover above 10% as forests in the tree-cover maps for the corresponding years. In a post-classification change detection approach, the F/NF maps from the three different sources (national, GFC, and GLCF) were used to obtain three different *deforestation* and *no-change* maps (**Figure 4-1b**). For consistency with the national forest definition the minimum mapping unit of 0.5-ha and the tree-cover threshold of 10% was used for all maps.

Spatial operations of union and intersection were applied to derive combinations of pairs of deforestation maps or combinations of the three deforestation maps. These intersections and unions plus the original three maps resulted in a total of 11 maps: three individual maps (National, GFC, GLCF), four combinations of intersected maps ( $\text{Nat} \cap \text{GFC}$ ,  $\text{Nat} \cap \text{GLCF}$ ,  $\text{GFC} \cap \text{GLCF}$ ,  $\text{Nat} \cap \text{GFC} \cap \text{GLCF}$ ), and four combinations of union of maps ( $\text{Nat} \cup \text{GFC}$ ,  $\text{Nat} \cup \text{GLCF}$ ,  $\text{GFC} \cup \text{GLCF}$ ,  $\text{Nat} \cup \text{GFC} \cup \text{GLCF}$ ). The purpose of these operations is to validate combinations of maps, quantify their errors of omission and commission and identify if higher accuracies are achieved by combining maps.

### 4.3.2 Reference data

#### 4.3.2.1 Sample design

To quantify the classification errors of the deforestation maps and their combinations, as well as the magnitude and causes of those errors, we designed a sampling scheme to collect reference observations. We selected a stratified random sampling scheme with the deforestation maps and their combinations forming the basis of the stratification. A simple random sampling strategy would have allowed validation of the maps and also to make inferences based only on the sample (Stehman, 2013; Olofsson et al., 2020; Chen et al., 2023). However, because the areas of the deforestation classes are rare comparatively to the *no-change* classes (ranging from less than 1% in the GFC to 5% in the National map; see **Table A.3.1**), a stratified random approach was selected instead to ensure that these small classes were adequately sampled (Stehman, 2012). Therefore, our reference sample was randomly selected with the map classes defined as the strata (i.e. *deforestation* and *no-change*). We followed the recommendations for stratified estimators in the accuracy assessment of remote sensing maps (Olofsson et al., 2013; Olofsson et al., 2014a). We first estimated the area proportion of each class of *deforestation* and *no-change* to use as strata weights. Because one of the conditions in a probability sample is that the inclusion probability for each class must be greater than zero (Stehman, 2001), we needed to ensure that all classes had samples allocated to them. Therefore, in addition to *deforestation* from the individual maps (National, GFC, GLCF), we have also included the rare classes of agreement of deforestation between maps ( $\text{Nat} \cap \text{GFC}$ ,  $\text{Nat} \cap \text{GLCF}$ ,  $\text{GFC} \cap \text{GLCF}$ ,  $\text{Nat} \cap \text{GFC} \cap \text{GLCF}$ ) in the stratification. We did a proportional split of the total sample size according to the area weight of the strata. However, we also followed the good practice of increasing the sample size of the smaller classes to a minimum of 50 units (Olofsson et al., 2014a)(**Table A.3.1**). The result was a compromise of allocation of sample units between equal sample size (typically with lower commission errors) and proportional allocation (typically with lower omission errors and overall error; Stehman, 2012).

### 4.3.2.2 Sources of data

To identify map classification errors and area bias, we collected a reference dataset by visually interpreting high-resolution satellite imagery between 2007 and 2010. Although our reference period is 2007-2010, we also visually interpreted an additional image around 2019 ( $\pm 2$  years) to confirm if the land use conversion had been a permanent conversion. We used the application Collect Earth (Bey et al., 2016) to facilitate access and visualization of high-resolution satellite data from Google Earth (including DigitalGlobe, SPOT, Sentinel 2, Landsat and MODIS imagery) combined with access to the full Landsat archive in Google Earth Engine (Gorelick et al., 2017). The latter data source, with its higher temporal resolution, is very useful to confirm the year of forest conversion or disturbance. For consistency in the classification, any sample unit with no high-resolution imagery in the beginning or end of the reference period (i.e., 2007 and 2010) was excluded from the sample. The reference sample included a total of 899 sample units visually interpreted with Google Earth imagery and 341 sample units where Google Earth imagery was not available for the period 2007-2010 (**Figure 4-1c**, in blue and yellow, respectively).

### 4.3.2.3 Classification protocol

We developed a response design to assign the sample to the class *deforestation* or *no-change* (including stable forest, and stable non-forest) (**Figure 4-2**). We classified our sample units of 0.5-ha using a systematic grid of 49 points within each sample unit to determine the proportion of land use and tree cover in each sample unit (**Figure 4-3**). The method is similar to that described in the guidance for the use of Collect Earth (Finegold and Ortmann, 2016; Tzamtzis et al., 2019) and used in similar research studies (e.g., Bastin et al., 2017), and is also frequently applied in countries' submissions to the UNFCCC using sample-based area estimate approaches (e.g. see REDD+ Forest Reference Level submissions from Mozambique 2018, Malawi 2020, Ghana 2021, Saint Lucia 2023 (Melo et al., 2023)). A sample unit is classified as forest if forest is the land use covering the larger proportion of the unit (i.e., more than 50% of the grid of points in forest land) and more than 10% of the unit is covered by trees (**Figure 4-2**). If the sample unit is not forest (NF in **Figure 4-2**), the prevailing land use is noted. In our classification, forest disturbances showed a reduction in tree cover but no sign of other land use (considered temporarily unstocked areas in **Figure 4-2**). However, if the prevailing land use is not forest in more than 50% of the sample unit (for example from conversion of mangrove forest to swamped rice field as in **Figure 4-3b**, or conversion of forest to tree crop, cropland, or settlement) the sample unit is classified as deforestation, even if the tree cover is above 10%. This is because settlements can have urban trees, cropland can have remaining trees standing, and tree crops are entirely covered by trees but are

not forest land use. Therefore, although quantifying canopy cover supported the classification of the sample unit, we did not attribute land use of a sample unit based solely on the percentage of canopy cover.

Shifting agriculture deserves particular attention in the class attribution of our reference sample. Many ethnic groups in Guinea-Bissau practice sustainable shifting agriculture characterised by long fallow periods, short crop cycles, and leaving most of the trees standing (Temudo, 2011; Temudo and Abrantes, 2013). Here, we considered that these practices were not land use conversion because the land remained forest or fallow for the entire reference period and no evidence of other use was visible in the available imagery. However, if shifting agriculture was in a crop cycle in more than 50% of the sample unit and there was a reduction of tree cover below the 10% of the national definition during the reference period, this unit was classified as *deforestation*. A sample unit with crop prevailing land use in less than 50% of the unit and tree cover above 10% could also be considered *deforestation* if the trees are suspected to be tree crops or if the surrounding area shows evidence of expansion of tree crop plantations. This is because of the wide-spread conversion to cashew plantations in the country and the fact that these conversions are typically preceded by crop cycles (Temudo and Abrantes, 2014). Here, again, percentage tree cover supports the classification but does not solely determine land use. Similarly, we classified the sample unit as *deforestation* in the case of conversion to settlement in more than 50% of the sample unit, regardless of the canopy tree cover percentage, because in Guinea-Bissau, remaining trees around settlements are very likely tree crops or fruit trees (e.g., cashew trees or mango trees).

The response design implemented in the analysis set clear rules for interpretation and attribution of land use and land use change to each sample unit. To increase the consistency and accuracy of the results, with each 100 units classified, the interpreter reviewed the entire set of classified units from the beginning. This post-interpretation review procedure ensured more consistency in the criteria applied i) spatially, when interpreting different regions of the country with different dominant ethnic groups, different practices, and different drivers of deforestation; and ii) in time given the increased experience of the interpreter as more sample units were classified and the implementation of the response design protocol became clearer.

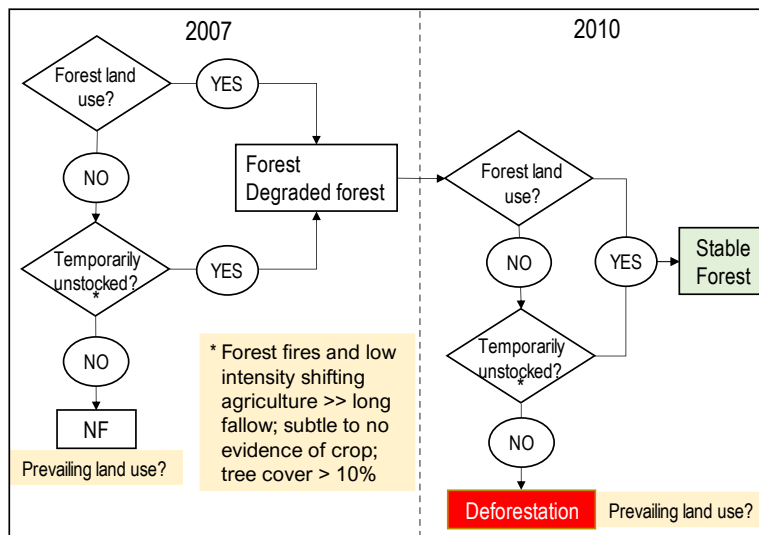
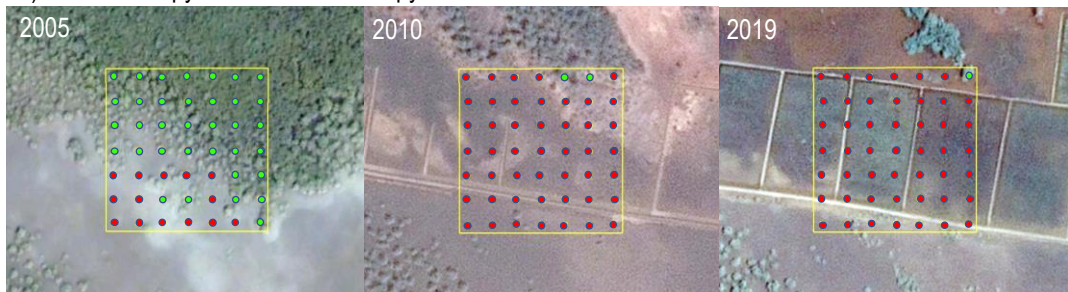


**Figure 4-2.** Response design or decision tree for the classification of the sampling units using Google Earth imagery to determine the prevailing land use in the year 2007 and 2010 and eventual land use changes in the reference period. Sample unit classified as “temporarily unstocked” correspond to areas affected by fire, logging, or low intensity shifting agriculture where the percentage tree cover is not reduced more than 30% and is not below the threshold of the national definition of forest in 2010 (i.e., 10% in Guinea-Bissau). When the land use is not forest (NF), the interpreter takes note of prevailing land use and percentage tree cover before and after conversion. Imagery available between 2010 and 2022 was also assessed to support and increase trust in the decision.

a) ● Tree canopy and ● no tree canopy cover



b) ● Forest land use and ● other land use



**Figure 4-3.** Example of a time-series of google earth imagery between 2005 and 2019 used to classify one sampling unit and the use of the grid of 49 points used to determine land use and land use change between 2005 and 2010. For each sample unit, the proportion of a) tree cover and a) land use was assessed in at least two time points through visual interpretation of very high-resolution satellite images. In this example, mangrove is converted to swamp rice cultivation (deforestation) between 2005 and 2010 with a reduction of a) tree canopy cover from 71% (35/49 points) to 4% (4/49 points) and a reduction of b) 88% (43/49 points) to 8% (4/49 points) of mangrove forest land use. An image from 2019 is also analysed to confirm the land use transition.

### 4.3.3 Map validation and bias correction of area estimates

To assess the accuracy of the available deforestation maps, we produced error matrices with a cross-tabulation between the *deforestation* and *no-change* classes allocated by the maps and reference data. We produced 11 error matrices: for the three individual maps (National, GFC, GLCF), for four combinations of intersected maps (Nat  $\cap$  GFC,

Nat  $\cap$  GLCF, GFC  $\cap$  GLCF, Nat  $\cap$  GFC  $\cap$  GLCF), and for four combinations of the union of maps (Nat  $\cup$  GFC, Nat  $\cup$  GLCF, GFC  $\cup$  GLCF, Nat  $\cup$  GFC  $\cup$  GLCF). The confusion matrices have the form:

		Reference dataset	
		Deforestation	No-change
Map classification	Deforestation	$n_{11}$ (true deforestation)	$n_{12}$ (false deforestation)
	No-change	$n_{21}$ (false no-change)	$n_{22}$ (true no-change)

Based on the error matrix we estimated the errors of the *deforestation* classes of each of the 11 maps, namely: i) commission error (CE, eq. 1; complementary measure to user's accuracy) given as the probability that the sample unit is wrongly classified as *deforestation* in the map because it is *no-change* (either stable forest or stable non-forest) in the reference data; and ii) omission error (OE, eq. 2; complementary measure to producer's accuracy) as the probability that the sample unit is wrongly classified as *no-change* (either stable forest or stable non-forest) in the map because it is *deforestation* in the reference data.

$$CE = \frac{n_{12}}{n_{11} + n_{12}} \quad (\text{eq. 1})$$

$$OE = \frac{n_{21}}{n_{11} + n_{21}} \quad (\text{eq. 2})$$

We used the reference data to correct the bias attributable to map classification error of the areas of *deforestation* of each map and combination of maps and to estimate its standard errors following best practices from Olofsson et al (2014). According to the authors, overall accuracy and omission errors (eq. 2) should not be estimated from the error matrix because sample units from the two different strata (deforestation and no-change) require different weights. Commission error (eq. 1), on the other hand, is quantified using data from the same strata only and therefore can be calculated directly from the error matrix of sample counts. Accordingly, here we derived the estimators of the overall map accuracy, omission error and commission error from the error matrix area proportions, or estimated error matrix (see equations 6-8, Olofsson et al., 2013).

#### 4.3.4 Spatial distribution of the errors and causes of the classification errors

We used the Hotspot analysis tool in ArcGIS to identify statistically significant clusters of sample units correctly (1) and incorrectly (0) classified as *deforestation* and as *no-change* in the 11 deforestation maps assessed. A hotspot is a cluster of high values (1) surrounded by other high values. Here, it corresponds to clusters of sample units correctly classified. A coldspot is a cluster of low values (0) surrounded by other low

values, and in our analysis corresponds to clusters of sample units wrongly classified in the maps. Our objective is to understand if there are spatial patterns and specific areas with high concentrations. The tool measures the spatial autocorrelation of the attribute values and display the results in a thematic map showing the location and intensity of hotspots and coldspots.

## 4.4 Results and discussion

### 4.4.1 Deforestation areas and classification errors of the maps

Comparing the deforestation areas of the three individual deforestation maps (National, GFC, and GLCF) with the area obtained by the combination of the maps confirms the findings from Melo et al (2018) of striking disagreements between these maps. The intersection of all maps shows that the area of agreement (1.3 kha; **Table 4.1**) corresponds to less than 1% of the area mapped as deforestation by the National map, 1.5% of the area mapped as deforestation in the GLCF, and 6% of the GFC. Comparing the maps and combining them confirms the spatial disagreement and highlights the different magnitudes in the deforestation estimates (**Table 4.1, Figure 4-4**). However, after adjustment of the mapped deforestation area (from pixel-counting) to eliminate bias from map classification error, the variability is significantly less striking between deforestation measurements from the three maps and their combinations. The coefficient of variation (CV) of the corrected deforestation areas is 43% compared to 100% in the original areas. Deforestation was greatly underestimated in all maps, as shown by the large omission errors (**Figure 4-4**). Note that it is considered statistical good practice (Olofsson et al (2013)) to use the stratified estimator to adjust the map area obtained from pixel-counting to account for the large omission error of deforestation. Consequently, the deforestation areas reported after correction are considerably higher than the original areas (**Table 4.1, Figure 4-4**) with increases ranging from 43% (Nat U GFC U GLCF) to 100% (in the intersection of maps).

**Table 4.1.** Aggregated deforestation between 2007 and 2010 obtained from the individual deforestation maps (National, GFC, and GLCF), the intersection of maps (National  $\cap$  GFC; National  $\cap$  GLCF; GFC  $\cap$  GLCF; National  $\cap$  GFC  $\cap$  GLCF) and union of maps (National U GFC; National U GLCF; GFC U GLCF; National U GFC U GLCF) before and after correction of classification bias calculated as in Olofsson et al. 2014

deforestation map	original (kha)	corrected (kha)
National	158.3	746.5
GFC	22.6	479.0
GLCF	84.4	737.9
Nat U GFC	177.7	337.7
Nat U GLCF	229.4	459.7
GFC U GLCF	103.0	341.8
Nat U GFC U GLCF	246.1	188.6
Nat $\cap$ GFC	1.9	857.3
Nat $\cap$ GLCF	11.9	956.6
GFC $\cap$ GLCF	2.7	877.0
Nat $\cap$ GFC $\cap$ GLCF	1.3	886.0

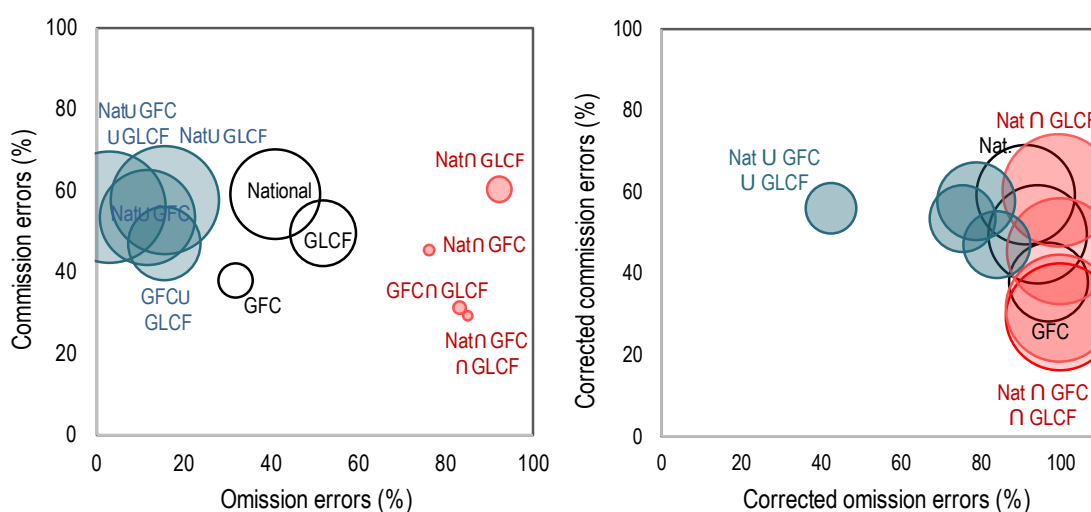


**Figure 4-4.** Omission and commission errors of the individual maps (National, GFC, and GLCF), intersection of maps (National  $\cap$  GFC; National  $\cap$  GLCF; GFC  $\cap$  GLCF; National  $\cap$  GFC  $\cap$  GLCF) and union of maps (National U GFC; National U GLCF; GFC U GLCF; National U GFC U GLCF) a) before and b) after correction of classification bias. The size of each circle is proportional to the area mapped as deforestation by each map (black circle), intersection of maps (red) or union of maps (blue), a) before, and b) after correction for classification bias.

The accuracy assessment from the visually interpretation of 899 sample units using very-high resolution imagery accessed through Collect Earth shows that, for the 2007-2010 reference period, the GFC deforestation map was the most accurate of the three individual deforestation maps analysed, with the highest number of sample units correctly classified and the lowest number wrongly classified (**Figure 4-5; Table A.3.2**). It had an overall accuracy (OA) of 85%, compared to 77% of the GLCF and 76% of the national deforestation map. Its OA is always higher when combined with the other two maps (Nat U GFC, GFC U GLCF, Nat U GFC U GLCF) ranging from 89% OA to 93%, with the highest OA obtained from the union of the three deforestation maps (Nat U GFC U GLCF). All maps show high omission and commission errors both before and after correction (**Figure 4-4**). Before correction the GFC shows the lowest errors, both of omission and commission (OE and CE, respectively; **Figure 4-4, Table A.3.2**). However,

omission errors need to be quantified and adjusted using the estimator from the proportion matrix (**Table A.3.3**) before drawing conclusions on the accuracy of the maps (Olofsson et al., 2014a). The omission error of the GFC increases more than any other map when considering the low area proportion of the *deforestation* class, moving the GFC from the *deforestation* map with lowest (32%) to the highest (97%) OE of all individual maps (**Figure 4-4, Table A.3.2, Table A.3.3**) This result was expected considering the GFC has the lowest mapped area of deforestation of the three maps analysed (**Table 4.1**).

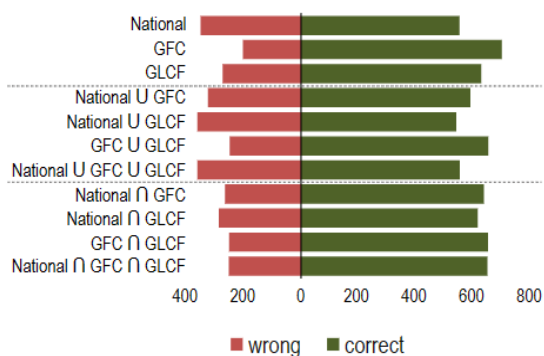


**Figure 4-5.** Number of the total 899 sampling units corresponding (correct, green) or not corresponding (wrong, red) to the classification of deforestation and stable forest or non-forest from the individual deforestation maps (National, GFC, and GLCF), the intersection of maps (National ∩ GFC; National ∩ GLCF; GFC ∩ GLCF; National ∩ GFC ∩ GLCF) and union of maps (National U GFC; National U GLCF; GFC U GLCF; National U GFC U GLCF)

Omission errors are reduced in all three individual maps when combined with another deforestation map (**Figure 4-4, Table A.3.2**) with the lowest being obtained in the union of all three maps (OE = 42%). Intersecting maps always increases the already high (in the individual maps) omission error. These reach as high as 99.9% in the intersection of National and GFC maps. Intersecting the three maps renders the lowest commission error of all 11 maps (**Figure 4-4, Table A.3.2**). Variations in the commission error vary depending on the map and map combinations. For the National deforestation map, it slightly decreases with the union with any of the other maps, with the maximum reduction being from 59% to 53% when combined with GFC. Conversely, the GFC map always increases its commission error if combined with any of the other maps. The National map commission error decreases if intersected with the GFC, and for both the GFC and GLCF it decreases if intersected with each other. However, reductions in commission errors are very small, with the lowest value, from the combination of all three maps, remaining high (CE = 29%).

#### 4.4.2 Sampling design as a source of bias

Our accuracy assessment of deforestation maps shows exacerbated omission errors leading to apparently exacerbated area corrections, particularly in the intersection of maps (**Table 4.1**). While research is still needed on how to contain the effects of omission

errors, the main causes of this effect are known. In our case, the area of *no-change* is very large relative to the area of *deforestation*, particularly in the intersection of maps (**Table 4.1**). Because of the very large difference in the weights of the two classes, omissions of deforestation in the class *no-change* carried a very large weight in the error matrices expressed as error proportions (**Table A.3.3**). This difference means that a single error of omission represents a large area proportion while a single sample correctly classified as deforestation carries a much lower area proportion weight. Olofsson et al (2020) provide practical suggestions to address these exacerbated errors by splitting the large strata into sub-classes. For example, by applying a buffer around areas of *deforestation* corresponding to areas of *no-change* in the maps with higher probability of having been deforested (Tyukavina et al., 2013; Arevalo et al., 2020; Olofsson et al., 2020). While we did not apply a buffer to the deforestation areas, by combining maps we are biasing our reference data to areas of likely deforestation as well. Consequences of this decision are discussed below.

Firstly, our sample is not allocated proportionally to the size of each class (**Table A.3.1**). This was because we wanted to ensure the small classes were adequately sampled and therefore we increased the sample size of the smaller classes to a minimum of 50 units. Furthermore, a large proportion of the sample units without Google Earth data were from the classes of *no-change* which means these classes were under-sampled while the deforestation classes were oversampled relative to their size. Consequently, the omission errors that are expected to be reduced in proportional allocation are always very high in our case because we had less sample units in a class that carried a very large area weight (*no-change*).

Secondly, we used the same sample of 899 units for the accuracy assessment of all 11 maps containing only two classes: *deforestation* and *no-change*. However, many of the sample units mapped as *no-change* by any of the maps, were very likely mapped by another map as *deforestation* (**Table A.3.1**). In practice, using independent maps of deforestation to identify areas of *no-change* that are more likely to contain omission errors than the class of agreement of *no-change* (class 1 in **Table A.3.1**) is the same concept as incorporating a spatial buffer around deforested areas. Hypothetically, it could even be considered a better alternative in the case of mosaic deforestation as opposed to fish bone deforestation in tropical forests. One possible solution to address the issue of including areas of more likelihood of omission errors would be to assign weights to each sample unit based on their probability of selection. Nevertheless, we note that Arevalo et al. (2020), presenting a methodology for monitoring and estimating areas of deforestation removing the classification bias of wall-to-wall maps, also used the combined sample units from the classes *no-change* and *buffer* as *no-change* to assess the effectiveness of the buffer to contain omission errors.

Therefore, while we must use our subjective judgment and point to the limitations of the sample and the likely bias of the estimates, we must also acknowledge that estimating an area that is assumed to be <1% of the population in all deforestation maps except the union of independent maps is inherently difficult. However, our sample still provides useful information because it is still sufficiently large and randomly selected from the population (Stehman, 2012; Olofsson et al., 2014a), specially to identify the main sources of classification errors in the most widely used global maps of deforestation (Hansen et al., 2013; Sexton et al., 2013) and to identifying the challenges faced by technical teams producing domestic deforestation maps.

#### 4.4.3 Causes of classification errors and drivers of deforestation

The interpretation of the post deforestation land use in the reference dataset showed that most of the classification errors, both commission and omission, are linked to shifting agriculture (**Figure 4-6**). Most of the errors in the National and the GFC deforestation maps are from wrongly identifying areas of stable cropland and shifting agriculture as deforestation (commission errors). Both had an equal number of sample units in stable cropland wrongly classified as deforestation ( $n = 78$  and  $n = 74$  for National and GFC, respectively). However, because more units are wrongly classified in the National map than the GFC (**Figure 4-5, Table A.3.2**), the proportion of errors due to stable cropland is lower in the National map (36% of wrongly classified sample units) than in the GFC (22%, **Figure 4-6a**). The GLCF also had most of its commission errors from wrongly classifying deforestation in areas of shifting agriculture ( $n = 62$ , 22%). However, the highest proportion of errors in this map was of omission errors in forest converted to shifting agriculture ( $n = 92$ , 33%).

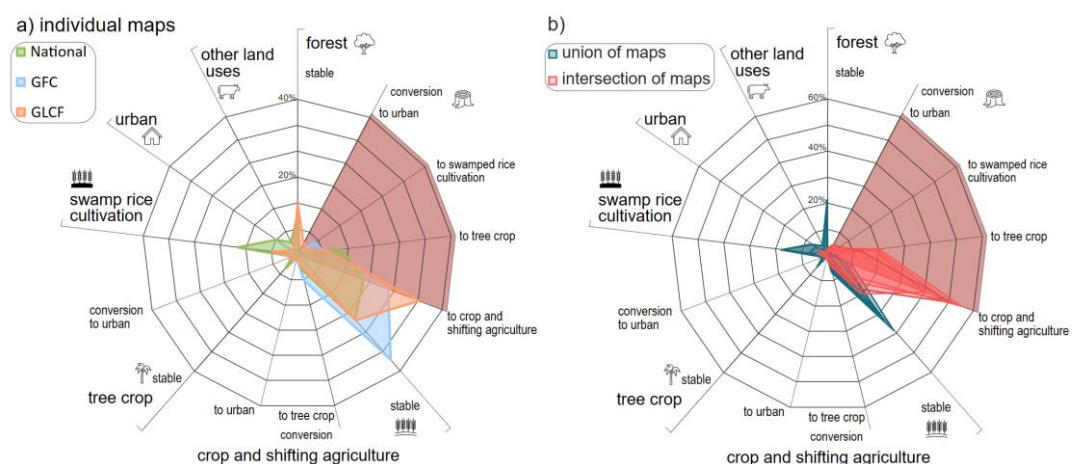


**Figure 4-6.** Percentage of classification errors of the satellite-based deforestation maps analysed by land use and land use conversion. Conversions from forest to other land uses (i.e., deforestation) is highlighted in red and errors in these classes are omission errors in the maps. Errors in the remaining classes with no red shading correspond to omission errors in the maps. In a) the individual maps (National, GFC, and GLCF) and b) the main errors of union and intersection of maps of the three maps.

Other causes of omission errors in the National map were mostly found to be in forest conversion to tree crops (n=40, 11%), in the GFC from forest conversion to tree crops (n=14, 7%) and from mangroves to swamped rice cultivation (n=11, 5%), and in the GLCF also mostly from forest conversion to tree crops (n=21, 8%). Other main causes of commission errors in addition to shifting agriculture are mostly from wrong classification of deforestation in stable swamped rice cultivation fields (n=55, 16%) and stable forest (n=37, 11%) in the National map, in stable forest (n=16, 8%) and shifting agriculture to tree crops (n=14, 7%; both classes in cropland land use) in the GFC, and stable forest (n=36, 13%) and swamped rice cultivation fields (n=18, 7%) in the GLCF.

The intersection of maps have higher omission errors (**Figure 4-4**) mostly from missed conversions from forest land to shifting agriculture (ranging from 40% to 55% of wrongly classified sample units) and to tree crops (ranging from 13% to 20%) (**Figure 4-6b**). Commission errors in the intersection of maps are due to the wrong classification of deforestation in areas of stable cropland (including shifting agriculture) and ranged from 9% to 20% of wrongly classified sample units. Unions of maps have a lower proportion of sample units wrongly classified as deforestation (**Figure 4-6b**), due to the lower omissions errors (**Figure 4-4**). For example, only 1% to 10% of the sample units are classified as stable forest instead of forest converted to shifting agriculture in the union of maps. Most errors are commission errors, or stable areas wrongly mapped as deforestation, such as in the case of stable shifting agriculture (29-38%), stable swamp rice cultivation (7-18%) and stable forest (15-21%).

Because we selected a stratified sampling design to ensure we had data in all our small classes of deforestation, we cannot use our sample for direct area estimation (Stehman, 2014). However, the information collected provides important insight on the main drivers of deforestation in Guinea-Bissau during the period 2007-2010. From the analysis of the reference dataset, the main post deforestation land use was cropland, including intensive shifting agriculture (**Figure 4-7**). In the period 2007-2010, 64% of deforestation corresponded to a transition to this land use, with most of the forest having already some evidence of past disturbance (degraded forest in **Figure 4-7**). The second most frequent post deforestation land use was tree crops (23%). This analysis confirms the findings from global studies identifying shifting agriculture as the main driver of deforestation (Curtis et al., 2018) but also highlights that existing maps often miss conversion of forest to commodities such as tree crops. The uncertainty in attribution between commodity-driven deforestation and shifting agriculture in sub-Saharan Africa was also noted by Harris et al. (2021). This observation is consistent with our findings showing that the main cause of classification errors are found in the transition from forest land to shifting agriculture and tree crops (**Figure 4-6**) which is not surprising when these were the dominant drivers of deforestation in the study period.

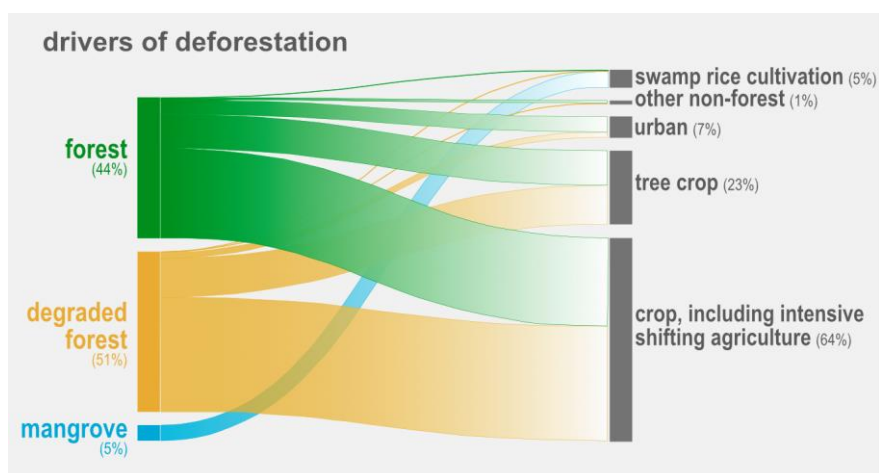


**Figure 4-7.** Drivers of deforestation in Guinea-Bissau, estimated from the reference dataset comprising 899 sample units where Google Earth imagery was visually interpreted to assess the accuracy of existing deforestation maps. Forest land use is separated by classes: forest, degraded forest and mangrove. The proportion of these forest classes converted to other land use (crop/shifting agriculture, tree crops, swamp rice cultivation, urban, and other non forest land uses not clearly identified) between 2007 and 2010 is identified in the chart by the size of the channels.

The spatial analysis of the autocorrelation of errors (in red, **Figure 4-8**) shows that clusters of errors are found mostly around the capital city of Bissau in the National and GFC maps, but not on the GLCF map. The GLCF has most clusters of errors in the northern region, closer to the border with Senegal and in the northwest drylands. With the intersection of maps, most of the clusters of errors are not in larger cities but in the western drylands, while in the union of maps errors are all clustered around the capital city of Bissau. Therefore, most errors are close to more populated areas or drylands. The union of maps increases the clusters of errors around the capital city, while the intersection of maps had all their clusters of errors in the western region of the country, which is mostly dominated by savannas. This pattern indicates that most commission errors (false deforestation in stable classes) are around cities while most omissions from conversion of forest to shifting agriculture and tree crops (**Figure 4-6**) are in the western drylands (**Figure 4-8**). This finding is intuitive given that large urban centres are more likely to have been converted to other land uses in the past in a, known but not well quantified, process of intensification of shifting agriculture cycles and transition to cashew plantations (Temudo and Abrantes, 2013; Temudo and Abrantes, 2014).

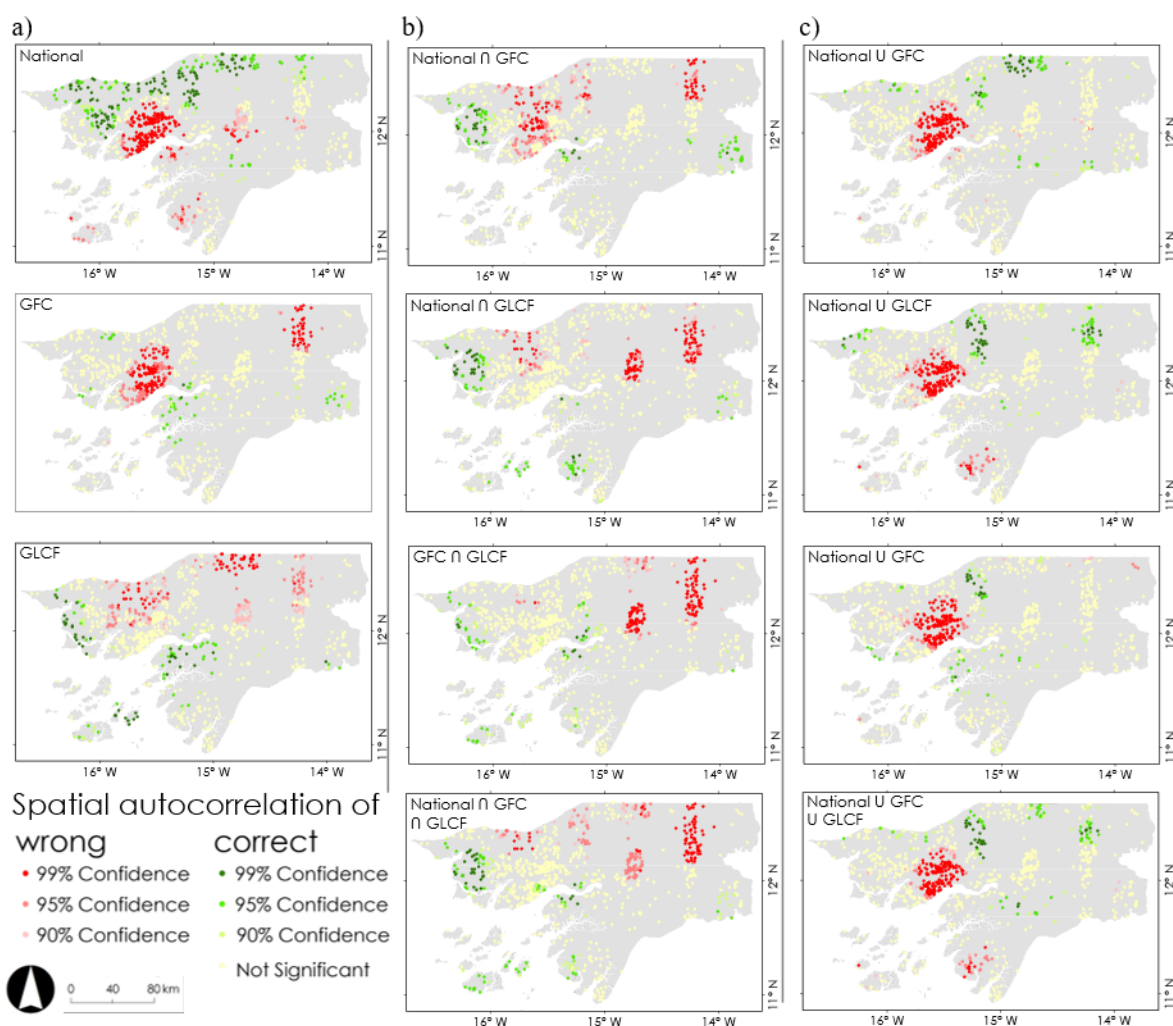


**Figure 4-8.** Map of the study area (Guinea-Bissau) showing high concentrations or clusters of the 899 sample units wrongly (red) or correctly (green) classified in the maps as deforestation or stable land use. One figure of the study area for each of the 11 maps or combination of maps: individual deforestation maps - National, GFC, and GLCF; intersection of maps - National  $\cap$  GFC, National  $\cap$  GLCF, GFC  $\cap$  GLCF; and union of maps - National U GFC, National U GLCF, GFC U GLCF, National U GFC U GLCF.

#### 4.4.4 Trends in the 21<sup>st</sup> century

This analysis shows that the assumed magnitude of deforestation in Guinea-Bissau in the period 2007-2010 is low (varying between 8 and 53 kha per year in the three individual maps; **Table 4.1**) and identifies the main drivers of deforestation, as well as the main sources of errors in available global deforestation maps. We also validated and explored possible uses of the most widely used global maps of forest change both in research (Harris et al., 2021; Feng et al., 2022) and in national reporting to the UNFCCC (Melo et al., 2023). If global maps derived from satellite data are deemed suitable to be adapted to national definitions to provide near real-time information on deforestation, they would ease the burden on national teams from least developed countries with lower MRV capacity who can only produce domestic deforestation maps with a great deal of effort.

For a comparison between national and global data sources, we had to restrict our analysis to the first decade on the 21<sup>st</sup> century. However, several global studies show a sharp increase in deforestation in West Africa during 2010-2020 (Feng et al., 2022; Harris et al., 2021). In Guinea-Bissau specifically, deforestation has increased sharply after the political coup in 2012, due to the foreign interest in African rosewood (*Pterocarpus Erinaceus*) coupled with political instability, which translated in the widespread felling and export of this species. According to the latest nationally determined contribution (NDC, (Guinea-Bissau, 2021)), deforestation in 2020 has an order of magnitude 3 times greater than in 2010. The average annual emissions in 2013-2020 was close to 4 Mt CO<sub>2</sub>e which was a striking increase considering the sector was a net sink in 2006-2012 (with an average annual removal of 230 kt CO<sub>2</sub>e). The Government issued a 5-year moratorium to all timber felling and export to stabilize clear cut rates. During that period, it accumulated one of the largest timber stockpiles on the continent, estimated to be greater than 400,000 logs (Eia, 2018). At present, and despite the moratorium imposed by the Government, the global maps continue to show that land clearing between 2013 and 2023 remained much higher than in the pre-2012 period ((Hansen et al., 2013) updated in the Global Forest Watch portal).

Here, we show that all maps have large errors and that the main drivers of deforestation were shifting agriculture and conversion to tree crops. Guinea-Bissau has not been able to update its deforestation maps to cover the 2010-2020 decade and the latest NDC used information downloaded from the Global Forest Watch portal. Understanding the magnitude of deforestation, its trends, and the new drivers of deforestation in a more recent period post military coup is of the utmost urgency to protect the country's remaining forests from such unprecedented pressure. Our analysis shows that the Earth Observation community has a great potential to support countries achieving the climate change mitigations objectives of the UNFCCC but further efforts are needed to produce more accurate maps. To produce accurate maps, national definitions and classification protocols need to include clear information on shifting agriculture and trees outside forest.

## 4.5 Conclusions

Comparing a national deforestation map of Guinea-Bissau (West Africa) with two global deforestation maps covering the period 2007-2010 showed large differences in the magnitude (CV = 77%) and spatial distribution of deforestation (1-6% of their area overlap with each other). The reference dataset of 899 sample units collected to validate the maps showed the three maps had large errors both of omission (91-97%) and commission (38-59%). Although still high, combining the maps (intersect and union) reduces the errors. The lowest omission error is obtained by the union of the three maps

(43%) and the lowest commission error by their intersection (29%). Combining maps can therefore contribute to mitigating the impact of exacerbated omission errors and corresponding exacerbated omission areas corrections. The causes of classification errors are similar in all maps and mostly linked to shifting agriculture and tree crops. Most of the commission errors (ranging from 1% to 38% of the sample units wrongly classified) are around the main urban areas and correspond to the wrong attribution of deforestation in the maps to areas of stable cropland (including shifting agriculture or tree crops). Most of the omission errors (ranging from 2% to 55%) are due to missed forest conversions to shifting agriculture or tree crops and are found in clusters in the western region of the country which is mostly dominated by dry forests. More accurate deforestation maps in mosaics of highly dynamic dry forests and conversion to shifting agriculture and tree crops are needed to harness the potential offered by the satellite Earth Observation community in support of the pressing needs of national Governments and the UNFCCC.

## 4.6 References

Achard, F., Eva, H. D., Stibig, H. J., Mayaux, P., Gallego, J., Richards, T., and Malingreau, J. P.: Determination of deforestation rates of the world's humid tropical forests, *Science*, 297, 999-1002, 10.1126/science.1070656, 2002.

Arevalo, P., Olofsson, P., and Woodcock, C.: Continuous monitoring of land change activities and post-disturbance dynamics from Landsat time series: A test methodology for REDD plus reporting, *Remote Sensing of Environment*, 238, 10.1016/j.rse.2019.01.013, 2020.

Bastin, J., Berrahmouni, N., Grainger, A., Maniatis, D., Mollicone, D., Moore, R., Patriarca, C., Picard, N., Sparrow, B., Abraham, E., Aloui, K., Atesoglu, A., Attorre, F., Bassullu, C., Bey, A., Garzuglia, M., Garcia-Montero, L., Groot, N., Guerin, G., Laestadius, L., Lowe, A., Mamane, B., Marchi, G., Patterson, P., Rezende, M., Ricci, S., Salcedo, I., Diaz, A., Stolle, F., Surappaeva, V., and Castro, R.: The extent of forest in dryland biomes, *Science*, 356, 635-+, 10.1126/science.aam6527, 2017.

Bey, A., Diaz, A., Maniatis, D., Marchi, G., Mollicone, D., Ricci, S., Bastin, J., Moore, R., Federici, S., Rezende, M., Patriarca, C., Turia, R., Gamoga, G., Abe, H., Kaidong, E., and Miceli, G.: Collect Earth: Land Use and Land Cover Assessment through Augmented Visual Interpretation, *Remote Sensing*, 8, 10.3390/rs8100807, 2016.

Chen, S., Olofsson, P., Saphangthong, T., and Woodcock, C.: Monitoring shifting cultivation in Laos with Landsat time series, *Remote Sensing of Environment*, 288, 10.1016/j.rse.2023.113507, 2023.

Curtis, P., Slay, C., Harris, N., Tyukavina, A., and Hansen, M.: Classifying drivers of global forest loss, *Science*, 361, 1108-1111, 10.1126/science.aau3445, 2018.

Diniz, C., Souza, A., Santos, D., Dias, M., da Luz, N., de Moraes, D., Maia, J., Gomes, A., Narvaes, I., Valeriano, D., Maurano, L., and Adami, M.: DETER-B: The New Amazon Near Real-Time Deforestation Detection System, *IEEE Journal of Selected Topics in*

Applied Earth Observations and Remote Sensing, 8, 3619-3628, 10.1109/JSTARS.2015.2437075, 2015.

Doblas, J., Reis, M., Belluzzo, A., Quadros, C., Moraes, D., Almeida, C., Maurano, L., Carvalho, A., Sant'Anna, S., and Shimabukuro, Y.: DETER-R: An Operational Near-Real Time Tropical Forest Disturbance Warning System Based on Sentinel-1 Time Series Analysis, *Remote Sensing*, 14, 10.3390/rs14153658, 2022.

EIA: Authorized Plunder: Massive Rosewood Sale Backed by Global Wildlife Convention Fuels Forest Crimes in Guinea-Bissau. Media Release. (available online: <https://us.eia.org/press-releases/20181212-guinea-bissau-authorized-plunder-pr/>) (last accessed: June 2023), 2018.

Federici, S., Grassi, G., Harris, N., Lee, D., Neeff, T., Penman, J., Sanz, M. J., and Wolosin, M.: GHG Fluxes from Forests: An assessment of national GHG estimates and independent research in the context of the Paris Agreement., Available at: <https://www.climateandlandusealliance.org/reports/ghg-fluxes-forests/> (last access October 2022), 2017.

Feng, Y., Zeng, Z., Searchinger, T., Ziegler, A., Wu, J., Wang, D., He, X., Elsen, P., Ciais, P., Xu, R., Guo, Z., Peng, L., Tao, Y., Spracklen, D., Holden, J., Liu, X., Zheng, Y., Xu, P., Chen, J., Jiang, X., Song, X., Lakshmi, V., Wood, E., and Zheng, C.: Doubling of annual forest carbon loss over the tropics during the early twenty-first century, *Nature Sustainability*, 5, 444-451, 10.1038/s41893-022-00854-3, 2022.

Finegold, Y. and Ortmann, A.: Map Accuracy Assessment and Area Estimation: A Practical Guide, Rome, Italy, 2016.

Finer, M., Novoa, S., Weisse, M., Petersen, R., Mascaro, J., Souto, T., Stearns, F., and Martinez, R.: 3 Combating deforestation: From satellite to intervention, *Science*, 360, 1303-1305, 10.1126/science.aat1203, 2018.

Gorelick, N., Hancher, M., Dixon, M., Ilyushchenko, S., Thau, D., and Moore, R.: Google Earth Engine: Planetary-scale geospatial analysis for everyone, *Remote Sensing of Environment*, 202, 18-27, 10.1016/j.rse.2017.06.031, 2017.

Grassi, G., Conchedda, G., Federici, S., Abad Viñas, R., Korosuo, A., Melo, J., Rossi, S., Sandker, M., Somogyi, Z., Vizzarri, M., and Tubiello, F. N.: Carbon fluxes from land 2000–2020: bringing clarity to countries' reporting, *Earth Syst. Sci. Data*, 14, 4643-4666, 10.5194/essd-14-4643-2022, 2022.

Guinea-Bissau: REDD+ Forest Reference Level submitted by the Government of Guinea-Bissau to the UNFCCC, 2019.

Guinea-Bissau: First Biennial Update Report (BUR1) submitted by the Government of Guinea-Bissau to the UNFCCC, 2020.

Guinea-Bissau: Updated Nationally Determined Contribution in the framework of the Paris Agreement, 2021.

Hansen, M. C., Potapov, P. V., Moore, R., Hancher, M., Turubanova, S. A., Tyukavina, A., Thau, D., Stehman, S. V., Goetz, S. J., Loveland, T. R., Kommareddy, A., Egorov, A., Chini, L., Justice, C. O., and Townshend, J. R. G.: High-Resolution Global Maps of

21st-Century Forest Cover Change, *Science*, 342, 850-853, 10.1126/science.1244693, 2013.

Harris, N., Gibbs, D., Baccini, A., Birdsey, R., de Bruin, S., Farina, M., Fatoyinbo, L., Hansen, M., Herold, M., Houghton, R., Potapov, P., Suarez, D., Roman-Cuesta, R., Saatchi, S., Slay, C., Turubanova, S., and Tyukavina, A.: Global maps of twenty-first century forest carbon fluxes, *Nature Climate Change*, 11, 10.1038/s41558-020-00976-6, 2021.

Hegglin, M. I., Bastos, A., Bovensmann, H., Buchwitz, M., Fawcett, D., Ghent, D., Kulk, G., Sathyendranath, S., Shepherd, T. G., Quegan, S., Röthlisberger, R., Briggs, S., Buontempo, C., Cazenave, A., Chuvieco, E., Ciais, P., Crisp, D., Engelen, R., Fadnavis, S., Herold, M., Horwath, M., Jonsson, O., Kpaka, G., Merchant, C. J., Mielke, C., Nagler, T., Paul, F., Popp, T., Quaife, T., Rayner, N. A., Robert, C., Schröder, M., Sitch, S., Venturini, S., van der Schalie, R., van der Vliet, M., Wigneron, J.-P., and Woolway, R. I.: Space-based Earth observation in support of the UNFCCC Paris Agreement, *Frontiers in Environmental Science*, 10, 10.3389/fenvs.2022.941490, 2022.

McNicol, I., Ryan, C., and Mitchard, E.: Carbon losses from deforestation and widespread degradation offset by extensive growth in African woodlands, *Nature Communications*, 9, 10.1038/s41467-018-05386-z, 2018.

McRoberts, R.: Satellite image-based maps: Scientific inference or pretty pictures?, *Remote Sensing of Environment*, 115, 715-724, 10.1016/j.rse.2010.10.013, 2011.

Melo, J., Baker, T., Nemitz, D., Quegan, S., and Ziv, G.: Satellite-based global maps are rarely used in forest reference levels submitted to the UNFCCC, *Environmental Research Letters*, 18, 10.1088/1748-9326/acba31, 2023.

Melo, J., Ziv, G., Baker, T., Carreiras, J., Pearson, T., and Vasconcelos, M.: Striking divergences in Earth Observation products may limit their use for REDD, *Environmental Research Letters*, 13, 10.1088/1748-9326/aae3f8, 2018.

Miles, L., Newton, A., DeFries, R., Ravillious, C., May, I., Blyth, S., Kapos, V., and Gordon, J.: A global overview of the conservation status of tropical dry forests, *Journal of Biogeography*, 33, 491-505, 10.1111/j.1365-2699.2005.01424.x, 2006.

Nesha, K., Herold, M., De Sy, V., Duchelle, A., Martius, C., Branthomme, A., Garzuglia, M., Jonsson, O., and Pekkarinen, A.: An assessment of data sources, data quality and changes in national forest monitoring capacities in the Global Forest Resources Assessment 2005-2020, *Environmental Research Letters*, 16, 10.1088/1748-9326/abd81b, 2021.

Ochiai, O., Poulter, B., Seifert, F. M., Ward, S., Jarvis, I., Whitcraft, A., Sahajpal, R., Gilliams, S., Herold, M., Carter, S., Duncanson, L. I., Kay, H., Lucas, R., Wilson, S. N., Melo, J., Post, J., Briggs, S., Quegan, S., Dowell, M., Cescatti, A., Crisp, D., Saatchi, S., Tadono, T., Steventon, M., and Rosenqvist, A.: Towards a roadmap for space-based observations of the land sector for the UNFCCC global stocktake, *iScience*, 106489, <https://doi.org/10.1016/j.isci.2023.106489>, 2023.

Olofsson, P., Foody, G. M., Stehman, S. V., and Woodcock, C. E.: Making better use of accuracy data in land change studies: Estimating accuracy and area and quantifying

- uncertainty using stratified estimation, *Remote Sensing of Environment*, 129, 122-131, 10.1016/j.rse.2012.10.031, 2013.
- Olofsson, P., Foody, G., Herold, M., Stehman, S., Woodcock, C., and Wulder, M.: Good practices for estimating area and assessing accuracy of land change, *Remote Sensing of Environment*, 148, 42-57, 10.1016/j.rse.2014.02.015, 2014.
- Olofsson, P., Arevalo, P., Espejo, A., Green, C., Lindquist, E., McRoberts, R., and Sanz, M.: Mitigating the effects of omission errors on area and area change estimates, *Remote Sensing of Environment*, 236, 10.1016/j.rse.2019.111492, 2020.
- Reiche, J., Mullissa, A., Slagter, B., Gou, Y., Tsendbazar, N., Odongo-Braun, C., Vollrath, A., Weisse, M., Stolle, F., Pickens, A., Donchyts, G., Clinton, N., Gorelick, N., and Herold, M.: Forest disturbance alerts for the Congo Basin using Sentinel-1, *Environmental Research Letters*, 16, 10.1088/1748-9326/abd0a8, 2021.
- Sexton, J. O., Song, X. P., Feng, M., Noojipady, P., Anand, A., Huang, C. Q., Kim, D. H., Collins, K. M., Channan, S., DiMiceli, C., and Townshend, J. R.: Global, 30-m resolution continuous fields of tree cover: Landsat-based rescaling of MODIS vegetation continuous fields with lidar-based estimates of error, *International Journal of Digital Earth*, 6, 427-448, 10.1080/17538947.2013.786146, 2013.
- Shimada, M., Itoh, T., Motooka, T., Watanabe, M., Shiraishi, T., Thapa, R., and Lucas, R.: New global forest/non-forest maps from ALOS PALSAR data (2007–2010), *Remote Sensing of Environment*, 155, 13-31, <http://dx.doi.org/10.1016/j.rse.2014.04.014>, 2014.
- Stehman, S.: Statistical rigor and practical utility in thematic map accuracy assessment, *Photogrammetric Engineering and Remote Sensing*, 67, 727-734, 2001.
- Stehman, S.: Impact of sample size allocation when using stratified random sampling to estimate accuracy and area of land-cover change, *Remote Sensing Letters*, 3, 111-120, 10.1080/01431161.2010.541950, 2012.
- Stehman, S.: Estimating area from an accuracy assessment error matrix, *Remote Sensing of Environment*, 132, 202-211, 10.1016/j.rse.2013.01.016, 2013.
- Stehman, S.: Estimating area and map accuracy for stratified random sampling when the strata are different from the map classes, *International Journal of Remote Sensing*, 35, 4923-4939, 10.1080/01431161.2014.930207, 2014.
- Sunderland, T., Apgaua, D., Baldauf, C., Blackie, R., Colfer, C., Cunningham, A., Dexter, K., Djoudi, H., Gautier, D., Gumbo, D., Ickowitz, A., Kassa, H., Parthasarathy, N., Pennington, R., Paumgarten, F., Pulla, S., Sola, P., Tng, D., Waeber, P., and Wilme, L.: Global dry forests: a prologue, *International Forestry Review*, 17, 1-9, 10.1505/146554815815834813, 2015.
- Temudo, M. P.: Planting Knowledge, Harvesting Agro-Biodiversity: A Case Study of Southern Guinea-Bissau Rice Farming, *Human Ecology*, 39, 309-321, 10.1007/s10745-011-9404-0, 2011.
- Temudo, M. P. and Abrantes, M.: The Cashew Frontier in Guinea-Bissau, West Africa: Changing Landscapes and Livelihoods, *Human Ecology*, 42, 217-230, 10.1007/s10745-014-9641-0, 2014.

Temudo, M. P. and Abrantes, M. B.: Changing Policies, Shifting Livelihoods: The Fate of Agriculture in Guinea-Bissau, *Journal of Agrarian Change*, 13, 571-589, 10.1111/j.1471-0366.2012.00364.x, 2013.

Tyukavina, A., Baccini, A., Hansen, M. C., Potapov, P. V., Stehman, S. V., Houghton, R. A., Krylov, A. M., Turubanova, S., and Goetz, S. J.: Aboveground carbon loss in natural and managed tropical forests from 2000 to 2012, *Environmental Research Letters*, 10, 14, 10.1088/1748-9326/10/7/074002, 2015.

Tyukavina, A., Stehman, S. V., Potapov, P. V., Turubanova, S. A., Baccini, A., Goetz, S. J., Laporte, N. T., Houghton, R. A., and Hansen, M. C.: National-scale estimation of gross forest aboveground carbon loss: a case study of the Democratic Republic of the Congo, *Environmental Research Letters*, 8, 10.1088/1748-9326/8/4/044039, 2013.

Tzamtzis, I., Federici, S., and Hanle, L.: A Methodological Approach for a Consistent and Accurate Land Representation Using the FAO Open Foris Collect Earth Tool for GHG Inventories, *Carbon Management*, 10, 437-450, 10.1080/17583004.2019.1634934, 2019.

UNFCCC: 'Decision 19/CMA.1: Adoption of the Paris Agreement', 2015.

UNFCCC: 'Decision 19/CMA.1: Matters relating to article 14 of the Paris Agreement and paragraphs 99–101 of decision 1/CP.21', 2019a.

UNFCCC: 'Annex to decision 18/CMA.1: Modalities, procedures and guidelines for the transparency framework for action and support referred to in Article 13 of the Paris Agreement'. 2019b.

Valentini, R., Arneeth, A., Bombelli, A., Castaldi, S., Gatti, R. C., Chevallier, F., Ciais, P., Grieco, E., Hartmann, J., Henry, M., Houghton, R. A., Jung, M., Kutsch, W. L., Malhi, Y., Mayorga, E., Merbold, L., Murray-Tortarolo, G., Papale, D., Peylin, P., Poulter, B., Raymond, P. A., Santini, M., Sitch, S., Laurin, G. V., van der Werf, G. R., Williams, C. A., and Scholes, R. J.: A full greenhouse gases budget of Africa: synthesis, uncertainties, and vulnerabilities, *Biogeosciences*, 11, 381-407, 10.5194/bg-11-381-2014, 2014.

Vancutsem, C., Achard, F., Pekel, J., Vieilledent, G., Carboni, S., Simonetti, D., Gallego, J., Aragao, L., and Nasi, R.: Long-term (1990-2019) monitoring of forest cover changes in the humid tropics, *Science Advances*, 7, 10.1126/sciadv.abe1603, 2021.

Vittekk, M., Brink, A., Donnay, F., Simonetti, D., and Desclee, B.: Land Cover Change Monitoring Using Landsat MSS/TM Satellite Image Data over West Africa between 1975 and 1990, *Remote Sensing*, 6, 658-676, 10.3390/rs6010658, 2014.

# Thesis Conclusions

## 5.1 Cross chapter synthesis

The research in this thesis aimed at understanding whether satellite-based EO products are supporting or could support countries in their reporting of emissions from deforestation to the UNFCCC and in planning mitigation actions in the forest and land use sector. In Chapter 2, I show that despite the large investments made by Space Agencies, there is a notable underutilization of EO products in forest reference level submissions to the UNFCCC. Of all the available maps of deforestation and land cover change, only the Global Forest Change (GFC; Hansen et al., 2013) was used to measure forest loss, and this often involved some level of ingenuity to adapt it to national definitions and to correct classification errors. The GFC was used for Activity Data (AD) in 29% of the submissions, or 43% if considering its use for comparison of results (i.e., verification or quality control, not as a source of AD). The use of satellite-based biomass maps is almost negligible – they only contributed to the submissions of four countries (out of 56 countries with 75 forest reference levels submitted up to 2022) and only indirectly, such as for comparing with biomass estimates from field plot measurements or to IPCC defaults. Nevertheless, I also show that, overall, the availability of EO products enhances MRV capacity: 70% of LDCs and 65% of African States with forest reference level submissions relied on EO products, and for 22 of the countries using EO products in their submission, this was their first reviewing process under the UNFCCC. The analysis presented in Chapter 2, coincided with the end of the first Global Stocktake and may serve as a baseline to assess progress by the EO community in their objective of enhancing the uptake of satellite-based global datasets in NGHGs.

The following chapters (Chapter 3 and Chapter 4) used Guinea-Bissau as a case study and focused on understanding and addressing why the uptake of EO products is so low. Guinea-Bissau is a LDC in West Africa mostly covered by highly dynamic and inherently challenging to measure forest-savanna mosaics (Vittekk et al., 2014; Mcnicol et al., 2018). These dry forests have been under unprecedented pressure with the widespread felling of African rosewood and conversion to tree crops (EIA, 2018). However, the country's forest monitoring capacity is very low, there is no national forest monitoring system in place to quantify such pressure, its trends and location, and therefore no capacity to plan adequate action. Guinea-Bissau is a good example of the (still far too) many countries that cannot answer the most fundamental question in their NGHGs – what is the extent and trend of deforestation and associated carbon emissions in the first two decades of the 21<sup>st</sup> century? With all the investments made in observing the Earth surface from

space, by now, arguably every government should have a timely, accurate and straightforward answer to this question.

In Chapter 3, I combined and compared available global EO products to quantify deforestation and associated carbon emissions as a possible solution to the lack of domestic systems. I showed that *in situ* above-ground biomass data and the available above-ground biomass maps relying on more sophisticated remote sensing approaches do not vary substantially. In contrast, deforestation maps show striking differences in both the magnitude (CV = 77%) and spatial distribution of deforestation, with almost total spatial disagreement between datasets (only 1-6% of overlapping area), which hinders their use for national reporting.

In Chapter 4, I assessed the accuracies of the deforestation maps produced in Chapter 3 and their combinations (union and intersection of maps). Following good practice (Olofsson et al., 2014; GFOI, 2020) and the examples from other countries using global deforestation maps in official reporting (seen in Chapter 2), I collected circa 900 sample units using very high-resolution imagery to validate the maps, correct their areas, and understand the causes of the classification errors. I concluded that the classification errors of the deforestation class are high in all maps. The Global Forest Change (GFC) dataset is the most widely used EO product in domestic reporting to the UNFCCC (Chapter 2) and is also the map with most sample units correctly classified as deforestation in Guinea-Bissau (Chapter 4). However, the area-corrected errors of omission and commission are very large, even when combining maps. Commission error varies from 29% to 60%, with the lowest commission error (CE = 29%) obtained by the intersection of the three deforestation maps. Omission error can reach as high as 99.9% with the lowest omission error (OE = 43%) obtained by the union of the three deforestation maps. The sources of errors are similar in all maps with most of the classification errors being linked to shifting agriculture (45-69%). Although the magnitude of deforestation is very different in the three individual maps, the corrected area is relatively similar regardless of the map used to stratify the sample (CV=102% in the original areas and CV=23% after correction).

### **5.1.1 Summary answers to the research questions raised in the previous chapters**

***How extensively are the wide range of EO products offered by the EO community being used in national reporting and are thus contributing to the Global Stocktake?***

I addressed this question in Chapter 2, revealing a notable underutilization of EO products in forest reference levels reported to the UNFCCC between 2014 and 2022, with a lack of diversity in those used for AD and their very limited use to map fire and support estimates of EFs. Only one out of the 12 global land cover maps listed in **Table 2.2** was used (see **Table 2.3**). The Global Forest Change (GFC) was used for Activity Data (AD) in 29% of the submissions, and was used by almost half the countries (n=24 or 43% of the total 56 countries with forest reference level submissions) if considering its use for comparison of results (i.e., verification or quality control). No country used available global biomass maps to derive EFs but two maps (out of the 9 listed in **Table 2.2**; Saatchi et al., (2011) and Baccini et al., (2012)) were used indirectly in four out of 75 submissions (**Table 2.3**). Of the 16 countries including emissions from forest fires or non-CO<sub>2</sub> emissions from biomass burning from deforestation, only three used fire EO products (MODIS Burned Area, MODIS Active Fire and NOAA fire hotspots). The uptake is limited but improved the MRV capacity of 22 countries. Nevertheless, it is important to note a limitation of chapter 2 to answer the question posed. I used a sample of 56 developing countries (out of 155) with REDD+ submissions under the UNFCCC, because REDD+ submissions are more detailed and transparent than National Communications and Biennial Update Reports (BURs) that include all sectors and don't focus exclusively on LULUCF, and because at the time the study was undertaken almost 80% of developing countries had never submitted a BUR. Using REDD+ reduces the uncertainty of the results because it is difficult to extract information on data sources from National Communications and BURs. However, it is possible that my sample of 56 countries is targeting the developing countries with higher MRV capacity and therefore are not representative of the population of developing countries. In principle, countries with REDD+ submissions are those with more REDD+ readiness support and consequently higher MRV capacity and higher use of EO data. It is likely, although unquantified, that the remaining developing countries rely on statistics when reporting fluxes from LULUCF.

The GFC is used to directly quantify deforestation by 10 countries, to quantify other REDD+ activities by 6 countries (noting the overlap), and as auxiliary data (for example as training data or map correction) by 6 countries. Furthermore, 14 countries used it indirectly, e.g., for quality control or verification. It was used directly, for example, to fill cloud gaps, to produce forest maps according to the national thresholds in the national definition of forest selecting the tree cover threshold and resampling pixel blocks and a reference dataset for the correct attribution of land use. It was also used in combination with other data, including very high-resolution imagery, to train a map classifier or to correct mapped areas. Two biomass maps (Saatchi et al., 2011; Baccini et al., 2012)

were used indirectly in four (5%) submissions, for example to compare estimates with the reported values in the FRL (verification). Fire products were used directly to map burnt areas for activity data by two countries. However, Ghana dropped the wall-to-wall mapping and the use of MODIS Burned Area product in subsequent submissions, choosing instead to use a systematic sample approach and interpretation of very high-resolution imagery, including to quantify emissions from fire occurrences. See summary of uses in **Table 2.3** and **Table 2.4**, and a more detailed and disaggregated description country by country in **Table A.1.2**.

The results from the analysis on Chapter 2 suggest that a low uptake in national reporting means a low contribution to the Global Stocktake. Furthermore, the aggregation of countries GHG inventories is used as input data (decision 19/CMA.1, para 37a). While the consistency and harmonization in data and methods used for REDD+ and GHG inventories submitted in National Communications and Biennial Update Reports (soon to be replaced by Biennial Transparency Reports) is expected, many countries are still working towards that objective.

Building on the knowledge and results from Chapter 2, in the next Chapters (3 and 4), I explored the possibility of using EO products to estimate emissions from deforestation using a least developed country in West Africa (Guinea-Bissau) as a case study. In Chapter 3 I delved into the question:

**Is the uncertainty in the EO-based carbon flux estimates mostly linked to land and land use change (Activity Data) or biomass (Emission/Removal factors)?**

Results for 20 combinations of EO products (four maps of deforestation and four biomass maps plus the national AGB plot data), show that AD and EF derived from different datasets render very different annual emission estimates (MtCO<sub>2</sub> yr<sup>-1</sup>; **Table 3.3**). The spread of all emissions estimates is high (overall CV of 64%) and using the National deforestation map and biomass plot data produced an estimate 10-times higher than that obtained when combining the GFC global map and the above-ground biomass map for African savannas published by Bouvet et al (2018).

The results highlight that the magnitude of variation is dominated by differences in the deforestation dataset (AD), with CV ranging between 58 and 71% when compared to the 20-32% variation in EFs (**Table 3.3**). Deforestation rates ranged between 0.3 and 1.8 % yr<sup>-1</sup> (**Table A.2.4**) and the maps show almost complete spatial disagreement (**Figure 3-4**) with only 1-6% overlap of deforestation area and over 90% of the 10-km pixels having a CV above 50%.

The aggregated AGB mean for the entire country varies little between products (**Figure 3-2**). All AGB estimates range between 54 and 65 t ha<sup>-1</sup> and are consistent with IPCC default for sub-tropical dry forests in the 2019 refinement to the 2006 Guidelines (65.2 t ha<sup>-1</sup>; Table 4.7 in IPCC, 2019). Note that Chapter 3 of this thesis was published in Environmental Research Letters in 2018 and at the time I used (in **Figure 3-2**) the much higher default value of the 2006 guidelines (130 t ha<sup>-1</sup>; IPCC, 2006).

### **What are the reasons for the main discrepancies and errors?**

In Chapter 3, I explored the potential reasons for the different patterns and magnitude of deforestation using i) expert knowledge, ii) information from the EO data used in each product, iii) time series of high-resolution imagery where available to illustrate random examples (**Figure 3-6** and **Figure 3-7**). The main issues appear to be: i) the different imagery acquisition dates (GFC uses imagery from the wet season and National from the dry season) coupled with ii) difficulties in distinguishing seasonality (e.g., from rice cultivation and its green signal in the wet season, and use of fire in shifting agriculture cycles in the dry season) from deforestation, and iii) issues related with forest definitions and the complexities of using land-cover change and tree-cover change as proxy for land-use change (including confusion between forests and tree crops). The potential reasons discussed in Chapter 3 are supported by the results of the map validation in Chapter 4 which uses a reference dataset based on a stratified sample and the visual interpretation of high-resolution imagery from google earth.

The reference dataset collected in Chapter 4 showed that for the period 2007-2010, the GFC deforestation map had the highest number of sample units correctly classified and the lowest number wrongly classified (**Figure 4-5; Table A.3.2**). It had an area-adjusted overall accuracy (OA) of 85%, compared to 77% of the GLCF and 76% of the national deforestation map (**Table A.3.3**). However, deforestation was greatly underestimated in all maps, as shown by the large omission errors (**Figure 4-4**). The deforestation areas reported after correction are considerably higher than the original areas (**Table 4.1, Figure 4-4**) but vary less among products (CV=102% in the original areas and CV=23% after correction). The GFC had the highest area-adjusted omission error (97%) and the corrected deforestation area was more than 20 times greater than the original mapped area. This issue of a single error in a very large class having a much stronger weight than an error in a small class with consequent exacerbated omission areas leading to exacerbated area corrections is well recognized when stable classes (in my case, the class of no deforestation) represent more than 90% of the total area (Olofsson et al., 2020 and Arevalo et al., 2020).

The sources of errors are similar in all maps with most of the classification errors being linked to shifting agriculture (45-69%), swamped rice cultivation in mangrove areas (5-16%), or tree crops (11-17%). Most commission errors are in clusters around urban areas, where vegetation is expected to be more humanized, while most omission errors are in the western region dominated by dry forests. For all maps the highest percentage of both omission and commission errors is linked to shifting agriculture areas, noting that in this analysis and according to the national definition, shifting agriculture is considered forest land if of low intensity with long fallow cycles and most trees left standing, but it is considered cropland if in shorter fallow cycles, if it shows reduction of canopy cover, or evidence of conversion to permanent cropland in subsequent years (we analysed high resolution imagery up to 2019 but assessed changes only between 2007 and 2010). The results of the analysis in Chapter 4 confirmed the suspicion in Chapter 3 – the GFC is the only map missing/omitting conversion of mangrove to swamped rice fields. The national map misses more conversion of forest to tree crops than the other maps, and wrongly classifies stable rice fields as deforestation, maybe due to the burning of the fields.

#### **How can the combination of maps improve the estimates?**

In Chapter 4 I tested if combining deforestation maps could reduce the errors of their estimates. In the individual products, commission error varies from 29% to 60%, and omission error reached as high as 99.9%. The errors are reduced when combining deforestation maps, by intersecting areas of deforestation or the union of those areas. The lowest commission error (CE = 29%) is obtained by the intersection of the three deforestation maps, and the lowest omission error (OE = 43%) obtained by their union. The union of the maps, where the class of deforestation is larger than in the individual maps, is the least affected by the exacerbated omission areas. Given the political implications of these exacerbated areas corrections, in the context of REDD+ results-based payments, this study suggests it could be advantageous to use a union of deforestation maps to reduce the area of the stable classes and consequently the impact of exacerbated area corrections. At least until better recommendations on how to contain, mitigate and potentially eliminate the effects of omission errors are provided (Olofsson et al., 2020).

## **5.2 Contributions to the overarching questions and future directions to science and policy**

The main conclusion of this thesis is that available EO products are not as widely employed nor as accurate as perceived within the EO community. Accurately mapping deforestation in dry forests, where the main driver of deforestation is shifting agriculture, is very complex. The mapping difficulties and map errors are not only linked to the small scale and more subtle change in the spectral signal which can be mistaken with seasonality. It is also connected with difficulties in the correct attribution between satellite image and tree canopy cover and land use. And even in the attribution of shifting agriculture to the right land use. Throughout this thesis I have discussed how EO products are very timely and needed and can be of support if some attention is given to the way they are handled and presented. This section reflects on the findings from Chapters 2, 3 and 4, and suggests future directions with a focus on the contributions from this thesis to the overarching questions.

The results shown in the chapters above highlighted opportunities and limitations to the uptake of EO products in national reporting to the UNFCCC largely linked to the need for compliance with IPCC methods and good practice. A first short answer from this study to the overarching questions posed is below.

### ***Why do we get conflicting estimates from the aggregation of land carbon fluxes from GHG inventories submitted to the UNFCCC and independent global estimates from EO products?***

Firstly, we get conflicting messages between estimates from EO products and GHG inventories because i) the maps can have large errors and ii) map classes may not correspond to the land categories used in the inventory. For example, if shifting agriculture is considered forest land remaining forest land in the inventory but is included in deforestation in the EO products. The future directions sections below will expand on these ideas.

### ***How has the EO community contributed to the first Global Stocktake if their independent estimates and the conclusions from the Global Stocktake are divergent?***

Secondly, the contribution to the first Global Stocktake was lower than expected by the EO community. Namely because: i) the independent submissions from the EO community using the black pathway **Figure 1-5** (e.g., ESA, 2022) were not considered in the synthesis reports by the UNFCCC secretariat; ii) the conclusions from the

synthesis reports included information from the land use sector that is contrasting to the estimates from the EO community (e.g. reporting decreasing emissions from deforestation in developing countries compared to the increasing emissions from deforestation from EO products in the tropics); and iii) Chapter 2 identifies an underutilization of EO products in countries reporting to the UNFCCC, and the uptake of the GFC was only possible if adapted or corrected to adhere to national definitions with consequent changes in the trend and magnitude of associated carbon fluxes. The future directions sections below will expand on these ideas with a focus on proposing ways to enhance the uptake of EO products in the next Global Stocktake.

The future directions suggested in this section are motivated by the findings of Chapters 2, 3 and 4, and by the necessity to provide further recommendations to address the overarching questions ahead of the next Global Stocktake in 2028. The discussion is primarily directed to space agencies and the EO scientific community wishing to support the Global Stocktake but are also relevant to national teams preparing their reports to the UNFCCC.

### **5.2.1 Provision of high quality EO data for maps and sampling approaches.**

Chapter 2 found that in forest reference level submissions to the UNFCCC, there is a trend towards reduced dependency on wall-to-wall maps to derive AD, which partially explains the limited uptake of EO products. Of the 76 submissions analysed, 70% used a reference dataset to estimate AD, of which 40% stratified the sample with a map (including the GFC product), as recommended to reduce omission errors (Olofsson et al., 2020; GFOI, 2020), and 30% relied only on the sample. One reason for the change in trend in the approach used is that pixel-counting methods introduce bias in the estimate from map classification errors (McRoberts, 2011; Olofsson et al., 2013). Stratified area estimation corrects the bias and the area. This approach also corrects any temporal inconsistencies from changes in the classification algorithm (Ceccherini et al., 2021), or changes in the source data, for example, due to sensor degradation or sensor and technology changes between successive missions (Roy et al., 2016; Vogeler et al., 2018) or due to adding additional higher-quality data in more recent years. Ultimately, it helps ensuring time-series consistency, a fundamental IPCC requirement. Chapter 4 showed a case study where the available deforestation maps had large classification errors and the corresponding emissions were very different depending on the deforestation maps that were selected (Chapter 3). In this case, correction of the estimates with a reference dataset was essential (Chapter 4).

Developing the NGHGI should be done in synergy with other policy needs and requirements, and therefore wall-to-wall maps, even with errors, are useful. For example, for planning actions in priority areas in the NDCs, to monitor natural disturbances (a memo item in the new reporting tables), or for developing and maintaining operational alert systems (e.g., the alert system DETER in Brazil is used also to report emissions from forest degradation in the Amazon in the 2023 forest reference level). For example, even if the maps in Guinea-Bissau have large errors, the intersection of the maps (with the lowest commission errors) could provide timely and important information on hotspots for action, in a conservative way, to avoid false positives and waste of resources on ground intervention. This thesis, therefore, supports the recommendation in GFOI MGDs (GFOI, 2020) of moving towards using stratified area estimation and the priority action point in the CEOS AFOLU roadmap (Poulter et al., 2023) for the EO community to work towards providing to national teams, including the inventory community, access to quality imagery for statistical estimates and maps. Furthermore, satellite data and derived maps should have long-term continuity and backward compatibility, and be properly documented in terms of the data sources used, classification algorithm changes, and any other information required to correct inconsistencies.

### **5.2.2 Improve mapping of shifting agriculture.**

Chapter 4 identified land areas under shifting agriculture cycles as the main source of error in all the deforestation maps, both errors of commission and omission. Furthermore, the reference dataset of circa 900 sample units collected in a stratified random sampling design identified shifting agriculture as the main cause of deforestation in Guinea-Bissau for the period 2007-2010. Other studies report similar findings in other countries (e.g., Ryan et al., 2014; Chen et al., 2023) and, at the global level, the impact of shifting agriculture in global tree cover loss is also considerable (Curtis et al., 2018). According to the study of Curtis et al (2018) on global drivers of tree cover loss from deforestation and other disturbances, shifting agriculture is responsible for 24% of tree cover loss at global level, and is the dominant driver of loss in sub-Saharan Africa, representing 92 to 93% of tree cover loss depending on which method is used, map-based (with the GFC dataset) or sample-based, respectively. However, the authors note the difficulty in accurately separating shifting agriculture from commodity driven agriculture in sub-Saharan Africa because the small-scale clearing pattern is similar, and some commodity driven agriculture areas are wrongly classified as shifting agriculture in their model. In fact, Curtis et al (2018), accessed in the global forest watch portal (GFW, 2023), quantified that in Guinea-Bissau shifting agriculture was responsible for 98-100% of tree cover loss in the period 2007-2010 (GFW, 2023). In Chapter 4, I found that shifting

agriculture together with permanent agriculture were responsible for 64% of deforestation in Guinea-Bissau in the same period 2007-2010 (**Figure 4-7**). This difference indicates a large overestimation of the share of shifting agriculture in the drivers of deforestation by Curtis et al. (2018).

The EO flux model from Harris et al (2021) uses the map of global drivers from Curtis et al (2018) and, in their sensitivity analysis, the global effect of the classification errors was minimal. Nevertheless, given the relevance of shifting agriculture as driver of tree cover loss, and the large errors in mapping those areas identified in Chapter 4 and independent studies, it is important that the EO community is aware of this challenge, particularly because technical national teams who rely on EO data as main source of AD (**Figure 2-2**) also face the same challenge. This finding is consistent with other studies reporting omission errors mapping small scale changes in sub-Saharan Africa and drylands with lower canopy cover (Tyukavina et al., 2013; Tyukavina et al., 2015).

### **5.2.3 Better alignment between EO products and IPCC categories.**

In Chapter 2.5.1, I discussed some of the factors included in the IPCC Guidelines (IPCC, 2019) that need to be considered by producers of EO products for alignment with national requirements and uptake of their products in countries' NGHGI. These factors include spatial and temporal resolution, and temporal coverage and consistency. Links with time-series consistency were also discussed above (5.2.1). Failing to consider a single one of these factors can render the product unsuitable for reporting to the UNFCCC and therefore all of these criteria need to be taken into account in future developments by the EO community. This section does not replace nor repeat the discussion in Chapter 2.5.1 but is intended to emphasise the issue of the disconnect between EO products and the national definitions and of attribution of land use and land use change according to the IPCC categories (**Table 1.1**). Although discussed in Chapter 2.5.1, it is mentioned here again because the importance of considering national definitions and the correct attribution of land use binds all the chapters of this thesis – it is connected to i) the low diversity in the choice of EO products to map deforestation (Chapter 2), ii) the low accuracy of the maps at national level (Chapter 3 and 4), iii) the option and recommendation of using a stratified area approach (Chapter 2 and 4), and iv) the reconciliation between datasets (wider scope in Chapter 1).

The flexibility to adhere to varying national definitions is one of the attractive characteristics of the GFC (Hansen et al., 2013) and reason for its use by half the countries with forest reference level submission between 2014 and 2022 (Chapter 2). Rigid thematic classes (for example, of land cover) cannot possibly match the IPCC

categories of all countries simultaneously (e.g., Forest Land, Cropland, see **Table 1.1**), and products that impose a definition (e.g., from **Table 2.2**) are not as attractive to national teams. There is no universal definition of Forest Land, not in terms of biophysical parameters, nor other characteristics of land use. Nations, that are sovereign, make the decision on how they define their own land. For example, for Forest Land, canopy cover thresholds vary between 10 and 60% among the forest definitions used in the forest reference level submissions analysed in Chapter 2 (**Table A.1.2**). Furthermore, palm trees, mangroves or shifting agriculture can constitute a forest or not, and timber plantations are considered Forest Land in the NGHGI but are typically excluded in REDD+. The GFC, when used to directly derive AD in national submissions (Chapter 2), is always used in combination with national maps, or a sample of visually interpreted high-resolution imagery. While the authors of the GFC product are clear in noting that “forest loss” employed in the study is defined as the removal or mortality of all tree cover in a Landsat pixel (Hansen et al., 2014), the use of the term “forest loss” is misleading and means the GFC data must be handled with care to match the categories in the NGHGIs (**Table 1.1**). This is because under the UNFCCC, the carbon removals of all trees in a timber plantation (harvest) are reported in the category Forest Land remaining Forest Land and is not forest conversion to other land use category.

I'll use again the shifting agriculture example discussed in this thesis because the challenges of accurately mapping and quantifying it are not only spectral (Chen et al., 2023; Miettinen et al., 2014; Ryan et al., 2012), but are also related to national definitions and attribution to IPCC categories. From the comprehensive analysis in Chapter 2 on 76 reference level submissions, it was noted that the land use of areas under shifting agriculture cycles are not always clearly defined by national teams nor are the protocols for land classification properly developed and implemented. This issue must, therefore, be addressed by both the EO community and the national technical teams. In Chapter 4, Guinea-Bissau illustrates an approach implemented by many other countries as well of using a sample of very-high resolution imagery for the correct attribution of land use (e.g., Ghana, Malawi, Mozambique). The classification protocol is described in Section 4.3.2.3 and was designed considering that shifting agriculture can be: i) a temporary tree cover loss in forest land remaining forest land if the fallow period is long and most trees remain standing (i.e., stable forest); ii) cropland (or stable non-forest) if in intensive management with short cycles and lower canopy coverage; or iii) deforestation if the management intensifies with reduction of tree canopy cover and can transition to permanent agriculture or tree crop. The difference between the findings in Chapter 4, i.e. shifting agriculture responsible for 64% of deforestation, and Curtis et al. (2018), i.e. shifting agriculture responsible for 98-100% of tree cover loss for the same period, can

potentially be explained by attribution to land use categories and national definitions. In this thesis, I am only looking at deforestation and, according to the national definition, did not include sustainable shifting agriculture cycles in forest land remaining forest land nor more intensive crop cycles in cropland remaining cropland. Those losses may not be included in national LULUCF fluxes in incomplete NGHGI if only emissions from deforestation are quantified.

These two examples, harvest and shifting agriculture, indicate the need to move from forest area change to land use change and from forest change to a land-based approach that includes all other IPCC land use categories. For example, in the NGHGI, GHG fluxes from shifting agriculture can be included in Forest Land or Cropland, and fluxes from harvest included in Forest Land. Also, GFC worked well for REDD+ (Chapter 2) but REDD+ focuses on Forest Land and forest land conversion while the NGHGI reports fluxes in the LULUCF sector, which is more comprehensive. This recommendation of moving towards a land-based approach is aligned with the priority action points to the EO community in the CEOS AFOLU roadmap (Poulter et al., 2023).

#### **5.2.4 Link EO products to IPCC variables**

Because Chapter 3 identified Activity Data (in this thesis, deforestation) as the main source of variability when estimating emissions from deforestation, Chapter 4 of this thesis focused on the challenges of mapping deforestation and not the biomass component. However, countries report fluxes to the UNFCCC (in NGHGI, REDD+, NDCs) in  $\text{tCO}_2\text{yr}^{-1}$  using different methods (Section 1.2.3). Even in NDCs, countries are encouraged to include quantitative metrics but especially, GHG targets (also in  $\text{tCO}_2\text{yr}^{-1}$ ; see **Table 2.1**). To estimate land fluxes according to the IPCC Guidance and to facilitate communication with national technical teams to develop practical demonstrations of uptake of EO products, EO products should be linked to IPCC variables (**Table 1.2**).

Furthermore, the different groups in the EO community, working on land dynamic, on fire mapping, and on biomass mapping, must work together to prioritize research developments because the variables need information from more than one expert EO group. Here, I present a very preliminary and coarse attempt to identify EO data requirements for each IPCC variable (**Table 5.1**). The requirements consider the IPCC factors discussed in section 2.5.1 (spatial resolution, temporal resolutions, and temporal coverage) and differ depending on how the product is used. The requirements in this table were based on the examples found in country submissions in Chapter 2 and must be explored further, including with specific EO products. The table is intended to present the idea of preliminary work that can be done to bridge the EO and NGHGI communities

and does not contain a final set of criteria. Additionally, this table is simplified. For area representation, for example, all the complexities on the attribution to the correct category and sub-category of land must be considered.

**Table 5.1.** Preliminary reflections on the requirements in terms of spatial and temporal resolutions and temporal coverage for satellite-based products to estimate emissions and removals from the LULUCF, i.e., to the IPCC variable to report (IPCC, 2006). The options of products, uses and characteristics are not exhaustive and only builds on the range of data and uses in Forest Reference Level submissions from the analysis in Chapter 2

Map	Use 1	Use 2	Spatial resolution	temporal resolution, temporal coverage or Year
Area representation	directly derive area of conversion ( $AD_{ij}$ )	Post-classification change detection Direct change detection	0.5 to 1 ha	Start and end of reference period ranging ~10-15 years
	Stratification	Strata are areas of conversion ( $AD_{ij}$ ) Strata are areas of land $i$ ( $i = 1$ to $n$ ) to support field inventory and determine EFs per land type	Coarser resolutions are possible	One point in time is enough. The year is flexible
Biomass	$B_{BEFORE}$ or $B_{AFTER}$	Average biomass value for each land type $i$ ( $i = 1$ to $n$ ) Stratification. Strata are classes of biomass density combined with the land stratification map. Average value = $B_{BEFORE}$ or $B_{AFTER}$ for each combination of biomass density class and land strata	Coarser resolutions are possible	One point in time is enough. The year is flexible but needs to be the same year of the land stratification map
Biomass change	A per pixel estimate of biomass change corresponds to applying the two Equations 2.15 and 2.16 (IPCC, 2006) of the Gain-loss method: $B_{BEFORE}$ , $B_{AFTER}$ , $AD_{ij}$ , $\Delta C_G$ and $\Delta C_L$		0.5 to 1 ha	Start and end of reference period ranging ~10-15 years
	$\Delta C_G$ and $\Delta C_L$ In large and homogeneous strata		Coarser resolutions are possible	At last in two different years representing two inventory round. Resolution ~10 years
	$C_{t1}$		0.5 to 1ha	Start of the reference period or proxy
	$C_{t2}$		0.5 to 1ha	End of the reference period or proxy
Burnt areas	to estimate the area affected by fire and the non- $CO_2$ emissions from fires separated by driver: to be combined with AD deforestation and AD forest remaining forest (degradation)		Coarser resolutions are possible	Annual, for the duration of the reference period or matching the years of the conversion maps

### 5.2.5 Implement a collaborative interface between national and global land monitoring experts.

The divergences found in existing EO products (Chapter 3) and their large errors (Chapter 4) demonstrates there are technical issues in the EO products that limited their use in national submissions to the UNFCCC (Chapter 2). While actions are undertaken within countries to address institutional capacity gaps and poor governance (Ochieng et al., 2016), developers of EO products should in parallel make an effort to interact with groups responsible for GHG inventories and experts familiar with IPCC guidance so to improve their products and make them suitable for national reporting, and thus contribute to the processes under the UNFCCC (**Figure 1-5**). This collaboration could include sharing of data for calibration of maps and their improvement, steps for identifying

together the needs and requirements in national reporting, for handling and presenting them in a way that is consistent with the IPCC Guidelines. Such collaborative efforts could, ultimately, enhance the uptake of EO products in national reporting and support more complete, accurate and transparent NGHGI and a stronger Global Stocktake.

It is worth noting that some cases, e.g., use of biomass maps, are still areas of active research, the IPCC Guidelines (IPCC, 2019) have only generic text, and there are not many examples on the practical implementation of the guidance. The existing examples using satellite data to produce biomass maps in national reporting are too few (Zambia 2017, Honduras 2020 and Togo 2020, **Figure 2-2, Table A.1.2**), including using airborne measurements, for example in Brazil (Ometto et al., 2023; in the latest forest reference level submitted in 2023). Enhancing the uptake of EO products in national reporting to the UNFCCC (CEOS AFOLU roadmap recommendation 2, Box 1.2, Poulter et al., 2023) will be more successfully achieved if the disconnect between producers and users is addressed and an interface for collaboration between EO global biomass monitoring, GHG inventory, and national forest inventory experts is created (CEOS AFOLU roadmap recommendation 3, Box 1.2, Poulter et al., 2023). Such an interface exists to some extent in capacity building programmes although the approaches used tend to be more of imposing data and methods rather than listening.

The objective of this section is to highlight that capacity building works both ways and for the purpose of enhancing the uptake of EO products, the way that these are handled and presented by the people that develop them to potential users is crucial. Therefore, below are some suggestions of requirements and steps for an effective engagement between the EO community developing global maps and NGHGI experts for the purpose of developing practical examples of uptake in national reporting to the UNFCCC:

- i. first, it is necessary to recognize that only individual countries, given their national circumstances, can determine if satellite-based data and derived products developed over large areas are suitable for use in national GHG inventories,
- ii. a well-established relationship with Government institutions responsible for reporting to the UNFCCC through the use of existing channels, i.e. long-standing relationships and trust takes time and consistency to build,
- iii. a champion in the national team and a champion in the EO group for each country cluster of selected scientists and national teams to explore nationally appropriate opportunities for the use of EO data and derived maps,
- iv. at least one member with GHG inventory experience included in the cluster (e.g. from the UNFCCC roster of experts) that may help in the interface, for example in understanding differences in definitions used,

- v. preparation steps ahead of the introduction meeting are undertaken, e.g., understanding the MRV capacity of the country and knowing the key priority areas of technical improvement identified in country reports,
- vi. link country needs and priorities with IPCC variables and existing EO data and methods to collaboratively explore opportunities to use satellite data and derived maps to estimate those variables following IPCC Guidelines and Principles.

Such an interface would address the disconnect and facilitates the collaboration and sharing of data between groups. Furthermore, it sets a framework for the best scientists in the remote sensing field to collaborate with GHG inventory experts to address some of the outstanding issues that hinder the use of maps by national teams preparing their reports to the UNFCCC. This is also essential and very timely for tropical countries and least developed countries given the impending more stringent reporting requirements they have committed to under the enhanced transparency framework of the Paris Agreement. Accordingly, these ideas are reflected in some of the outputs of the CEOS AFOLU harmonization ongoing efforts (Ochiai et al., 2023; Poulter et al., 2023; Hunka et al., 2023).

### **5.2.6 Reconcile the differences at national and global level.**

One important topic discussed in the motivation for this thesis was the need to reconcile or at least explain the differences in the estimates of carbon fluxes informing the Global Stocktake. Such reconciliation could potentially help converge the conflicting estimates from aggregation of carbon fluxes from NGHGI and independent estimates from EO products (one of the overarching questions of this thesis). This thesis focuses on deforestation, because the magnitude and trends of deforestation from different estimates are still conflicting at the global level. These conflicting messages were also observed in this thesis' case study – in Guinea-Bissau the deforestation maps were very divergent in magnitude and spatial distribution (1-6% area overlap), and all had large classification errors (area-corrected OE = 91-97% CE = 38-59%) linked to shifting agriculture.

So far, there is no systematic review of the impacts of shifting agriculture in LULUCF emissions in the aggregated NGHGI. This is because it is not clear in every inventory, nor in the IPCC Guidelines, what is the prevailing land use in shifting agriculture. There is no global consensus either. According to the IPCC Guidance, if the prevailing land use is cropland, then the fluxes should be reported in the corresponding category in the NGHGI. Curtis et al (2018) identifies it as tree loss other than deforestation, although it remains unclear if the authors mean to say these losses correspond to emissions in the

IPCC categories forest land remaining forest land, or cropland remaining cropland. Other local studies describe it as driver of deforestation (e.g., Ryan et al., 2014; Chen et al., 2023). Ultimately, it is up to nations, who are sovereign, to make decisions on what is considered forest or other land uses in their territory and, accordingly, the UNFCCC and the IPCC Guidelines do not prescribe a common definition (discussed in section 5.2.3).

The most recent GCB (Friedlingstein et al, 2023) quantifies for the first time the impact of shifting agriculture in the total land use fluxes and split total emissions from deforestation into permanent deforestation and deforestation from shifting agriculture, as well as total removals from forest recovery into afforestation/reforestation and regrowth from shifting agriculture (**Figure 5-1**). Averaged over the 2013–2022 period and over the three bookkeeping estimates, fluxes from total deforestation amount to 6.97 GtCO<sub>2</sub>yr<sup>-1</sup> of which 2.94 GtCO<sub>2</sub>yr<sup>-1</sup> are due to shifting agriculture and are entirely balanced out by removals during fallow. Emissions from permanent deforestation are therefore around 4 GtCO<sub>2</sub>yr<sup>-1</sup> which is of the same magnitude of emissions from deforestation in the aggregation of NGHGI in Grassi et al (2022) (**Figure 5-1**) and may explain the remaining gap in Grassi et al (2023). Overlaying data from the GFC (Hansen et al., 2013) updated annually on Global Forest Watch combined with Curtis et al (2018) to exclude emissions from the drivers shifting agriculture and wildfires (GFW, 2023), still shows a large gap and maintains the different trend. The Forestry class was not excluded because although including harvest, it also includes deforestation of primary forest which, in the NGHGI, are reported in different categories. In the case of the GFW, it seems the disagreements are not explained by shifting agriculture.

For the future, it is important to explore where these differences come from to increase confidence in the EO products by making sure the contrasting estimates are not due to conceptual differences. To explain all the differences, assessments at the national levels are required because MRV capacity, completeness, and accuracy of the NGHGI, as well as the drivers of deforestation are largely different and the reasons for the disagreements will vary from country to country accordingly. Doing this exercise in articulation with the recommendations above is encouraged.

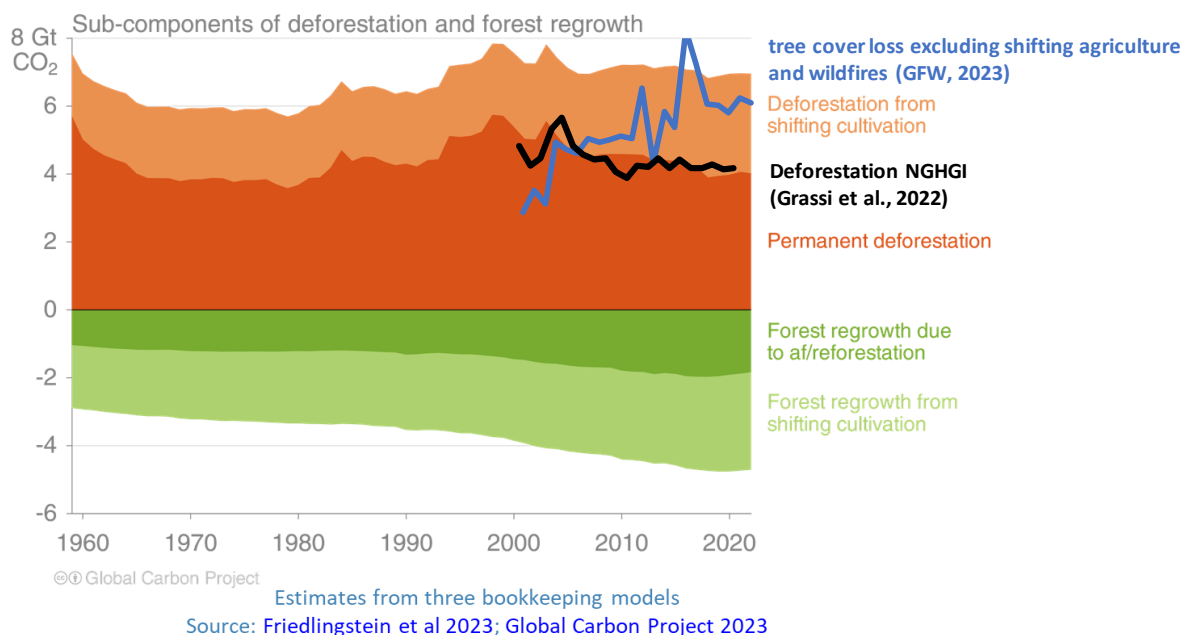


**Figure 5-1** Figure 7(d) from the *Global Carbon Budget 2023* (Friedlingstein et al, 2023) overlaid with emissions from deforestation from the aggregated NGHGI in Figure 2(a) of Grassi et al (2022) (in black) and the global emissions from tree cover loss (Hansen et al., 2013) combined with the map of drivers from Curtis et al. (2018) to exclude emissions from shifting agriculture (in blue; from Global Forest Watch, GFW, 2023). The figure from Friedlingstein et al, (2023) shows the sub-components of “deforestation” and of “forest (re)growth” in the component of emissions from land use (ELUC): (i) deforestation in shifting cultivation cycles, (ii) permanent deforestation, (iii) forest (re)growth due to afforestation and/or reforestation, and (iv) forest regrowth in shifting cultivation cycles.

### 5.3 Closing Remarks

Accurate and timely information on the carbon fluxes from forests and land use is required to plan climate change mitigation actions and address the greatest challenge humanity is facing this century. The science is clear that we need to act very fast (IPCC, 2022; UNEP, 2023). With the end of the first Global Stocktake (UNFCCC, 2023), scientists are expressing frustration about the slow political response to the “broken record” messages of the IPCC ARs and requesting power to prescribe policies (Neslen, 2023 December 7). The work presented in this thesis disagrees with the idea that scientists reached a point where they can no longer “be policy relevant without being prescriptive”.

This thesis reveals that, despite the large investments made by Space Agencies and the EO community to provide satellite data and derived global maps to measure carbon fluxes from land, there is a notable underutilization of EO products in national reporting. One reason for their low uptake is exactly the disconnect between science and policy, or between the available maps and the IPCC requirements used in NGHGI to report to the UNFCCC. I show that maps relying on more sophisticated satellite data and remote sensing approaches have large errors at national levels, many times simply because they don’t use the same definitions and therefore present results that are conceptually

different. On the land use sector, the message from the scientific community, including modelling and EO experts, is still not crystal clear. In fact, the most widely used satellite-based forest loss global map (GFC, Hansen et al., 2013; Harris et al., 2021) had an area-corrected omission error of 97% in my case-study and using national definitions and IPCC Guidelines, for a time period (2007-2010) prior to the 2016 methodological change and sharp increase in detected forest loss (Galiatsatos et al., 2020; Palahi et al., 2021; Ceccherini et al., 2021). The errors, which are mostly linked to shifting agriculture, were equally large in other satellite-based maps and can be connected to the same conceptual differences.

Nations are sovereign, governments make decisions on land definitions and on mitigation actions on their land. The role of the research community is to provide clear, accurate, timely information so that all countries that wish to, have the necessary data to make informed decisions and can answer in their NGHGI the most fundamental question – what is the extent and trend of deforestation and associated carbon emissions in the first two decades of the 21<sup>st</sup> century? If many countries do not have a straightforward answer yet, and at the global level we still have contradictory messages, more effort is required to translate science, to handle and present data in a way that resonates with policy makers and technical teams. Tropical forests are vulnerable and the enhanced transparency that accurate and adequate EO maps and products bring to the climate change arena is essential given that many developing countries are still far from being ready to implement domestic monitoring systems. Their forests, including the carbon they store and removal capacity that are so essential to achieve climate neutrality objectives, are too vulnerable to wait.

## 5.4 References

Arevalo, P., Olofsson, P., and Woodcock, C.: Continuous monitoring of land change activities and post-disturbance dynamics from Landsat time series: A test methodology for REDD plus reporting, *Remote Sensing of Environment*, 238, 10.1016/j.rse.2019.01.013, 2020.

Ceccherini, G., Duveiller, G., Grassi, G., Lemoine, G., Avitabile, V., Pilli, R., and Cescatti, A.: Concerns about reported harvests in European forests Reply to Wernick, I. K. et al.; Palahi, M. et al., *Nature*, 592, E18-E23, 10.1038/s41586-021-03294-9, 2021.

Chen, S., Olofsson, P., Saphangthong, T., and Woodcock, C.: Monitoring shifting cultivation in Laos with Landsat time series, *Remote Sensing of Environment*, 288, 10.1016/j.rse.2023.113507, 2023.

Curtis, P., Slay, C., Harris, N., Tyukavina, A., and Hansen, M.: Classifying drivers of global forest loss, *Science*, 361, 1108-1111, 10.1126/science.aau3445, 2018.

EIA: Authorized Plunder: Massive Rosewood Sale Backed by Global Wildlife Convention Fuels

ESA (2022) The Role of Systematic Earth Observations in the Global Stocktake. Version 28 February. Available at: <https://unfccc.int/documents/462475> (last accessed: October 2022).

Forest Crimes in Guinea-Bissau. Media Release. (available online: <https://us.eia.org/press-releases/20181212-guinea-bissau-authorized-plunder-pr/>) (last accessed: June 2023), 2018.

Friedlingstein, P., O'Sullivan, M., Jones, M. W., Andrew, R. M., Bakker, D. C. E., Hauck, J., Landschützer, P., Le Quéré, C., Lujikx, I. T., Peters, G. P., Peters, W., Pongratz, J., Schwingshackl, C., Sitch, S., Canadell, J. G., Ciais, P., Jackson, R. B., Alin, S. R., Anthoni, P., Barbero, L., Bates, N. R., Becker, M., Bellouin, N., Decharme, B., Bopp, L., Brasika, I. B. M., Cadule, P., Chamberlain, M. A., Chandra, N., Chau, T. T. T., Chevallier, F., Chini, L. P., Cronin, M., Dou, X., Enyo, K., Evans, W., Falk, S., Feely, R. A., Feng, L., Ford, D. J., Gasser, T., Ghattas, J., Gkritzalis, T., Grassi, G., Gregor, L., Gruber, N., Gürses, Ö., Harris, I., Hefner, M., Heinke, J., Houghton, R. A., Hurtt, G. C., Iida, Y., Ilyina, T., Jacobson, A. R., Jain, A., Jarníková, T., Jersild, A., Jiang, F., Jin, Z., Joos, F., Kato, E., Keeling, R. F., Kennedy, D., Klein Goldewijk, K., Knauer, J., Korsbakken, J. I., Körtzinger, A., Lan, X., Lefèvre, N., Li, H., Liu, J., Liu, Z., Ma, L., Marland, G., Mayot, N., McGuire, P. C., McKinley, G. A., Meyer, G., Morgan, E. J., Munro, D. R., Nakaoka, S. I., Niwa, Y., O'Brien, K. M., Olsen, A., Omar, A. M., Ono, T., Paulsen, M., Pierrot, D., Pockock, K., Poulter, B., Powis, C. M., Rehder, G., Resplandy, L., Robertson, E., Rödenbeck, C., Rosan, T. M., Schwinger, J., Séférian, R., Smallman, T. L., Smith, S. M., Sospedra-Alfonso, R., Sun, Q., Sutton, A. J., Sweeney, C., Takao, S., Tans, P. P., Tian, H., Tilbrook, B., Tsujino, H., Tubiello, F., van der Werf, G. R., van Ooijen, E., Wanninkhof, R., Watanabe, M., Wimart-Rousseau, C., Yang, D., Yang, X., Yuan, W., Yue, X., Zaehle, S., Zeng, J., and Zheng, B.: Global Carbon Budget 2023, 15, 5301-5369, 2023.

Galiatsatos, N., Donoghue, D., Watt, P., Bholanath, P., Pickering, J., Hansen, M., and Mahmood, A.: An Assessment of Global Forest Change Datasets for National Forest Monitoring and Reporting, *Remote Sensing*, 12, 10.3390/rs12111790, 2020.

GFOI: Integration of remote-sensing and ground-based observations for estimation of emissions and removals of greenhouse gases in forests: Methods and Guidance from the Global Forest Observations Initiative, Edition 3.0., 2020.

Grassi, G., Conchedda, G., Federici, S., Vinas, R., Korosuo, A., Melo, J., Rossi, S., Sandker, M., Somogyi, Z., Vizzarri, M., and Tubiello, F.: Carbon fluxes from land 2000-2020: bringing clarity to countries' reporting, *Earth System Science Data*, 14, 4643-4666, 10.5194/essd-14-4643-2022, 2022.

Hansen, M., Potapov, P., Margono, B., Stehman, S., Turubanova, S., and Tyukavina, A.: Response to Comment on "High-resolution global maps of 21st-century forest cover change", *Science*, 344, 1, 10.1126/science.1248817, 2014.

Hansen, M. C., Potapov, P. V., Moore, R., Hancher, M., Turubanova, S. A., Tyukavina, A., Thau, D., Stehman, S. V., Goetz, S. J., Loveland, T. R., Kommareddy, A., Egorov, A., Chini, L., Justice, C. O., and Townshend, J. R. G.: High-Resolution Global Maps of 21st-Century Forest Cover Change, *Science*, 342, 850-853, 10.1126/science.1244693, 2013.

Harris, N., Gibbs, D., Baccini, A., Birdsey, R., de Bruin, S., Farina, M., Fatoyinbo, L., Hansen, M., Herold, M., Houghton, R., Potapov, P., Suarez, D., Roman-Cuesta, R.,

Saatchi, S., Slay, C., Turubanova, S., and Tyukavina, A.: Global maps of twenty-first century forest carbon fluxes, *Nature Climate Change*, 11, 10.1038/s41558-020-00976-6, 2021.

Hunka et al, N.: On the NASA GEDI and ESA CCI biomass maps: aligning for uptake in the UNFCCC global stocktake, *Environ. Res. Lett.* 18 124042 DOI 10.1088/1748-9326/ad0b60, 2023.

IPCC: 2019 Refinement to the 2006 IPCC Guidelines for National Greenhouse Gas Inventories, 2019.

IPCC: Climate Change 2022: Mitigation of Climate Change. Contribution of Working Group III to the Sixth Assessment Report of the Intergovernmental Panel on Climate Change, 2022.

McNicol, I., Ryan, C., and Mitchard, E.: Carbon losses from deforestation and widespread degradation offset by extensive growth in African woodlands, *Nature Communications*, 9, 10.1038/s41467-018-05386-z, 2018.

McRoberts, R.: Satellite image-based maps: Scientific inference or pretty pictures?, *Remote Sensing of Environment*, 115, 715-724, 10.1016/j.rse.2010.10.013, 2011.

Miettinen, J., Stibig, H., and Achard, F.: Remote sensing of forest degradation in Southeast Asia-Aiming for a regional view through 5-30 m satellite data, *Global Ecology and Conservation*, 2, 24-36, 10.1016/j.gecco.2014.07.007, 2014.

Neslen, A.: "We need power to prescribe climate policy, IPCC scientists say". *The Guardian*, 7 December 2023. Available online: <https://www.theguardian.com/environment/2023/dec/07/we-need-power-to-prescribe-climate-policy-ipcc-scientists-say>.

Ochiai, O., Poulter, B., Seifert, F. M., Ward, S., Jarvis, I., Whitcraft, A., Sahajpal, R., Gilliams, S., Herold, M., Carter, S., Duncanson, L. I., Kay, H., Lucas, R., Wilson, S. N., Melo, J., Post, J., Briggs, S., Quegan, S., Dowell, M., Cescatti, A., Crisp, D., Saatchi, S., Tadono, T., Steventon, M., and Rosenqvist, A.: Towards a roadmap for space-based observations of the land sector for the UNFCCC global stocktake, *iScience*, 106489, <https://doi.org/10.1016/j.isci.2023.106489>, 2023.

Ochieng, R., Visseren-Hamakers, I., Arts, B., Brockhaus, M., and Herold, M.: Institutional effectiveness of REDD plus MRV: Countries progress in implementing technical guidelines and good governance requirements, *Environmental Science & Policy*, 61, 42-52, 10.1016/j.envsci.2016.03.018, 2016.

Olofsson, P., Foody, G. M., Stehman, S. V., and Woodcock, C. E.: Making better use of accuracy data in land change studies: Estimating accuracy and area and quantifying uncertainty using stratified estimation, *Remote Sensing of Environment*, 129, 122-131, 10.1016/j.rse.2012.10.031, 2013.

Olofsson, P., Foody, G., Herold, M., Stehman, S., Woodcock, C., and Wulder, M.: Good practices for estimating area and assessing accuracy of land change, *Remote Sensing of Environment*, 148, 42-57, 10.1016/j.rse.2014.02.015, 2014.

Olofsson, P., Arevalo, P., Espejo, A., Green, C., Lindquist, E., McRoberts, R., and Sanz, M.: Mitigating the effects of omission errors on area and area change estimates, *Remote Sensing of Environment*, 236, 10.1016/j.rse.2019.111492, 2020.

Ometto, J., Gorgens, E., Pereira, F., Sato, L., de Assis, M., Cantinho, R., Longo, M., Jacon, A., and Keller, M.: A biomass map of the Brazilian Amazon from multisource remote sensing, *Scientific Data*, 10, 10.1038/s41597-023-02575-4, 2023.

Palahi, M., Valbuena, R., Senf, C., Acil, N., Pugh, T., Sadler, J., Seidl, R., Potapov, P., Gardiner, B., Hetemaki, L., Chirici, G., Francini, S., Hlasny, T., Lerink, B., Olsson, H., Olabarria, J., Ascoli, D., Asikainen, A., Bauhus, J., Berndes, G., Donis, J., Fridman, J., Hanewinkel, M., Jactel, H., Lindner, M., Marchetti, M., Marusak, R., Sheil, D., Tome, M., Trasobares, A., Verkerk, P., Korhonen, M., and Nabuurs, G.: Concerns about reported harvests in European forests, *Nature*, 592, E15-E17, 10.1038/s41586-021-03292-x, 2021.

Poulter, B., Ochiai, O., Siefert, F.-M., Albergel, C., Dowell, M., Duncanson, L., Gilliams, S., Harris, N., Herold, M., Hunka, N., Friendship-Kay, H., Jarvis, I., Lucas, R., Meijer, Y., Melo, J., Quegan, S., Rosenquist, A., Sloat, L., Sohl, T., Requena Suarez, D., Viciano, L., Ward, S., Whitcraft, A., and Wilson, S.: CEOS Roadmap for Space-Based Support of Agriculture, Forestry and Other Land Use (AFOLU) Emissions and Removals of Greenhouse Gases. Version 1.0 endorsed by the Principals at the 37th Committee on Earth Observation Satellites Plenary, Thailand November 2023. Last accessed online at:

[https://ceos.org/document\\_management/Meetings/Plenary/37/Supporting%20Documents/CEOS\\_AFOLU\\_roadmap\\_FINAL\\_V1.0.pdf](https://ceos.org/document_management/Meetings/Plenary/37/Supporting%20Documents/CEOS_AFOLU_roadmap_FINAL_V1.0.pdf), 2023.

Roy, D., Kovalsky, V., Zhang, H., Vermote, E., Yan, L., Kumar, S., and Egorov, A.: Characterization of Landsat-7 to Landsat-8 reflective wavelength and normalized difference vegetation index continuity, *Remote Sensing of Environment*, 185, 57-70, 10.1016/j.rse.2015.12.024, 2016.

Ryan, C. M., Berry, N. J., and Joshi, N.: Quantifying the causes of deforestation and degradation and creating transparent REDD plus baselines: A method and case study from central Mozambique, *Applied Geography*, 53, 45-54, 10.1016/j.apgeog.2014.05.014, 2014.

Ryan, C. M., Hill, T., Woollen, E., Ghee, C., Mitchard, E., Cassells, G., Grace, J., Woodhouse, I. H., and Williams, M.: Quantifying small-scale deforestation and forest degradation in African woodlands using radar imagery, *Global Change Biology*, 18, 243-257, 10.1111/j.1365-2486.2011.02551.x, 2012.

Tyukavina, A., Baccini, A., Hansen, M. C., Potapov, P. V., Stehman, S. V., Houghton, R. A., Krylov, A. M., Turubanova, S., and Goetz, S. J.: Aboveground carbon loss in natural and managed tropical forests from 2000 to 2012, *Environmental Research Letters*, 10, 14, 10.1088/1748-9326/10/7/074002, 2015.

Tyukavina, A., Stehman, S. V., Potapov, P. V., Turubanova, S. A., Baccini, A., Goetz, S. J., Laporte, N. T., Houghton, R. A., and Hansen, M. C.: National-scale estimation of gross forest aboveground carbon loss: a case study of the Democratic Republic of the Congo, *Environmental Research Letters*, 8, 10.1088/1748-9326/8/4/044039, 2013.

UNEP: Emissions Gap Report 2023: Broken Record – Temperatures hit new highs, yet world fails to cut emissions (again), Nairobi, 2023.

UNFCCC: ' Outcome of the first global stocktake '. REVISED ADVANCE VERSION 13 December 2023, 2023.

Vittek, M., Brink, A., Donnay, F., Simonetti, D., and Desclee, B.: Land Cover Change Monitoring Using Landsat MSS/TM Satellite Image Data over West Africa between 1975 and 1990, *Remote Sensing*, 6, 658-676, 10.3390/rs6010658, 2014.

Vogeler, J., Braaten, J., Slesak, R., and Falkowski, M.: Extracting the full value of the Landsat archive: Inter-sensor harmonization for the mapping of Minnesota forest canopy cover (1973-2015), *Remote Sensing of Environment*, 209, 363-374, 10.1016/j.rse.2018.02.046, 2018.

# Appendix 1

We selected REDD+ FRLs as our data source because our focus is on the use of EO products to monitor forests and conversions to/from forests; this is the part of LULUCF where most GHG fluxes are reported and where most of the uncertainties exist. FRLs provide the most detailed technical information on the data and methods used to derive carbon flux estimates in tropical forests and are technically assessed under the UNFCCC. Alternative sources not included in this study are NDCs, national communications and biennial update reports, of which only the latter are technically reviewed. However, many countries have never submitted a biennial update report, or if they have, this may exclude the LULUCF sector or use IPCC default values due to lack of national data.

Furthermore, REDD+ decisions establish that the data, methodologies and procedures used in FRLs should be consistent with corresponding anthropogenic forest-related GHG emissions by sources and removals by sinks as contained in the national GHG inventory (GHGi). Hence, the use of satellite data and EO products in the FRL is evidence of the opportunity for its use in the LULUCF sector of the GHGi. Although methodologies are often not yet harmonized between FRLs and GHGi, countries are working towards that objective.

REDD+ activities and the classes in our study can be mapped to the IPCC categories used in GHGi (**Table A.1.1**). For example, the class 'deforestation' in our study includes uses of EO products for AD or EF in carbon flux estimates of 'forest land converted to' either 'cropland', 'grassland', 'wetlands', 'settlements', or 'other land' in the GHGi. Also, the class 'other REDD+ activities' includes uses of EO products for AD or EF in estimates of the sub-categories of the GHG inventory 'land converted to forest land' and 'forest land remaining forest land'. Due to the focus of REDD+ on forest land, uses of EO products for other sub-categories of the GHG inventory are not included in the analysis. Furthermore, some of the sub-categories of the GHGi corresponding to fluxes to and within forest land (in our study, 'other REDD+ activities') may be under-represented. For example, although most countries included fluxes from forest degradation (DEG, n=32, 57%) and enhancement of forest carbon stocks (ECS, n=35, 63%) in their FRLs, only a few included the remaining activities (conservation of forest carbon stocks CCS=18%, and sustainable management of forests SMF=18%).

**Table A.1.1.** IPCC categories for the land use, land use change and forestry (LULUCF) sector in GHG inventories reported to the UNFCCC (see LULUCF tabs of the common reporting tables) mapped to the activities reported under the UNFCCC REDD+ framework and the classes in this study ('deforestation' and 'other REDD+ activities'). This mapping is not fixed, though. For REDD+, some countries choose a land-based approach and may report emissions and removals from most land-use categories under 'sustainable management of forests' (SMF) or 'conservation of forest carbon stocks' (CCS), or on the contrary, include the activities SMF and CCS in the other three activities. For example, India's forest reference level only has the activity SMF covering fluxes from afforestation as a management practice, harvesting, thinning and forest conservation as a management practice. Given the focus of REDD+ on forest land, some categories in the GHG inventory have no correspondence to REDD+ activities, hence NA = not applicable

IPCC land-use categories and sub-categories	REDD+ activity	categories in this study
forest land remaining forest land (4.A.1.)	forest degradation (DEG) enhancement of forest carbon stocks (ECS) sustainable management of forests (SMF) conservation of forest carbon stocks (CCS)	included
land converted to forest land (4.A.2.)		EO uses to estimate fluxes from 'other REDD+ activities'
cropland converted to forest land (4.A.2.a)		
grassland converted to forest land (4.A.2.b)		
wetlands converted to forest land (4.A.2.c)	enhancement of forest carbon stocks (ECS)	
settlements converted to forest land (4.A.2.d)		
other land converted to forest land (4.A.2.e)		
cropland remaining cropland (4.B.1.)	NA	not included
land converted to cropland (4.B.2.)		
forest land converted to cropland (4.B.2.a)	deforestation (DEF)	included. EO uses for 'deforestation'
other land uses converted to cropland (4.B.2.b-e)	NA	not included
grassland remaining grassland (4.C.1.)	NA	not included
land converted to grassland (4.C.2.)		
forest land converted to grassland (4.C.2.a)	deforestation (DEF)	included. EO uses for 'deforestation'
other land uses converted to grassland (4.C.2.b-e)	NA	not included
wetlands remaining wetlands (4.D.1.)	NA	not included
land converted to wetlands (4.D.2.)		
forest land converted to wetlands (4.D.2.a)	deforestation (DEF)	included. EO uses for 'deforestation'
other land uses converted to wetlands (4.D.2.b-e)	NA	not included
settlements remaining settlements (4.E.1.)	NA	not included
land converted to settlements (4.E.2.)		
forest land converted to settlements (4.E.2.a)	deforestation (DEF)	included. EO uses for 'deforestation'
other land uses converted to settlements (4.E.2.b-e)	NA	not included
other land remaining other land (4.F.1.)	NA	not included
land converted to other land (4.F.2.)		
forest land converted to other land (4.F.2.a)	deforestation (DEF)	included. EO uses for 'deforestation'
other land uses converted to other land (4.F.2.b-e)	NA	not included

**Table A.1.2.** List of the 56 country Parties to the UNFCCC with a total of 75 REDD+ Forest Reference Emission Levels / Forest reference Level (FREL/FRL) submissions to the UNFCCC since 2014 and up to 2022. Identification of the REDD+ activities included in the FREL/FRL (DEF: deforestation, DEG: forest degradation, SMF: Sustainable Management of Forests, CCS: Conservation of forest Carbon Stocks, or ECS: Enhancement of forest Carbon Stocks. ECS can include fluxes from ‘forest land remaining forest land’ (F>F) or only fluxes from conversion of non-forest land to forest land (NF>F). If only one component is included, that information is included). Identification of the greenhouse gases reported in the FREL/FRL, and some biophysical parameters of the national definition of forest land. Identification of the technical method used to derive Activity Data (AD, area of land converted to other land-use or remaining in the same land-use) and description of how AD and Emission Factors and Removal Factors (EF/RFs, biomass and biomass change) were estimated, and if and how satellite data and derived products contributed to these estimates. Countries are listed alphabetically with symbols identifying the UN geopolitical and negotiating groups mentioned in this study († Latin American and Caribbean States; ‡ African States; § Asian and the Pacific States; & Least Developed Countries). Following the step-wise approach (Decision 12/CP.17), 17 countries submitted more than one FREL/FRL (Brazil, Cambodia, Colombia, Dominican Republic, Ecuador, Ghana, Honduras, Indonesia, Madagascar, Malaysia, Mexico, Nigeria, Panama, Paraguay, Peru, Suriname, and Zambia), although Brazil has separate sub-national FRELs for biomes. Submissions marked with \* in the submission year are still undergoing technical assessment (n=6; from Ecuador, Ghana, Dominica, Guatemala, Indonesia, and Paraguay) and changes are expected in a future modified submission (cut-off date December 2022).

Country	Technical Assess. year(s)	Activity	Non-CO <sub>2</sub> Gases	Forest definition Biophysical thresholds	AD method	Notes on Emission Factors (EFs), including satellite-based data sources	Notes on Activity Data (AD), including satellite-based data sources	Use of products derived from satellite data?
Argentina †	2019	DEF	No	0.5-ha 5-20% canopy cover	pixel-counting	NFI volumetric plot data	Landsat: manual editing and accuracy assessment.	No
Bangladesh §.&	2019	DEF DEG ECS	No	0.5-ha 10% canopy cover	stratified area estimate	Harmonized national and subnational forest inventories	Landsat, SPOT and Sentinel-2: land-cover maps and change detection for the activities DEF, DEG and ECS Collect Earth imagery: reference data to correct bias. Low confidence in the attribution of AD method. The area values in the FRL from Table 12 (AD) and Table 18 (Uncertainty) don't match. The map bias-corrected areas may not have been used to derive the FREL (Table 15).but the method was left left bias-correction approach to match FAO (2020a) analysis	No
Belize †	2020	DEF DEG SMF CCS ECS	Yes	0.5-ha 30% canopy cover	systematic sampling	No NFI. Data from research studies, IPCC default values, and expert judgment	Collect Earth and Google Earth Engine to access NASA and ESA archive (Landsat, MODIS, Sentinel-2) Land-based approach. Mapathon. Visual interpretation of sample units to identify initial and final land-use and units affected by fire to estimate non-CO2 emissions.	No
Bhutan §.&	2020	DEF DEG SMF CCS ECS	Yes	0.5-ha 10% canopy cover	stratified area estimate	NFI and harvested timber records maintained by the Department of Forests and Park Services	Landsat: stacking imagery to obtain two layers with multi-temporal segmentation. GFC yearly loss dataset was aggregated by down-sampling the product to reach the minimum mapping unit 0.5 ha (see page 8 of FRL submission). Yearly GFC loss was combined with multi-temporal segmentation based on Landsat imagery using zonal statistics to produce information at the polygon level in SEPAL. GFC gain was assumed to be equally distributed between the different years. Using a stratified random sampling approach, sample units were assessed in the Collect Earth interface. The error matrix was used to correct the bias of the map estimates Forest fire burnt area obtained from annual forest fire statistics maintained by the Department of Forests and Park Services, and no mention to satellite data use.	Yes. Global Forest Change (GFC) for AD
Brazil †	Amazonia 2014 2018  Cerrado 2017	DEF	Yes, for Cerrado only	0.5-ha 10% canopy cover	pixel-counting	Amazonia: RADAMBRASIL project constructed a carbon map for the Amazonia biome using airborne radar sensors and dendrometric measurements from plots Cerrado: scientific publications and default IPCC values	Amazonia: PRODES gross deforestation mapping using Landsat data (complemented with imagery from other satellites - CBERS-2, CBERS-2B, Resourcesat-1, and UK-DMC2) on a wall-to-wall basis. Reference to Ometto et al (2014) comparing and highlighting large differences between the Amazon RADAM-based carbon map and Saatchi et al (2011) and Baccini et al (2012) maps  Cerrado: Mainly Landsat. Collect Earth for validation and to assist in the thematic mapping process. Assumption that all forest conversion led to a post-conversion fire and AD fire is not estimated separately from AD DEF	No

Country	Technical Assess. year(s)	Activity	Non-CO <sub>2</sub> Gases	Forest definition Biophysical thresholds	AD method	Notes on Emission Factors (EFs), including satellite-based data sources	Notes on Activity Data (AD), including satellite-based data sources	Use of products derived from satellite data?
Burkina Faso †,‡	2020	DEF DEG ECS	Yes	0.5-ha 10% canopy cover	pixel-counting	NFI (2nd cycle)	Landsat land cover mapping and post classification change detection Not clear what was the source of data for validation Forest fire historical data observations from a station of the Monitoring for Environment and Security in Africa (MESA) programme. Third National Communication	No
Cambodia §,¶	2017 2021	DEF DEG ECS	No	0.5-ha 10% canopy cover	stratified area estimate -- pixel-counting in the previous 2017 submission	No NFI. Forest AGB from harmonized plot data from subnational forest inventories. IPCC (2003) default values for pine forests and plantations. Post-deforestation carbon stock assumed to be zero. ECS: a carbon stock value was assumed to be reached without carbon sequestration increasing as forests matured. Bamboo AGB assumed to be zero.	Landsat, SPOT and Sentinel-2: Segmentation and classification of segments into two land cover maps. Post-classification change detection. The land-cover class of each segment of the initial map being compared with the corresponding segment of the subsequent map. Collect Earth synchronized with Earth Engine and with the GLAD tree canopy cover to collect a reference dataset which was used to correct the area estimates of the maps.	No
Chile †	2016	DEF DEG CCS ECS	Yes. For DEG only	0.5-ha 10-25% canopy cover	pixel-counting	NFI for forests, literature for other land uses	DEF: mostly based on the national cadastral data that uses aerial photogrammetry or interpretation of Landsat MSS complemented with aero photos. DEG, C, ECS: Landsat to estimate variations in FL>FL. Spot and RapidEye images to update the final maps. Collect Earth: reference dataset to validate change Assessment Team compared DEF estimates with the Global Forest Watch (i.e. GFC) as well as Landsat time series for the respective reference periods available for each region.	Yes. Global Forest Change (GFC) to compare results
Colombia †	2015 2020	DEF	No	1-ha 30% canopy cover	pixel-counting	NFI (1st cycle)	Mainly Landsat. Other sources to complement in case of cloud coverage (CBERS, RapidEye, ASTER and Sentinel 2). Direct change detection to measure deforestation biennially. Accuracy assessment: visual interpretation of sampling units following a stratified random sampling design. Landsat and other high-resolution images available in Google Earth were used for this assessment.	No
Congo (Republic of the) †	2016	DEF DEG	No	0.5-ha 30% canopy cover	stratified area estimate	NFI for forests. Croplands carbon stocks (post-deforestation land-use) assumed to be zero Saatchi et al. (2011) above-ground density map used by the Party and assessment team to compare with the NFI estimates. Baccini et al. (2012) to compare rate of emissions	The approach followed to map deforestation used a combination of three products, including the GFC and two Landsat-based national maps (FACET, GAF). Polygons are identified as loss/deforestation if there is agreement between at least two of the three maps. The maps have different spatial resolutions (from 0.09, 0.36 and 1-ha) not compatible with the national definition but the combined map has segments with a minimum mapping unit of 0.5-ha. Collect Earth imagery: reference data to correct bias. GFC used to support some decisions regarding the choice of adjustment of the FRL	Yes. Global Forest Change (GFC) for AD-DEF and indirectly. Saatchi et al (2011) to compare AGB (AT). Baccini et al. (2012) to compare rate of emissions (Guyana approach).
Costa Rica †	2016	DEF ECS	Yes	1-ha 30% canopy cover	pixel-counting	NFI (partially complete) complemented with data published in the literature for non-forest classes and secondary forests.	AD were estimated by combining all land-use maps based on Landsat data (post-classification change detection). RapidEye and Google Earth imagery used to collect training sites and improve the maps, e.g. by removing shrubland, urban areas and eliminate improbable transitions in mangrove and palm forests. GFC dataset used to fill cloud gaps. The supporting report (Agregta, 2015; FCPF) describes how the global mosaics for 2000 ("first") and 2012 ("last") from GFC and a selection of RapidEye images were used to derive a tree cover index and non-parametric regression models to estimate tree cover for the entire country. The two tree cover maps were compared to derive a spatially explicit map of changes within the forest stratum (ECS)	Yes. Global Forest Change (GFC) for AD

Country	Technical Assess. year(s)	Activity	Non-CO <sub>2</sub> Gases	Forest definition Biophysical thresholds	AD method	Notes on Emission Factors (EFs), including satellite-based data sources	Notes on Activity Data (AD), including satellite-based data sources	Use of products derived from satellite data?
Cote d'Ivoire †	2017	DEF	No	0.1-ha 30% canopy cover	stratified area estimate	No NFI. DEF: plot data for Forests AGB (not representative of the whole country); post-deforestation carbon stocks assumed to be zero ECS: literature annual increment values for teak.	Mainly Landsat data complemented with one Sentinel-2 image to produce land cover maps for three years. Post-classification change detection. Google Earth imagery used for training the classifier.	No
Democratic Republic of the Congo †&	2018	DEF	No	0.5-ha 30% canopy cover	stratified area estimate	No NFI. AGB from harmonized plot data from pre-NFI testing sites in some provinces combined with other plot data from two other initiatives (JICA and WWF). A national AGB map based on airborne lidar was described in the annex and the average results compared with the FRL estimates, but it was not used in the FRL.	Landsat mosaics for three years (12,500 images) created in Google Earth Engine. Direct change detection using the same algorithm as the GFC product. Google Earth Engine also used to collect training data and Collect Earth for reference samples. Deforestation maps were overlapped with the Landsat mosaics to identify false changes. GFC used to understand the implications of selecting an operational tree cover threshold.	Yes. Global Forest Change (GFC) used indirectly to support decisions
Dominica †	*2022	SMF CCS ECS	Yes	1-ha 60% canopy cover	systematic sampling	AGB was obtained from the NFI from Saint Lucia (2009), as both islands share the same forest types and there is no recent Forest inventory	Collect Earth: national systematic grid of sample units were visually interpreted following a hierarchical key	No
Dominican Republic †	2020 2022	DEF DEG (inc. SMF, CCS) ECS	Yes. For DEG only	1-ha 30% canopy cover	systematic sampling	NFI for forest AGB, including for annual increments (ECS). AGB of other land uses (post-deforestation carbon stock) are IPCC defaults	Collect Earth: AD were collected through visual interpretation of sample units distributed over the country in a systematic grid. Fluxes from forest land remaining forest land are measured by changes in % canopy cover. E.g., DEG = transition from higher tree cover to lower tree cover while remaining above the % tree cover threshold of the definition of forest	No
Ecuador †	2015 *2020	DEF	No	1-ha 30% canopy cover	pixel-counting	NFI for forests. Post-deforestation carbon stocks assumed to be zero	Landsat imagery processed in SEPAL. Land Cover map with IPCC classes for the reference year and subsequent gross forest loss mapping for two periods. Plantations are separated and excluded from AD-DEF --- Assessment team of the 2015 submission compared deforestation estimates in the FREL with those obtained with the GFC product.	Yes. Global Forest Change (GFC) to compare results (1 <sup>st</sup> submission)
El Salvador †	2021	DEF DEG ECS	No	0.5-ha 30% canopy cover	systematic sampling	NFI for forest land. Post deforestation carbon stocks were estimated on the basis of the number of trees remaining on site and assuming forest cover correlates 1:1 with biomass. Same for DEG EFs, as well as RF for forest land remaining forest land. Default IPCC factors for conversion to forest (ECS).	Collect Earth: AD were collected through visual interpretation of sample units distributed over the country in a systematic grid in three points in time. A LIDAR image was used to check tree heights. Fluxes from forest land remaining forest land are measured by changes in % canopy cover. E.g., DEG = transition from higher tree cover to lower tree cover while remaining above the % tree cover threshold of the definition of forest	No
Equatorial Guinea †	2020	DEF DEG	No	1-ha 30% canopy cover	stratified area estimate	No NFI. IPCC defaults were used and the decision supported through comparison with independent estimates from Saatchi et al. (2011) biomass map, values reported by neighbouring countries and expert judgement	Segmentation of the GFC Landsat mosaics for mainland and Bioko, and mosaics of Landsat, ALOS, Sentinel-1 for island of Annobon. Classification of stable, deforested or degraded segments with support from GFC (see TAR, para 14). DEG was classified with visual inspection of tree cover loss in VHR images collected over selected segments. GFC also used to support the definition of forest including tree cover threshold (30%) and minimum area (1-ha). See page 19 of FRL. Collect Earth: visual interpretation of sample units following a stratified random sampling design. Reference dataset used to correct bias (upward adjustment of 74%) MODIS Burnt Area to justify omission of non-CO <sub>2</sub> emissions.	Yes. Global Forest Change (GFC) for AD (DEF and DEG) and indirectly to support decisions Saatchi et al. (2011) for comparison MODIS Burnt Area to justify omission of non-CO <sub>2</sub> emissions

Country	Technical Assess. year(s)	Activity	Non-CO <sub>2</sub> Gases	Forest definition Biophysical thresholds	AD method	Notes on Emission Factors (EFs), including satellite-based data sources	Notes on Activity Data (AD), including satellite-based data sources	Use of products derived from satellite data?
Ethiopia †,§	2016	DEF ECS (F>F)	No	0.5-ha 20% canopy cover	stratified area estimate	NFI (1st cycle) plot data following a stratified systematic sampling. To estimate emissions and removals from land converted to forest land, Ethiopia applied the removal of the full carbon stock in a single year.	Forest change (both gain and loss) is detected through supervised classification using Landsat imagery (direct change detection). Plantations are not separated. GFC used to collect training data. Points for loss and gains from the GFC were carefully assessed through visual interpretation of Landsat time series, vegetation indices and VHR imagery through the Collect Earth tool. GFC product also used to compare results and to identify an historical increase of emissions which could be used in the future to justify a trend approach instead of historical average.	Global Forest Change (GFC) as auxiliary data for AD and to compare results
Gabon †	2021	DEF DEG SMF CCS ECS (F>F)	No	1-ha 30% canopy cover	systematic sampling	The EFs were obtained from Gabon's national resource inventory, additional measurements and IPCC default values.	AD were extracted from a historical time series of land-use maps. Digitalization of the land-use /land cover segments in sampling units using Landsat, SPOT and Sentinel data. Collect Earth also used to support the classification	No
Ghana †	2017 *2021	DEF DEG ECS (F>F)	Yes	1-ha 15% canopy cover	systematic sampling -- Pixel-counting in the previous 2017 submission	Biomass data for BBEFORE and BAFTER were derived from a subnational project or the literature	Collect Earth: interpretation of sample points on a systematic grid across the country with different levels of intensification. This reference dataset is used for all activities included in the FRL and to identify burned areas. DEG and ECS are quantified by measuring tree canopy losses in the sample units by identifying tree cover loss within the thresholds for forest (i.e., transition from higher tree cover to lower tree cover while remaining above the % tree cover threshold of the definition of forest = DEG) -- MODIS Burned Area product (500 m spatial resolution) was used to map fires in the 2017 submission and combined with IPCC defaults to estimate non-CO <sub>2</sub> emissions from forest fires, i.e., for DEG only. In the 2021 submission, the product is not used anymore. Fire occurrences are identified in the samples by visual interpretation of active fires or fire scars. Due to the low temporal resolution of Google Earth imagery for burnt area mapping, underestimation of non-CO <sub>2</sub> emissions estimates is likely. Low confidence in the attribution of the AD method in the 2017 submission because Ghana states in the latest 2021 submission that the approach was stratified area estimate. It was not possible to confirm with the technical team if that was a mistake. Our classification as pixel-counting agrees with FAO (2020a)	Yes. MODIS Burned Area in the 2017 submission but abandoned in the most recent 2021 submission
Guatemala †	*2022	DEF DEG ECS	No	0.5-ha 30% canopy cover	systematic sampling	Map of carbon obtained by combining field plot data with bioclimatic strata from WorldClim. carbon estimate is extracted for each sampling unit for AGB of forest before conversion or degradation DEG: carbon stock losses estimated on the basis of % canopy remaining and assuming that forest cover correlates 1:1 with biomass	Collect Earth: interpretation of sample points on a systematic grid	No
Guinea-Bissau †,§	2019	DEF	No	0.5-ha 10% canopy cover	stratified area estimate	harmonized national and subnational forest inventories	Land cover maps classified using Landsat imagery. Post-classification change detection. Maps were manually corrected for classification errors through visual inspection of hot stops with expert judgement and VHR imagery from Google Earth. "The process revealed that many of the mapped change areas were in fact stable classes (either F to F or NF to NF). For example, 41% of the manually reclassified pixels corresponded to reclassifications from NF>F to NF>NF, and 33% from SA>NF to NF>NF. Many of these cases were identified as cashew plantations" (page 15) Collect Earth: reference dataset to correct bias	No

Country	Technical Assess. year(s)	Activity	Non-CO <sub>2</sub> Gases	Forest definition Biophysical thresholds	AD method	Notes on Emission Factors (EFs), including satellite-based data sources	Notes on Activity Data (AD), including satellite-based data sources	Use of products derived from satellite data?
Guyana †	2015	DEF DEG	No	1-ha 30% canopy cover	pixel-counting	C stocks from plot data installed in concession areas. Post-deforestation carbon stocks equal to zero.	DEF: Land cover maps classified using Landsat, Landsat and RapidEye, and full wall-to-wall coverage with RapidEye depending on the year. Post-classification change detection DEG: records on volume of timber extracted (including illegal logging).	Yes. Baccini et al. (2012) to obtain the average annual global forest carbon stock emissions % for the ref. period. Used to adjust the FRL
Honduras †	2017 2020	DEF DEG SMF CCS ECS (F>F)	No	1-ha 10% canopy cover (although for mapping deforestation the 30% threshold was used)	pixel-counting	NFI. Carbon change map produced for two points in time to assess DEG. Not very transparent in the submission.	Landsat mosaics. VHR imagery and NFI as training data for all classes (including degradation and enhancement). Classification of mosaics using the Random Forest algorithm. Manual edition of classification errors Google Earth images for validation. -- In the 2017 FRL GFC was used in the quality control phase to help improve the map classification.	Yes. In the first FRL (2017) Global Forest Change (GFC) as auxiliary data.
India §	2018	SMF	No	1-ha 10% canopy cover	pixel-counting	NFI and complemented by a separate inventory on smaller trees (<10cm dbh).	AD based on wall-to-wall mapping using IRS-LISS-3 satellite data. Classification according to the density of forest cover using the NDVI Index in three time points. Accuracy assessed with sample plots from the NFI and VHR imagery. Information on plantations from national records.	No
Indonesia §	2016 *2022	DEF DEG ECS (F>F)	Yes	0.25-ha 30% canopy cover  (Official definition. Indonesia defines a working definition too with minimum area = 6.25-ha)	pixel-counting	NFI permanent plots complemented with temporary plots and basal area for mangroves. GFC for stratification to support the selection of carbon stocks of non-forest classes (shrub, agriculture and transmigration) obtained from the literature and research groups. The combination between % canopy cover and carbon stock was used to determine weighting score for each category. Parameters to estimate peat fire emissions from the literature.	Landsat: wall-to-wall land cover maps digitised manually for each monitoring year. Plantations and oil palm excluded. Burn areas visually interpreted using Landsat and Sentinel 2A and 2B, and validated using MODIS and NOAA hotspot, ground truthing data and burn area model based on normalized burnt ratio. Map of peatland distribution was already available and was based on high-resolution imagery and soil survey data. GFC used for comparison (GLAD) and to enhance confidence in the national maps (in the study of Margono et al, 2014)	Yes. Global Forest Change (GFC) indirectly, for stratification of NFI plots and to compare results. MODIS and NOAA Active Fire products to support and validate the classification of burnt areas for non-CO <sub>2</sub> emissions.
Kenya ‡	2020	DEF DEG SMF ECS	No	0.5-ha 15% canopy cover	pixel-counting	No NFI. Data from pilot forest inventories. Post-deforestation carbon stocks (BAFTER) assumed to be zero and stocks from land-use following deforestation from IPCC defaults. Growth rates for ECS also IPCC defaults.	Landsat: 5 land cover maps produced using a semi-automated method and stratified into ecozones and % tree cover classes Training and validation data included ground surveys complemented by Google Earth imagery.	No.
Lao People's Democratic Republic §&	2018	DEF DEG ECS	No	0.5-ha 20% canopy cover	stratified area estimate	NFI (2nd cycle) and default parameters from IPCC 2006. ECF: zero annual increment from forest growth was assumed because using the IPCC default would result in overestimation.	SPOT and RapidEye for wall-to-wall mapping (object-based classification). Forest type map for a reference year and direct change detection for the following periods. Collect Earth: visual interpretation of sample units. Reference dataset used to correct bias. GFC used for map correction related with shifting agriculture and fallow. Mature forests where vegetation loss was confirmed in the past one to eight years with GFC loss product, were revised to secondary forests. Low confidence in the attribution of method to derive AD. FAO (2020) classifies as pixel-counting. Not clearly stated in the FRL and TAR, however, the tables in Annex 1 after stratified area estimate (Table 18-21 in the FRL) are the final AD estimates for the FRL shown in Table 11 and 12 (see FRL submission)	Yes. Global Forest Change (GFC) as auxiliary data
Liberia ‡.&	2020	DEF DEG	No	1-ha 30% canopy cover	stratified area estimate	NFI. Values are above the upper threshold of defaults IPCC (2006).	GFC (Hansen et al. 2013) tree cover and tree cover loss layers were combined with additional national data layers depicting agricultural extents. Collect Earth: The sample was stratified using the available classes from the map Stratified Area Estimation approach. Not clear in the submission if the map area estimates for all strata (stable forest, stable non-forest, deforestation from intact and secondary forest, DEG and ECS) were used, and the bias corrected with the sample. Low confidence in the attribution of stratified area estimate based on the submission but confirmed in personal communication with the technical team	Yes. Global Forest Change (GFC) for AD

Country	Technical Assess. year(s)	Activity	Non-CO <sub>2</sub> Gases	Forest definition Biophysical thresholds	AD method	Notes on Emission Factors (EFs), including satellite-based data sources	Notes on Activity Data (AD), including satellite-based data sources	Use of products derived from satellite data?
Madagascar <sup>±, &amp;</sup>	2017 2018	DEF	Yes	1-ha 30% canopy cover	stratified area estimate -- Pixel-counting in the previous 2017 submission	Harmonized data from and old NFI, subnational inventories and a study on mangroves. Post-deforestation carbon stocks were obtained from the literature.	Fusion of data to create a deforestation map of four forest types: 1) a historical time series of Landsat satellite imagery to produce forest type maps. Post-classification change detection to map forest loss; 2) forest loss from GFC. Collect Earth: visual interpretation of sample units following a stratified sampling design to adjust the AD estimates. -- In the 2017 submission (pixel-based approach) the GFC product was also used to complement the national map in areas of cloud coverage and to select hotspots for validation	Yes. Global Forest Change (GFC) for AD (in a pixel-counting approach in 2017, and stratified area estimate in 2018) Also indirectly in 2017 for validation.
Malawi <sup>±, &amp;</sup>	2020	DEF DEG ECS	No	0.5-ha 10% canopy cover	systematic sampling	harmonized plot measurements from the NFI The carbon stocks after conversion were estimated under the assumption that all land that was deforested was converted to grassland	Collect Earth: interpretation of sample points on a systematic grid. Simple random sampling approach, without stratification (DEF, and ECS) Wisdom model for DEG (fuelwood harvest)	No
Malaysia <sup>§</sup>	2015 2018 2019	DEF SMF CCS	Yes	0.5-ha 30% canopy cover	pixel-counting	NFI data for gross tree growth rates, default biomass conversion and expansion factor (IPCC 2006) and information from literature for growth rates of specific forest types.	The total forest area was obtained from gazette notification and geospatial maps, which were developed by the forestry department through analysis of satellite images. SPOT imagery used biennially to update the geospatial maps. The reported area damaged by fire is very small (source of data not clear in the FRL) In the 2015 submission only national statistics were used, no satellite data and no AD methods as defined in this study. Satellite data (Landsat) was used for validation	No
Mexico <sup>†</sup>	2015 2020	DEF DEG	No	1-ha 10% canopy cover	stratified systematic sampling -- Pixel-counting in the previous 2015 submission	NFI for forests before conversion (mainly from the 2nd cycle). Post-disturbance carbon stock of remaining woody vegetation also from the NFI and zero assumed when no NFI information exists --	Collect Earth: interpretation of sample points on a systematic grid with different intensification according to forest type (stratified). For each sample, if there is a total loss of canopy cover but there is no evidence of conversion to other land-use, that sample unit is classified as DEG -- Previous submission (2015) used a pixel-counting approach and relied on SPOT and Landsat imagery. The second FRL is considerably lower than that of the first FRL (20,339,240 versus 44,388,620 t CO <sub>2</sub> eq/year)	No
Mongolia <sup>§</sup>	2018	DEF DEG ECS (F>F)	No	1-ha 10% canopy cover	stratified systematic sampling	data from NFI plots aligned with the AD samples for only one forest class	Collect Earth: interpretation of sample points on a systematic grid with different intensification according to the forest type (stratified, boreal forests and other) The optimal size of the sampling grid was determined with support from the GFC product	Yes. Global Forest Change (GFC) to support decisions
Mozambique <sup>±, &amp;</sup>	2018	DEF	No	1-ha 30% canopy cover	systematic sampling	NFI for forests. No post-deforestation emissions or removals were considered (i.e., 100% instant oxidation) IPCC (2006) default values for the post-deforestation carbon stocks for conversion to cropland and grassland, while a complete loss of carbon stock was assumed for other land-use conversions.	Collect Earth: interpretation of sample points on a systematic grid. Each point from the internal grid has a weight coverage of 4%. The FRL submission compares results to those obtained in the REDD+ strategy (study from CEAGRE and Winrock international) producing independent estimates using global datasets to derive AD (GFC) and EF (Saatchi et al). Information not directly in the FRL, found in the REDD+ strategy	Yes. Global Forest Change (GFC) and Saatchi et al. (2011) to compare results
Myanmar <sup>§, &amp;</sup>	2018	DEF ECS (F>F)	No	0.5-ha 10% canopy cover	stratified area estimate	NFI data but only for pre-deforestation carbon stocks and only for a few districts with protected status ECS: default values for biomass consumption for all savannah grasslands (IPCC 2003) and biomass increment (IPCC 2006)	Collect Earth: interpretation of stratified random samples based on the stratification obtained from GFC maps adjusted for the national forest definition. Two options to estimate AD were tested: a) modified GFC loss map corrected for bias with the reference sample (176,680 hayr-1); and b) Sample-based estimates with confidence intervals (428,984 ha/yr). ECS: database on the area of forest plantations maintained by the forest department. Low confidence in the attribution of AD method. FAO (2020a) identifies the method as stratified area estimate, also confirmed by personal communication and from	Yes. Global Forest Change (GFC) to support decisions

Country	Technical Assess. year(s)	Activity	Non-CO <sub>2</sub> Gases	Forest definition Biophysical thresholds	AD method	Notes on Emission Factors (EFs), including satellite-based data sources	Notes on Activity Data (AD), including satellite-based data sources	Use of products derived from satellite data?
							page 47: "The stratified area estimate of annual deforestation is estimated with 428,984 ha per year during 2005-2015" Not entirely clear only because Table 7.5 in the submission shows two options to estimate AD: a) GFC Map (modified), or bias-corrected, area = 1766799 ha for the 10 years of the reference period = 176,680 ha/yr; and b) Sample-based estimates = 4289839 ha = 428,984 ha/yr. The reader would assume the approach selected was simple sampling and not stratified area estimate.	
Nepal §&	2017	DEF DEG ECS (F>F)	No	0.5-ha 10% canopy cover	stratified area estimate	NFI permanent sample plots	Landsat mainly and ASTER, SRTM-DEM and RapidEye used as ancillary data. Object-based multi-resolution segmentation image analysis (e-Cognition). Collect Earth: reference dataset for stratified area estimate. GFC used to compare results magnitude DEG: Land cover maps based on RapidEye and Forest Type map were used as input to WISDOM to model fuelwood harvesting	Yes. Global Forest Change (GFC) to compare results
Nicaragua †	2019	DEF DEG ECS (F>F)	No	1-ha 30% canopy cover	systematic sampling	NFI. A linear regression model was developed to estimate average carbon stock of NFI plots with canopy cover classes visually interpreted for AD. The model demonstrated the relationship between canopy cover and above-ground biomass carbon stock as measured in the NFI, which was applied to obtain biomass carbon stocks ECS: Forest growth rates from national studies using sampling plots	Collect Earth: interpretation of sample points on a systematic grid	No
Nigeria †	2018, 2019	DEF	No	0.5-ha 15% canopy cover	stratified area estimate	NFI. No information on post-deforestation carbon stocks and AGB of non-forest classes	Collect Earth: visual interpretation of sampling units. The reference dataset was collected following a probability based stratified random sampling design. GFC product adjusted to national definitions was used to obtain a 3-class map with stable forest, stable non-forest and deforestation. AD DEF the GFC-derived map used for stratification and the final estimates correspond to the areas in the map corrected with the reference dataset (same in the first 2018 submission). Information obtained through personal communication with the technical team and FAO. The modified FRL (page 31) reads the opposite and hence is not transparent: "The Nigeria map was created from Landsats 7 and 8, 30-metre resolution imagery using the following three classes: stable forest, stable non-forest, forest loss based on the GFC map with a tree cover threshold of 15% and a loss period from 2006-2016. The activity data (AD) is however derived from the reference data, the map is only used for stratification and the final estimates do not correspond to the areas in the map." GFC used to justify the omission of DEG (2019 TAR, para 14) - pixel-counting as a preliminary indicator of the magnitude of degradation at the national scale.	Yes. Global Forest Change (GFC) for AD DEF and to justify omission of DEG.
Pakistan §	2020	DEF	No	0.5-ha 10% canopy cover	sampling	Pilot NFI complemented by subnational inventory plot data. Post-deforestation carbon stocks also from NFI plots measured in non-forest plots with woody vegetation and AGB of post-deforestation land uses assumed to be zero	Landsat for wall-to-wall land-cover mapping in three points in time. Post-classification change detection and the resulting change maps used for stratification Collect Earth: visual interpretation of sampling units over a stratified systematic grid complemented with random units over deforestation hotspots Low confidence in the attribution of AD method. The FRL and TAR are not clear. FAO (2020a) identifies as bias-correction but from personal communication with FAO team, it was clarified as sampling given the areas of the map were not used to derive AD	No
Panama †	2018 2022	DEF DEG SMF CCS	Yes	0.5-ha 30% canopy cover	stratified sampling --	NFI (complete in the 2022 FRL for all forest types)	Collect Earth: visual interpretation of sampling units in a "Mapathon" exercise. The reference dataset was collected following a stratified random sampling design using four strata (stable forests, mangroves, areas of land-use change and other land) and post-stratification according to three climate regions. (systematic design	No

Country	Technical Assess. year(s)	Activity	Non-CO <sub>2</sub> Gases	Forest definition Biophysical thresholds	AD method	Notes on Emission Factors (EFs), including satellite-based data sources	Notes on Activity Data (AD), including satellite-based data sources	Use of products derived from satellite data?
		ECS			systematic sampling (2018)	ECS: assumed the complete stock secondary forests is available immediately after conversion	in the 2018 submission). Existing maps were used for stratification. DEG: Fire occurrences and fuelwood from regional tabular records.	
Papua New Guinea §	2017	DEF DEG ECS (F>F)	No	1-ha 10% canopy cover	systematic sampling	DEF: research study and IPCC defaults depending on the ecological zone. Post-deforestation growth from IPCC defaults DEG: assumption that carbon stock of degraded forests = 65.5% of those in the primary forests.	Collect Earth: interpretation of sample points on a systematic grid with different intensifications Comparison of results obtained by the sampling method used for the FRL and a wall-to-wall map produced for 2015 using the TerraAmazon software (Landsat imagery) with an agreement of 89%	No
Paraguay †	2016 *2022	DEF	No	1-ha 30% canopy cover	stratified area estimate	NFI	Landsat. Supervised classification of a time series. Segmentation with direct change detection. Landsat mosaics and VHR imagery used in ArcGis and Qgis to interpret a reference dataset for stratified area estimate of the estimates	No
Peru †	2016 2021	DEF	No	0.5-ha 30% canopy cover	stratified systematic sampling -- pixel-counting (2016)	plot data from the ongoing NFI complemented by plot data from research studies (e.g. ForestPlots.net)	Collect Earth: visual interpretation of sampling units selected randomly in a systematic grid. Landsat mosaics were used for the deforestation map used to stratify the sample (ex-post). Stratification based on ecozones, deforestation and buffer around deforestation	No
Saint Lucia †	2021	DEF DEG CCS ECS	Yes	1-ha 60% canopy cover	systematic sampling	EFs were obtained from the NFI carried out in 2009 and the FAO GSOCmap, and complemented by IPCC default values of the 2006 IPCC Guidelines, 2013 IPCC Wetlands supplement and 2019 Refinement to the 2006 IPCC Guidelines	Collect Earth: interpretation of sample points on a systematic grid. Land based approach using IPCC categories The information on wood removals was derived from the Collect Earth assessment as % tree cover loss instead of volume loss. Losses due to Hurricanes, Fires, Logging and Shifting Cultivation, specifically on Forest lands were also identified Ground truthing to validate the findings from the Collect Earth exercise	No
Solomon Islands §&	2019	DEF DEG ECS (F>F)	No	1-ha 10% canopy cover	systematic sampling	No NFI. EFs obtained from IPCC defaults (DEF) and country-specific data from Papua New Guinea (assumption that carbon stocks in degraded forests are 65.5 per cent of those in the primary forests)	Collect Earth: interpretation of sample points on a systematic grid. GFC data used to assess tree cover loss and support the identification of the sample units. Re-assessment of all plots where Hansen data shows a tree cover loss >10 ha within a surrounding area of 100 ha but neither deforestation nor forest degradation was recorded by Collect Earth assessment. All the plots were re-assessed where deforestation or forest degradation was recorded in Collect Earth but the GFC showed a tree cover loss < 5 ha within 100 ha around the plot. Page 21. In most cases the differences between Collect Earth data and Hansen data occurred due to the lack of detail in the land cover interpretation in the Hansen data. For instance, harvesting and replanting of oil palm plantations is reported as tree cover loss and gain in Hansen data but in Collect Earth assessment, this is considered cropland remaining cropland.	Yes. Global Forest Change (GFC) for AD
Sri Lanka §	2017	DEF ECS (F>F)	No	0.5-ha 10% canopy cover	stratified area estimate	No NFI. Use of IPCC defaults	The GFC tree cover map and a national forest map were combined to adapt the GFC to national definitions (e.g. exclude agriculture and agroforestry lands). The estimates from the GFC loss dataset adapted to national definitions were corrected using a reference dataset compiled in Collect Earth through visual interpretation of sample units. The distribution of the reference data points follows a stratified random sampling. Sri Lanka also used the GFC gain layer to include ECS but during the technical assessment, it was noted that, because the existing methodology cannot clearly identify horticultural, rubber and coconut plantations, the area under reforestation could be overestimated owing to the possible inclusion of such areas, which are not included in the forest definition. Sri Lanka listed the use of high-resolution satellite imagery instead of the mid-resolution imagery available from the GFC product for preliminary change assessment as a potential future improvement.	Yes. Global Forest Change (GFC) for AD

Country	Technical Assess. year(s)	Activity	Non-CO <sub>2</sub> Gases	Forest definition Biophysical thresholds	AD method	Notes on Emission Factors (EFs), including satellite-based data sources	Notes on Activity Data (AD), including satellite-based data sources	Use of products derived from satellite data?
Sudan <sup>‡, &amp;</sup>	2020	DEF ECS (F>F)	No	0.4-ha 30% canopy cover	stratified area estimate	NFI for DEF, IPCC defaults for ECS The NFI stratified sampling design used a combination of maps, including CGIAR-CSI and Africover2000, to stratify forests and select number of plots per stratum (assumed domestic EO product). Assumptions: Carbon stocks after forest conversion to other land uses were zero; for ECS the annual decrease in carbon stocks from harvesting, fuelwood and disturbances on land converted to forest was zero.	Landsat for 2010, 2014, 2018; Aster for 2006. Object based analysis approach using segmentation (eCognition). The polygons were visually interpreted Collect Earth: reference dataset for stratified area estimate following a systematic sampling design with different intensifications according to strata (vegetation density). The Sudan used records of planted areas to establish AD for ECS instead of data from the land-cover.	No.
Suriname <sup>†</sup>	2018 2021	DEF DEG	Yes	1-ha 30% canopy cover	stratified area estimate	No NFI. DEF: Harmonization of plot data from different inventories and additional plots measured for mangroves. DEG: average from same plots and literature values for shifting cultivation.	Landsat imagery. Forest Non-Forest wall to wall maps. Post classification change detection. Sentinel-2A imagery was used from 2017 onwards. Unbiased area estimates produced using a stratified random sampling approach with visual inspection of sample units in Landsat and Sentinel images (using SEPAL). Fire AD from post-deforestation LULC maps. DEF: includes shifting cultivation converted to non-forest area although emissions from the use of fire are excluded. DEG: Conversions to shifting agriculture measured through tree cover losses also combined with fire occurrences for non-CO <sub>2</sub> emissions; harvest through tabular recordings on extracted volume, and same for fuelwood. Illegal logging is not included. Low confidence in the attribution of AD method. The error matrices are not available and it is not clear how the values in the FRL (Table 2) and TAR are obtained. From the table caption 'the stratified estimated areas will be used in further we assumed 'stratified area estimates' (same as FAO, 2020a).	No
Tanzania (Republic of) <sup>‡, &amp;</sup>	2017	DEF	No	0.5-ha 10% canopy cover	pixel-counting	NFI (from two comprehensive inventory initiatives), including post-disturbance carbon stock of remaining woody vegetation.	Landsat for mainland and ortho-photographs and RapidEye images for Zanzibar Islands. Training data collected from Landsat (layer stacked bi-temporal) and the GFC to map deforestation, stable forest, wetland, water and other non-forest classes. Classification of the bi-temporal stacked scenes was carried out using the Random forests algorithm (direct change detection).	Yes. Global Forest Change (GFC) as auxiliary data
Thailand <sup>§</sup>	2021	DEF DEG ECS	No	0.5-ha 10% canopy cover	stratified area estimate	NFI (cycle 1 and 3) complemented by plot data on mangroves. The emission and removal factors were calculated as the difference between the carbon stock of the NFI cycle 1 and 3 divided by the time period between the two inventories. The IPCC default carbon stock of annual crop was chosen as the carbon stock for non-forest.	Landsat imagery combined in best pixel mosaics for two time points. Forest areas were visually interpreted and manually digitized through inspection of Landsat, high-resolution images from Google Earth, and national auxiliary data sets. Unbiased area estimates produced using a stratified random sampling approach with visual inspection of sample units in Collect Earth. DEG was not mapped; instead, emissions were calculated using NFI data from two cycles	No
Togo <sup>‡, &amp;</sup>	2020	DEF ECS (F>F)	No	0.5-ha 10% canopy cover  operational definitions: >30% tree cover are included	pixel-counting	Worldclim and Landsat data for 2018 calibrated with field data to generate a biomass map. RapidEye images and orthophotomaps used to support the NFI by classifying the sample unit prior to the field measurements. Global Forest Watch portal used for comparison.	Wall to wall mapping using Landsat imagery. F/NF maps produced for 4 time points. Post-classification change detection. Google Earth data and Landsat used for training for validation of the F/NF maps. Bias-corrected areas were also derived but chosen not to be used. The reference dataset was used for validation of the maps only. Global Forest Watch portal used for comparison in the introduction section only.	Yes. Global Forest Watch portal / Global Forest Change (GFC) used to compare results
Uganda <sup>‡, &amp;</sup>	2017	DEF	No	1-ha 30% canopy cover	stratified area estimate	No NFI. Harmonization of field plots from different sources, including exploratory inventories with permanent plots, and planting statistics. The forest average carbon stock was calculated using an area weighted mean with area proportions from the land cover maps.	Land cover maps for 5 years classified using SPOT and Landsat. One of the maps used a Landsat mosaic to produce a F/NF mask. Training data from land cover maps from the two closer periods and from the GFC dataset. The F/NF mask was combined with the Africover 2000 land cover map (assumed domestic EO product). Unbiased area estimates produced using a stratified random sampling approach with visual inspection of sample units in Collect Earth. GFC for comparison.	Yes. Global Forest Change (GFC) as auxiliary data and to compare results.

Country	Technical Assess. year(s)	Activity	Non-CO <sub>2</sub> Gases	Forest definition Biophysical thresholds	AD method	Notes on Emission Factors (EFs), including satellite-based data sources	Notes on Activity Data (AD), including satellite-based data sources	Use of products derived from satellite data?
Viet Nam §	2016	DEF DEG ECS	No	0.5-ha 10% canopy cover  (includes timber forest plantations)	pixel-counting	NFI (cycles I to IV). EF/RF matrices for each combination of classes. Assuming all NF classes (including cropland) with 0 carbon stock	SPOT and Landsat to produce land cover maps for 4 years. Google Earth Engine tool was applied to mosaic Landsat images. Object-based interpretation (using the software eCognition) for automated segmentation was used as well as a process (decision tree) to correct illogical changes. Post-classification change detection between pairs of land cover maps. Accuracy assessment through observation of sample points over Landsat imagery using Collect Earth	No
Zambia †,‡	2016 2021	DEF DEG	No	0.5-ha 10% canopy cover	systematic sampling -- Stratified area estimate (2016)	NFI (two cycles) for DEF and DEG (classes of canopy coverage). Carbon stock of non-forest classes also available from the NFI -- The 2016 submission included a spatially explicit carbon map with carbon density classes derived from plot data and optical and Radar (ALOS) data	Collect Earth: interpretation of sample points using a random systematic sampling approach with different intensifications of the grid. DEG: reduction in tree cover in forest land remaining forest land of an intact forest by at least two tree canopy cover predetermined classes. As QC, random samples or samples flagged as low confidence should be compared with other datasets from a list. -- The 2016 submission used wall-to-wall maps based on Landsat using GFC aggregated at 5x5 pixel blocks to create an initial point training dataset for stable forest, non-forest and deforestation (stratifier). The Assessment team (AT) of the 2016 FRL submission compared results with Global Forest Watch	Yes. Auxiliary data in 2021. A list of available products is included in the quality control protocol to assist in the interpretation of samples for AD. -- In the 2016 submission, Global Forest Change (GFC) is used as auxiliary data and for comparing results (AT)

†Latin American and the Caribbean States; ‡African States; §Asian and the Pacific States; ¶Least Developed Countries

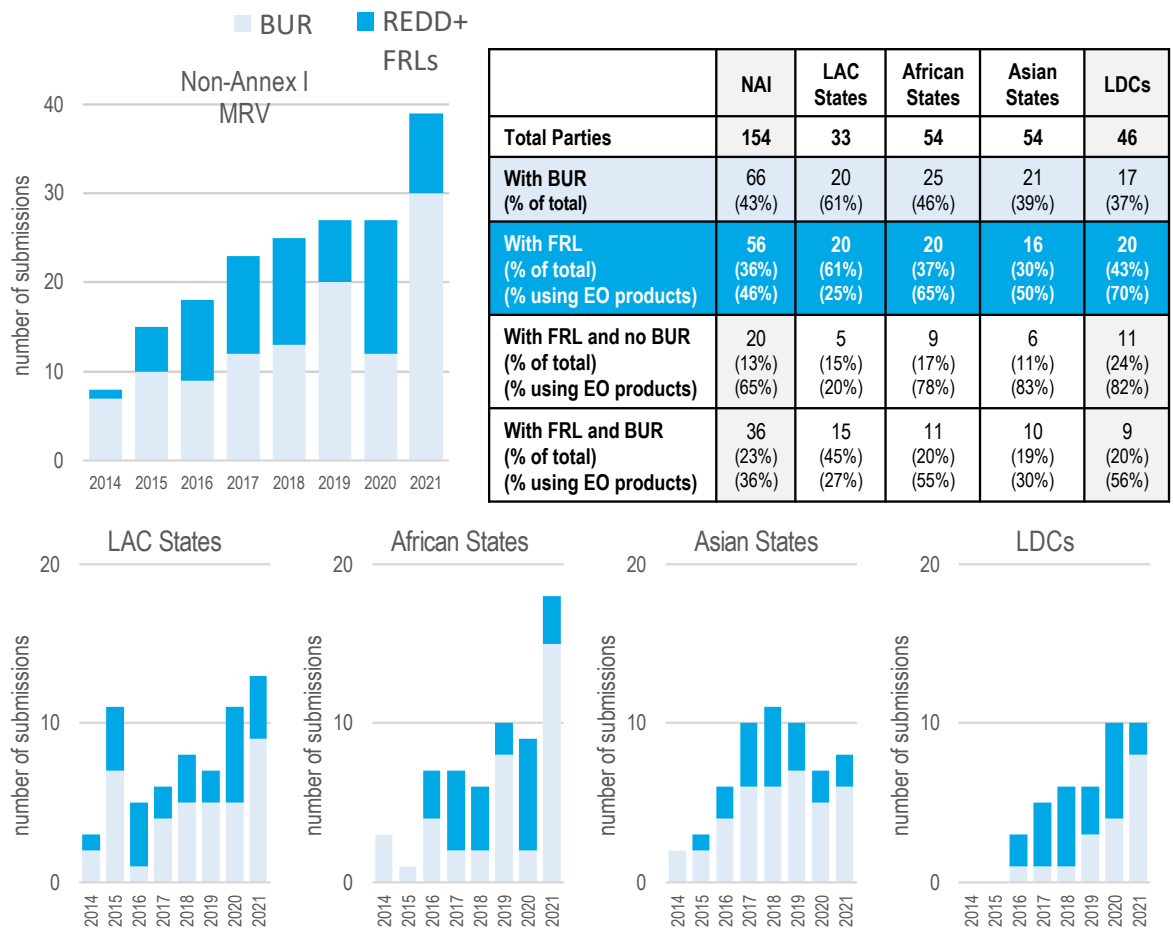


**Figure A.1.1.** Indicators of Measurement, Reporting and Verification (MRV) capacity and contribution of EO products (in percentage of countries with FRL submissions). Number of submissions of GHG fluxes in biennial update reports (BUR) and REDD+ forest reference emission levels / forest reference levels (FRLs) from non-Annex I (NAI) country-Parties to the UNFCCC up to 2021 (for BURs) or 2022 (for REDD+ FRLs). Includes NAI Parties from the Latin American and Caribbean (LAC) States, African States, Asian States, and Least Developed Countries. Adapted and expanded from Federici et al (2017) using information available in the UNFCCC web portal for BUR submissions (<https://unfccc.int/BURs>) and REDD+ FRLs information, including on the use of EO products, compiled for this study. Except for LAC States, the main contribution of EO products is for country Parties which have never submitted a BUR but have submitted a FRL. The bar charts show the timeline with BUR and FRL submitted every year since 2014. Note that the number of submissions in the bar charts is larger than number of countries in the table with absolute number in 2014-2021 (or 2014-2022 for FRLs) because while some Parties have never submitted a BUR, others have submitted four.

**Table A.1.3.** List of the 56 developing countries that have submitted at least one Forest Reference Level / Forest Reference Emission Level (FRL/FREL) to the UNFCCC between 2014 and 2022, listed alphabetically and identified by Regional group and Least Developed Country († Latin American and the Caribbean States; ‡ African States; § Asian and the Pacific States; & Least Developed Countries). For each country Party, it is identified if the FRL/FREL uses satellite-based global maps (or EO products) in its construction or verification, and if, when, and how many Biennial Update Reports (BUR) were submitted to the UNFCCC. The dates of submission indicate if the FRL/FREL was submitted before or after the BUR including a national GHG inventory.

Party	BUR1	total BURs	FRL year	EO products in FRL?
Argentina †	2015	4	2019	-
Bangladesh §&	-	0	2019	-
Belize †	2021	1	2020	-
Bhutan §&	-	0	2020	yes
Brazil †	2014	4	2014, 2017, 2018	-
Burkina Faso ‡&	2021	1	2020	-
Cambodia §&	2020	1	2021	-
Chile †	2015	4	2016	yes
Colombia †	2015	3	2015, 2020	-
Congo ‡	-	0	2016	yes
Costa Rica †	2015	2	2016	yes
Cote d'Ivoire ‡	2018	1	2017	-
DRC ‡&	-	0	2018	yes
Dominica †	-	0	2022	-
Dominican Republ. †	2020	1	2020, 2022	-
Ecuador †	2017	1	2015, 2020	yes
El Salvador †	2018	1	2021	-
Equatorial Guinea ‡	-	0	2020	yes
Ethiopia ‡&	-	0	2016	yes
Gabon ‡	2021	1	2021	-
Ghana ‡	2015	3	2017, 2021	yes
Guatemala †	-	0	2022	-
Guinea-Bissau ‡&	2020	1	2019	-
Guyana †	-	0	2015	yes
Honduras †	2020	1	2017, 2020	yes
India §	2016	3	2018	-
Indonesia §	2016	3	2016, 2022	yes
Kenya ‡	-	0	2020	-
Lao §&	2020	1	2018	yes
Liberia ‡&	2021	1	2020	yes
Madagascar ‡&	-	0	2017, 2018	yes
Malawi ‡&	2021	1	2020	-
Malaysia §	2016	3	2015, 2018, 2019	-
Mexico †	2015	3	2015, 2020	-
Mongolia §	2017	1	2018	yes
Mozambique ‡&	-	0	2018	yes
Myanmar §&	-	0	2018	yes
Nepal §&	-	0	2017	yes
Nicaragua †	-	0	2019	-
Nigeria ‡	2018	2	2019	yes
Pakistan §	2022	1	2020	-
Panama †	2018	2	2019	-
Papua New Guinea §	2019	2	2017	-
Paraguay †	2015	3	2018, 2022	-
Peru †	2014	2	2016, 2021	-
Saint Lucia †	2021	1	2021	-
Solomon Islands §&	-	0	2019	yes
Sri Lanka §	-	0	2017	yes
Sudan ‡&	-	0	2020	-
Suriname †	-	0	2018, 2021	-
Tanzania ‡&	-	0	2017	yes
Thailand §	2015	3	2021	-
Togo ‡&	2017	2	2020	yes
Uganda ‡&	2019	1	2017	yes
Viet Nam §	2014	3	2016	-
Zambia ‡&	2020	1	2016, 2021	yes

† Latin American and the Caribbean States; ‡ African States; § Asian and the Pacific States; & Least Developed Countries

## Appendix 2

### National deforestation and above-ground biomass data

#### Description of existing *National* data

Land-cover maps produced and above-ground biomass (AGB) data collected under the CARBOVEG-GB nation-wide project and a subsequent project in three protected areas (IBAP 2015, Vasconcelos et al. 2015) were used for this analysis and are referred throughout this study as *National* data. More detailed information on the production of land-cover maps, as well as field protocol and plot location is described in (Vasconcelos et al., 2015).

Under these projects, Landsat TM and ETM+ images covering the entire territory of Guinea-Bissau during the late dry season in 2007 and 2010 were processed and used to discriminate four forest classes using supervised classification algorithms. The four homogeneous sub-classes of forest (Closed-Forest, Open-Forest, Savanna-Woodland and Mangrove) were aggregated into Terrestrial Forests and Mangrove to improve overall accuracy from 69% and 96%.

Tree AGB data was also collected under these projects at the plot level. A 250 x 250 meter stratified systematic sampling grid was created covering the entire national territory and used as a basis for plot location. In each location (randomly selected over the grid) a circular nested plot (4, 14, and 20 m concentric sub-plots) was installed following the measurement methodology described in (Pearson, 2005). The sampling design was stratified by forest class (Closed-Forest, Open-Forest, Savanna-Woodland and Mangrove) and a total of 492 plots were measured between 2007 and 2012. Several tree parameters were recorded, including diameter at breast height (DBH), height (h) and individuals identified at the species level. For some species where no wood density values were found in the literature, wood samples were also collected to estimate their specific wood density.

#### Carbon assessment of *in-situ* data

For this study, an exhaustive process of quality control of the data led to the exclusion of plots without coordinates, plots where heights of trees were not measured, or plots with other missing information. From the entire dataset a total of 309 plots were used with 49 plots measured in Closed-Forests, 120 in Open-Forests, 70 in Savanna-Woodlands, and 70 in Mangroves. These data were compiled and analysed here to

estimate carbon densities ( $\text{Mg ha}^{-1}$ ) per forest class and total forest. For that, three different equations for estimation of AGB were selected (**Table A.2.1**). To estimate AGB of terrestrial forests we used the pantropical model proposed by Chave et al. (2014) requiring information on tree DBH, height (H) and wood density ( $\rho$ ). For mangrove species, the Chave et al. (2005) common allometric equation for mangroves requiring only two parameters (DBH and  $\rho$ ) was proposed due to the advantage of having used a bigger sample ( $n=84$ ) for its construction, and having more similar DBH classes than other species specific models available. No palm biomass equations were found that were specific to Guinea-Bissau, the West Africa region or even the tropics as a whole. Therefore, we selected the example allometric equation from the IPCC Good Practice Guidance (GPG) for LULUCF (IPCC 2003; Table 4A.2, GPG-LULUCF) for estimating AGB of palm trees relying only on height measurements as key predictor for AGB. For both terrestrial forest and mangrove species where specific wood density was required, values from a national database were used. This database includes values from literature revision (when available) and values calculated from tree wood samples collected and analyzed under the CARBOVEG-GB project. When the species was not known or wood density values were not published/available, an average wood density was calculated from the data collected under CARBOVEG-GB ( $\rho=0.731 \text{ g cm}^{-3}$ ). AGB data obtained at plot level was extrapolated to the area of 1-ha ( $10,000 \text{ m}^2$ ) by calculating the proportion that is occupied by a given plot using a dimensional scaling factor (e), defined by the equation  $e = (10,000/\pi \cdot r^2)$ , where r is the plot radius in meters (Pearson et al. 2005). Resulting AGB estimates are shown for the sampled forest sub-classes (Closed-Forests, Open-Forests, Savanna-Woodlands and Mangroves) and for the total forest as the weighted average of the AGB density in all forest classes (**Table A.2.2**).

**Table A.2.1** Allometric equations used to estimate above-ground biomass of terrestrial forest species, mangroves species, and palm trees; diameter at breast height (1.3 m; DBH), height (H), wood density ( $\rho$ )

Equation	Strata	Source
$0.0673 \times (\rho \times \text{DBH}^2 \times H)^{0.976}$	Terrestrial Forest	Chave et al. (2014)
$0.168 \times \rho \times \text{DBH}^{2.47}$	Mangrove	Chave et al. (2005)
$6.666 + 12.826 \times H^{0.5} \times \ln H$	Palm	IPCC (2003) (Table 4.A.2, GPG-LULUCF)

**Table A.2.2** In-situ mean AGB density ( $\text{Mg ha}^{-1}$ ) per forest sub-class Closed-Forests (CF), Open-Forests (OF), Savanna-Woodlands (SW), Mangroves (M), and area-weighted average for total forest. Margin of error (MoE, 95% confidence) included as measure of spread. The area-weighted average AGB density is used as National emission factor after conversion from  $\text{t ha}^{-1}$  to  $\text{CO}_2 \text{ ha}^{-1}$ .

Strata	Number of plots	AGB density ( $\text{t ha}^{-1}$ )	Standard deviation	MoE (95% CI)	Error (as % of mean)
Closed-Forests	49	180.5	122.5	34.7	19
Open-Forests	120	86.3	38.7	11.3	20
Savanna-Woodlands	70	53.2	62.7	12.2	13
Mangroves	70	45.6	51.9	9.1	23
Total area-weighted	309	62.8	54.3	6.1	10

## Remote sensing datasets and methods to derive deforestation and associated emissions

### Global forest cover datasets to derive deforestation

Available global datasets were used to derive deforestation. Firstly, the University of Maryland Global Forest Change (GFC) 30-m resolution dataset based on a time-series of Landsat images from the growing season (Hansen et al., 2013) was used to estimate forest cover change from 2007 to 2010. This product includes a global percent tree-cover map from 2000 and a map identifying the year when removal of all tree cover was observed (Hansen et al., 2013; 2014). This global dataset is freely available in 10x10 degree tiles and the tile corresponding to Guinea-Bissau (granule with top-left corner at 20°N, 20°W) was downloaded as version 1.3 ([https://earthenginepartners.appspot.com/science-2013-global-forest/download\\_v1.3.html](https://earthenginepartners.appspot.com/science-2013-global-forest/download_v1.3.html)). For this study only data corresponding to the period 2000-2010 was used. Therefore limitations of interannual consistency when integrating 2000-2010 data and the updated 2011-2016 data should not have any impact in our analysis. This product is thereafter referred to as *GFC*.

Secondly, we used the global dataset of tree-cover at 30-m resolution (Sexton et al., 2013) which is freely available for download at the Global Land Cover Facility (GLCF) website (<http://glcfapp.glcg.umd.edu/data/>). This dataset uses the 250-m MODIS Vegetation Continuous Fields (VCF) rescaled to 30-m resolution using Landsat data. For this study we used the percent tree-cover layer for 2005 and 2010. Landsat scenes acquisition dates varied greatly (between November 2005 and December 2006 for the 2005 product, and between October 2009 and November 2010 for the 2010 product). As consequence, it becomes harder to compare this product to the *National* product that uses Landsat imagery from the dry season, or the *GFC* with imagery from the growing season. This product is referred to as *GLCF* product.

Thirdly we used the 25-m spatial resolution Forest/Non-Forest (F/NF) global mosaics from (Shimada et al., 2014) based on the Japan Aerospace Exploration Agency (JAXA) ALOS PALSAR. This product uses the lower levels of the L-band Synthetic Aperture Radar (SAR) backscatter as a threshold for mapping the transition of forest to non-forest, with forests being defined as areas of woody vegetation above 10% tree cover. Mosaics are available annually between 2007 and 2010 but only the maps for 2007 and 2010 were used in this analysis ([http://www.eorc.jaxa.jp/ALOS/en/palsar\\_fnf/fnf\\_index.htm](http://www.eorc.jaxa.jp/ALOS/en/palsar_fnf/fnf_index.htm)). In contrast with the *GFC* and *GLCF* products, which require a cloud screening and a stack of layers to create a per-pixel set of cloud-free observations, SAR penetrates

through clouds (a unique ability when compared to optical and lidar data). Therefore it does not require cloud screening processing and multi-temporal compositing, although has been recognized these mosaics should be generated with data acquired in the dry season to avoid the impact of rainfall events (Lucas et al., 2010). With this product we also don't have a reference year, but rather four independent F/NF, and two options could have been chosen for estimating deforestation. The option followed in this analysis recognizes that post-classification change detection leads to increased errors in the estimates and prioritizes having more comparable datasets. Therefore, only the F/NF maps for 2007 and 2010 were used and any deforestation captured in between is not accounted for if it regrows in 2010 (e.g., F>NF>NF>F). These mosaics covering Guinea-Bissau in 2007 and 2010 are referred to as the *JAXA* product. Acquisition dates are from the growing season between June and August of 2007 and from June to September of 2010.

A spatial tracking approach was used to estimate gross deforestation over the 2007-2010 temporal boundary. This period was selected due to the availability of data. The processing included the following steps:

- a) Producing mosaics from *GLCF* and *JAXA* scenes/tiles. *National* and *GFC* were already available in a single seamless raster;
- b) Resampling all datasets to a common spatial resolution (25-m) and coordinate system (UTM Zone 28N, WGS84 datum). A nearest neighbour algorithm was used to resample all datasets to a common resolution, thus not changing the original values of each dataset;
- c) "Water" and "No data" were eliminated by developing and applying a common land mask. In each dataset "water" and "no data" were reclassified to 0 and all other values to 1. The individual land masks were then combined to produce a common binary land mask. This common land mask was finally applied to all individual datasets to exclude "water" and "no data" from any given product;
- d) Generating Forest/Non-Forest (F/NF) maps. *National*: The two *National* 5-class land cover maps (Closed-Forest, Open-Forest, Savanna-Woodland, Mangrove, Non-Forest) were reclassified into F/NF maps. *GFC*: F/NF maps were generated for the years 2007 and 2010 using the 2000 percent tree-cover reclassified to F/NF with a threshold of 10% and annual loss maps in the period 2001-2007 and 2001-2010. *GLCF*: F/NF maps were generated for the years 2005 and 2010 by reclassifying areas with tree cover above 10% as forests in the tree cover maps for the corresponding years. *JAXA*: maps were already available as F/NF for 2007 and 2010. For both *National* and *JAXA* the threshold for forest is 10% tree cover, which is consistent with the national forest definition (FAO FRA 2010);

- e) Selection of continuous patches of forest with area equal or larger than 0.5 ha (8 pixels) to be consistent with the national forest definition of “Land spanning more than 0.5 hectares with trees higher than 5 meters and a canopy cover of more than 10 percent” (FAO FRA 2010);
- f) Generating deforestation maps for 2007-2010. For each product F/NF maps were combined to generate all transitions on a pixel-by-pixel basis. Deforestation maps were generated by reclassifying all possible transitions to *deforestation* and *no-change* between 2007 and 2010.

### AGB datasets

We used four available maps of AGB. Two AGB pantropical maps are based on Lidar and were developed at grid scales of 1-km (Saatchi et al., 2011) and 500-m (Baccini et al., 2012). They used similar input data layers of sparse transects derived from the Lidar dataset obtained by GLAS onboard the Ice, Cloud and land Elevation Satellite (ICESat) before its failure in 2009. However, they are based on different field data for calibration, different data for upscaling from MODIS data only (Baccini et al., 2012) or MODIS and Quick Scatterometer (QuikSCAT) data (Saatchi et al., 2011), and different methodologies for spatial modeling (Random Forests and Maxent respectively). Their reference year is 2000 for (Saatchi et al., 2011) and 2007-2008 for (Baccini et al., 2012). Both maps were downloaded from (<https://carbon.jpl.nasa.gov/data/dataMain.cfm> and <http://whrc.org/publications-data/datasets/pantropical-national-level-carbon-stock/> respectively) and are referred to as *SA11* and *BA12* respectively.

The other two AGB maps used ALOS PALSAR data. (Carreiras et al., 2012) created a country-scale mosaic of ALOS PALSAR data from 2008 and subsequently used a machine learning algorithm (boosted regression trees) to calibrate AGB observations obtained from national field data from 2007 and 2008 (Guinea-Bissau, 2011) as a function of ALOS PALSAR Fine Beam Dual (HH+HV polarization) backscatter intensity data to produce an AGB map for Guinea-Bissau at 50-m spatial resolution. Similarly, (Bouvet et al., 2018) used data from the same sensor but already in a mosaic format for the year 2010 (Shimada et al., 2014) over the entire African continent. They also used *in-situ* AGB data collected in eight African countries between 2000 and 2013 to produce a 25-m spatial resolution AGB map of African savannas, woodlands and dry forests. The method relies on a Bayesian inversion of a model relating ALOS PALSAR backscatter intensity as a function of AGB. Due to the saturation limitations of the L-band backscatter at higher AGB values (Collins et al., 2009; Mitchard et al., 2009) and its sensitivity to surface moisture conditions (Lucas et al., 2010), closed-forests and mangroves were masked out by using the ESA Climate Change Initiative Land Cover 2010 map. (Carreiras et al., 2012) map and the map corresponding to the bounding box of Guinea-

Bissau from (Bouvet et al., 2018) were made available for this study by the authors, and are referred to here as *CA12* and *BO18* respectively.

AGB maps were resampled to a common spatial resolution (25-m) and coordinate system (UTM Zone 28N, WGS84 datum), and a mask was applied to eliminate water values in all datasets as well as all values above 100 t/ha in *BO18* which correspond to other classes rather than biomass (100 - dense forest, 160 - inundated forest, 170 – mangroves, 190 – urban, and 210 – water; see Bouvet et al. 2018 for details).

## Supplementary results

**Table A.2.3** Mean above-ground biomass (AGB, t ha<sup>-1</sup>) ( $\pm$  standard deviation) from SA11, BA12, CA12, BO18 (maps) and National (field plots) for the entire country and corresponding to deforested areas mapped by each activity data product: GFC, GLCF, JAXA, and National.

	Country-wide	AD-GFC	AD-GLCF	AD-JAXA	AD-National
<b>EF-SA11</b>	55.4 ( $\pm$ 33.0)	65.6 ( $\pm$ 39.1)	42.4 ( $\pm$ 22.7)	50.2 ( $\pm$ 27.0)	42.4 ( $\pm$ 24.1)
<b>EF-BA12</b>	66.4 ( $\pm$ 25.9)	72.0 ( $\pm$ 29.3)	57.6 ( $\pm$ 19.0)	61.1 ( $\pm$ 24.4)	49.7 ( $\pm$ 18.1)
<b>EF-CA12</b>	62.8 ( $\pm$ 35.9)	63.5 ( $\pm$ 36.5)	53.5 ( $\pm$ 34.5)	55.8 ( $\pm$ 33.3)	36.2 ( $\pm$ 32.2)
<b>EF-BO18</b>	55.4 ( $\pm$ 21.8)	45.4 ( $\pm$ 21.6)	45.5 ( $\pm$ 22.8)	38.6 ( $\pm$ 21.1)	33.5 ( $\pm$ 24.4)
<b>EF-National</b>			62.8 ( $\pm$ 54.3)		

**Table A.2.4** Deforestation values and rates obtain by different products between 2007 and 2010.

Product	Deforested area (ha)	Deforestation rate	
		ha yr <sup>-1</sup>	% yr <sup>-1</sup>
<b>AD-National</b>	158,290	52,763	1.8
<b>AD-GFC</b>	22,631	7,544	0.3
<b>AD-GLCF</b>	84,383	16,877	0.6
<b>AD-JAXA</b>	112,626	37,542	1.3

**Table A.2.5** Forest Reference Emission Level (in MtCO<sub>2</sub> yr<sup>-1</sup>) given as the multiplication of deforestation (Activity Data, AD, ha yr<sup>-1</sup>) derived from each product (AD-GFC, AD-GLCF, AD-JAXA, and AD-National) and the above-ground biomass for tropical and sub-tropical dry forests (Tier 1, [Table 4.12](#) IPCC 2006) as pre-deforestation carbon stock or Emission Factor (EF-Tier1).

	AD-GFC	AD-GLCF	AD-JAXA	AD-National
<b>EF-Tier1</b>	1.69	3.78	8.41	11.82

## References

Baccini, A., Goetz, S. J., Walker, W. S., Laporte, N. T., Sun, M., Sulla-Menashe, D., Hackler, J., Beck, P. S. A., Dubayah, R., Friedl, M. A., Samanta, S., and Houghton, R. A.: Estimated carbon dioxide emissions from tropical deforestation improved by carbon-density maps, *Nature Climate Change*, 2, 182-185, 10.1038/nclimate1354, 2012.

Bouvet, A., Mermoz, S., Toan, T. L., Villard, L., Mathieu, R., Naidoo, L., and Asner, G. P.: An above-ground biomass map of African savannahs and woodlands at 25 m resolution derived from ALOS PALSAR, *Remote Sensing of Environment*, 206, 156-173, 10.1016/j.rse.2017.12.030, 2018.

Carreiras, J. M. B., Vasconcelos, M. J., and Lucas, R. M.: Understanding the relationship between aboveground biomass and ALOS PALSAR data in the forests of Guinea-Bissau (West Africa), *Remote Sensing of Environment*, 121, 426-442, 10.1016/j.rse.2012.02.012, 2012.

Collins, J. N., Hutley, L. B., Williams, R. J., Boggs, G., Bell, D., and Bartolo, R.: Estimating landscape-scale vegetation carbon stocks using airborne multi-frequency polarimetric synthetic aperture radar (SAR) in the savannahs of north Australia, *International Journal of Remote Sensing*, 30, 1141-1159, 10.1080/01431160802448935, 2009.

Guinea-Bissau, R. o.: Second National Communication of Guinea-Bissau to the UNFCCC, SEAT, Bissau, 2011.

Hansen, M., Potapov, P., Margono, B., Stehman, S., Turubanova, S., and Tyukavina, A.: Response to Comment on "High-resolution global maps of 21st-century forest cover change", *Science*, 344, 1, 10.1126/science.1248817, 2014.

Hansen, M. C., Potapov, P. V., Moore, R., Hancher, M., Turubanova, S. A., Tyukavina, A., Thau, D., Stehman, S. V., Goetz, S. J., Loveland, T. R., Kommareddy, A., Egorov, A., Chini, L., Justice, C. O., and Townshend, J. R. G.: High-Resolution Global Maps of 21st-Century Forest Cover Change, *Science*, 342, 850-853, 10.1126/science.1244693, 2013.

Lucas, R., Armston, J., Fairfax, R., Fensham, R., Accad, A., Carreiras, J., Kelley, J., Bunting, P., Clewley, D., Bray, S., Metcalfe, D., Dwyer, J., Bowen, M., Eyre, T., Laidlaw, M., and Shimada, M.: An Evaluation of the ALOS PALSAR L-Band Backscatter-Above Ground Biomass Relationship Queensland, Australia: Impacts of Surface Moisture Condition and Vegetation Structure, *IEEE Journal of Selected Topics in Applied Earth Observations and Remote Sensing*, 3, 576-593, 10.1109/jstars.2010.2086436, 2010.

Mitchard, E. T. A., Saatchi, S. S., Woodhouse, I. H., Nangendo, G., Ribeiro, N. S., Williams, M., Ryan, C. M., Lewis, S. L., Feldpausch, T. R., and Meir, P.: Using satellite radar backscatter to predict above-ground woody biomass: A consistent relationship across four different African landscapes, *Geophysical Research Letters*, 36, 6, 10.1029/2009gl040692, 2009.

Pearson, T., Walker, S., and Brown, S.: Sourcebook for land use, land-use change and forestry projects, Winrock International, Little Rock, AK, 64 p., 2005.

Saatchi, S. S., Harris, N. L., Brown, S., Lefsky, M., Mitchard, E. T. A., Salas, W., Zutta, B. R., Buermann, W., Lewis, S. L., Hagen, S., Petrova, S., White, L., Silman, M., and Morel, A.: Benchmark map of forest carbon stocks in tropical regions across three continents, *Proceedings of the National Academy of Sciences of the United States of America*, 108, 9899-9904, 10.1073/pnas.1019576108, 2011.

Sexton, J. O., Song, X. P., Feng, M., Noojipady, P., Anand, A., Huang, C. Q., Kim, D. H., Collins, K. M., Channan, S., DiMiceli, C., and Townshend, J. R.: Global, 30-m resolution continuous fields of tree cover: Landsat-based rescaling of MODIS vegetation continuous fields with lidar-based estimates of error, *International Journal of Digital Earth*, 6, 427-448, 10.1080/17538947.2013.786146, 2013.

Shimada, M., Itoh, T., Motooka, T., Watanabe, M., Shiraishi, T., Thapa, R., and Lucas, R.: New global forest/non-forest maps from ALOS PALSAR data (2007–2010), *Remote Sensing of Environment*, 155, 13-31, <http://dx.doi.org/10.1016/j.rse.2014.04.014>, 2014.

Vasconcelos, M. J., Cabral, A. I. R., Melo, J. B., Pearson, T. R. H., Pereira, H. D., Cassama, V., and Yudelman, T.: Can blue carbon contribute to clean development in West-Africa? The case of Guinea-Bissau, *Mitigation and Adaptation Strategies for Global Change*, 20, 1361-1383, [10.1007/s11027-014-9551-x](https://doi.org/10.1007/s11027-014-9551-x), 2015.

## Appendix 3

**Table A.3.1** calculations to derive the required sample size to validate and correct the deforestation maps (National, GFC, and GLCF and their combinations - columns on the left) following a stratified sampling design.

Nat	GFC	GLCF	Class	Ui	Si	Pixels	Wi	ni	area proportion	reference dataset
0	0	0	1	0.95	0.2179	46,978,348	0.9	516	0.923	293
0	1	0	2	0.7	0.4583	266,361	0.0	3	0.005	57
0	0	1	3	0.7	0.4583	1,094,434	0.0	12	0.021	84
0	1	1	4	0.7	0.4583	43,959	0.0	0	0.001	67
1	0	0	5	0.7	0.4583	2,289,963	0.0	25	0.045	168
1	0	1	6	0.7	0.4583	190,887	0.0	2	0.004	53
1	1	0	7	0.7	0.4583	30,936	0.0	0	0.001	119
1	1	1	8	0.95	0.2179	20,846	0.0	0	0.000	58
								<b>n</b>	559	<b>899</b>
								<b>S(O)</b>	0.01	

**Table A.3.2** Error matrices of the maps expressed as number of reference units with estimate of commission errors (CE, %), omission errors (OE, %) and overall accuracy (OA, %) for a) the individual maps, b) union of maps, and c) intersection of maps

Individual maps		Deforestation	No change	Total	CE (%)
<b>National</b>	Deforestation	162	236	398	59
	no change	113	388	501	23
	Total	275	624	899	61% OA
	OE (%)	41	38		
<b>GFC</b>	Deforestation	187	114	301	38
	no change	88	510	598	15
	Total	275	624	899	78% OA
	OE (%)	32	18		
<b>GLCF</b>	Deforestation	132	130	262	50
	no change	143	494	637	22
	Total	275	624	899	70% OA
	OE (%)	52	21		

Union of maps		Deforestation	No change	Total	CE (%)
<b>Nat U GFC</b>	Deforestation	243	279	522	53
	no change	32	345	377	8
	Total	275	624	899	65% OA
	OE (%)	12	45		
<b>Nat U GLCF</b>	Deforestation	232	317	549	58
	no change	43	307	350	12
	Total	275	624	899	60% OA
	OE (%)	16	51		
<b>GFC U GLCF</b>	Deforestation	232	206	438	47
	no change	43	418	461	9
	Total	275	624	899	72% OA
	OE (%)	16	33		
<b>Nat U GFC U GLCF</b>	Deforestation	267	339	606	56
	no change	8	285	293	3
	Total	275	624	899	61% OA
	OE (%)	3	54		

Intersection of maps		Deforestation	No change	Total	CE (%)
<b>Nat ∩ GFC</b>	Deforestation	65	54	119	45
	no change	210	570	780	27
	Total	275	624	899	71% OA
	OE (%)	76	9		
<b>Nat ∩ GLCF</b>	Deforestation	21	32	53	60
	no change	254	592	846	30
	Total	275	624	899	68% OA
	OE (%)	92	5		
<b>GFC ∩ GLCF</b>	Deforestation	46	21	67	31
	no change	229	603	832	28
	Total	275	624	899	72% OA
	OE (%)	83	3		
<b>Nat ∩ GFC ∩ GLCF</b>	Deforestation	41	17	58	29
	no change	234	607	841	28
	Total	275	624	899	72% OA
	OE (%)	85	3		

**Table A.3.3** Error matrix of deforestation and no-change expressed as the proportion of area as suggested by good practice recommendations (Olofsson et al., 2014a) with estimate of the corrected commission errors (CE, %), omission errors (OE, %) and overall accuracy (OA, %) for a) the individual maps, b) union of maps, and c) intersection of maps

a) Individual maps		Deforestation	No change	Total	CE (%)
<b>National</b>	Deforestation	0.02	0.03	0.05	59
	no change	0.21	0.74	0.95	23
	Total	0.23	0.77	<b>76%</b>	<b>OA</b>
	OE (%)	91	4		
<b>GFC</b>	Deforestation	0.00	0.00	0.01	38
	no change	0.15	0.85	0.99	15
	Total	0.15	0.85	<b>85%</b>	<b>OA</b>
	OE (%)	97	0		
<b>GLCF</b>	Deforestation	0.01	0.01	0.03	50
	no change	0.22	0.75	0.97	22
	Total	0.23	0.77	<b>77%</b>	<b>OA</b>
	OE (%)	94	2		

b) Union of maps		Deforestation	No change	Total	CE (%)
<b>Nat U GFC</b>	Deforestation	0.03	0.03	0.056	53
	no change	0.08	0.86	0.944	8
	Total	0.11	0.89	<b>89%</b>	<b>OA</b>
	OE (%)	76	3		
<b>Nat U GLCF</b>	Deforestation	0.03	0.04	0.072	58
	no change	0.11	0.81	0.928	12
	Total	0.14	0.86	<b>84%</b>	<b>OA</b>
	OE (%)	79	5		
<b>GFC U GLCF</b>	Deforestation	0.02	0.02	0.032	47
	no change	0.09	0.88	0.968	9
	Total	0.11	0.89	<b>89%</b>	<b>OA</b>
	OE (%)	84	2		
<b>Nat U GFC U GLCF</b>	Deforestation	0.03	0.04	0.077	56
	no change	0.03	0.90	0.923	3
	Total	0.06	0.94	<b>93%</b>	<b>OA</b>
	OE (%)	43	5		

c) Intersection of maps		Deforestation	No change	Total	CE (%)
<b>Nat ∩ GFC</b>	Deforestation	0.00	0.00	6E-04	45
	no change	0.27	0.73	0.999	27
	Total	0.27	0.73	<b>73%</b>	<b>OA</b>
	OE (%)	100	0		
<b>Nat ∩ GLCF</b>	Deforestation	0.00	0.00	0.004	60
	no change	0.30	0.70	0.996	30
	Total	0.30	0.70	<b>70%</b>	<b>OA</b>
	OE (%)	100	0		
<b>GFC ∩ GLCF</b>	Deforestation	0.00	0.00	9E-04	31
	no change	0.28	0.72	0.999	28
	Total	0.28	0.72	<b>72%</b>	<b>OA</b>
	OE (%)	100	0		
<b>Nat ∩ GFC ∩ GLCF</b>	Deforestation	0.00	0.00	4E-04	29
	no change	0.28	0.72	1	28
	Total	0.28	0.72	<b>72%</b>	<b>OA</b>
	OE (%)	100	0		